ASME PTC 19.5-2004

Flow Measurement

Performance Test Codes

AN AMERICAN NATIONAL STANDARD

The American Society of Mechanical Engineers

Intentionally left blank

ASME PTC 19.5-2004

Flow Measurement

Performance Test Codes

AN AMERICAN NATIONAL STANDARD

The American Society of Mechanical Engineers

Three Park Avenue • New York, NY 10016

Date of Issuance: July 25, 2005

The 2004 edition of ASME PTC 19.5 is being issued with an automatic addenda subscription service. The use of addenda allows revisions made in response to public review comments or committee actions to be published as necessary. This Supplement will be revised when the Society approves the issuance of a new edition.

ASME issues written replies to inquiries as code cases and interpretations of technical aspects of this document. Code cases and interpretations are published on the ASME Web site under the Committee Pages at http://www.asme.org/codes/ as they are issued.

The American Society of Mechanical Engineers
Three Park Avenue, New York, NY 10016-5990

CONTENTS

Tables

NOTICE

All Performance Test Codes must adhere to the requirements of ASME PTC 1, General Instructions. The following information is based on that document and is included here for emphasis and for the convenience of the user of the Supplement. It is expected that the Code user is fully cognizant of Sections 1 and 3 of ASME PTC 1 and has read them prior to applying this Supplement.

ASME Performance Test Codes provide test procedures that yield results of the highest level of accuracy consistent with the best engineering knowledge and practice currently available. They were developed by balanced committees representing all concerned interests and specify procedures, instrumentation, equipment-operating requirements, calculation methods, and uncertainty analysis.

When tests are run in accordance with a Code, the test results themselves, without adjustment for uncertainty, yield the best available indication of the actual performance of the tested equipment. ASME Performance Test Codes do not specify means to compare those results to contractual guarantees. Therefore, it is recommended that the parties to a commercial test agree before starting the test and preferably before signing the contract on the method to be used for comparing the test results to the contractual guarantees. It is beyond the scope of any Code to determine or interpret how such comparisons shall be made.

FOREWORD

The history of this Instruments and Apparatus Supplement began with the Research Committee on Fluid Meters being organized in 1916. One of its stated objectives was "the preparation of a textbook on the theory and use of fluid meters sufficient as a standard reference." In carrying out this objective, the first edition of Part 1 of this report was published in 1924, received immediate approval, and was widely referenced by the users of fluid meters and educators. As originally planned by the Committee, the report was to be issued in three parts: Part 1, Theory and Application, was the first one published; followed by Part 2, Description of Meters; and Part 3, Installation. Part 1 was so well received that the second and third editions of this Part were needed before the preparation of the other two parts could occur. The second edition of Part 1 was considerably different from the first, though it followed about the same format and arrangement; the third edition was very similar to the second. These were published in 1927 and 1930, respectively.

Part 2 of the report was published in 1931 and contained a complete description of the physical characteristics of the meters then being manufactured. However, it was found that the material in this Part became obsolete rapidly and it was decided to inform anyone interested in these descriptions that they should be secured from the manufacturers, since their literature must necessarily be up to date.

Part 3, published in 1933, gave instructions for correct installation of meters and discussed the effect of incorrect installation. However, Part 3 was abandoned also because the Committee decided the material in it should be an integral part of the complete report of the Committee.

The fourth edition of Part 1 was prepared in 1937 and was a completely new draft of this Part of the report. It was altered because there had been considerable criticism of the fact that the material presented was difficult to put to practical use. The changed format and additional material presented apparently corrected this condition, since this edition went through many printings.

The fifth edition, issued in 1959, followed the same general format as the fourth and included material gained in the long interval since the last edition. Another publication by the Committee was a manual, Flowmeter Computation Handbook, which was issued in 1961. The procedures in it could be adapted to computer programming.

The format of the sixth edition differed slightly from that of the fourth and fifth editions. Each section by itself was complete so that altering one section would not affect preceding or following sections.

The sixth edition, somewhat like the third edition and its Part 3, was divided into two parts. The material on installation and application were both a part of the complete report and a separate publication, which became ASME PTC 19.5, Flow Measurement, in accordance with an agreement made between the Research Committee on Fluid Meters and the Performance Test Code Committee in 1964. Practically all of the material in ASME PTC 19.5 was taken from Fluid Meters, and most of the writers also were members of the Research Committee on Fluid Meters. It was the decision of the two committees that combining the material into one publication, in such a way that the sections dealing with specifications and instructions could be published separately, would reduce the work of the committees and the number of separate publications. However, this publication prompted considerable criticism that the material presented was difficult to put to practical use. Consequently, the Board on Performance Test Codes formed a committee to address these concerns, and the result is the current version of ASME PTC 19.5, Flow Measurement.

This edition includes a much broader range of methods of flow measurement than any of its predecessors. Even so, it does not include every method — only those that were judged at the time to meet the requirements and needs of Test Codes by providing results of the highest level of accuracy consistent with the best engineering knowledge and practice currently available.

This edition was approved by the Board of Performance Test Codes on April 16, 2001 and February 18, 2004 and by the ANSI Board of Standards Review as an American National Standard on July 10, 2002 and March 10, 2004.

PERFORMANCE TEST CODE COMMITTEE 19.5 ON FLOW MEASUREMENT

(The following is the roster of the Committee at the time of approval of this Code.)

OFFICERS

D. R. Keyser, *Chair*
J. R. Friedman, *Vice Chair*
M. Brookes, *Secretary*

COMMITTEE PERSONNEL

B. T. Arnberg, Consultant
D. B. Cox, Florida Power Corp.
J. R. Friedman, Siemens-Westinghouse Corp.
F. C. Lowell, Jr., Accusonic Technologies Inc.
D. R. Keyser, U.S. Navy, Naval Air Systems

MEMBERS EMERITI

R. F. Bruner, E. I. du Pont de Nemours & Co., Inc.
E. D. Mannherz, Fisher & Porter Co.
W. J. Sumner, General Electric Co.

NECROLOGY

R. P. Benedict, Westinghouse Electric Corp.
C. P. Kittredge, Princeton University
J. W. Murdock, Drexel University and U.S. Navy
D. A. Sullivan, Fern Engineering

BOARD ON PERFORMANCE TEST CODES

OFFICERS

P. M. Gerhart, *Chair*
S. J. Korellis, *Vice Chair*
W. O. Hays, *Secretary*

BOARD PERSONNEL

P. G. Albert
R. P. Allen
R. L. Bannister
D. S. Beachler
J. M. Burns
W. C. Campbell
M. J. Dooley
A. J. Egli
J. R. Friedman
G. J. Gerber
Y. Goland
T. C. Heil
T. S. Jonas
D. R. Keyser
P. M. McHale
J. W. Milton
G. H. Mittendorf, Jr.
S. P. Nuspl
A. L. Plumley
R. R. Priestley
J. W. Siegmund
J. A. Silvaggio, Jr.
W. G. Steele,Jr.
J. C. Westcott
J. G. Yost

CORRESPONDENCE WITH THE PTC 19.5 COMMITTEE

General. ASME Codes are developed and maintained with the intent to represent the consensus of concerned interests. As such, users of this Supplement may interact with the Committee by requesting interpretations, proposing revisions, and attending Committee meetings. Correspondence should be addressed to:

Secretary, PTC 19.5 Standards Committee
The American Society of Mechanical Engineers
Three Park Avenue
New York, NY 10016-5990

Proposing Revisions. Revisions are made periodically to the Supplement to incorporate changes that appear necessary or desirable, as demonstrated by the experience gained from the application of the Supplement. Approved revisions will be published periodically.

The Committee welcomes proposals for revisions to this Supplement. Such proposals should be as specific as possible, citing the paragraph number(s), the proposed wording, and a detailed description of the reasons for the proposal, including any pertinent documentation.

Interpretations. Upon request, the PTC 19.5 Committee will render an interpretation of any requirement of the Supplement. Interpretations can only be rendered in response to a written request sent to the Secretary of the PTC 19.5 Standards Committee.

The request for interpretation should be clear and unambiguous. It is further recommended that the inquirer submit his/her request in the following format:

Subject:	Cite the applicable paragraph number(s) and the topic of the inquiry.
Edition:	Cite the applicable edition of the Supplement for which the interpretation is being requested.
Question:	Phrase the question as a request for an interpretation of a specific requirement suitable for general understanding and use, not as a request for an approval of a proprietary design or situation. The inquirer may also include any plans or drawings, which are necessary to explain the question; however, they should not contain proprietary names or information.

Requests that are not in this format will be rewritten in this format by the Committee prior to being answered, which may inadvertently change the intent of the original request.

ASME procedures provide for reconsideration of any interpretation when or if additional information that might affect an interpretation is available. Further, persons aggrieved by an interpretation may appeal to the cognizant ASME Committee or Subcommittee. ASME does not "approve," "certify," "rate," or "endorse" any item, construction, proprietary device, or activity.

Attending Committee Meetings. The PTC 19.5 Standards Committee regularly holds meetings, which are open to the public. Persons wishing to attend any meeting should contact the Secretary of the PTC 19.5 Standards Committee or check our Web sitehttp://www.asme.org.org/codes/.

Intentionally left blank

FLOW MEASUREMENT

Section 1
Object and Scope

1-1 OBJECT

The object of this Supplement is to define and describe the proper measurement of any flow required or recommended by any of the Performance Test Codes. Flow measurements performed as specified herein satisfy the requirements of all relevant ISO flow measurement standards in effect at the time of publication.

1-2 SCOPE

This Supplement describes the techniques and methods of all flow measurements required or recommended by the Performance Test Codes. Newer flow measurement techniques of comparably high accuracy are included to provide alternative flow measurements for special situations in which deviations from the requirements of a code are agreed to be necessary. This is a supplementary document that does not supersede the mandatory requirements of any code unless such an agreement has been expressed in writing prior to testing.

Section 2
Definitions, Values, and Descriptions of Terms

Except where specifically noted, the equations in this Edition are written in the primary system of units explained below. The reason for this practice is to simplify the text and focus on the physical, scientific principles involved in the measurement of flow. There are too many customary units in use throughout the various industries to publish all such physically identical variations in this book. It behooves the user, therefore, to convert his particular units into these primary units, calculate the flow, and reconvert the result back into his desired units. For international use, equations written in which force is in pounds, mass is in slugs, length is in feet, and time is in seconds appear identical to equations in which force is in newtons, mass is in kilograms, length is in meters, and time is in seconds.

2-1 PRIMARY DEFINITIONS AND SYSTEMS OF UNITS

(a) The force of 1 lb applied to a mass of 1 slug (also known as the geepound) will accelerate said mass at the rate of 1 ft/sec^2.

(b) The force of 1 N applied to a mass of 1 kg will accelerate said mass at the rate of 1 m/s^2.

(c) Equations written in these units will appear identical. Converting measured values for the test from English units commonly used to the above primary U.S. Customary units can simplify the expression of test results in Systeme Internationale (SI) units.

(d) By way of contrast and for clarification, the force of 1 lb applied to a mass of 1 lb will accelerate said mass at the rate of g_c in feet per second squared. This fact is the origin of the appearance of the conversion factor g_c in engineering equations expressed in traditional English units. Note that g_c is not the local acceleration of gravity at the test site.

(e) The required source for precise physical values, conversion factors, and definitions is ASME PTC 2.

2-2 HISTORICAL DEFINITIONS OF UNITS OF MEASUREMENTS

It is often useful to be aware of the historic physical bases for many of the units of performance measurement. The reader is cautioned that the numerical values of these physical definitions have been refined over the years, so that the following historic definitions may be no longer numerically exact and should not be used in Code tests under those circumstances. Nonetheless, the embodied physical concepts can improve one's understanding of a measurement or test result.

British thermal unit (Btu): a unit of heat energy equal to the heat needed to raise the temperature of a 1-lb mass of air-free water from 60°F to 61°F at a constant pressure of 1 standard atm; the mean Btu is equal to $^1/_{180}$ of the heat needed to raise a 1-lb mass of air-free water from its freezing point to its boiling point at a constant pressure of 1 standard atm [1].

calorie: the amount of heat energy required to raise the temperature of 1 g of pure water from 14.5°C to 15.5°C at a constant pressure of 1 standard atm [1].

Celsius: a thermometer invented in 1742 by Anders Celsius, a Swedish astronomer, who graduated the interval between the freezing point of water and its boiling point into 100° (wherefrom centigrade) at an atmospheric pressure of 760 mmHg. The present scale has the freezing point at 0°C and the boiling point at 100°C, just the reverse of the numbering by Celsius [2].

Fahrenheit: the scale used by Daniel Gabriel Fahrenheit, who invented a thermometer containing alcohol in 1709 and a mercury thermometer in 1714. The zero point on the scale was established by mixing equal quantities by weight of snow and common salt. The freezing point of water was found to be at 32° of graduation and the boiling point very near 212° under standard atmospheric pressure [2].

foot: one-third of a yard, originally based on the length of a man's foot [2].

force: units of pound or newton; no one has ever seen a force.

geepound or slug: 1 slug weighs 32.174 lb at sea level and 45 deg of latitude [2].

gram: the mass of 1 cc of pure water in a vacuum at its maximum density [2].

heat: energy in transit between a source at a higher temperature from which the energy is coming to a sink toward which the energy is going. Other types of energy in transit are called work [1].

inch: the twelfth part of a foot, originally established by statute, apparently of Edward II, given in the Cottonian

Manuscripts (Claudius D.2) to be that of three grains of barley dry and round placed end to end lengthwise [2].

joule: the unit of work or energy equal to the work done by a force of 1 N when the point at which the force is applied is displaced 1 m in the direction of said force. Also known as a newton-meter of energy. It is also practically equivalent to the energy expended by an electric current of 1 A flowing for 1 s through a resistance of 1 Ω [1, 2].

meter: an SI unit of length, originally one ten-millionth of the distance along a meridian on earth from the equator to the pole [2].

second: a measure of an interval in time, originally the period of a pendulum, 1 m in length at sea level and 45 deg of latitude [2].

temperature: the property of an object that determines the direction of heat flow when that object is placed in thermal contact with another object at a different temperature [1].

yard: a unit of length containing 36 in.; in Great Britain, it is the distance, at 62°F, between two transverse lines in gold plugs set in a bronze bar, called the British Imperial Yard, and kept at the Standards office of the Board of Trade at Westminster [2].

2-2.1 References for Para. 2-2

[1] Lapedes, D., ed. *Dictionary of Scientific and Technical Terms.* New York: McGraw-Hill Book Co.; 1974.

[2] *Webster's New International Dictionary,* 2nd edition unabridged. Springfield, MA: Merriam Co.; 1934.

2-3 SYMBOLS AND DIMENSIONS

A = area, L^2
B = magnetic flux density, Tesla
C = coefficient of discharge
C^* = critical flow function
D = diameter, usually of pipe, L
D = drag torque coefficient, for turbine meters, subscripted
E = relative error
F = fluorescence
F = velocity of approach factor
G = mass flux, $M/(L^2T)$
K = structural blockage coefficient
M, Ma = Mach number
P, p = pressure, F/L^2
Pr = Prandtl number
Q, q = flow, L^3/T
R = gas constant, FL/M deg
Re = Reynolds number
S = frontal area, L^2
S = velocity profile correction factor
T = temperature, deg
V, v = velocity, L/T
Z = compressibility factor for a gas
c = mass concentration
c = specific heat, FL/M
d = diameter, usually of meter bore, L
d = spacing, separation dimension, L
e = electrode voltage, V
f = frequency, Hz, 1/T
g = local acceleration of gravity, L/T^2
h = enthalpy, or convective heat transfer coefficient, FL/M
k = loss coefficient for a flow conditioner
l = length or distance, as to the pressure tap loci, L
s = entropy, FL/M deg
s = streamline coordinate, L
u = uncertainty, %
v = specific volume, 1/density, L^3/M
w = weighting factor
w, q_m = mass flow, M/T
z = elevation, as in head, L
α = acoustic velocity, speed of sound, L/T
β = diameter ratio, d/D
Δ = difference operator
δ = small difference, sometimes an operator
ϵ = expansion factor of a flowing compressible fluid
Φ = angle of the divergent, rad or deg
Γ = average isentropic exponent of a real gas
γ = ratio of specific heats, constant pressure/constant volume
η = efficiency, as in volumetric
= isentropic exponent, as in the expansion or compression of gas
λ = friction factor of a conduit
μ = absolute viscosity, M/LT
= kinematic viscosity, L^2/T
ρ = density, M/L^3
σ = standard deviation
Ω, ω = frequency, rad/sec in both U.S. Customary and SI units, 1/T

Subscripts and superscripts

B = back (pressure)
D = based on pipe diameter
L = local
R = real gas
a = area
c = constant, as in the proportionality between slugs and lbm
d = based on bore or throat diameter
f = fringe, as in light interference patterns
i = ideal
m = mass
meas = measured value
o = plenum inlet or stagnation conditions
p = constant pressure

t = at throat conditions
u = universal
v = constant volume
$*$ = at sonic or critical conditions

2-3.1 Common Conversion Factors

See Tables 2-3.1-1 through 2-3.1-8 for common conversion factors.

2-4 THERMAL EXPANSION

This paragraph deals with piping and primary element materials. In most cases, the piping and primary element diameters are measured at room temperature but are used at the actual temperature of the flowing fluid (assumed to be the same as piping and primary element temperature). It is customary to assume, unless given otherwise, that the dimensional measurement takes place at 68°F (20°C).

2-4.1 Linear Thermal Expansion

The mean coefficient of linear thermal expansion is defined by

$$\alpha = \left(\frac{1}{L_b}\right)\frac{dL}{dt} \qquad (2\text{-}4.1)$$

where
α = mean coefficient of linear expansion from base temperature b to actual temperature t, $(1/t)$
L_b = length at base temperature b

The ratio of length at temperature t to base temperature b is given by

$$L_t/L_b = 1 + \alpha(t - b) \qquad (2\text{-}4.2)$$

where
L_t = length at temperature t

2-4.2 Tables of Linear Thermal Expansion for Selected Materials

Table 2-4.2-1 contains values of α and L_t/L_b in SI units and Table 2-4.2-2 contains the same values in U.S. Customary units. These data are for informational purposes only, and it should not be implied that materials are suitable for all the temperature ranges shown.

2-4.3 Automatic Data Processing

Table 2-4.2-1 was generated using the following equation:

$$10^6\alpha = a + bt + ct^2 + dt^3 \qquad (2\text{-}4.3)$$

where
α = mean coefficient of linear expansion from 20°C to indicated temperature, mm/(mm/°C)
t = temperature, °C

Values of coefficients of Eq. (2-4.3) for the selected materials are given in Table 2-4.3.

Similarly, Table 2-4.2 for U.S. Customary units was calculated by multiplying Eq. (2-4.3) by $^5/_9$ and substituting equivalent values of t in °C.

2-5 SOURCES OF FLUID AND MATERIAL DATA

Abramowitz, M.; Stegun, I. *Handbook of Mathematical Functions With Formulas, Graphs, and Mathematical Tables.* NBS-AMS 55. Washington, D.C.: U.S. Department of Commerce; 1964.

ASHRAE Brochure in Psychrometry. Atlanta: American Society of Heating, Refrigerating and Air-Conditioning Engineers.

ASHRAE Thermodynamic Properties of Refrigerants. Atlanta: American Society of Heating, Refrigerating and Air-Conditioning Engineers; 1991.

ASME Fluid Meters: Their Theory and Application, 6th edition. New York: American Society of Mechanical Engineers; 1971.

ASME Steam Tables: Thermodynamic and Transport Properties of Steam, 6th edition. New York: American Society of Mechanical Engineers; 1993.

Avallone, E.; Baumeister, T. *Mark's Standard Handbook for Mechanical Engineers.* New York: McGraw-Hill; 1987.

Aviation Fuel Properties. Warrendale, PA: Society of Automotive Engineers; 1970.

CTI Publication ATC-105 Field Test Handbook. Houston, TX: Cooling Tower Institute.

Eshbach, O.; Sanders, M. *Handbook of Engineering Fundamentals.* New York: John Wiley & Sons; 1975.

Handbook of Chemistry and Physics. Cleveland: The Chemical Rubber Co.; 1978.

Joint-Army-Navy-Air-Force (JANAF) Thermochemical Tables. Melville, NY: American Institute of Physics; 1998.

Kutz, M. *Mechanical Engineers' Handbook.* New York: John Wiley & Sons; 1955.

Machinery's Handbook. New York: Industrial Press.

Miller, R. W. *Flow Measurement Engineering Handbook,* 3rd. New York: McGraw-Hill; 1996.

Table 2-3.1-1 Conversions to SI (Metric) Units

Quantity	Conversion		Multiplication Factor	
	From	To		
Acceleration, linear	ft/sec^2	m/s^2	3.048 [Note (1)]	E − 01
	standard gravity	m/s^2	9.806 65 [Note (1)]	E + 00
Area	in.^{2}	m^2	6.451 6	E − 04
	ft^2	m^2	9.290 304 [Note (1)]	E − 02
Coefficient of thermal expansion	°R^{-1}	K^{-1}	1.8 [Note (1)]	E + 00
Density	lbm/ft^3	kg/m^3	1.601 846	E + 01
	slugs/ft^3	kg/m^3	5.153 788	E + 02
Energy, work, heat	Btu (IT)	J	1.055 056	E + 03
	ft-lbf	J	1.355 818	E + 00
Flow rate, mass	lbm/sec	kg/s	4.535 924	E − 01
	lbm/min	kg/s	7.559 873	E − 03
	lbm/hr	kg/s	1.259 979	E − 04
	slugs/sec	kg/s	1.459 390	E + 01
Flow rate, volume	ft^3/min	m^3/s	4.719 474	E − 04
	ft^3/sec	m^3/s	2.831 685	E − 02
	gallons (U.S. liquid)/min	m^3/s	6.309 020	E − 05
Force	lbf (avoirdupois)	N	4.448 222	E + 00
Frequency	sec^{-1}	Hz	1 [Note (1)]	E + 00
Gas constant	Btu/lbm-°R	J/(kg · K)	4.186 8 [Note (1)]	E + 03
	ft-lbf/lbm-°R	J/(kg · K)	5.380 320	E + 00
Heat rate	Btu/kWh	kJ/kWh	1.055 056	E + 00
Heat transfer coefficient	Btu/hr-ft^2-°R	W/(m^2 · K)	5.678 263	E + 00
Length	in.	m	2.54 [Note (1)]	E − 02
	ft	m	3.048 [Note (1)]	E − 01
	mile (U.S.)	m	1.609 344 [Note (1)]	E + 03
Mass	lbm (avoirdupois)	kg	4.535 924	E − 01
	slug	kg	1.459 390	E + 01
Plane angle	deg	rad	1.745 329	E − 02
Power	Btu(IT)/hr	W	2.930 711	E − 01
	ft-lbf/sec	W	1.355 818	E + 00
	hp (550 ft-lbf/sec)	W	7.456 999	E + 02
Pressure	standard atmosphere	Pa	1.013 25 [Note (1)]	E + 05
	bar	Pa	1 [Note (1)]	E + 05
	lbf/ft^2	Pa	4.788 026	E + 01
	lbf/in.^{2}	Pa	6.894 757	E + 03
Rotational frequency	min^{-1}	s^{-1}	1.666 667	E − 02
Specific enthalpy	Btu/lbm	J/kg	2.326	E + 03
Specific entropy	Btu/lbm-°R	J/(kg · K)	4.186 8 [Note (1)]	E + 03
Specific heat	Btu/lbm-°R	J/(kg · K)	4.186 8	E + 03
Specific internal energy	Btu/lbm	J/kg	2.326	E + 03
Specific volume	ft^3/lbm	m^3/kg	6.242 797	E − 02
Specific weight (force)	lbf/ft^3	N/m^3	1.570 875	E + 02
Surface tension	lbf/ft	N/m	1.459 390	E + 01
Temperature interval	°F	°C	5.555 556	E − 01
Temperature, measured	°F	°C	$t_C = (t_F - 32)/1.8$	
Temperature, thermodynamic	°C	K	$T_K = t_C + 273.15$	
	°F	K	$T_K = (t_F + 459.67)/1.8$	
	°R	K	$T_K = T_R/1.8$	
Thermal conductivity	Btu-ft/hr-ft^2-°R	W/(m · K)	1.730 735	E + 00
Time	hr	s	3.6 [Note (1)]	E + 03
	min	s	6 [Note (1)]	E + 01
Torque	lbf-in.	N · m	1.129 848	E + 01
	lbf-ft	N · m	1.355 818	E + 00
Velocity	ft/hr	m/s	8.466 667	E − 05
	ft/min	m/s	5.08 [Note (1)]	E − 03
	ft/sec	m/s	3.048 [Note (1)]	E − 01
	knot (international)	m/s	5.144 444	E − 01
	mile (U.S.)/hr	m/s	4.470 4 [Note (1)]	E − 01

Table 2-3.1-1 Conversions to SI (Metric) Units (Cont'd)

Quantity	Conversion		Multiplication Factor	
	From	To		
Viscosity, dynamic	centipoise	Pa · s	1 [Note (1)]	E – 03
	poise	Pa · s	1 [Note (1)]	E – 01
	lbm/ft-sec	Pa · s	1.488 164	E + 00
	lbf-sec/ft^2	Pa · s	4.788 026	E + 01
	slug/ft-sec	Pa · s	4.788 026	E + 01
Viscosity, kinematic	centistoke	m^2/s	1 [Note (1)]	E – 06
	stoke	m^2/s	1 [Note (1)]	E – 04
	ft^2/sec	m^2/s	9.290 304	E – 02
Volume	gallon (U.S. liquid)	m^3	3.785 412	E – 03
	ft ^{3}	m^3	2.831 685	E – 02
	in^3	m^3	1.638 706	E – 05
	liter	m^3	1 [Note (1)]	E – 03

GENERAL NOTE: The factors are written as a number greater than one and less than ten with six decimal places. The number is followed by the letter E (for exponent), a plus or minus symbol, and two digits that indicate the power of 10 by which the number must be multiplied to obtain the correct value. For example:

3.785 412 E – 03 is 3.785 412 × 10^{-3} or 0.003 785 412

NOTE:

(1) Exact relationship in terms of the base units.

Perry, Chilton, Kilpatrick. *Perry's Chemical Engineer's Handbook.* New York: McGraw-Hill; 1984.

Sea Water Properties From Reproduced Charts. Contract No. 14-30-2639. Washington, D. C.: Office of Saline Water, U.S. Dept. of Interior; 1930.

Tube Properties: HEI Standards for Steam Surface Condensers, 8th edition. Cleveland: Heat Exchange Institute; 1984.

Table 2-3.1-2 Conversion Factors for Pressure (Force/Area)

To obtain → / Multiply, by ↓	atm	bar	$\frac{lbf}{in.^2}$	in. Hg (0°C)	ft H_2O (20°C)	mmHg (0°C)	$\frac{kp}{cm^2}$	kPa
atm	1	1.013 25	$\frac{1\,013\,250 \times 2.54^2}{980.665 \times 453.592\,37} = 14.695\,948\,8$	$\frac{1\,013\,250/980.665}{13.595\,088\,9 \times 2.54} = 29.921\,280\,0$	$\frac{1\,013\,250/980.665}{0.998\,278\,282 \times 30.48} = 33.957\,002\,9$	$\frac{10\,132\,500/980.665}{13.595\,088\,9} = 760.000\,512$	$\frac{1.013\,25}{0.980\,665} = 1.033\,227\,45$	101.325
bar	$\frac{1.0}{1.013\,25} = 0.986\,923\,267$	1	$\frac{2.54^2 \times 10^6}{980.665 \times 453.592\,37} = 14.503\,773\,8$	$\frac{10^6/980.665}{13.595\,088\,9 \times 2.54} = 29.530\,007\,4$	$\frac{10^6/980.665}{0.998\,278\,282 \times 30.48} = 33.512\,956\,2$	$\frac{10^7/980\,665}{13.595\,088\,9} = 750.062\,188$	$\frac{10^3}{980.665} = 1.019\,716\,21$	100
$\frac{lbf}{in.^2}$	$\frac{980.665 \times 453.592\,37}{1\,013\,250 \times 2.54^2} = 0.068\,045\,963\,9$	$\frac{980.665 \times 453.592\,37}{2.54^2 \times 10^6} = 0.068\,947\,572\,9$	1	$\frac{453.592\,37/2.54^3}{13.5950889} = 2.036\,022\,34$	$\frac{453.592\,37/2.54^3}{0.998\,278\,282 \times 12} = 2.310\,636\,99$	$\frac{453.592\,37 \times 10}{13.595\,088\,9 \times 2.54^2} = 51.714\,967\,4$	$\frac{453.592\,37}{2.54^2 \times 10^3} = 0.070\,306\,958\,0$	$\frac{980.665 \times 453.592\,37}{2.54^2 \times 10^4} = 6.894\,757\,29$
in. Hg (0°C)	$\frac{13.595\,088\,9 \times 2.54}{1\,013\,250/980.665} = 0.033\,421\,030\,1$	$\frac{13.595\,088\,9 \times 2.54}{10^6/980.665} = 0.033\,863\,858\,8$	$\frac{13.595\,088\,9 \times 2.54^3}{453.592\,37} = 0.491\,153\,746$	1	$\frac{13.595\,088\,9}{0.998\,278\,282 \times 12} = 1.134\,878\,01$	25.4	$\frac{13.595\,088\,9 \times 2.54}{10^3} = 0.034\,531\,525\,8$	$\frac{13.595\,088\,9 \times 2.54}{10^4/980.665} = 3.386\,385\,88$
ft H_2O (20°C)[1]	$\frac{0.998\,278\,282 \times 30.48}{1\,013\,250/980.665} = 0.029\,449\,006\,6$	$\frac{0.998\,278\,282 \times 30.48}{10^6/980.665} = 0.029\,839\,205\,9$	$\frac{0.998\,278\,282 \times 12}{453.592\,37/2.54^3} = 0.432\,781\,092$	$\frac{0.998278282 \times 12}{13.595\,088\,9} = 0.881\,151\,971$	1	$\frac{9.982\,782\,82 \times 30.48}{13.595\,088\,9} = 22.381\,260\,1$	$\frac{0.998\,278\,28 \times 30.48}{10^3} = 0.030\,427\,522\,0$	$\frac{0.998\,278\,28 \times 30.48}{10^4/980.665} = 2.983\,920\,59$
mm Hg (0°C)	$\frac{13.595\,088\,9}{10\,132\,500/980.665} = 0.001\,315\,788\,59$	$\frac{13.595\,088\,9}{10^7/980.665} = 0.001\,333\,222\,79$	$\frac{13.595\,088\,9 \times 2.54^2}{453.592\,37 \times 10} = 0.019\,336\,761\,7$	$\frac{1.0}{25.4} = 0.039\,370\,078\,7$	$\frac{13.595\,088\,9}{9.982\,782\,82 \times 30.48} = 0.044\,680\,236\,8$	1	$13.595\,088\,9 \times 10^{-4} = 0.001\,359\,508\,89$	$\frac{13.595\,088\,9}{10^5/980.665} = 0.133\,322\,279$
$\frac{kp}{cm^2}$	$\frac{980.665}{1\,013.25} = 0.967\,841\,105$	0.980 665	$\frac{2.54^2 \times 10^3}{453.592\,37} = 14.223\,343\,3$	$\frac{10^3}{13.595\,088\,9 \times 2.54} = 28.959\,044\,7$	$\frac{10^3}{0.998\,278\,282 \times 30.48} = 32.864\,983\,2$	$\frac{10^4}{13.595\,088\,9} = 735.559\,736$	1	$\frac{9.806\,65}{10^{-1}} = 98.066\,5$
kPa	$\frac{1.0}{101.325} = 0.009\,869\,232\,67$	0.01	$\frac{2.54^2 \times 10^4}{980.665 \times 453.592\,37} = 0.145\,037\,738$	$\frac{10^4/980.665}{13.595\,0889 \times 2.54} = 0.295\,300\,074$	$\frac{10^4/980.665}{0.998\,278\,282 \times 30.48} = 0.335\,129\,562$	$\frac{10^5/980.665}{13.595\,088\,9} = 7.500\,621\,88$	$\frac{0.1}{9.806\,65} = 0.010\,197\,162$	1

Example: 1 bar = 1 bar × 0.986 923 267 atm/bar = 0.986 923 267 atm = (1/1.013 25) atm

From definitions: 1 lbf = 0.453 592 37 kp (kilopond = kgf) = 4.448 221 161 N; 1Pa = $1N/m^2$

Table 2-3.1-3 Conversion Factors for Specific Volume (Volume/Mass)

To obtain → / Multiply, by ↓ ↘	$\frac{ft^3}{lbm}$	$\frac{in.^3}{lbm}$	$\frac{U.S.\ gal}{lbm}$	$\frac{liter}{kg}$	$\frac{m^3}{kg}$
$\frac{ft^3}{lbm}$	1	1 728	$\frac{1\ 728}{231}$ = 7.480 519 48	$\frac{30.48^3}{453.592\ 37}$ = 62.427 960 6	$\frac{30.48^3 \times 10^{-6}}{0.453\ 592\ 37}$ = 0.062 427 960 6
$\frac{in^3}{lbm}$	$\frac{1.0}{1\ 728}$ = 0.000 578 703 704	1	$\frac{1.0}{231}$ = 0.004 329 004 33	$\frac{2.54^3}{453.592\ 37}$ = 0.036 127 292 0	$\frac{2.54^3 \times 10^{-6}}{0.453\ 592\ 37}$ = 0.000 036 127 292
$\frac{U.S.\ gal}{lbm}$	$\frac{231}{1\ 728}$ = 0.133 680 556	231	1	$\frac{231 \times 2.54^3}{453.592\ 37}$ = 8.345 404 45	$\frac{231 \times 2.54^3 \times 10^{-6}}{0.453\ 592\ 37}$ = 0.008 345 404 45
$\frac{liter}{kg}$	$\frac{453.592\ 37}{30.48^3}$ = 0.016 018 463 4	$\frac{453.592\ 37}{2.54^3}$ = 27.679 904 7	$\frac{453.592\ 37}{231 \times 2.54^3}$ = 0.119 826 427	1	0.001
$\frac{m^3}{kg}$ [Note (1)]	$\frac{0.453\ 592\ 37}{30.48^3 \times 10^{-6}}$ = 16.018 463 4	$\frac{0.453\ 592\ 37}{2.54^3 \times 10^{-6}}$ = 27 679.904 7	$\frac{0.453\ 592\ 37}{231 \times 2.54^3 \times 10^{-6}}$ = 119.826 427	1 000	1

GENERAL NOTE: All values given in the rational fractions are exact except 1 U.S. gal = 231 $in.^3$ (NBS Misc. Pub. 233 P5).

Example: 1 U.S. gal/lbm = 0.133 680 556 ft^3/lbm

NOTE:

(1) SI units for ASME use.

Table 2-3.1-4 Conversion Factors for Specific Enthalpy and Specific Energy (Energy/Mass)

To obtain → / Multiply, by ↓ ↘	$\frac{Btu}{lbm}$	$\frac{ft \times lbf}{lbm}$	$\frac{hp \times hr}{lbm}$	$\frac{lbf/in.^2}{lbm/ft^3}$	$\frac{kp \times m}{g}$	$\frac{kcal}{g}$	$\frac{kJ}{kg}$
$\frac{Btu}{lbm}$	1	$\frac{2.326 \times 10^7}{980.665 \times 30.48} = 778.169\ 262$	$\frac{2.326}{980.665 \times 30.48 \times 0.198} = 3.930\ 147\ 79 \times 10^{-4}$	$\frac{2.326 \times 10^7}{980.665 \times 30.48 \times 144} = 5.403\ 953\ 21$	$\frac{2.326}{9.806\ 65} = 0.237\ 185\ 991$	$\frac{2.326}{4\ 186.8} = 5.555\ 555\ 6 \times 10^{-4}$	2.326
$\frac{ft \times lbf}{lbm}$	$\frac{980.665 \times 30.48}{2.326 \times 10^7} = 0.001\ 285\ 067\ 46$	1	$\frac{1.0}{1\ 980\ 000} = 5.050\ 505\ 05 \times 10^{-7}$	$\frac{1.0}{144} = 0.006\ 944\ 444\ 44$	$30.48 \times 10^{-5} = 0.000\ 304\ 8$	$\frac{980.665 \times 30.48}{4\ 186.8 \times 10^7} = 7.139\ 263\ 69 \times 10^{-7}$	$980.665 \times 30.48 \times 10^{-7} = 0.002\ 989\ 066\ 920$
$\frac{hp \times hr}{lbm}$	$\frac{980.665 \times 30.48 \times 0.198}{2.326} = 2\ 544.433\ 58$	1 980 000	1	$\frac{1\ 980\ 000}{144} = 13\ 750$	$30.48 \times 19.8 = 603.504$	$\frac{980.665 \times 30.48}{4\ 186.8/0.198} = 1.413\ 574\ 21$	$\frac{980.665 \times 30.48 \times 198}{1000} = 5\ 918.352\ 50$
$\frac{lbf/in^2}{lbm/ft^3}$	$\frac{980.665 \times 30.48 \times 144}{2.326 \times 10^7} = 0.185\ 049\ 715$	144	$\frac{144}{1\ 980\ 000} = 7.272\ 727\ 27 \times 10^{-5}$	1	$30.48 \times 144 \times 10^{-5} = 0.043\ 891\ 2$	$\frac{980.665 \times 30.48 \times 144}{4\ 186.8 \times 10^7} = 1.028\ 053\ 97 \times 10^{-4}$	$\frac{980.665 \times 30.48 \times 144}{10^7} = 0.430\ 425\ 636$
$\frac{kp \times m}{g}$	$\frac{9.806\ 65}{2.326} = 4.216\ 100\ 60$	$\frac{10^5}{30.48} = 3\ 280.839\ 90$	$\frac{1.0}{30.48 \times 19.8} = 0.001\ 656\ 989\ 85$	$\frac{10^5}{30.48 \times 144} = 22.783\ 610\ 4$	1	$\frac{9.806\ 65}{4\ 186.8} = 0.002\ 342\ 278\ 11$	9.806 65
$\frac{kcal}{g}$	$\frac{4\ 186.8}{2.326} = 1800$	$\frac{4\ 186.8 \times 10^7}{980.665 \times 30.48} = 1\ 400\ 704.67$	$\frac{4\ 186.8 \times 10^3}{980.665 \times 30.48 \times 198} = 0.707\ 426\ 602$	$\frac{4\ 186.8 \times 10^7}{980.665 \times 30.48 \times 144} = 9\ 727.115\ 78$	$\frac{4\ 186.8}{9.806\ 65} = 426.934\ 784$	1	4 186.8
$\frac{kJ}{kg}$	$\frac{1.0}{2.326} = 0.429\ 922\ 614$	$\frac{10^7}{980.665 \times 30.48} = 334.552\ 563$	$\frac{10^3}{980.665 \times 30.48 \times 198} = 1.689\ 659\ 41 \times 10^{-4}$	$\frac{10^7}{980.665 \times 30.48 \times 144} = 2.323\ 281\ 69$	$\frac{1.0}{9.806\ 65} = 0.101\ 971\ 621$	$\frac{1.0}{4\ 186.8} = 2.388\ 458\ 97 \times 10^{-4}$	1

GENERAL NOTE: All values given in the rational fractions are exact except 1hp = 550 ft-lbf/sec = 1,980,000 ft-lbf/hr.

Example: $1\ \frac{Btu}{lbm} = 1kN{\cdot}m\ \frac{1Btu}{lbm} \times 778.169\ 262\ \frac{ft \times lbf/lbm}{Btu/lbm} = 778.169\ 262\ \frac{ft \times lbf}{lbm}$

From definitions: $1\ \frac{Joule}{g} = 1\ \frac{J}{g} = 10^7\ \frac{erg}{g} = 10^7\ \frac{dyne{\cdot}cm}{g} = 10^3\ \frac{J}{kg} = 1\ \frac{kW{\cdot}sec}{kg} = 10\ \frac{bar{\cdot}cm^3}{g}$

$1kJ = 1/(0.45359237 \times 2.326) = 0.947817120$ Btu; $1\ kcal = \frac{1.8}{0.45359237} = 3.96832072$ Btu

Table 2-3.1-5 Conversion Factors for Specific Entropy, Specific Heat, and Gas Constant [Energy/(Mass × Temperature)]

To obtain → / Multiply, by ↓	$\frac{Btu}{lbm \times R}$	$\frac{ft \times lbf}{lbm \times R}$	$\frac{kw \times hr}{lbm \times R}$	$\frac{bar \times cm^3}{g \times K}$	$\frac{kcal}{g \times K}$	$\frac{kp \times m}{g \times K}$	$\frac{kJ}{kg \times K}$
$\frac{Btu}{lbm \times R}$	1	$\frac{2.326 \times 10^7}{980.665 \times 30.48}$ = 778.169 262	$\frac{2.326 \times 453.592\ 37}{3\ 600\ 000}$ = 0.000 293 071 070	41.868	0.001	$\frac{4.186\ 8}{9.806\ 65}$ = 0.426 934 784	4.186 8
$\frac{ft \times lbf}{lbm \times R}$	$\frac{980.665 \times 30.48}{2.326 \times 10^7}$ = 0.001 285 067 46	1	$\frac{453.592\ 37 \times 30.48}{3.6 \times 10^{13}/980.665}$ = $3.766\ 160\ 97 \times 10^{-7}$	$\frac{30.48 \times 980.665 \times 9/5}{10^6}$ = 0.053 803 204 6	$\frac{980.665 \times 30.48}{2\ 326 \times 10^7}$ = $1.285\ 067\ 46 \times 10^{-6}$	$30.48 \times 10^{-5} \times 9/5$ = 0.000 548 64	$\frac{980.665 \times 30.48 \times 10^{-7}}{5/9}$ = 0.005 380 320 46
$\frac{kw \times hr}{lbm \times R}$	$\frac{3\ 600\ 000}{2.326 \times 453.592\ 37}$ = 3 412.141 63	$\frac{3.6 \times 10^{13} / 980.665}{453.592\ 37 \times 30.48}$ = 2 655 223.73	1	$\frac{3.6 \times 10^7 \times 9/5}{453.592\ 37}$ = 142 859.546	$\frac{3\ 600\ 000}{2\ 326 \times 453.592\ 37}$ = 3.412 141 63	$\frac{3.6 \times 10^8 \times 9\ /\ 5}{980.665 \times 453.592\ 37}$ = 1 456.761 95	$\frac{3.6 \times 10^6 \times 9\ /\ 5}{453.592\ 37}$ = 14 285.954 6
$\frac{bar \times cm^3}{g \times K}$	$\frac{1.0}{41.868}$ = 0.023 884 589 7	$\frac{10^6}{30.48 \times 980.665 \times 9/5}$ = 18.586 253 5	$\frac{453.592\ 37}{3.6 \times 10^7 \times 9/5}$ = $6.999\ 882\ 25 \times 10^{-6}$	1	$\frac{1.0}{41\ 868}$ = $2.388\ 458\ 97 \times 10^{-5}$	$\frac{1.0}{98.066\ 5}$ = 0.010 197 1621	0.1
$\frac{kcal}{g \times K}$	1000	$\frac{2\ 326 \times 10^7}{980.665 \times 30.48}$ = 778 169.262	$\frac{2\ 326 \times 453.592\ 37}{3\ 600\ 000}$ = 0.293 071 070	41 868	1	$\frac{4\ 186.8}{9.806\ 65}$ = 426.934 784	4 186.8
$\frac{kp \times m}{g \times K}$	$\frac{9.806\ 65}{4.186\ 8}$ = 2.342 278 11	$\frac{10^5}{30.48 \times 9/5}$ = 1 822.688 83	$\frac{980.665 \times 453.592\ 37}{3.6 \times 10^8 \times 9/5}$ = 0.000 686 453 953	98.066 5	$\frac{9.806\ 65}{4\ 186.8}$ = 0.002 342 278 11	1	9.806 65
$\frac{kJ}{kg \times K}$	$\frac{1.0}{4.186\ 8}$ = 0.238 845 897	$\frac{10^7 \times 5/9}{980.665 \times 30.48}$ = 185.862 535	$\frac{453.592\ 37}{3.6 \times 10^6 \times 9/5}$ = $6.999\ 882\ 25 \times 10^{-5}$	10	$\frac{1.0}{4\ 186.8}$ = 0.000 238 845 897	$\frac{1.0}{9.806\ 65}$ = 0.101 971 621	1

GENERAL NOTE: All values given in the rational fractions are exact.

Example: 1 Btu / (lbm × R) = 778.169 262 ft × lbf / (lbm × R)

Table 2-3.1-6 Conversion Factors for Viscosity (Force × Time/Area ~ Mass/Length × Time)

To obtain → / Multiply by ↓	Pa × s	$\frac{\text{lbf} \times \text{sec}}{\text{ft}^2}$	$\frac{\text{lbm}}{\text{ft} \times \text{sec}}$	$\frac{\text{lbm}}{\text{hr} \times \text{ft}}$	$\frac{\text{g}}{\text{cm} \times \text{s}}$ (poise)	$\frac{\text{kg}}{\text{m} \times \text{s}}$
Pa × s	1	$\frac{(0.3048)^2}{9.80665 \times 0.453\,592\,37} = 0.020\,885\,434\,2$	$\frac{0.3048}{0.453\,592\,37} = 0.671\,968\,975$	$\frac{0.3048 \times 3600}{0.453\,592\,37} = 2419.088\,31$	10	1
$\frac{\text{lbf} \times \text{sec}}{\text{ft}^2}$	$\frac{9.806\,65 \times 0.453\,592\,37}{(0.3048)^2} = 47.880\,259\,0$	1	$\frac{980.665}{30.48} = 32.174\,048\,6$	$\frac{980.665 \times 3\,600}{30.48} = 115\,826.575$	$\frac{980.665 \times 453.592\,37}{30.48^2} = 478.802\,590$	$\frac{980.665 \times 453.592\,37}{10 \times 30.48^2} = 47.880\,259\,0$
$\frac{\text{lbm}}{\text{ft} \times \text{sec}}$	$\frac{0.453\,592\,37}{0.3048} = 1.488\,163\,94$	$\frac{30.48}{980.665} = 0.031\,080\,950\,2$	1	3 600	$\frac{453.592\,37}{30.48} = 14.881\,639\,4$	$\frac{453.592\,37}{304.8} = 1.488\,163\,94$
$\frac{\text{lbm}}{\text{hr} \times \text{ft}}$	$\frac{0.453\,592\,37}{0.3048 \times 3600} = 0.413\,378\,873 \times 10^{-3}$	$\frac{30.48}{980.665 \times 3\,600} = 8.633\,597\,27 \times 10^{-6}$	$\frac{1.0}{3\,600} = 0.000\,277\,777\,778$	1	$\frac{453.592\,37}{30.48 \times 3\,600} = 0.004\,133\,788\,73$	$\frac{453.592\,37}{304.8 \times 3\,600} = 0.000\,413\,378\,873$
$\frac{\text{g}}{\text{cm} \times \text{s}}$ (poise)	0.1	$\frac{30.48^2}{980.665 \times 453.592\,37} = 0.002\,088\,543\,42$	$\frac{30.48}{453.592\,37} = 0.067\,196\,897\,5$	$\frac{3\,600 \times 30.48}{453.592\,37} = 241.908\,831$	1	0.1
$\frac{\text{kg}}{\text{m} \times \text{s}}$	1	$\frac{10 \times 30.48^2}{980.665 \times 453.592\,37} = 0.020\,885\,434\,2$	$\frac{304.8}{453.592\,37} = 0.671\,968\,975$	$\frac{10 \times 3\,600 \times 30.48}{453.592\,37} = 2\,419.088\,31$	10	1

GENERAL NOTE: All values given in the rational fractions are exact.

Example: 1 lbf × sec/ft^2 = 32.174 048 6 lbm/(ft × sec)

From definitions: 1 poise = 1 P = 1 g/cm × s = 1 dyne × s/cm^2 = 0.1 kg/m × s = 0.1 N × s/m^2 = 0.1 Pa × s

Table 2-3.1-7 Conversion Factors for Kinematic Viscosity (Area/Time)

To obtain → / Multiply, by ↓	$\frac{m^2}{s}$ [Note (1)]	$\frac{ft^2}{sec}$	$\frac{cm^2}{s}$ (stoke)	$\frac{cm^2}{hr}$	$\frac{m^2}{hr}$
$\frac{m^2}{s}$ [Note (1)]	1	$\frac{1.0}{(0.3048)^2} = 10.763\ 910\ 4$	$(100)^2 = 10\ 000$	$(100)^2 \times 3\ 600 = 36 \times 10^6$	3 600
$\frac{ft^2}{sec}$	$(0.3048)^2 = 0.092\ 903\ 04$	1	$(30.48)^2 = 929.030\ 4$	$(30.48)^2 \times 3\ 600 = 3\ 344\ 509.440\ 000$	$(0.304\ 8)^2 \times 3\ 600 = 334.450\ 944\ 000$
$\frac{cm^2}{s}$ (stoke)	$\frac{1.0}{(100)^2} = 10^{-4}$	$\frac{1.0}{(30.48)^2} = 0.001\ 076\ 391\ 04$	1	3 600	$\frac{3\ 600}{(100)^2} = 0.36$
$\frac{cm^2}{hr}$	$\frac{1.0}{(100)^2 \times 3\ 600} = 27.777\ 777\ 8 \times 10^{-9}$	$\frac{1.0}{(30.48)^2 \times 3\ 600} = 0.298\ 997\ 512 \times 10^{-6}$	$\frac{1.0}{3\ 600} = 0.000\ 277\ 777\ 778$	1	$\frac{1.0}{(100)^2} = 0.000\ 1$
$\frac{m^2}{hr}$	$\frac{1.0}{3\ 600} = 277.777\ 778 \times 10^{-6}$	$\frac{1.0}{(0.3048)^2 \times 3\ 600} = 2.989\ 975\ 12 \times 10^{-3}$	$\frac{(100)^2}{3\ 600} = 2.777\ 777\ 78$	$(100)^2 = 10\ 000$	1

GENERAL NOTE: All values given in the rational fractions are exact.

Example: 1 $ft^2/sec = 3600\ ft^2/hr$

NOTE:
(1) SI units for ASME use.

Table 2-3.1-8 Conversion Factors for Thermal Conductivity (Energy/Time × Length × Temperature Difference ~ Power/Length × Temperature Difference)

To obtain → / Multiply, by ↓ ↘	$\frac{Btu}{hr \times ft \times F}$	$\frac{ft \times lbf}{hr \times ft \times F} = \frac{lbf}{hr \times F}$	$\frac{W}{ft \times F}$	$\frac{W}{m \times C}$	$\frac{kp \times m}{hr \times m \times C} = \frac{kp}{hr \times C}$	$\frac{cal}{sec \times cm \times C}$	$\frac{kcal}{hr \times m \times C}$
$\frac{Btu}{hr \times ft \times F}$	1	$\frac{2.326 \times 10^7}{980.665 \times 30.48}$ = 778.169 262	$\frac{2.326 \times 453.592\ 37}{3\ 600}$ = 0.293 071 070	$\frac{4.186\ 8 \times 453.592\ 37}{3\ 600 \times 0.304\ 8}$ = 1.730 734 67	$\frac{4.186\ 8 \times 453.592\ 37}{980.665 \times 30.48 \times 10^{-4}}$ = 635.348 952	$\frac{453.592\ 37}{3\ 600 \times 30.48}$ = 0.004 133 788 73	$\frac{453.592\ 37}{10 \times 30.48}$ = 1.488 163 94
$\frac{ft \times lbf}{hr \times ft \times F}$	$\frac{980.665 \times 30.48}{2.326 \times 10^7}$ = 0.001 285 067 46	1	$\frac{980.665 \times 453.592\ 37}{3\ 600 \times 10^7/30.48}$ = 0.000 376 616 097	$\frac{980.665 \times 453.592\ 37}{3\ 600 \times 10^5 \times 5/9}$ = 0.002 224 110 81	$\frac{453.592\ 37 \times 9/5}{1\ 000}$ = 0.816 466 266 000	$\frac{980.665 \times 453.592\ 37}{3\ 600 \times 2.326 \times 10^7}$ = 5.312 197 40 × 10^{-6}	$\frac{980.665 \times 453.592\ 37}{2.326 \times 10^8}$ = 0.001 912 391 06
$\frac{W}{ft \times F}$	$\frac{3\ 600}{2.326 \times 453.592\ 37}$ = 3.412 141 63	$\frac{3\ 600 \times 10^7\ /\ 30.48}{980.665 \times 453.592\ 37}$ = 2 655.223 74	1	$\frac{9/5}{0.304\ 8}$ = 5.905 511 81	$\frac{3\ 600 \times 10^4 \times 9/5}{980.665 \times 30.48}$ = 2 167.900 61	$\frac{1.0}{30.48 \times 2.326}$ = 0.014 105 072 6	$\frac{360}{30.48 \times 2.326}$ = 5.077 826 15
$\frac{W}{m \times C}$	$\frac{3\ 600 \times 0.304\ 8}{4.186\ 8 \times 453.592\ 37}$ = 0.577 789 316	$\frac{3\ 600 \times 10^5 \times 5/9}{980.665 \times 453.592\ 37}$ = 449.617 886	0.304 8 × 5/9 = 0.169 333 333	1	$\frac{3\ 600 \times 100}{980.665}$ = 367.097 837	$\frac{1.0}{418.68}$ = 0.002 388 458 97	$\frac{360}{418.68}$ = 0.859 845 228
$\frac{kp \times m}{hr \times m \times C}$	$\frac{980.665 \times 30.48 \times 10^{-4}}{4.186\ 8 \times 453.592\ 37}$ = 0.001 573 938 22	$\frac{10^3 \times 5/9}{453.592\ 37}$ = 1.224 790 35	$\frac{980.665 \times 30.48 \times 5/9}{3\ 600 \times 10^4}$ = 0.000 461 275 759	$\frac{980.665}{3\ 600 \times 100}$ = 0.002 724 069 44	1	$\frac{980.665}{3\ 600 \times 4.186\ 8 \times 10^4}$ = 6.506 328 09 × 10^{-6}	$\frac{980.665}{4.186\ 8 \times 10^5}$ = 0.002 342 278 11
$\frac{cal}{sec \times cm \times C}$	$\frac{3\ 600 \times 30.48}{453.592\ 37}$ = 241.908 831	$\frac{3\ 600 \times 2.326 \times 10^7}{980.665 \times 453.592\ 37}$ = 188 246.017	2.326 × 30.48 = 70.896 48	418.68	$\frac{3\ 600 \times 4.186\ 8 \times 10^4}{980.665}$ = 153 696.522	1	360
$\frac{kcal}{hr \times m \times C}$	$\frac{10 \times 30.48}{453.592\ 37}$ = 0.671 968 975	$\frac{2.326 \times 10^8}{980.665 \times 453.592\ 37}$ = 522.905 602	$\frac{2.326 \times 30.48}{360}$ = 0.196 934 667	$\frac{418.68}{360}$ = 1.163	$\frac{4.186\ 8 \times 10^5}{980.665}$ = 426.934 784	$\frac{1.0}{360}$ = 0.002 777 777 78	1

GENERAL NOTE: All values given in the rational fractions are exact.

Example: $1\ \frac{W}{ft \times F} = 1\ \frac{W}{ft \times F} \times 3.412\ 141\ 632\ \frac{Btu\ /\ (hr \times ft \times F)}{W\ /\ (ft \times F)} = 3.412\ 141\ 632\ \frac{Btu}{hr \times ft \times F}$

Table 2-4.2-1 Thermal Expansion Data for Selected Materials — SI Units

Material	Item	Temperature, °C											
		−200	−100	0	20	100	200	300	400	500	600	700	800
Carbon steel: carbon-moly steel low-chrome steels (through 3Cr)	$10^6\alpha$	9.04	9.90	10.73	10.89	11.53	12.28	12.97	13.60	14.14	14.58	14.92	15.14
	L_t/L_{20}	0.998 01	0.998 81	0.999 79	1.000 00	1.000 92	1.002 21	1.003 63	1.005 17	1.006 79	1.008 46	1.010 15	1.011 81
Intermediate alloy steels (5Cr–Mo through 9Cr–Mo)	$10^6\alpha$	8.46	9.36	10.15	10.29	10.84	11.43	11.95	12.41	12.81	13.17	13.51	13.83
	L_t/L_{20}	0.998 14	0.998 88	0.999 80	1.000 00	1.000 87	1.002 06	1.003 35	1.004 71	1.006 15	1.007 64	1.009 19	1.010 79
Austenitic stainless steels	$10^6\alpha$	14.70	15.53	16.22	16.35	16.80	17.28	17.68	18.02	18.34	18.64	18.96	19.31
	L_t/L_{20}	0.996 77	0.998 14	0.999 68	1.000 00	1.001 34	1.003 11	1.004 95	1.006 85	1.008 80	1.010 81	1.012 89	1.015 06
Straight chromium stainless steels (12Cr, 17Cr, and 27Cr)	$10^6\alpha$	7.73	8.53	9.26	9.39	9.90	10.47	10.98	11.41	11.77	12.08	12.32	12.51
	L_t/L_{20}	0.998 30	0.998 98	0.999 81	1.000 00	1.000 79	1.004 89	1.003 07	1.004 33	1.005 65	1.007 01	1.008 38	1.009 76
25Cr–20Ni	$10^6\alpha$	11.44	12.40	13.24	13.39	13.95	14.56	15.08	15.51	15.87	16.18	16.43	16.65
	L_t/L_{20}	0.997 48	0.998 51	0.999 74	1.000 00	1.001 12	1.002 62	1.004 22	1.005 89	1.007 62	1.009 38	1.011 17	1.012 99
Monel (67Ni–30Cu)	$10^6\alpha$	10.24	11.89	13.17	13.39	14.15	14.90	15.49	16.00	16.49	17.05	17.73	18.62
	L_t/L_{20}	0.997 75	0.998 57	0.999 74	1.000 00	1.001 13	1.002 68	1.004 34	1.006 08	1.007 92	1.009 89	1.012 06	1.014 52
Monel [66Ni–29(Cu–Al)]	$10^6\alpha$	9.84	11.36	12.57	12.78	13.53	14.29	14.93	15.50	16.06	16.68	17.42	18.33
	L_t/L_{20}	0.997 83	0.998 64	0.999 75	1.000 00	1.001 08	1.002 57	1.004 18	1.005 89	1.007 71	1.009 68	1.011 84	1.014 30
Aluminum	$10^6\alpha$	17.72	19.80	21.67	22.01	23.26	24.52	25.39	25.81	...	...	...	...
	L_t/L_{20}	0.996 10	0.997 62	0.999 57	1.000 00	1.001 86	1.004 41	1.007 11	1.009 81				
Gray cast iron	$10^6\alpha$	...	...	9.84	9.95	10.39	10.96	11.55	12.13	12.72	13.28	...	...
	L_t/L_{20}			0.999 80	1.000 00	1.000 83	1.001 97	1.003 23	1.004 61	1.006 10	1.007 70		
Bronze	$10^6\alpha$	14.87	16.10	17.06	17.22	17.80	18.35	18.77	19.09	19.36	19.62	19.91	...
	L_t/L_{20}	0.996 73	0.998 07	0.999 66	1.000 00	1.001 42	1.003 30	1.005 26	1.007 26	1.009 29	1.011 38	1.013 54	
Brass	$10^6\alpha$	14.57	15.62	16.59	16.77	17.50	18.35	19.16	19.93	20.66	21.38	22.08	...
	L_t/L_{20}	0.996 79	0.998 13	0.999 67	1.000 00	1.001 40	1.003 30	1.005 36	1.007 57	1.009 92	1.012 40	1.015 02	
Wrought Iron	$10^6\alpha$	10.19	11.44	12.40	12.56	13.13	13.69	14.14	14.54	14.95	15.42	...	...
	L_t/L_{20}	0.997 76	0.998 63	0.999 75	1.000 00	1.001 05	1.002 46	1.003 96	1.005 52	1.007 17	1.008 95		
Copper–nickel (70Cu–30Ni)	$10^6\alpha$	11.93	13.36	14.51	14.71	15.39	15.99	16.30	...	...	...	...	...
	L_t/L_{20}	0.997 37	0.998 40	0.999 71	1.000 00	1.001 23	1.002 88	1.004 56					

Table 2-4.2-1 Thermal Expansion Data for Selected Materials — SI Units (Cont'd)

Material	Item	Temperature, °C											
		−200	−100	0	20	100	200	300	400	500	600	700	800
Hastelloy B	$10^6\alpha$	...	...	8.90	9.28	10.69	12.25	13.56	14.64	15.48	16.09	16.47	16.62
	L_t/L_{20}			0.999 82	1.000 00	1.000 86	1.002 20	1.003 80	1.005 56	1.007 43	1.009 33	1.011 20	1.012 96
Hastelloy C	$10^6\alpha$	...	7.62	9.12	9.42	10.61	12.06	13.42	14.65	15.71	16.58	17.20	17.53
	L_t/L_{20}		0.999 09	0.999 82	1.000 00	1.000 85	1.002 17	1.003 76	1.005 57	1.007 54	1.009 61	1.011 69	1.013 67
Inconel X annealed	$10^6\alpha$	...	10.59	12.34	12.64	13.69	14.73	15.55	16.23	16.87	17.56	18.38	19.43
	L_t/L_{20}		0.998 73	0.999 75	1.000 00	1.001 10	1.002 65	1.004 35	1.006 17	1.008 10	1.010 18	1.012 50	1.015 15
Haynes Stellite 25 (L605)	$10^6\alpha$	...	...	7.54	8.16	10.27	12.24	13.58	14.46	15.00	15.36	15.67	16.08
	L_t/L_{20}			0.999 85	1.000 00	1.000 82	1.002 20	1.003 80	1.005 49	1.007 20	1.008 91	1.010 65	1.012 54
Copper (ASTM B 124, B 133, B 152)	$10^6\alpha$	...	...	16.18	16.38	17.13	17.98	18.76	19.51	20.27	21.09	21.99	23.02
	L_t/L_{20}			0.999 68	1.000 00	1.001 37	1.003 24	1.005 25	1.007 41	1.009 73	1.012 23	1.014 95	1.017 95
Beryllium copper 25 (ASTM B 194)	$10^6\alpha$	...	14.01	15.95	16.17	16.67	16.95	17.61	...	...	...	...	...
	L_t/L_{20}		0.998 32	0.999 68	1.000 00	1.001 33	1.003 05	1.004 93					
Titanium	$10^6\alpha$	7.91	8.12	8.36	8.41	8.62	8.90	9.18	9.44	9.68	9.88	10.02	10.10
	L_t/L_{20}	0.998 26	0.999 03	0.999 83	1.000 00	1.000 69	1.001 60	1.002 57	1.003 59	1.004 65	1.005 73	1.006 81	1.007 88
Tantalum	$10^6\alpha$	5.31	5.85	6.27	6.34	6.59	6.81	6.96	7.06	7.12	7.17	7.21	7.263 35
	L_t/L_{20}	0.998 83	0.999 30	0.999 87	1.000 00	1.000 53	1.001 23	1.001 95	1.002 68	1.003 42	1.004 16	1.004 90	1.005 67

GENERAL NOTE:

$$L_t/L_{20} = 1 + \alpha(t - 20)$$

where

L_t = length at temperature t in degrees centigrade
L_{20} = length at 20°C
α = mean coefficient of thermal expansion in going from 20°C to indicated temperature, mm/mm/°C

Table 2-4.2-2 Thermal Expansion Data for Selected Materials — U.S. Customary Units

Material	Item	Temperature, °F											
		−300	−200	−100	68	100	200	400	600	800	1000	1200	1400
Carbon steel: Carbon-moly steel low-chrome steels (through 3Cr)	$10^6\alpha$	5.10	5.36	5.62	6.05	6.13	6.37	6.84	7.26	7.64	7.95	8.20	8.37
	L_t/L_{68}	0.998 12	0.998 56	0.999 06	1.000 00	1.000 20	1.000 84	1.002 27	1.003 86	1.005 59	1.007 41	1.009 28	1.011 15
Intermediate alloy steels (5Cr–Mo through 9Cr–Mo)	$10^6\alpha$	4.78	5.06	5.32	5.72	5.79	6.00	6.36	6.68	6.95	7.20	7.41	7.61
	L_t/L_{68}	0.999 02	0.999 25	0.999 50	1.000 00	1.000 10	1.000 44	1.001 17	1.001 97	1.002 83	1.003 73	1.004 66	1.005 63
Austenitic stainless steels	$10^6\alpha$	8.24	8.50	8.74	9.08	9.14	9.31	9.61	9.85	10.06	10.25	10.44	10.65
	L_t/L_{68}	0.998 32	0.998 73	0.999 18	1.000 00	1.000 16	1.000 68	1.001 77	1.002 91	1.004 09	1.005 31	1.006 57	1.007 88
Straight chromium stainless steels (12Cr, 17Cr, and 27Cr)	$10^6\alpha$	4.37	4.62	4.85	5.22	5.28	5.48	5.83	6.14	6.40	6.61	6.78	6.91
	L_t/L_{68}	0.999 11	0.999 31	0.999 55	1.000 00	1.000 09	1.000 40	1.001 08	1.001 81	1.002 60	1.003 42	1.004 26	1.005 12
25Cr–20Ni	$10^6\alpha$	6.44	6.74	7.02	7.44	7.51	7.73	8.10	8.42	8.67	8.89	9.06	9.20
	L_t/L_{68}	0.998 68	0.999 00	0.999 34	1.000 00	1.000 13	1.000 57	1.001 49	1.002 49	1.003 53	1.004 60	1.005 70	1.006 81
Monel (67Ni–30Cu)	$10^6\alpha$	5.85	6.37	6.82	7.44	7.54	7.83	8.29	8.65	8.96	9.27	9.64	10.13
	L_t/L_{68}	0.998 80	0.999 05	0.999 36	1.000 00	1.000 13	1.000 57	1.001 53	1.002 56	1.003 64	1.004 80	1.006 07	1.007 50
Monel [66Ni–29(Cu–Al)]	$10^6\alpha$	5.61	6.09	6.51	7.10	7.20	7.48	7.96	8.35	8.69	9.05	9.46	9.97
	L_t/L_{68}	0.998 85	0.999 09	0.999 39	1.000 00	1.000 13	1.000 55	1.001 47	1.002 47	1.003 54	1.004 69	1.005 95	1.007 38
Aluminum	$10^6\alpha$	10.03	10.68	11.29	12.23	12.39	12.87	13.65	14.16	...	...	...	...
	L_t/L_{68}	0.997 95	0.998 41	0.998 95	1.000 00	1.000 22	1.000 94	1.002 52	1.004 18				
Gray cast iron	$10^6\alpha$	...	...	...	5.53	5.58	5.75	6.10	6.46	6.83	7.18	...	...
	L_t/L_{68}				1.000 00	1.000 10	1.000 42	1.001 13	1.001 91	1.002 78	1.003 72		
Bronze	$10^6\alpha$	8.38	8.76	9.10	9.57	9.65	9.86	10.21	10.46	10.65	10.81	10.98	...
	L_t/L_{68}	0.998 29	0.998 70	0.999 15	1.000 00	1.000 17	1.000 72	1.001 88	1.003 09	1.004 33	1.005 60	1.006 90	
Brass	$10^6\alpha$	8.19	8.51	8.82	9.32	9.41	9.69	10.21	10.71	11.18	11.63	12.07	...
	L_t/L_{68}	0.998 33	0.998 73	0.999 18	1.000 00	1.000 17	1.000 71	1.001 88	1.003 17	1.004 55	1.006 02	1.007 59	
Wrought Iron	$10^6\alpha$	5.78	6.17	6.51	6.98	7.05	7.27	7.62	7.89	8.14	8.40	...	...
	L_t/L_{68}	0.998 82	0.999 08	0.999 39	1.000 00	1.000 13	1.000 53	1.001 40	1.002 33	1.003 31	1.004 35		
Copper–nickel (70Cu–30Ni)	$10^6\alpha$	6.76	7.21	7.61	8.17	8.26	8.52	8.89	...	...	...	...	...
	L_t/L_{68}	0.998 62	0.998 93	0.999 29	1.000 00	1.000 15	1.000 62	1.001 64					

Table 2-4.2-2 Thermal Expansion Data for Selected Materials — U.S. Customary Units (Cont'd)

Material	Item	Temperature, °F											
		−300	−200	−100	68	100	200	400	600	800	1000	1200	1400
Hastelloy B	$10^6\alpha$	. . .	3.46	4.12	5.15	5.34	5.88	6.84	7.64	8.27	8.74	9.06	9.21
	L_t/L_{68}		0.999 49	0.999 62	1.000 00	1.000 09	1.000 43	1.001 26	1.002 26	1.003 36	1.004 53	1.005 70	1.006 82
Hastelloy C	$10^6\alpha$	. . .	4.00	4.46	5.24	5.38	5.84	6.73	7.57	8.31	8.93	9.40	9.69
	L_t/L_{68}		0.999 40	1.999 58	1.000 00	1.000 10	1.000 43	1.001 24	1.002 24	1.003 38	1.004 62	1.005 91	1.007 17
Inconel X annealed	$10^6\alpha$	. . .	5.55	6.17	7.02	7.16	7.56	8.21	8.70	9.11	9.51	9.96	10.54
	L_t/L_{68}		0.999 17	0.999 42	1.000 00	1.000 13	1.000 55	1.001 51	1.002 57	1.003 71	1.004 92	1.006 27	1.007 80
Haynes Stellite 25 (L605)	$10^6\alpha$	. . .	. . .	. . .	4.53	4.82	5.62	6.84	7.64	8.13	8.42	8.61	8.83
	L_t/L_{68}				1.000 00	1.000 09	1.000 41	1.001 26	1.002 26	1.003 31	1.004 36	1.005 42	1.006 54
Copper (ASTM B 124, B 133, B 152)	$10^6\alpha$	. . .	. . .	. . .	9.10	9.20	9.49	10.01	10.49	10.95	11.43	11.95	12.55
	L_t/L_{68}				1.000 00	1.000 16	1.000 70	1.001 85	1.003 10	1.004 45	1.005 92	1.007 52	1.009 29
Beryllium copper 25 (ASTM B 194)	$10^6\alpha$	6.01	7.28	8.16	8.98	9.07	9.25	9.43	9.89	. . .	. . .	. . .	. . .
	L_t/L_{68}	0.998 77	0.998 92	0.999 24	1.000 00	1.000 16	1.000 68	1.001 74	1.002 92				
Titanium	$10^6\alpha$	4.41	4.47	4.54	4.67	4.70	4.78	4.95	5.12	5.28	5.42	5.53	5.60
	L_t/L_{68}	0.999 10	0.999 33	0.999 58	1.000 00	1.000 08	1.000 35	1.000 91	1.001 51	1.002 15	1.002 81	1.003 48	1.004 14
Tantalum	$10^6\alpha$	3.00	3.17	3.32	3.52	3.56	3.65	3.79	3.88	3.93	3.97	3.99	4.020 93
	L_t/L_{68}	0.999 39	0.999 53	0.999 69	1.000 00	1.000 06	1.000 27	1.000 70	1.001 15	1.001 60	1.002 05	1.002 51	1.002 98

GENERAL NOTE:

$$L_t/L_{68} = 1 + \alpha(t - 68)$$

where

L_{68} = length at 68°F
L_t = length at temperature t in degrees fahrenheit
α = mean coefficient of thermal expansion in going from 68°F to indicated temperature, in./in./°F

Table 2-4.3 Coefficients for Thermal Expansion Equation in °C

Material	Coefficients				Data Source Reference
	a	*b*	*c*	*d*	
Carbon steel: carbon-moly steel	10.728 0	0.008 172 5	−1.695 1E−06	−2.037 4E−09	(a)
Intermediate alloy steels	10.150 0	0.007 338 0	−5.064 2E−06	2.058 0E−09	(a)
Austenitic stainless steels	16.224 0	0.006 307 6	−5.957 5E−06	3.609 8E−09	(a)
Straight chromium stainless steels	9.255 9	0.006 841 8	−3.845 1E−06	4.744 1E−09	(a)
25Cr–20Ni	13.237 0	0.007 726 4	−5.885 9E−06	1.952 9E−09	(a)
Monel(67Ni–30Cu)	13.172 0	0.011 153 0	−1.503 7E−05	1.201 2E−08	(a)
Monel [66Ni–29(Cu–Al)]	12.571 0	0.010 714 0	−1.256 6E−05	1.021 7E−08	(a)
Aluminum	21.672 0	0.017 401 0	−1.375 9E−05	−9.776 9E−09	(a)
Gray cast iron	9.839 5	0.005 353 0	1.569 9E−06	−1.540 4E−09	(a)
Bronze	17.059 0	0.008 427 9	−1.118 3E−05	7.092 0E−09	(a)
Brass	16.587 0	0.009 381 9	−3.127 9E−06	1.342 3E−09	(a)
Wrought iron	12.396 0	0.008 353 1	−1.146 7E−05	9.920 7E−09	(a)
Copper–nickel (70Cu–30Ni)	14.510 0	0.010 174 0	−1.370 5E−05	−9.622 3E−10	(a)
Hastelloy B	8.896 3	0.019 182 0	−1.223 2E−05	4.042 6E−10	(b)
Hastelloy C	9.123 4	0.015 018 0	−3.973 3E−07	−6.546 0E−09	(b)
Inconel X annealed	12.343 0	0.015 353 0	−2.006 9E−05	1.493 1E−08	(c)
Haynes Stellite 25(L605)	7.542 7	0.031 572 0	−4.530 1E−05	2.397 5E−08	(d)
Copper	16.178 0	0.010 221 0	−7.335 3E−06	6.560 4E−09	(e)
Beryllium copper 25	15.954 0	0.011 952 0	−6.142 9E−05	1.333 3E−07	(f)
Titanium	8.358 6	0.002 560 6	1.241 3E−06	−2.156 2E−09	(g)
Tantalum	6.273 7	0.003 642 9	−5.348 5E−06	2.926 5E−09	(h)

GENERAL NOTE: The equation for the coefficient of thermal expansion at temperature, T, °C, is

$$10^6\alpha = a + bT + cT^2 + dT^3$$

DATA SOURCE REFERENCES:

(a) ANSI/ASME B31.1-1986 Edition, Power Piping, Appendix B.

(b) Y. S. Touloukian et al. "Thermal Expansion of Metallic Elements — Alloys," *Thermophysical Properties of Matter,* Vol. 12, p. 1245, IF/Plenum Press, 1975.

(c) *American Institute of Physics Handbook,* 3rd Ed., p. 4-136, McGraw-Hill, 1975.

(d) *Reactor Handbook — Volume I — Materials,* 2nd Ed., p. 522, 1960.

(e) Y. S. Touloukian et al. "Thermal Expansion of Metallic Elements — Alloys," *Thermophysical Properties of Matter,* Vol. 12, p. 77, IF/Plenum Press, 1975.

(f) "Mechanical Properties of Metals and Alloys," NBS Circular C447, 12/1/43, p. 148.

(g) Beaton C. F. and G. F. Hewitt (Eds.). *Physical Property Data for the Design Engineer,* p. 386, Hemisphere Publishing Corp., 1989.

(h) *American Institute of Physics Handbook,* 3rd Ed., p. 4-131, McGraw-Hill, 1975.

Section 3
Differential Pressure Class Meters

3-0 NOMENCLATURE

Some symbols are also shown in para. 2-3 and are repeated here for convenience. Refer to this list for Sections 3 through 5; dimensions are L = length, T = time, M = mass, and θ = temperature.

A = cross-sectional area of pipe or of flow element, L^2
C = discharge coefficient of flow meter, dimensionless
C_P = specific heat at constant pressure, $L^2T^{-2}\theta^{-1}$
D = diameter of pipe, L
Eu = Euler number, dimensionless
L = ratio of location of a pressure to D, dimensionless
MW = molecular weight, M
P = pressure, $ML^{-1}T^{-2}$
Q = heat, L^2MT^{-2}
Re or R = Reynolds number, dimensionless
T = absolute temperature, θ
U = energy, L^2MT^{-2}
U = uncertainty, in units of measure
V = velocity, LT^{-1}
W = work, L^2MT^{-2}
d = diameter of flow element, sometimes called bore diameter, L
g_C = proportionality constant, see Table 3-1
g_L = local acceleration of gravity, LT^{-2}
l_1 or l_2 = dimension for spacing a pressure tap as measured from its centerline, L
n = units conversion factor for general equation of flow through a differential pressure class meter; see Table 3-1 for dimensions
q_m = mass flow, MT^{-1}
q_{m_c} = mass flow (compressible), MT^{-1}
q_{m_i} = mass flow (incompressible), MT^{-1}
q_{m_t} = mass flow (theoretically compressible), MT^{-1}
$q_{m_{ti}}$ = mass flow (theoretically incompressible), MT^{-1}
q_v = volumetric flow, L^3T^{-1}
r = pressure ratio, dimensionless
z = elevation, L
α_p = pipe material thermal expansion factor, θ^{-1}
α_{pe} = flow element material thermal expansion factor, θ^{-1}
β = ratio of bore to pipe diameters, d/D, dimensionless
Δ = finite difference operator, as in differential pressure ΔP
δ = calculus differential operator, as in change in heat δQ
ϵ = expansion factor correction for compressible fluids, dimensionless
= isentropic exponent, dimensionless
ρ = density, ML^{-3}
μ = absolute viscosity, $ML^{-1}T^{-1}$

Subscripts

D = based on pipe diameter
d = based on bore or throat diameter
meas = measured
1 = upstream location, cross-section, or conditions
2 = downstream location, cross-section, or conditions

3-1 GENERAL EQUATION FOR MASS FLOW RATE THROUGH A DIFFERENTIAL PRESSURE CLASS METER

(a) The general equation for mass flow is as follows:

$$q_m = n\frac{\pi}{4}d^2C\epsilon\sqrt{\frac{2\rho(\Delta P)g_C}{1-\beta^4}} \qquad (3\text{-}1.1)$$

Equation (3-1.1) is applied to flow calculations for all orifices, nozzles, and venturis described in Sections 4 through 6, and is valid both for liquids and for gases flowing at subsonic velocity.

(b) Values of n and g_c for commonly used combinations of units are shown in Table 3-1. SI units are the first set of units shown. The second set is from U.S. Engineering units, which are commonly used in the United States. The third set is U.S. Absolute Engineering units, which are less commonly used, but, similar to the SI units, derived by setting the proportionality constant equal to unity. Use of other units for any parameter(s) in the general equation is permissible, provided the n factor is correctly determined.

(c) If manometers are used to measure the differential pressure, then the acceleration of gravity g_L at the location of use must be taken into consideration. Refer to ASME PTC 19.2. When manometers are used, $P = \rho h(g_L/g_c)$, where h is the height of manometer fluid and the

Table 3-1 Values of Constants in the General Equation for Various Units

	Mass Flow Rate Units, q_m	Meter Geometry Units, d or D	Fluid Density Units, ρ	Differential Pressure Units, ΔP	Values of Constants	
					Proportionality Constant, g_c	Units Conversion Constant, n
(1)	$\frac{kg}{s}$	m	$\frac{kg}{m^3}$	Pa	$g_c \equiv 1.0$ dimensionless	$n \equiv 1.0 \left(\frac{kg}{m\text{-}s^2\text{-}Pa}\right)^{1/2}$
(2)	$\frac{lbm}{hr}$	in.	$\frac{lbm}{ft^3}$	$\frac{lbf}{in.^2}$	$g_c = 32.174\,048\,6 \frac{lbm\text{-}ft}{lbf - sec^2}$	$n \equiv 300.0 \frac{ft^2}{sec^2}\left(\frac{in.^2}{ft^2} \cdot \frac{sec^2}{hr^2}\right)^{1/2}$
(3)	$\frac{slugs}{sec}$	ft	$\frac{slug}{ft^3}$	$\frac{lbf}{ft^2}$	$g_c \equiv 1.0$ dimensionless	$n \equiv 1.0 \left(\frac{slug\text{-}ft}{lbf\text{-}sec^2}\right)^{1/2}$

density of the manometer fluid is corrected per ASME PTC 19.2.

(d) The development of the general equation follows.

3-2 BASIC PHYSICAL CONCEPTS USED IN THE DERIVATION OF THE GENERAL EQUATION FOR MASS FLOW

(a) The physical concepts and assumptions used for the derivation of Eq. (3-1.1) are well documented in the literature. The equation is derived from the principles of conservation of energy and mass between the upstream and downstream taps. Flow behavior and fluid properties are idealized, and errors introduced by these assumptions are corrected by the factors C and ϵ for accurate calculation of mass flow.

The coefficient of discharge, or discharge coefficient, C, corrects for the idealized theoretical assumptions of flow behavior made in the derivation of the flow equation.

The expansion factor, ϵ, corrects for the compressibility effects of a gas as it flows between 1 and 2.

(b) Energy Equation. Flow through a differential pressure meter is idealized as Newtonian steady state flow, with one-dimensional velocities across the flow areas.

$$\delta Q = \delta W + du + PdV + vdP + \frac{1}{g_C} VdV + \frac{g_L}{g_C} dz \qquad (3\text{-}2.1)$$

Each of the terms of Eq. (3-2.1) must be in consistent units of energy per unit mass.

Further idealizations are made by assuming that the flow through a differential pressure meter section is a reversible thermodynamic process in the absence of external work or heat.

$$0 = \frac{dP}{\rho} + \frac{VdV}{g_C} + \frac{g_L}{g_C} dz \qquad (3\text{-}2.2)$$

In those cases where installation in an inclined pipe is necessary, the elevation change between pressure taps $(z_2 - z_1)$ must be considered. The measured differential pressure is corrected for the difference in elevation of the pressure taps before the flow is calculated, so that the elevation term is always zero.

The integration of Eq. (3-2.2) depends further on whether the fluid is treated as incompressible or compressible.

(c) Conservation of Mass Equation. Under the assumptions of para. 3-2(b), conservation of mass is written in the form

$$q_m = \rho_1 V_1 A_1 = \rho_2 V_2 A_2 \qquad (3\text{-}2.3a)$$

or

$$V_1 = \frac{\rho_2}{\rho_1} \beta^2 V_2 \qquad (3\text{-}2.3b)$$

in any set of consistent units.

3-3 THEORETICAL FLOW RATE — LIQUID AS THE FLOWING FLUID

(a) For the special case where the flowing fluid is a liquid, or incompressible, integrating the energy equation [Eq.(3-2.2)] between the upstream tap and the downstream tap gives Bernoulli's equation.

$$\frac{P_1}{\rho} + \frac{V_1^2}{2g_C} + \frac{g_L}{g_C} z_1 = \frac{P_2}{\rho} + \frac{V_2^2}{2g_C} + \frac{g_L}{g_C} z_2 \qquad (3\text{-}3.1)$$

(b) Combining Eq. (3-3.1) with Eq. (3-2.3a) and applying $A_2 = \pi d^2/4$ gives the following theoretical flow rate:

$$q_{m_{ti}} = \frac{\pi}{4} d^2 \frac{1}{\sqrt{1 - \beta^4}} \sqrt{2\rho(\Delta P) g_C} \qquad (3\text{-}3.2)$$

(c) Equation (3-3.2) is equivalent to Eq. (3-1.1) before correction factors and units conversion are applied. It is the theoretical incompressible flow equation for the flow of fluids through differential pressure meters.

3-4 THEORETICAL FLOW RATE — GAS OR VAPOR AS THE FLOWING FLUID

(a) Assuming an ideal gas in an isentropic process,

$$r \equiv \frac{P_2}{P_1} = \left[\frac{\rho_2}{\rho_1}\right] = \left[\frac{T_2}{T_1}\right]^{\frac{}{-1}} \tag{3-4.1}$$

(b) Integrating the energy equation [Eq. (3-2.2)] for these conditions,

$$0 = \frac{}{-1}\left[\frac{P_2}{\rho_2} - \frac{P_1}{\rho_1}\right] + \left[\frac{V_2^2 - V_1^2}{2g_C}\right] \tag{3-4.2}$$

(c) Substituting Eq. (3-2.3b) to eliminate V_1 and Eq. (3-4.1), and from conservation of mass,

$$q_{m_{tc}} = \left(\frac{\pi}{4}d^2\right)\rho_2\left[\left(\frac{2g_C}{-1}\right)\left(\frac{P_1}{\rho_1}\right)\left(\frac{1 - r^{(\ -1)/}}{1 - \beta^4 r^{2/}}\right)\right]^{0.5} \tag{3-4.3}$$

(d) Equation (3-4.3) can be modified using $P_1 = \Delta P/(1 - r)$ and again by Eq. (3-4.1), and is written

$$q_{m_{tc}} = \frac{\pi}{4}d^2\frac{\sqrt{2\rho_1(\Delta P)g_C}}{\sqrt{1 - \beta^4}} \times \left[r^{2/}\left[\frac{}{-1}\right]\left[\frac{1 - r^{(\ -1)/}}{1 - r}\right]\left[\frac{1 - \beta^4}{1 - \beta^4 r^{2/}}\right]\right]^{0.5} \tag{3-4.4}$$

(e) Equation (3-4.4) is equivalent to Eq. (3-1.1) before correction factors and units conversion are applied and modified by the term in brackets. The bracketed term is the derived value of ϵ_1 for nozzles and venturis.

(f) The compressibility effects of flow through an orifice include sudden radial expansion. The minimum downstream pressure is, therefore, at a different location than that of the downstream pressure tap. Straightforward derivation of the values for ϵ to be used for orifices cannot be developed with the basic principles of this paragraph. The values for ϵ to be used for orifices are discussed in para. 3-8.

(g) Equation (3-4.4) is the theoretical compressible equation for subsonic flow of ideal, compressible fluids through differential pressure meters.

3-5 ERRORS INTRODUCED IN THEORETICAL MASS FLOW RATE BY IDEALIZED FLOW ASSUMPTIONS

The major reasons that q_{mti} and q_{mtc} must be corrected by the coefficient of discharge to achieve accurate measurement are as follows:

(a) In flowing from A_1 to A_2, the minimum cross-section of the flow stream does not coincide precisely with the bore or flow element area. This is particularly true for orifices.

(b) P_2 varies with pressure tap location. The correction to actual flow rate depends on pressure tap location, such as flange taps compared with corner taps.

(c) All static pressure taps exhibit an error in static pressure measurement.

(d) Velocity profiles are not uniform.

(e) In nozzles and venturis, there is some flow separation in the vicinity of the corner formed between the inlet pipe and nozzle face.

(f) No flow is frictionless or reversible.

3-6 DISCHARGE COEFFICIENT *C* IN THE INCOMPRESSIBLE FLUID EQUATION

(a) To correct errors introduced by the idealized flow assumptions built into the incompressible fluid equation, C is introduced and defined as

$$C \equiv \frac{q_{m_i}}{q_{m_{ti}}} \tag{3-6.1}$$

In practice, differential pressure meters are calibrated to determine C over a range of flows by means of liquid tests, usually water. The static weight/time technique is used to determine q_{mi}. A series of q_{mi} versus ΔP data is obtained during calibration, and, with q_{mti} defined by the hydraulic equation [Eq. (3-3.1)], C can be written as follows:

$$C \equiv \frac{q_{m_i}}{\frac{\pi}{4}d^2\frac{1}{\sqrt{1-\beta^4}}\sqrt{2\rho(\Delta P)g_C}} \tag{3-6.2}$$

(b) It has been found that, for a given meter type and size, C is a function of bore or pipe Reynolds number and β only. This can also be derived from dimensional analysis. Calibration data of different meters of the same type and size is extremely repeatable, provided that the meters are manufactured and installed in strict accordance with Sections 4, 5, and 7, including machining tolerances, dimensions, and straight length or flow conditioning requirements.

(c) Because the fluid properties that affect the discharge coefficient are inherently contained in Reynolds number, a water calibration of a given differential pressure device is applicable for any measured fluid without loss of accuracy. This includes gases, provided the corrections detailed in paras. 3-7 and 3-8 are made.

3-7 DISCHARGE COEFFICIENT *C* AND THE EXPANSION FACTOR ϵ FOR GASES

(a) For gases, C obtained by liquid calibration is modified by the expansion correction factor ϵ to account for

the effects of compressibility. For a given flow meter calibrated using liquid,

$$\epsilon \equiv \frac{q_{m_c}}{q_{m_i}} = \frac{q_{m_c}}{\frac{\pi}{4} d^2 C \frac{1}{\sqrt{1-\beta^4}} \sqrt{2\rho(\Delta P) g_C}} \quad (3\text{-}7.1)$$

(b) Hence, a water calibration used to determine C versus R_D for a differential pressure meter can also be used to measure gas flow if ϵ is known.

3-8 CALCULATION OF EXPANSION FACTOR ϵ

(a) The expansion factor for nozzles and venturi tubes, with density determined at the upstream pressure tap, has been derived [see Eq. (3-4.4)].

$$\epsilon_1 = \left[r^{2/} \left[\frac{}{-1} \right] \left[\frac{1 - r^{(-1)/}}{1 - r} \right] \left[\frac{1 - \beta^4}{1 - \beta^4 r^{2/}} \right] \right]^{0.5} \quad (3\text{-}8.1)$$

Equation (3-8.1) is valid for any gas or vapor for which is known.

(b) For orifices, abrupt radial as well as axial expansions take place, and the analytical derivation of Eq. (3-8.1) is invalid. It has been determined that the product of C and ϵ for subsonic flow orifices depends on R_d and the acoustic ratio $[\Delta P/(\ P_1)]$. Based on the data, if ρ_1 is the value of density used for the flow calculation, then

$$\epsilon_1 = 1 - (0.41 + 0.35\beta^4) \frac{\Delta P}{P_1} \quad (3\text{-}8.2)$$

(c) Equation (3-8.2) has been validated experimentally for air, natural gas, and steam only. However, it may also be used for any gas or vapor for which is known.

(d) Equations (3-8.1) and (3-8.2) are valid only for cases where $P_2/P_1 \geq 0.8$. Differential pressure meters must not be sized for compressible fluids such that the pressure ratio is lower than 0.8 to avoid Mach number effects.

(e) Temperature is measured downstream of the meter to avoid disturbing the flow profile. Static pressure is usually measured at the upstream tap. Temperature at the upstream tap T_1 can be calculated using Eq. (3-4.1) and the relationship $\Delta P = P_1 - P_2$. In most cases, T_1 may be assumed equal to T_2. Rigorous calculation is preferred if uncertainties introduced by this assumption are larger than the uncertainties introduced by the measurement of P_2, T_2, and ΔP, which is very rare.

(f) In some special cases when orifices are used, static pressure is measured at the downstream tap P_2 and density is determined from P_2. To derive ϵ_2, rewrite Eq. (3-7.1) in the following two valid formats:

$$q_{m_c} = \frac{\pi}{4} d^2 C \epsilon_1 \frac{1}{\sqrt{1-\beta^4}} \sqrt{2\rho_2(\Delta P) g_C} \quad (3\text{-}8.3)$$

$$q_{m_c} = \frac{\pi}{4} d^2 C \epsilon_2 \frac{1}{\sqrt{1-\beta^4}} \sqrt{2\rho_2(\Delta P) g_C} \quad (3\text{-}8.4)$$

By equating q_{mc} from Eqs. (3-8.3) and (3-8.4), it is seen that

$$\epsilon_2 = \epsilon_1 \sqrt{\frac{\rho_1}{\rho_2}} = \epsilon_1 \sqrt{\left(\frac{P_1}{P_2}\right)^{1/}} \quad (3\text{-}8.5)$$

P_1 may be obtained for use in Eq. (3-8.5) from $(\Delta P + P_2)$, and ρ_2 and ϵ_2 are then used in Eq. (3-1.1).

(g) Equations (3-8.3) and (3-8.4) can be rewritten in the appropriate units, based on the definition of ϵ given by Eq. (3-7.1), as the general Eq. (3-1.1). Thus, when the general equation is used for incompressible or liquid flows, $\epsilon \equiv 1.0$.

3-9 DETERMINING COEFFICIENT OF DISCHARGE FOR DIFFERENTIAL PRESSURE CLASS METERS

(a) It follows from paras. 3-6 through 3-8 that, for each type of differential pressure meter specified herein,

$$C = C\ (R_D, \beta, D) \quad (3\text{-}9.1)$$

Due to the repeatability of hydraulic laboratory calibration data for differential pressure meters of like type and size, relationships of C versus R_D are available for each type of meter described in Sections 4 and 5 over the range of allowable sizes and Reynolds numbers. This is based on the results of thousands of calibrations. The empirical C versus R_D relationship, along with the concomitant uncertainty of C, for each type of differential pressure meter is given in those sections.

(b) In Performance Test Code tests, application of the empirical formulations for discharge coefficient may be used for primary variables if uncertainty requirements are met. In some cases, it is preferable to perform a hydraulic laboratory calibration of a specific differential pressure meter to determine the specific C versus R_D number relationship for that meter.

(c) When a differential pressure flow meter is calibrated in a hydraulic laboratory to determine the C versus R_D relationship for that specific meter, the entire flow-metering section must be tested. This includes the upstream and downstream piping, manufactured such that the metering section meets the straight length and other dimensional requirements of Section 7. The calibration is not valid otherwise, except as a validation of the primary element only. Also, the metering run must be shipped as one piece, dirt and moisture free, and not taken apart at the flanges for shipping, installation, inspection, or any other reason for the hydraulic laboratory calibration to remain valid. If the primary element is removed for inspection, then the empirical formulation for discharge coefficient shall be used for the meter,

unless it could be reassembled precisely (i.e., dowel pins).

3-10 THERMAL EXPANSION/CONTRACTION OF PIPE AND PRIMARY ELEMENT

(a) In actual flow conditions, both d and D change from the measured values in the factory or laboratory because of thermal expansion or contraction. This occurs when the flowing fluid is at a different temperature than that at which the primary element and the pipe were measured.

$$d_{\text{actual}} = d_{\text{meas}} + \alpha_{pe} d_{\text{meas}} (T - T_{\text{meas}}) \quad (3\text{-}10.1)$$

$$D_{\text{actual}} = D_{\text{meas}} + \alpha_{p} D_{\text{meas}} (T - T_{\text{meas}}) \quad (3\text{-}10.2)$$

$$\beta_{\text{actual}} = \frac{d_{\text{actual}}}{D_{\text{actual}}} \quad (3\text{-}10.3)$$

(b) The actual values of d, D, and β are used to calculate q_m to account for thermal expansion or contraction. It is assumed that the flow element and pipe are at the same temperature as the flowing fluid. Either T_1 or T_2 may be used.

(c) For uncalibrated devices, 68°F (20°C) may be assumed if T_{meas} is unknown. For calibrated devices, T_{meas} is the fluid temperature of the calibration liquid if the calibration data were not corrected to standard temperature.

3-11 SELECTION AND RECOMMENDED USE OF DIFFERENTIAL PRESSURE CLASS METERS

The major considerations when selecting a differential pressure class meter are outlined in this paragraph.

3-11.1 Beta, Pipe Size, and Reynolds Number

Each meter described in Sections 4 and 5 has limiting values for these parameters. In selecting and sizing a meter, care must be taken to stay within these limits. If the metering run is laboratory calibrated, then it is sometimes necessary to extrapolate to higher Reynolds numbers from the calibrated data.

For example, if the chosen value of differential pressure for the design or expected flow rate in the sizing of an orifice results in a calculated β that exceeds the prescribed limits, it might be necessary to use a flow nozzle or venturi. Both devices have a higher capacity for the same size. Discharge coefficients for nozzles and venturi-metering runs are in the order of 1.0 compared to typical discharge coefficients of orifices in the order of 0.6.

In some cases, when there are sizing problems, pipe expanders or reducers are used at the flow section flanges so that the flow section diameter D is different from that of the surrounding process pipe. This is permissible provided the flow section, both upstream and downstream of the primary element, is of adequate length as prescribed herein.

3-11.2 Cost

Orifices are the least expensive devices; venturi meters are the costliest. It is important to consider also the costs of ancillary instrumentation, such as pressure and temperature instrumentation, installation costs, and costs to operation.

3-11.3 Uncertainty

The bias uncertainty of the empirical formulation of the discharge coefficient and the expansion factor in the general equation is given for each device in Sections 4 and 5, only if it is manufactured, installed, and used as specified herein. The results are summarized in Table 3-11.3.

Detailed calculation of overall uncertainty in flow measurement by differential pressure meters is discussed in Section 4. The uncertainty of the discharge coefficient usually is by far the most significant component of flow-measuring uncertainty, assuming that process and differential pressure instrumentation are satisfactory.

It is seen that, among differential pressure meters, orifice-metering runs are usually the choice in Performance Test Code work on an accuracy basis when using the empirical formulation for discharge coefficient.

Qualified hydraulic laboratories can usually calibrate within an uncertainty of 0.2%. Thus, with inherent curve-fitting inaccuracies, the uncertainty of the discharge coefficients of all meters may be made to be within approximately 0.3% or less with laboratory calibration, if the measured flow is within the Reynolds number range of the laboratory and the caveats of para. 3-9(c) are met.

The total measurement uncertainty of the flow contains components consisting of the uncertainty in the determination of fluid density, and of pressure, temperature, and differential pressure measurement uncertainty (see Section 4), in addition to the components caused by the uncertainty in C. For an orifice-metering run, the difference in the uncertainty of measured flow between meters with and without hydraulic calibration (about 0.3% maximum difference) is less significant than it is for nozzles or venturis. Due to higher uncertainty in the empirical formulation of discharge coefficient for nozzles and venturis, the improved accuracy of these meters when hydraulically calibrated is significant.

3-11.4 Overall Stagnation Pressure Loss

The overall nonrecoverable stagnation pressure loss due to the downstream portion of the primary element is significantly less for venturi tubes than for nozzle or orifice-metering runs because venturi tubes have a diffuser. Orifices have the highest nonrecoverable stagnation pressure loss relative to devices of the same β

Table 3-11.3
Summary Uncertainty of Discharge Coefficient and Expansion Factor

Location	Uncertainty of Discharge Coefficient, C	Uncertainty of Expansion Factor, ϵ, %
Orifice	0.6% for $\beta \le 0.6$ β% for $0.6 \le \beta \le 0.75$	$\frac{4\Delta P}{P_1}$
Venturi	0.7%	$\frac{(4 + 100\beta^8)\Delta P}{P_1}$
Nozzle, wall taps	1.0% for $0.2 \le \beta \le 0.8$	$\frac{2\Delta P}{P_1}$
Nozzle, throat taps	See Section 5 Normally calibrated	$\frac{2\Delta P}{P_1}$

and diameter. The nonrecoverable stagnation pressure losses for each device are given in Sections 4 and 5.

3-11.5 Installation

Orifices are the lightest weight and easiest to install or replace if laboratory calibrations are not required for a given line size. Venturi tubes have the heaviest weight for a given line size and require less upstream piping than nozzles and orifices.

3-12 RESTRICTIONS OF USE

The following restrictions must be met for proper use of these meters:

(a) The flow meter, flow section, pressure taps, and connecting tubing must be manufactured, installed, and used in strict accordance with the specifications herein.

(b) The pipe must be flowing full.

(c) Refer to pulsating flow in Section 7. The flow must be steady or changing very slowly as a function of time. Pulsations in the flow must be small compared with the total flow rate. The frequency of data collection must adequately cover several periods of unsteady flow.

(d) If the fluid does not remain in a single phase while passing through the meter, or if it has two phases when entering the meter, then it is beyond the scope of this Performance Test Code.

(e) If the fluid contains suspended particles, such as sand, flow measurement is beyond the scope of this Performance Test Code. Colloidal solutions with an index of dispersion not materially different from that of a homogenous liquid (e.g., milk) may be measured.

3-13 PROCEDURE FOR SIZING A DIFFERENTIAL PRESSURE CLASS METER

(a) When differential pressure class meters are being considered, they are sized to suit the user's needs. Usually the surrounding pipe diameter of the metering run and the fluid conditions over the expected flow range are known.

(b) One method of sizing the meter is to assume that the metering run pipe diameter D will be the same as that of the surrounding pipe, and to select a differential pressure to correspond to the maximum expected flow. All terms in Eq. (3-1.1) are known except C and d. Equation (3-1.1) may be used to solve for d by iteration or successive approximation.

(c) It can be preferable to specify the size of the meter, such as that corresponding to a β of 0.6 for an orifice-metering run (e.g., to optimize accuracy while minimizing pressure loss). All terms in Eq. (3-1.1) are then known except for differential pressure, which should be calculated by the user at maximum expected flow to ensure that the pressure ratio is within limits.

(d) The user must be careful when sizing a differential pressure class meter that the calculated β, d, and Reynolds number are within the specified ranges for each meter, as described in Sections 4 and 5. If any limitations are exceeded, then either a different size of the same meter type (d, D, or both) must be used or a different type of differential pressure class meter should be evaluated for the application. The metering run's length dimensions, per Section 7, must also be met and considered when sizing the meter.

(e) The values of d_{meas} and D_{meas} are the values of the diameters specified to the supplier (see para. 3-10).

3-14 FLOW CALCULATION PROCEDURE

(a) Equation (3-1.1) is used for all differential pressure class meters and is valid for both liquid and subsonic gas flow measurement.

(b) Used for gas flow, ϵ_1 is given by Eq. (3-8.1) for nozzles and venturi tubes; ϵ_1 and ϵ_2 are given by Eq. (3-8.2) and (3-8.5), respectively, for orifices; and, for liquid flows, $\epsilon_1 = \epsilon_2 \equiv 1.0$.

(c) Per para. 3-10, d and D are corrected to the fluid temperature of the measurement.

(d) The applicable fluid density is determined from pressure and temperature measurements, and, if the fluid is a mixture, such as natural gas, from the constituent analysis. Determine fluid viscosity to calculate Reynolds number. See Section 2 for references on fluid properties.

(e) All quantities in the general Eq. (3-1.1), except the discharge coefficient, are known once steps 3-14(b) through 3-14(d) have been completed. Because C depends on Reynolds number, which itself depends on flow rate, Eq. (3-1.1) is now solved by iteration. It is convenient to initially guess a discharge coefficient of $C = 1.0$ for nozzles and venturi tubes and 0.60 for orifices. The corresponding flow rate, and thus, Reynolds number, from the initially assumed discharge coefficient is then calculated. A reiteration is begun using the new value of the discharge coefficient as calculated from the new Reynolds number from the previous iteration.

(f) This process is continued until the difference between successive calculated flow rates is less than 2% of the estimated uncertainty of the measurement. For example, if the estimated uncertainty is 1.0%, the successive iterations must be within 0.02% of each other. It is also convenient to simply iterate until convergence to five significant digits is achieved. Usually convergence can be achieved with only two to four iterations.

(g) Another convenient algorithm is to initially guess the flow rate based on knowledge of the process, calculate the corresponding Reynolds number, and then find the corresponding discharge coefficient. Flow rate is then calculated with the new discharge coefficient and compared to the initial guess. Again, the iterative process is repeated until the same criterion as above is satisfied.

3-15 SAMPLE CALCULATION

A sample calculation of flow rate through an orifice-metering section, which is not calibrated in a hydraulic laboratory and given the appropriate process measurements and fluid constituent analysis, is shown for natural gas. The expected bias component of uncertainty in the flow measurement is 0.7%.

All fluid properties, materials properties, and procedures for calculation of fluid properties of mixtures are taken from the references in this Section and in Section 2.

U.S. Engineering units are used in this example.

(a) Orifice Geometry and Data

$D_{meas} = 7.981$ in.
$T_{meas} = 68°F$
$d_{meas} = 4.754$ in.

Taps: flange type
Orifice material: 316 stainless steel
Pipe material: carbon steel

Table 3-15 Natural Gas Analysis

Constituent	Mole Percent	Molar Mass
Nitrogen	0.656 3	28.013 4
Carbon dioxide	0.769 6	44.010 0
Methane	96.033 3	16.043 0
Ethane	1.965 8	30.043 0
Propane	0.328 3	44.097 0
N-butane	0.070 0	58.123 0
Isobutane	0.070 0	58.123 0
N-pentane	0.030 0	72.150 0
Isopentane	0.040 0	72.150 0
N-hexane	0.036 7	86.177 0
	100.00	Molecular weight = 16.828

Static pressure at the upstream side of the plate: 292.85 psia

Temperature at the downstream side of the plate: 53.56°F

Differential pressure: 1.4106 psi

For natural gas analysis, see Table 3-15.

(b) Temperature at the Upstream Side. Usually temperature at the upstream side of the orifice can be assumed to be equal to the temperature at the downstream side without significant loss of accuracy.

As an example for gases, is a function of the specific heat C_P and the molecular weight

$$= \frac{C_P}{C_P - \dfrac{1.986}{MW}} = \frac{0.5005}{0.5005 - \dfrac{1.986}{16.828}} = 1.309 \quad (3\text{-}15.1)$$

Assuming a pressure recovery of about 40% [ΔP to downstream thermowell is (0.6)(1.4106) = 0.846],

$$\frac{P_2}{P_1} = \left[\frac{T_2}{T_1}\right]^{(\ - 1)/}$$
$$\Rightarrow \frac{292.85 - 0.846}{292.85}$$
$$= \left[\frac{53.56 + 459.67}{T_1 + 459.67}\right]^{1.309/(1.309 \ - \ 1)}$$
$$\Rightarrow T_1 = 53.92°F \quad (3\text{-}15.2)$$

The estimated temperature difference is insignificant at 0.07% on an absolute basis.

(c) Fluid Properties. From the constituent analysis and at 53.56°F, 292.85 psia,

$\rho = 0.935810$ lbm/ft^3
$\mu = 7.40\text{E} - 06$ lbm/(ft-sec)

(d) Thermal Expansion Coefficients of Materials. At the temperature of the flowing fluid,

$\alpha_{PE} = 9.\text{E} - 06$ in./in. - °F
$\alpha_P = 6.\text{E} - 06$ in./in. - °F

(e) Calculation of d, D, and β. From Eq. (3-10.1),

$$\begin{aligned} d_{\text{actual}} &= d_{\text{meas}} + \alpha_{pe} d_{\text{meas}} (T - T_{\text{meas}}) \\ &= 4.754 + (9.\text{E} - 06)(4.754)(53.56 - 68) \\ \Rightarrow d_{\text{actual}} &= 4.753 \text{ in.} \end{aligned} \tag{3-15.3}$$

From Eq. (3-10.2),

$$\begin{aligned} D_{\text{actual}} &= D_{\text{meas}} + \alpha_p D_{\text{meas}} (T - T_{\text{meas}}) \\ &= 7.981 + (6.\text{E} - 06)(7.981)(53.56 - 68) \\ \Rightarrow D_{\text{actual}} &= 7.980 \text{ in.} \end{aligned} \tag{3-15.4}$$

From Eq. (3-10.3),

$$\beta_{\text{actual}} = \frac{d_{\text{actual}}}{D_{\text{actual}}} = \frac{4.753}{7.980} = 0.59561 \tag{3-15.5}$$

Note that at flowing temperatures close to 68°F, geometry is fundamentally unchanged when corrected to flowing temperature. Correction to geometry of higher temperature flows, such as for steam, can be far more significant.

(f) Expansion Factor. From Eq. (3-8.2),

$$\begin{aligned} \epsilon_1 &= 1 - (0.41 + 0.35\beta_4)\frac{\Delta P}{P_1} \\ &= 1 - \left[0.41 + (0.35)(0.59561)^4\right]\frac{1.4106}{(1.309)(292.85)} \\ &= 0.99833 \end{aligned} \tag{3-15.6}$$

(g) Iterations. All terms in the general Eq. (3-1.1) are now known except for the discharge coefficient. It is solved for iteratively. Equation (3-1.1) is repeated for convenience.

$$q_m = n\frac{\pi}{4} d^2 C \epsilon \sqrt{\frac{2\rho(\Delta P) g_C}{1 - \beta^4}} \tag{3-1.1}$$

$$\begin{aligned} q_m &= 300.0\frac{\pi}{4}(4.752)^2 C(0.99833) \\ &\quad \times \sqrt{\frac{(2)(0.935810)(1.4106)(32.17405)}{1 - (0.59561)^4}} \\ \Rightarrow q_m &= (52{,}361)C \end{aligned} \tag{3-15.7}$$

(1) Iteration 1. For the first iteration, guess $C = 0.6$.

$$\begin{aligned} q_m(\text{iteration 1}) &= (52{,}361)(0.600) \\ &= 31{,}417 \text{ lbm/hr} \end{aligned} \tag{3-15.8}$$

$$R_D = \frac{\rho V \frac{D}{12}}{\mu} = \frac{q_m}{75\mu\pi D} \tag{3-15.9}$$

From Eqs. (3-15.4), (3-15.8), and (3-15.9),

$$\begin{aligned} R_D(\text{iteration 1}) &= \frac{31{,}417}{(75)(7.40\text{E} - 6)(\pi)(7.980)} \\ &= 2{,}258{,}000 \end{aligned} \tag{3-15.10}$$

(2) Iteration 2. Discharge coefficient is a function of metering geometry and Reynolds number. Equation (4-8.4) is applicable and is given for convenience. (See Section 4 for empirical equations for discharge coefficients for orifice meters.)

$$\begin{aligned} C = 0.5959 &+ 0.0312\beta^{2.1} - 0.1840\beta^8 + \frac{0.0900\beta^4}{D(1 - \beta^4)} \\ &- \frac{0.0337\beta^3}{D} + \frac{91.71\beta^{2.5}}{R_D^{0.75}} \end{aligned} \tag{4-8.4}$$

For this specific meter, from Eqs. (3-15.4), (3-15.5), and (4-8.4), it is seen that C as a function of R_D is

$$C = 0.60465 + \frac{25.109}{R_D^{0.75}} \tag{3-15.11}$$

From Eqs. (3-15.10) and (3-15.11),

$$C(\text{iteration 2}) = 0.60465 + \frac{25.109}{2{,}258{,}000^{0.75}} = 0.60508 \tag{3-15.12}$$

Note that the difference = (0.60508 − 0.60000)/0.60000 = 0.85%. By the criteria of para. 3-14(f), this is far too large and another iteration is clearly required. With uncertainty requirements in the flow of 0.7%, convergence must be within 2% of 0.7%, or within 0.014%.

From Eq. (3-15.7), the corresponding flow to C (iteration 2) is

$$\begin{aligned} q_m(\text{iteration 2}) &= (52{,}361)C = (52{,}361)(0.60508) \\ &= 31{,}682 \text{ lbm/hr} \end{aligned} \tag{3-15.13}$$

(3) Iteration 3. From Eqs. (3-15.4), (3-15.9), and (3-15.13),

$$\begin{aligned} R_D(\text{iteration 3}) &= \frac{31{,}682}{(75)(7.40\text{E} - 06)(\pi)(7.980)} \\ &= 2{,}277{,}000 \end{aligned} \tag{3-15.14}$$

From Eqs. (3-15.11) and (3-15.14),

$$C(\text{iteration 3}) = 0.60465 + \frac{25.109}{2{,}277{,}000^{0.75}} = 0.60508 \tag{3-15.15}$$

The discharge coefficient, and therefore, the mass flow rate, have converged within five significant digits. This is less than 0.002% difference and well within the 0.014% criterion.

Thus, the calculated flow rate is 31,682 lbm/hr.

(h) Notes on Sample Calculation. It is seen from Eq. (3-15.11) that at large enough Reynolds numbers, the discharge coefficient is a very weak function of Reynolds number, which is why so few iterations are required for convergence. If enough about the measured process is known, then the alternative iterative process described in para. 3-14(g) can be used. Instead of initially guessing

the discharge coefficient, the initial guess would be the flow. With digital computational techniques, it is not critical which method is selected.

The low dependence of the discharge coefficient on the Reynolds number at higher Reynolds numbers makes the orifice-metering run a good candidate for extrapolation of laboratory calibration data to higher Reynolds numbers than are available in the laboratory. This is discussed in detail in Section 4 and in Appendix I.

If the pressure correction to temperature was used so that in this sample calculation 53.92°F was the fluid temperature [Eq. (3-15.2)], then the resulting flow would be 31,668 lbm/hr. The difference of 0.04% is small. The Code user may use the upstream temperature as estimated in this sample calculation, but it is not a requirement.

3-16 SOURCES OF FLUID AND MATERIAL DATA

AGA Report No. 8, *Compressibility and Supercompressibility for Natural Gas and Other Hydrocarbon Gases.* Washington, DC: American Gas Association; 1985.

ASME MFC-3M, *Measurement of Fluid Flow in Pipes Using Orifice, Nozzle, and Venturi.* New York: American Society of Mechanical Engineers; 1989.

ASTM D 1945, *Standard Test Method for Analysis of Natural Gas by Gas Chromatography.* West Conshohocken, PA: American Society for Testing and Materials; 1996.

ASTM D 3588, *Standard Practice for Calculating Heat Value, Compressibility Factor, and Relative Density of Gaseous Fuels.* West Conshohocken, PA: American Society for Testing and Materials; 1998.

Bean, H. S., ed. *Fluid Meters: Their Theory and Application,* 6th edition. New York: The American Society of Mechanical Engineers; 1971.

Benedict, R. P. *Fundamentals of Pipe Flow.* New York: John Wiley & Sons; 1980.

Benedict, R. P. *Fundamentals of Temperature, Pressure, and Flow Measurements.* New York: John Wiley & Sons; 1977.

ISO 5167-1(E), Measurement of Fluid Flow by Means of Pressure Differential Devices Part 1: Orifice Plates, Nozzles, and Venturi Tubes Inserted in Circular Cross-Section Conduits Running Full. Geneva: International Organization for Standardization; 1991.

ISO 5167-1(E), Measurement of Fluid Flow by Means of Pressure Differential Devices Part 1: Orifice Plates, Nozzles, and Venturi Tubes Inserted in Circular Cross-Section Conduits Running Full. Geneva: International Organization for Standardization; 1998.

Sabersky, Acosta, Hauptmann. *Fluid Flow.* New York: Macmillan; 1971.

Shapiro, *The Dynamics and Thermodynamics of Compressible Fluid Flow,***1**. New York: Ronald Press; 1953.

Section 4
Orifice Meters

4-0 NOMENCLATURE

See the nomenclature at the beginning of Section 3.

4-1 INTRODUCTION

This type of differential pressure class meter consists of a flat plate through which the diameter, d, in the general equation for mass flow [Eq. (3-1.1)], has been bored precisely and is thin relative to the diameter of the flow section. The upstream edges of the meter that are exposed to flow must be sharp. The primary element is, therefore, referred to as a thin-plate, square-edged orifice. It is the most widely used differential pressure class meter because of its low cost and high accuracy.

4-2 TYPES OF THIN-PLATE, SQUARE-EDGED ORIFICES

Thin-plate, square-edged orifices are classified based on the locations of their differential pressure taps. The following three types of tap geometries are recommended by this Supplement for primary data when conducting ASME performance tests in accordance with a code:

(a) flange taps
(b) D and $D/2$ taps
(c) corner taps

Pressure tap locations for flange taps and D and $D/2$ taps are given by the measured distance from the centerline of the pressure tap to the upstream face A or to the downstream face B of the orifice plate (Fig. 4-2-1). The thickness of the gaskets or other sealing material is included in the given dimension.

In a corner tap arrangement, the pressure holes open in the corner formed by the pipe wall and the orifice plate (Fig. 4-2-2). The pressure taps may have several locations.

4-3 CODE COMPLIANCE REQUIREMENTS

Thin-plate, square-edged orifice-metering runs must be manufactured and installed in accordance with this Section and Section 7 to be in compliance with this Supplement. Flow measurement accuracy is affected by

(a) thermal expansion and pressure-induced distortion affecting orifice geometry
(b) orifice plate dimensions and construction
(c) orifice bore concentricity to the pipe
(d) location of temperature and static pressure measurements
(e) Reynolds number limitations
(f) metering section and flange dimensions and construction
(g) effect of flow conditions on swirl or upstream obstructions on accuracy
(h) pressure tap construction and geometry

This Section addresses paras. 4-3(a) through (e). Compliance requirements for paras. 4-3(f) through (h) are discussed in Section 7.

4-4 MULTIPLE SETS OF DIFFERENTIAL PRESSURE TAPS

It is recommended that two sets of differential pressure taps separated by 90 deg or 180 deg be provided. It is sometimes necessary for them to be provided at 90 deg for situations where connecting tubing must be routed either vertically upward or horizontally or vertically downward or horizontally; the vertical positions are preferred.

Orifice degradation through use, dirt, or other irregularities can go unnoticed if only one set of taps are used. Differential pressure is measured at each set of taps. The flow calculation is done separately for each pair and averaged. Investigation is needed if the results differ from each tap set calculation by more than the flow measurement uncertainty.

When using a calibrated orifice for precise measurement, two sets of differential pressure taps are required.

4-5 MACHINING TOLERANCES, DIMENSIONS, AND MARKINGS FOR ORIFICE PLATE

Unless otherwise noted, all symbols correspond to those in Fig. 4-5.

4-5.1 Deflection and the Required Thickness *E* of Orifice Plate

Deflection of the orifice plate during flowing conditions is unavoidable (Fig. 4-5.1), but must be small enough so that the total deflection τ is less than $0.005(D - d)/2$ (assuming the plate was perfectly flat with zero differential pressure applied). Table 4-5.1 shows minimum orifice plate thickness E for stainless steel orifices.

The minimum plate thickness E shall be those values given in Table 4-5.1. Maximum plate thickness shall not

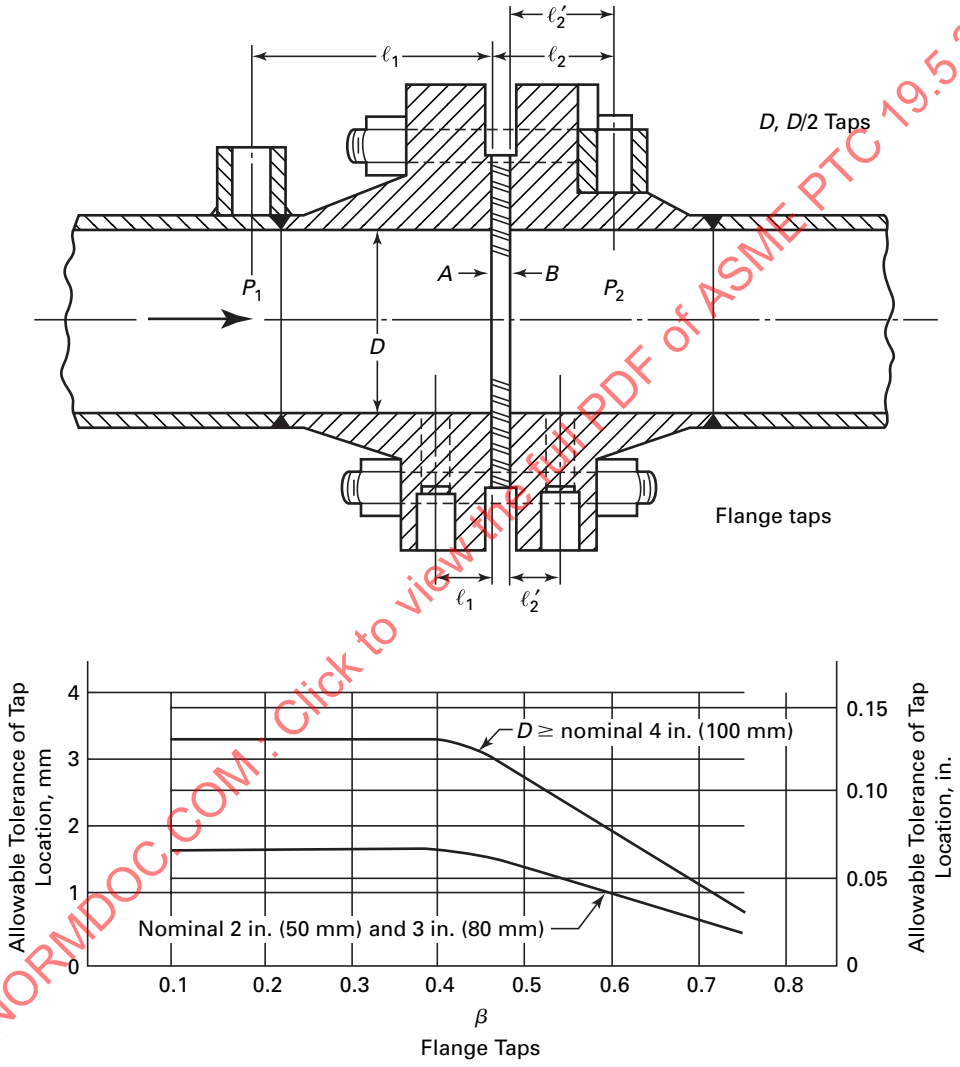

Fig. 4-2-1 Location of Pressure Taps for Orifices With Flange Taps and With *D* and *D*/2 Taps

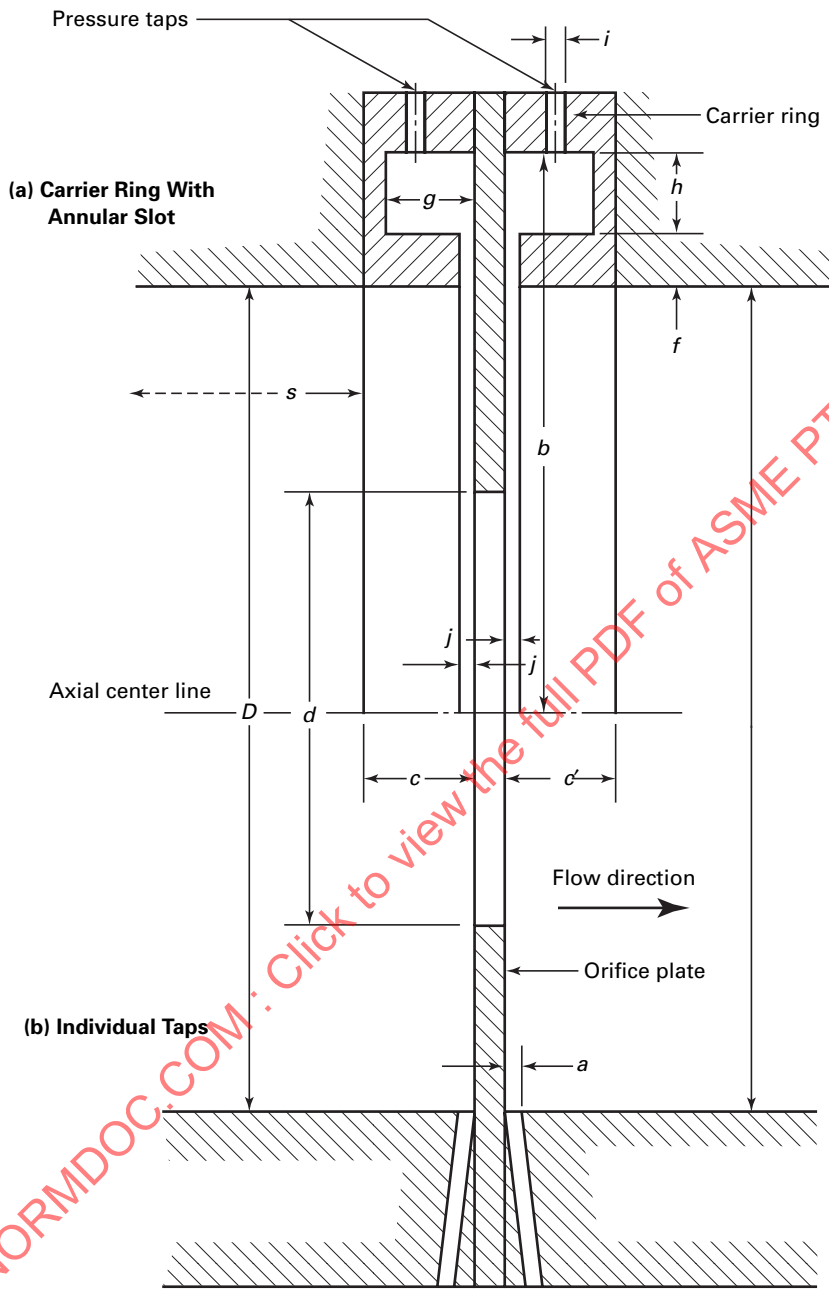

a = diameter of individual tap holes
b = diameter of the ring
c = length of upstream ring
c' = length of downstream ring
f = thickness of the slot
i = diameter of pressure tap in carrier ring
j = width of the upstream and downstream annular slots
s = distance from carrier ring to upstream step

Fig 4-2-2 Location of Pressure Taps for Orifices With Corner Taps

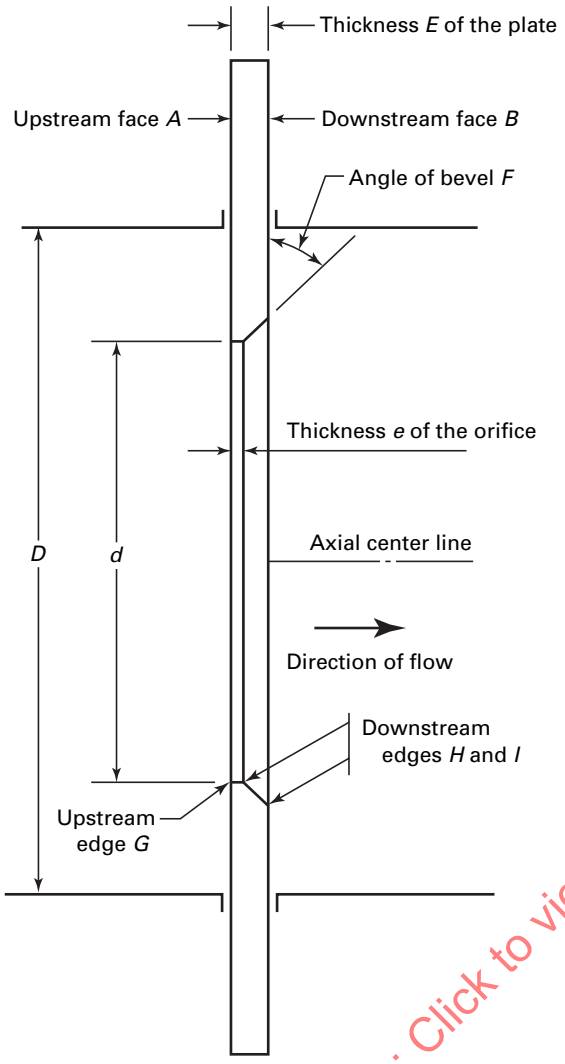

Fig. 4-5 Standard Orifice Plate

exceed 1.5 times the minimum value, and in no case can it be larger than 0.5 in. (13 mm).

The values of E measured at any point of the plate shall not differ among themselves by more than $0.001D$.

4-5.2 Upstream Face *A*

With zero differential pressure applied, the plate upstream face A must be flat within $0.01(D - d)/2$. The orifice plate mounting shall have no significant distorting effect on the plate.

The upstream face A must have a maximum roughness of no greater than 5 μin. (1.3 μm) within a circle whose diameter is not less than D and is concentric with the bore.

The lip-like upstream side of the orifice plate that extends out of the pipe called the tag shall be permanently marked with the following information:

(a) identification as the upstream side

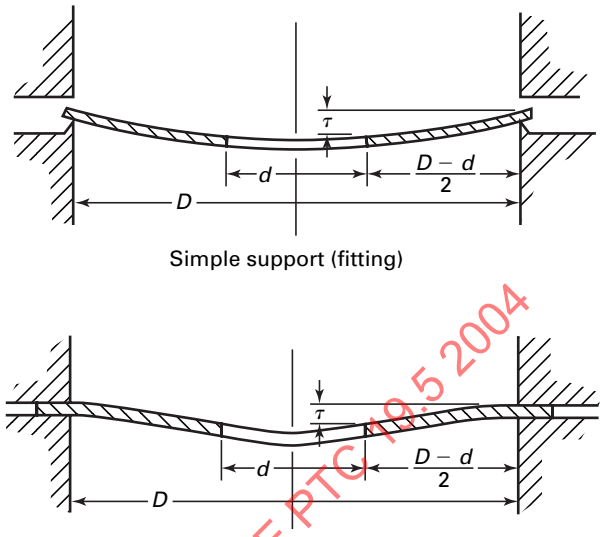

Fig. 4-5.1 Deflection of an Orifice Plate by Differential Pressure

(b) measured bore diameter to five significant digits

(c) measured upstream pipe diameter to five significant digits if it is from the same supplier as the orifice plate

(d) instrument or orifice identifying number

It is also suggested, but not mandatory, that the tag be marked with the plate thickness and angle of bevel, even if that is zero.

4-5.3 Downstream Face *B*

The downstream face B does not have to be machined to the same tolerances as the upstream face. Flatness and roughness can be judged acceptable by visual and tactile inspection.

4-5.4 Thickness *e*

The thickness of the cylindrical bore of the orifice e measured normal to the plane of the inlet face must be between $0.005D$ and $0.02D$, but it must never be less than 0.005 in. (125 mm).

The values of e measured around the bore shall not differ among themselves by more than $0.001D$.

4-5.5 Bevel

If the thickness of the orifice plate E is greater than the thickness e of the orifice, then the bevel shall be on the downstream side. The beveled surface has the same smoothness requirements as the upstream side of the orifice plate A. The angle of bevel F shall be 45 deg (+2, −0).

4-5.6 Edges *G*, *H*, and *I*

The upstream edge G and downstream edges H and I must be completely free of any burrs, nicks, wire edges,

Table 4-5.1 Minimum Plate Thickness, *E*, for Stainless Steel Orifice Plate

ΔP	D < 150 mm (D < 6 in.)	D < 250 mm (D < 10 in.)	D < 500 mm (D < 20 in.)	D ≤ 900 mm (D ≤ 36 in.)
$\beta \leq 0.5$				
$\Delta P \leq 250$ kPa (36.3 lbf/in.^{2})	3 mm (0.125 in.)	5 mm (0.188 in.)	10 mm (0.375 in.)	13 mm (0.500 in.) [Note (1)]
$\Delta P \leq 50$ kPa (7.25 lbf/in.^{2})	3 mm (0.125 in.)	3 mm (0.125 in.)	6 mm (0.250 in.)	10 mm (0.375 in.)
$\Delta P \leq 25$ kPa (3.63 lbf/in.^{2})	3.2 mm (0.125 in.)	3 mm (0.125 in.)	6 mm (0.250 in.)	10 mm (0.375 in.)
$\beta > 0.5$				
$\Delta P \leq 250$ kPa (36.3 lbf/in.^{2})	3 mm (0.125 in.)	5 mm (0.188 in.)	10 mm (0.375 in.)	13 mm (0.500 in.)
$\Delta P < 50$ kPa (7.25 lbf/in.^{2})	3 mm (0.125 in.)	3 mm (0.125 in.)	5 mm (0.188 in.)	10 mm (0.375 in.)
$\Delta P < 25$ kPa (3.63 lbf/in.^{2})	3 mm (0.125 in.)	3 mm (0.125 in.)	5 mm (0.188 in.)	6 mm (0.250 in.)

GENERAL NOTES:
(a) See para. 4-6 for maximum allowable plate thickness.
(b) Calculated based on U.S. engineering units, with minimum thickness expressed in multiples of one-sixteenth of an inch, as is common practice. SI units are rounded to the nearest millimeter.
(c) Sources: ASME MFC-3M, ASME Fluid Meters.

NOTE:
(1) At pipe diameters of 30 in. and higher, maximum differential pressure is 125 kPa (18.1 lbf/in.^{2}).

or other manufacturing deficiencies detectable by visual or tactile inspection.

The upstream edge G must be sharp. It is defined as sharp if the radius of the edge is not greater than $0.0004D$ for orifices up to $D = 3$ in. (75 mm) and not greater than 0.001 in. (0.025 mm) for orifices of $D > 3$ in. (75 mm).

Visual inspection of the G edge of orifices of $D > 1$ in. (25 mm) is sufficient to check edge sharpness compliance. If the edge does not appear to reflect a beam of light when viewed by the naked eye, the sharpness requirements are considered to be met. If there is any doubt, the edge radius must be measured. For orifices of $D < 1$ in. (25 mm), it is recommended to measure the edge radius. The edge radius can be measured by the lead foil impression method, casting method, or paper recording roughness method.

The downstream edges H and I do not have the same rigorous requirements as the G edge. This is because they are in the separated flow region. Small defects should be undetectable by the naked eye.

4-5.7 Orifice Diameter

The diameter D shall be such that $0.20 < \beta < 0.75$; however, it is recommended that a β of 0.70 is not exceeded. The manufactured diameter D is reported as the mean of four measured diameters at approximately 45 deg spacings. More diametral measurements can be specified but must be spaced in approximately equal radial angles to each other.

Caution must be exercised to avoid damaging the inlet edge G while measuring the diameter.

No measured diameter can differ by more than 0.05% from the mean for orifices of $D > 1$ in. (25 mm) or by more than 0.0004 in. (0.01 mm) for orifices with smaller diameters down to 0.40 in. (10 mm)

The orifice shall be cylindrical and perpendicular to the upstream face.

4-5.8 Eccentricity of Orifice in Metering Section

Centeredness of the orifice diameter with respect to the upstream metering run diameter, or eccentricity, is defined as the perpendicular distance between the orifice bore center and the metering section bore center. For line sizes greater than 4 in. (100 mm), eccentricity must not exceed $0.0025D/(0.1 + 2.3\beta^4)$. In smaller line sizes, eccentricity must not exceed 0.03 in. (0.8 mm) toward the taps, or 1.5% of D away from the taps.

An orifice plate must be perpendicular to the centerline of the metering run within 1 deg.

The manufacturing and installation requirements needed to comply with these restrictions are addressed in Section 7.

4-6 MACHINING TOLERANCES AND DIMENSIONS FOR DIFFERENTIAL PRESSURE TAPS

4-6.1 Flange Tap and *D* and *D*/2 Tap Orifice-Metering Runs — Shape, Diameter, and Angular Position

The centerline of the taps must meet the pipe centerline and be at right angles to it within ±2 deg.

At the point of breakthrough the hole must be circular. The edges must be flush with the internal surface of

the pipe wall and be as sharp as can be reasonably manufactured. Because of the criticality of eliminating burrs or wire wedges at the inner edge, rounding is permitted but it should be minimized. The radius caused by rounding must not exceed $0.0625d$. Visually, no irregularities could appear inside the connecting hole, on the edges of the hole drilled in the pipe wall, or in the pipe wall close to the pressure tap.

The maximum allowable diameters of the tap holes through the pipe wall or flange are given in Section 7. Interpolation for intermediate sizes is permitted. Upstream and downstream tap holes must be the same diameter. The minimum size of the tap holes is 0.25 in. (6 mm).

The pressure tap holes must be circular and cylindrical. They may be constructed such that they may abruptly increase in diameter at any location away from the inner wall. However, if they decrease in diameter, the decrease must not occur for at least 2.5 hole diameters away from the inner wall.

The axis of an upstream and its respective downstream tap may be located in different axial planes. Caution is advised concerning correct calculations based on elevation differences of taps and tubing installation that does not negatively affect the measurement. Also, if the metering run is installed downstream of a bend or a tee, it is recommended that, when using pairs of single taps, they be installed so that their axes are perpendicular to the plane of the bend or tee.

4-6.2 Flange Tap and *D* and *D*/2 Tap Orifice-Metering Runs — Spacing of Taps

The spacing l of a pressure tap is the distance between the centerline of the pressure tap and the plane of one specified face of the orifice plate. When installing the pressure taps, take into account the thickness of the gaskets and/or sealing material that are to be used.

(a) Spacing of Flange Taps. The center of the tap for P_1 is $l_1 = 1.00$ in. (25.4 mm) measured from the upstream face A of the orifice plate. The center of the tap for P_2 is $l_2 = 1.00$ in. (25.4 mm) measured from the downstream face B of the orifice plate. Manufacturing tolerances for flange tap locations are shown in Fig. 4-2.1.

(b) Spacing of D and D/2 Taps. The center of the tap for P_1 is $l_1 = D \pm 5\%$ from the upstream face A of the orifice plate. The center of the tap for P_2 is $l_2 = 1.00$ in. (25.4 mm) measured from the downstream face B of the orifice plate. Manufacturing tolerances for flange tap locations are shown in Fig. 4-2.1.

4-6.3 Corner Tap Orifice-Metering Runs

(a) The spacing between the centerlines of the taps and the respective faces of the plate is to be selected so that the tap holes break through the wall flush with the faces of the plate.

(b) The taps may be either single taps or annular slots. Both types of taps can be located either in the pipe, its flanges, or in carrier rings, as shown in Fig. 4-2.2.

(c) The diameter a of single taps or the width j of annular slots are given below. The minimum diameter is determined in practice by the likelihood of accidental blockage, such as by air bubbles or built-up dirt.

(1) For clean fluids and steam,

(a) for $\beta \le 0.65$, $0.005D \le a$ or $j \le 0.03D$

(b) for $\beta > 0.65$, $0.01D \le a$ or $j \le 0.02D$

(2) For any values of β,

(a) for clean fluids, 0.05 in. (1 mm) $\le a$ or $j \le 0.5$ in. (10 mm)

(b) for steam with annular chambers, 0.05 in. (1 mm) $\le a$ or $j \le 0.5$ in. (10 mm)

(c) for steam and liquefied gases with single taps, 0.16 in. (4 mm) $\le a$ or $j \le 0.5$ in. (10 mm)

(d) The annular slots usually break through the pipe over the entire perimeter with no break in continuity. If not, each chamber shall connect with the inside of the pipe by at least four openings, the axes of which are at equal angles to one another and the individual opening area of each being at least 0.02 in.^{2} (12 mm^2).

(e) If individual pressure taps are used, the centerline of the taps must cross the centerline of the pipe at as near a right angle (90 deg) as possible. If there are several individual pressure taps for the same upstream or downstream axial plane, their centerlines shall form equal angles with each other around the pipe. The pressure taps must be circular and cylindrical over a length of at least 2.5 times the diameter of the taps, measured from the inner wall of the pipe.

(f) The inner diameter b of the carrier rings must be equal to or greater than the diameter D of the pipe to ensure that the carrier rings do not protrude into the pipe. The inner diameter must not be greater than $1.0025D$.

(g) The following restrictions are placed on the geometry of the pressure taps for corner tap orifice-metering runs (see Fig. 4-2.2):

(1) $D \le b \le 1.0025D$

(2) $c \le 0.5D$

(3) $c' \le 0.5D$

(4) $f \ge 2j$

(5) area $gh \ge \pi jb/2$

(h) All surfaces of the ring that can be in contact with the measured fluid shall be clean and have a good machined finish.

(i) The pressure taps connecting the annular chambers to the secondary device are pipe-wall taps, circular at the point of breakthrough and with diameters a between 0.15 in. and 0.5 in. (4 mm and 10 mm).

(j) The upstream and downstream carrier rings are not necessarily symmetrical to each other, but they shall both comply with the specifications herein.

(k) The diameter D of the pipe to be used for the calculation of the diameter ratio is to be measured, as must be the arithmetic mean of measurements made in

at least four equally separated diameters in the plane of the upstream tap. The carrier ring is regarded as part of the primary device. The mean diameter of the carrier ring b must be used in the calculation. This also applies to the length requirement so that the length s is to be taken from the upstream edge of the recess formed by the carrier ring.

4-7 LOCATION OF TEMPERATURE AND STATIC PRESSURE MEASUREMENTS

The general equation for mass flow [Eq. (3-1.1)] was developed to calculate the velocity at the throat of the device. Thus, temperature and static pressure measurements for density and viscosity determination are preferably determined at the upstream side of the orifice. However, temperature measurement upstream can interfere with the flow pattern and introduce errors. Hence, the temperature well shall be located between $5D$ and $6D$ downstream of the orifice face B.

For a gas or vapor, with the requirement that $P_2/P_1 > 0.80$, or for a liquid, it is acceptable to assume that $T_1 = T_2$ without any loss of accuracy. This can be confirmed by assuming isentropic expansion of the fluid across the orifice and using the measured differential and static pressures, taking note that there is some pressure recovery.

The static pressure of the fluid is measured in the radial plane of the upstream pressure tap. This can be done using a separate pressure tap or by tee-in connection with the differential pressure measurement line. Care must be taken to avoid introducing errors when connecting static pressure measurement in common with a differential pressure measurement (see Section 7). In the case of corner tap orifices, static pressure can be measured by means of carrier ring taps.

It is acceptable to measure static pressure at the downstream tap if, for a gas or vapor, the expansion factor is calculated by Eq. (3-8.5).

4-8 EMPIRICAL FORMULATIONS FOR DISCHARGE COEFFICIENT C

4-8.1 General Formulation

The empirical formulation for the discharge coefficient for orifices is given by the following equation:

$$C = 0.5959 + 0.0312\beta^{2.1} - 0.1840\beta^{8} + \frac{0.0900L_1\beta^4}{(1-\beta^4)} - 0.0337L'_2\beta^3 + \frac{91.71\beta^{2.5}}{R_D^{0.75}} \quad (4\text{-}8.1)$$

where

L_1 = dimensionless correction for upstream tap location
= l_1/D, measured from upstream face A

L_2 = dimensionless correction for downstream tap location
= l_2/D, measured from upstream face A

L'_2 = dimensionless correction for downstream tap location
= $(l_2 - E)/D$, measured from downstream face B

4-8.2 Discharge Coefficient for Flange Tap Orifices (U.S. Customary Units)

For $D \geq 2.3$ in., $L_1 = L'_2$, and

$$C = 0.5959 + 0.0312\beta^{2.1} - 0.1840\beta^{8} + \frac{0.0900\beta^4}{D(1-\beta^4)} - \frac{0.0337\beta^3}{D} + \frac{91.71\beta^{2.5}}{R_D^{0.75}} \quad (4\text{-}8.2)$$

For 2 in. $\leq D <$ 2.3 in., $L_1 = 0.4333$, $L'_2 = 1/D$, and

$$C = 0.5959 + 0.0312\beta^{2.1} - 0.1840\beta^{8} + \frac{0.0390\beta^4}{(1-\beta^4)} - \frac{0.0337\beta^3}{D} + \frac{91.71\beta^{2.5}}{R_D^{0.75}} \quad (4\text{-}8.3)$$

4-8.3 Discharge Coefficient for Flange Tap Orifices (SI Units)

For $D \geq 58.6$ mm, $L_1 = L'_2 = 25.4/D$, and

$$C = 0.5959 + 0.0312\beta^{2.1} - 0.1840\beta^{8} + \frac{2.2860\beta^4}{D(1-\beta^4)} - \frac{0.8560\beta^3}{D} + \frac{91.71\beta^{2.5}}{R_D^{0.75}} \quad (4\text{-}8.4)$$

For 50.8 mm $\leq D \leq$ 58.6 mm, $L_1 = 0.4333$, $L'_2 = 25.4/D$, and

$$C = 0.5959 + 0.0312\beta^{2.1} - 0.1840\beta^{8} + \frac{0.0390\beta^4}{(1-\beta^4)} - \frac{0.8560\beta^3}{D} + \frac{91.71\beta^{2.5}}{R_D^{0.75}} \quad (4\text{-}8.5)$$

4-8.4 Discharge Coefficient for D and $D/2$ Tap Orifices (U.S. Customary and SI Units)

For both sets of units, $L_1 = 0.4333$, $L'_2 = 0.47$, and

$$C = 0.5959 + 0.0312\beta^{2.1} - 0.1840\beta^{8} + \frac{0.0390\beta^4}{(1-\beta^4)} - 0.01584\beta^3 + \frac{91.71\beta^{2.5}}{R_D^{0.75}} \quad (4\text{-}8.6)$$

Note that for D and $D/2$ orifices, $l'_2 = (l_2 - E)$, the distance from the downstream face B of the orifice plate to the center of the P_2 tap, is defined as $0.47D$.

4-8.5 Discharge Coefficient for Corner Tap Orifices (U.S. Customary and SI Units)

For corner taps, $L_1 = L'_2 = 0$, and

$$C = 0.5959 + 0.0312\beta^{2.1} - 0.1840\beta^{8} + \frac{91.71\beta^{2.5}}{R_D^{0.75}} \quad (4\text{-}8.7)$$

Note that, with the elimination of the dimensionless corrections, corner tap orifice-metering runs are the best to study for the development of formulations for discharge coefficient based on fluid dynamic theories for comparison to test data.

4-9 LIMITATIONS AND UNCERTAINTY OF EQS. (4-8.1) THROUGH (4-8.7) FOR DISCHARGE COEFFICIENT *C*

Equations (4-8.1) through (4-8.7) are valid only for metering tube sizes of 2 in. ≤ D ≤ 36 in. (50 mm ≤ D ≤ 900 mm), nominal sizes.

At pipe Reynolds numbers Re_D between 2,000 and 10,000, the bias uncertainty of the calculated discharge coefficient is $(0.6 + \beta)$%. Notice from the empirical formulations that, for these very low Reynolds numbers, the slope of the C versus Re_D curve is steep.

At pipe Reynolds numbers Re_D above 10,000, the calculated uncertainty is as follows:

(a) For $0.2 \le \beta \le 0.6$, the uncertainty of the discharge coefficient is 0.6%.

(b) For $0.6 \le \beta \le 0.75$, the uncertainty of the discharge coefficient is equal to β%.

The uncertainties in this paragraph are to be treated as bias uncertainties in the uncertainty analysis of flow. They are valid only if the orifice and metering section are manufactured and installed strictly in accordance with the requirements of this Section or Section 7 of this Code.

The upper Reynolds number limit for these equations is $Re_D = 10^8$.

4-10 UNCERTAINTY OF EXPANSION FACTOR ϵ

The numerical value of the uncertainty of the expansion factor ϵ, expressed as a percentage, is $4\Delta P/P$, with ΔP and P in the same units.

4-11 UNRECOVERABLE PRESSURE LOSS

The unrecoverable pressure loss $\Delta\omega$ is related to the pressure drop across the orifice ΔP by

$$\Delta\omega = \frac{\sqrt{1-\beta^4 - C\beta^2}}{\sqrt{1-\beta^4 + C\beta^2}}\Delta P \quad (4\text{-}11.1)$$

with $\Delta\omega$ and ΔP in the same units.

4-12 CALCULATIONS OF DIFFERENTIAL PRESSURE CLASS FLOW MEASUREMENT STEADY STATE UNCERTAINTY

4-12.1 Derivation

This uncertainty analysis is valid provided that the calculations of mass flow rate are performed and the metering runs and orifices are manufactured and installed strictly in accordance with this Code. Deviation from this Code in manufacture, installation, calculations, or any other requirement adversely affects uncertainty.

Sample calculations shown are for orifice-metering runs, which have the best accuracy levels of the empirical discharge coefficient (hydraulic laboratory calibration equalizes the discharge coefficient uncertainties among all the differential pressure devices.

Steam and gas are the chosen fluids for sample calculation of uncertainty because all terms are then used in the fundamental flow equation [Eq. (3-1.1)], which is repeated below for the user's convenience. Water or incompressible flow measurement uncertainty would be calculated similarly but without the expansion factor term coming into play.

$$q_m = n\frac{\pi}{4}d^2C\epsilon\sqrt{\frac{2\rho(\Delta P)g_C}{1-\beta^4}} \quad (3\text{-}1.1)$$

C = orifice discharge coefficient
d = diameter of orifice at flowing fluid temperature
n = units conversion factor for all units to be consistent
q_m = mass flow rate
β = ratio of orifice and pipe diameters (d/D), both diameters at the flowing fluid temperature
ΔP = differential pressure
ϵ = expansion factor for gas and vapor flow
ρ = fluid density

Defining U as the uncertainty in the units of measure of its subscripted variable,

$$U_m = \left[\left(\frac{\partial m}{\partial C}U_C\right)^2 + \left(\frac{\partial m}{\partial \epsilon}U_\epsilon\right)^2 + \left(\frac{\partial m}{\partial d}U_d\right)^2 + \left(\frac{\partial m}{\partial D}U_D\right)^2 + \left(\frac{\partial m}{\partial \rho}U_\rho\right)^2 + \left(\frac{\partial m}{\partial \Delta P}U_{\Delta P}\right)^2\right]^{0.5} \quad (4\text{-}12.1)$$

After differentiation, dividing by m to get fractional units, and algebra,

$$\frac{U_m}{m} = \left[\left(\frac{U_C}{C}\right)^2 + \left(\frac{U_\epsilon}{\epsilon}\right)^2 + \left(\frac{2\beta^4}{1-\beta^4}\right)^2\left(\frac{U_D}{D}\right)^2 + \left(\frac{2}{1-\beta^4}\right)^2\left(\frac{U_d}{d}\right)^2 + \left(\frac{U_{\Delta P}}{2\Delta P}\right)^2 + \left(\frac{U_\rho}{2_\rho}\right)^2\right]^{0.5} \quad (4\text{-}12.2)$$

Table 4-12.1
Sensitivity Coefficients in the General Equation for Differential Pressure Meters

Term in General Flow Rate Eq. (1)	Sensitivity Coefficient
C	1.00
ϵ	1.00
D	$\frac{2\beta^4}{1-\beta^4}$
d	$\frac{2}{1-\beta^4}$
ΔP	0.50
ρ	0.50

Uncertainty as a percentage is then equal to $100U_m/m$.

The square root of the coefficient of each term in Eq. (4-12.2) is the sensitivity coefficient of the particular variable X. The sensitivity coefficients are summarized from Eq. (4-12.2) in Table 4-12.1.

4-12.2 Uncertainty Calculation-General

The uncertainties of high-quality instrumentation for measurement of the fluid conditions and orifice differential pressure are used in the following calculations. Use of different quality instrumentation would result in different total uncertainty and must be considered for each application. Even if typical orifice and pipe geometries are used, each individual case has to be considered in practice.

There are no additional uncertainty considerations in completely steady state conditions using Eq. (4-12.2) for uncertainty analysis, if the parameters on the right side of Eq. (3-1.1) are independent. Although they are not entirely independent, the unaccounted-for cross-products are completely insignificant, as shown below.

The discharge coefficient C is a function of Reynolds number, which is calculated based on temperature, pressure, and constituent analysis if a gas mixture (for density and viscosity calculations). Consider that an error in the Reynolds number of 25% for typical geometries and flow rates results in an error in the discharge coefficient of much less than 0.1%; the error in the discharge coefficient caused by temperature, pressure, and analysis errors is trivial.

The expansion factor ϵ also depends on pressure and differential pressure.

$$\epsilon = 1 - (0.41 + 0.35\beta^4)\frac{\Delta P}{P_1}$$

The uncertainty of the empirical formulation of the expansion factor in the calculations overwhelms the uncertainty in ϵ due to process measurement error. As an example, consider a metering section with β ratio of 0.6 and measured differential pressure of 5.4 psi for a compressible fluid with a specific heat ratio of 1.3 at a pressure of 300 psi. The error in the ϵ calculation is 0.003% at typical instrument errors of 0.2%.

Three example uncertainty calculations are given; two are for steam mass flow rate and one is for natural gas fuel mass flow rate. It is emphasized that these are steady state uncertainties. A post-test uncertainty analysis would have to include random errors caused by data fluctuations per ASME PTC 19.1.

4-12.2.1 Example 1: Uncertainty of Typical Steam Flow Measurement, Orifice-Metering Run for $\beta \leq 0.6$. Orifice geometry and design flow conditions are as follows (see Table 4-12.2.1):

D_{meas} = 10.02 in.
d_{meas} = 4.9012 in.
β_{meas} = 0.4891
differential pressure = 18.046 psi
fluid pressure = 280 psia
fluid temperature = 430°F

4-12.2.2 Example 2: Uncertainty of Typical Steam Flow Measurement, Orifice-Metering Run for $\beta > 0.6$. Steam flow orifice geometry and flow conditions are as follows (see Table 4-12.2.2):

D_{meas} = 12.00 in.
d_{meas} = 8.400 in.
β_{meas} = 0.7000
differential pressure = 7.835 psi
fluid pressure = 65 psia
fluid temperature = 360°F

4-12.2.3 Example 3: Uncertainty of Typical Fuel Gas Flow Measurement, Orifice-Metering Run for $\beta < 0.6$. Fuel flow orifice geometry and flow conditions are as follows (see Table 4-12.2.3):

D_{meas} = 7.9810 in.
d_{meas} = 4.6834 in.
β_{meas} = 0.5868
differential pressure = 4.234 psi
fluid pressure = 375 psia
fluid temperature = 60°F

4-12.3 Precision Uncertainty Due to Data Fluctuations

The post-test uncertainty analysis must consider fluctuation of actual data. The differences in degrees of freedom of the required data should be considered in calculation of the random component of uncertainty. The analyses in this document just consider steady state uncertainty, which is usually treated as bias error only.

For example, consider that fuel samples are taken in 10-min intervals to determine the constituent analysis for the determination of density, and all other data are taken in 1-min intervals. Then, the two-tailed Student's t distribution for four degrees of freedom (2.776) is applied to the random uncertainty component of the constituent analysis portion for the density uncertainty

Table 4-12.2.1 Example 1: Steady State Uncertainty Analysis for Given Steam Flow Orifice–Metering Run

Parameter	Parameter Total Uncertainty, $\frac{U_X}{X}$, %	Sensitivity Factor on Flow Measurement, S	$\frac{U_X}{X} S$
Discharge coefficient, C	$U_C/C = 0.600$	1.00	0.6
Expansion factor, ϵ	$\frac{U_\epsilon}{\epsilon} = \frac{4\Delta P}{P}$, $4\left(\frac{18.046}{280}\right) = 0.26\%$	1.00	0.26
Pipe diameter, D	0.2%	$\frac{2\beta^4}{1-\beta^4} = 0.121$	0.0242
Orifice Diameter, d	0.05%	$\frac{2}{1-\beta^4} = 2.12$	0.106
Differential pressure, ΔP	0.25%	0.50	0.125
Density, ρ	$U_P/P = 0.25\%$, $U_T = 0.5°F$ $\Rightarrow U_\rho/\rho = 0.27\%$	0.50	0.135
Total steady state uncertainty	...	...	0.69%

Table 4-12.2.2 Example 2: Steady State Uncertainty Analysis for Given Steam Flow Orifice–Metering Run

Parameter	Parameter Total Uncertainty, $\frac{U_X}{X}$, %	Sensitivity Factor on Flow Measurement, S	$\frac{U_X}{X} S$
Discharge coefficient, C	$U_C/C = 0.700$	1.00	0.700
Expansion factor, ϵ	$\frac{U_\epsilon}{\epsilon} = \frac{4\Delta P}{P}$ $4\left(\frac{7.835}{65}\right) = 0.48\%$	1.00	0.48
Pipe diameter, D	0.2%	$\frac{2\beta^4}{1-\beta^4} = 0.632$	0.126
Orifice Diameter, d	0.05%	$\frac{2}{1-\beta^4} = 2.632$	0.132
Differential pressure, ΔP	0.25%	0.50	0.125
Density, ρ	$U_P/P = 0.25\%$, $U_T = 0.5°F$ $\Rightarrow U_\rho/\rho = 0.27\%$	0.50	0.135
Total steady state uncertainty	...	...	0.89%

Table 4-12.2.3 Steady State Uncertainty Analysis for Given Gas Flow Orifice-Metering Run

Parameter	Parameter Total Uncertainty, $\frac{U_X}{X}$, %	Sensitivity Factor on Flow Measurement, S	$\frac{U_X}{X}S$
Discharge coefficient, C	$U_C/C = 0.600$	1.00	0.600
Expansion factor, ϵ	$\frac{U_\epsilon}{\epsilon} = \frac{4\Delta P}{P}$ $4\left(\frac{4.234}{375}\right) = 0.045\%$	1.00	0.045
Pipe diameter, D	0.2%	$\frac{2\beta^4}{1-\beta^4} = 0.269$	0.054
Orifice Diameter, d	0.05%	$\frac{2}{1-\beta^4} = 2.269$	0.113
Differential pressure, ΔP	0.25%	0.50	0.125
Density, ρ	$U_P/P = 0.25\%$, $U_T = 0.5°F$ $\Rightarrow U_\rho/\rho = 0.27\%$, if perfect analysis Constituent analysis uncertainty: 0.2% Root mean square: 0.34%	0.50	0.17
Total steady state uncertainty	. . .	. . .	0.65%

determination and, for greater than 30 data points (2.000), for the temperature and pressure contributions to the random component of density uncertainty.

The relative random indices of the mean of density (using uncertainties in measurement of temperature, pressure, and chemical analysis) and of differential pressure due to fluctuations are computed and combined with the bias uncertainties, as calculated in these examples for the post-test uncertainty analysis.

Excellent examples of complete uncertainty analyses, including random uncertainty from fluctuation in data, are given in ASME PTC 19.1, Test Uncertainty. Reference is made to that Performance Test Code for details of post-test uncertainty analysis requirements.

4-12.4 Instrumentation Uncertainties for the Determination of Total Measurement Uncertainties

The following is a summary of the reasons for selection of the individual instrumentation uncertainties:

(a) Differential Pressure. Differential pressure transmitters installed specifically for test purposes are assumed to be of the 0.075% accuracy class. For the purposes of this calculation, it is assumed that transmitters are selected for a specific application so that their range does not affect uncertainty. It is also assumed that local ambient temperature is 80°F, and that there is insignificant water leg error.

Additional instrument uncertainties are caused by

(1) static pressure effects
(2) ambient temperature effects
(3) vibration effects

Other small error sources can be from power supply effects or RFI effects and are considered zero. Each manufacturer documents the influence of these effects on their instrumentation. Typical values and total differential pressure uncertainty at steady state conditions are given in Table 4-12.4-1. With the above assumptions, 0.23% represents the total instrument uncertainty in steady state. To be conservative, 0.25% is used for the uncertainty of differential pressure in the uncertainty calculations in this Section.

(b) Static Pressure. Making the same assumptions as for the differential pressure measurement, static pressure uncertainty at steady state conditions is estimated, for a 0.075% class gage pressure transmitter, in Table 4-12.4-2. With the above assumptions, 0.21% represents the total instrument error in steady state. To be conservative, 0.25% is used for the uncertainty of static pressure in

Table 4-12.4-1
Total Steady State Uncertainty, 0.075% Accuracy Class Differential Pressure Transmitter

Parameter	Sensitivity, %/%	Steady State Instrument Bias and Precision Error Combined	Sensitivity × Error
Calibration	1.0	0.075%	0.075%
Static pressure	1.0	0.1%	0.1%
Temperature effect	1.0	0.15%	0.15%
Vibration	1.0	0.1%	0.1%
Repeatability	1.0	0.05%	0.05%
Data acquisition system	1.0	0.04%	0.04%
Root sum square	. . .	. . .	0.23%

Table 4-12.4-2 Total Steady State Uncertainty, 0.075% Accuracy Class Static Pressure Transmitter

Parameter	Sensitivity, %/%	Steady State Precision and Bias Error Combined	Sensitivity × Error
Calibration	1.0	0.075%	0.075%
Temperature effect	1.0	0.15%	0.15%
Vibration	1.0	0.1%	0.1%
Repeatability	1.0	0.05%	0.05%
Data acquisition system	1.0	0.04%	0.04%
Barometric pressure	0.05	0.1%	nil
Root sum square	. . .	. . .	0.21%

the uncertainty calculations in this Section.

(c) Temperature. Several options exist to determine temperature within 0.5°F (assuming no temperature stratification). For example, RTDs typically have digital accuracies of 0.3°F in broad temperature ranges. Combined with data acquisition uncertainty and other effects, 0.5°F maximum uncertainty is achievable and can be improved with applied laboratory calibrations.

4-12.5 Uncertainty of Typical Gas Fuel Flow Measurement for a Laboratory-Calibrated Orifice-Metering Section

This shows the recalculation of the uncertainty of the natural gas flow rate measurement example, except that the metering section is assumed to be laboratory calibrated at the Reynolds number of the flow. The uncertainty is then significantly reduced due to the better knowledge of the discharge coefficient versus Reynolds number characteristics of the specific metering run.

If it is desired to use the reduced uncertainty number, then the metering section would have to be shipped in one piece and installed closely enough to the time of the test such that removing the orifice plate for pretest inspection, which by definition would change the calibration slightly, would not be necessary. In practice, this is cumbersome and out of the ordinary.

Water calibration of an orifice meter does not increase measuring uncertainty when the meter is used in gas flow measurements. The uncertainty of the ϵ expansion factor of the fundamental flow equation [Eq. (4-12.5)] is the same whether or not the orifice is water calibrated or air calibrated.

$$\epsilon = \frac{q_{m_c}}{q_{m_i}} \qquad (4\text{-}12.5)$$

As shown in para. 4-10, the uncertainty in the compressibility effects is proportional to the ratio of differential pressure and static pressure or the velocity of the fluid. This makes sense because as Mach number increases, compressibility effects also increase, as does the uncertainty in quantifying them.

The uncertainty in the discharge coefficient is treated separately from the uncertainty due to compressibility effects.

Water flow rate is claimed to be measurable in laboratories to within 0.2%. Data points from an orifice meter calibration tend to have much less scatter than for other devices. The correlation coefficients for orifice meter calibrations tend to be very nearly unity. A conservative estimate of the uncertainty of the discharge coefficient uncertainty of a laboratory-calibrated orifice-metering section is 0.25%.

Substituting 0.25% in Table 4-12.2.3 for the uncertainty of the discharge coefficient is shown in Table 4-12.5.

The laboratory-calibrated orifice-metering section has an uncertainty of 0.35% for fuel gas flow rate, reduced from 0.65% if the empirical formulation for the discharge coefficient is used.

4-13 PROCEDURE FOR FITTING A CALIBRATION CURVE AND EXTRAPOLATION TECHNIQUE

4-13.1 Discharge Coefficient Equations Based on Fluid Dynamic Theory

The derivation of the discharge coefficient based on fluid dynamic principles is presented in Appendix I of this Code. To fit an equation suitable for extrapolation, it is critical that it be based on such fluid dynamic theory rather than an empirical formulation based on curve-fits. Thus, the Appendix I equations are used for fitting a calibration curve and extrapolating the calibration beyond the highest Reynolds number that the orifice-metering run was calibrated. Some of the equations in Appendix I are repeated in this section for the user's convenience.

The fluid dynamics–based equation for flange and corner tap orifice-metering runs is as follows:

$$C = C_0 + a\beta^2 + b\beta^4 + d[f(Eu, Re_D)] + e\phi \qquad (4\text{-}13.1)$$

Table 4-12.5 Steady State Uncertainty Analysis for Given Gas Flow–Metering Run With a Laboratory Calibration

Parameter	Parameter Total Uncertainty $\frac{U_x}{X}$,%	Sensitivity Factor on Flow Measurement, S	$\frac{U_x}{X}S$
Discharge coefficient, C	$U_C/C = 0.25$ (laboratory calibration discharge coefficient vs Reynolds number signature used)	1.00	0.25
Expansion factor, ϵ	$\frac{U_\epsilon}{\epsilon} = \frac{4\Delta P}{P}$ $4\left(\frac{4.234}{375}\right) = 0.045\%$	1.00	0.045
Pipe diameter, D	0.2%	0.0	0.0
Orifice diameter, d	0.05%	0.0	0.0
Differential pressure ΔP	0.25%	0.50	0.125
Density, ρ	$U_P/P = 0.25\%$, $U_T = 0.5°F$ $\Rightarrow U_\rho/\rho = 0.27\%$, if perfect analysis Constituent analysis uncertainty: 0.2% Root mean square: 0.34%	0.50	0.17
Total steady state uncertainty	...	...	0.3%

where

C_0 = 0.5957 ± 0.000186 for an uncalibrated orifice-metering run
a = 0.03371 − 0.0239(L) ± 0.002141
b = 0.1496 ± 0.0318
d = 0.2232 ± 0.003417
e = −0.3343 + 0.2241(L) ± 0.0169

$$f(Eu, Re) = \frac{\sqrt{1-\beta^4}}{\sqrt{1-\frac{\beta^4}{(1-30.78Re_D^{-0.5})^2}}} - 1 \quad (4\text{-}13.2)$$

and

$$\phi \equiv \frac{1}{\sqrt{1-\beta^4}} - 1 \quad (4\text{-}13.3)$$

4-13.2 Calibration Fitting Procedure

Combining Eqs. (4-13.1) and (4-13.2) to consider laboratory calibration data,

$$C_{meas} = C_0 + d[f(Eu, Re_D)] \quad (4\text{-}13.4)$$

where C_{meas} is the coefficient of discharge determined from a laboratory calibration at a specific calibration point. Note that the missing terms from Eq. (4-13.1) are included in the measured coefficient of discharge term. Only the Euler/Reynolds number function remains for extrapolation.

Shifting the terms in Eq. (4-13.4) and distributing the value of d,

$$C_0 = C_{meas} - 0.2232\frac{\sqrt{1-\beta^4}}{\sqrt{1-\frac{\beta^4}{(1-30.78Re_D^{-0.5})^2}}} + 0.2232 \quad (4\text{-}13.5)$$

The C_0 term is the difference between the measured coefficient of discharge and the Euler/Reynolds number function.

Once a C_0 term has been computed for all of the given Reynolds numbers and corresponding coefficients of discharge of a calibration, the average of all these is computed by

$$\overline{C}_0 = \frac{\sum_{i=1}^{n} C_{0,i}}{n} \quad (4\text{-}13.6)$$

where

n = the number of calibration points

Table 4-13.3 Example Coefficient Curve Fit and Extrapolation for an Orifice–Metering Run

Tap Set A				Tap Set B			
Re_D	$C_{measured}$	C_0	C_{fitted}	Re_D	$C_{measured}$	C_0	C_{fitted}
664 900	0.607 4	0.606 0	0.607 0	664 900	0.607 6	0.606 2	0.607 0
733 400	0.607 2	0.605 9	0.606 9	733 400	0.607 3	0.606 0	0.607 0
790 000	0.607 2	0.606 0	0.606 9	790 000	0.607 4	0.606 2	0.606 9
801 900	0.607 7	0.606 5	0.606 9	801 900	0.607 8	0.606 6	0.606 9
850 000	0.607 1	0.605 9	0.606 8	850 000	0.607 3	0.606 1	0.606 9
917 400	0.607 0	0.605 8	0.606 8	917 400	0.607 1	0.605 9	0.606 8
975 500	0.606 9	0.605 8	0.606 7	975 500	0.607 0	0.605 9	0.606 8
1 043 300	0.606 8	0.605 7	0.606 7	1 043 300	0.606 7	0.605 6	0.606 8
1 088 000	0.606 7	0.605 6	0.606 7	1 088 000	0.606 8	0.605 7	0.606 7
1 171 000	0.606 6	0.605 6	0.606 6	1 171 000	0.606 6	0.605 6	0.606 7
1 228 900	0.606 6	0.605 6	0.606 6	1 228 900	0.606 5	0.605 5	0.606 7
1 293 800	0.606 3	0.605 3	0.606 6	1 293 800	0.606 2	0.605 2	0.606 6
1 358 000	0.606 5	0.605 6	0.606 6	1 358 000	0.606 4	0.605 5	0.606 6
1 423 700	0.606 5	0.605 6	0.606 5	1 423 700	0.606 6	0.605 7	0.606 6
1 482 900	0.606 1	0.605 2	0.606 5	1 482 900	0.606 2	0.605 3	0.606 6
1 539 100	0.605 9	0.605 0	0.606 5	1 539 100	0.606 0	0.605 1	0.606 6
1 568 000	0.606 3	0.605 4	0.606 5	1 568 000	0.606 3	0.605 4	0.606 6
1 664 300	0.606 3	0.605 5	0.606 5	1 664 300	0.606 3	0.605 5	0.606 5
1 738 300	0.606 1	0.605 3	0.606 5	1 738 300	0.606 1	0.605 3	0.606 5
1 791 000	0.606 0	0.605 2	0.606 4	1 791 000	0.606 1	0.605 3	0.606 5
20 000 000	...	...	0.605 9	20 000 000	...	...	0.605 9
30 000 000	...	...	0.605 8	30 000 000	...	...	0.605 9
40 000 000	...	...	0.605 8	40 000 000	...	...	0.605 8
50 000 000	...	...	0.605 8	50 000 000	...	...	0.605 8
	C_0 (avg) =	0.605 6			C_0 (avg) =	0.605 7	

The fitted calibration curve and the one from which coefficients of discharge for higher Reynolds number values may be extrapolated is

$$C = \overline{C}_0 + 0.2232 \frac{\sqrt{1-\beta^4}}{\sqrt{1-\dfrac{\beta^4}{(1-30.78Re_D^{-0.5})^2}}} - 0.2232 \qquad (4\text{-}13.7)$$

Equation (4-13.7) may be used to fit a calibration curve and for extrapolation of all corner tap or flange tap orifice-metering runs that are built in accordance with this Code.

4-13.3 Sample Calculations of Curve Fit and Extrapolation

Table 4-13.3 shows actual calibration data for an orifice-metering run for both sets of taps. The metering run is 7.9460 in. in diameter with a β ratio of 0.6024. Extrapolations were performed to pipe Reynolds numbers of 20, 30, 40, and 50 million.

As an example of the calculations, the average C_O for Tap Set A is 0.6056. At a pipe Reynolds number of 1,088,000, the fitted discharge coefficient is determined by substituting into equation 4-13.7.

$$C = 0.6056 + 0.2232 \frac{\sqrt{1-0.6024^4}}{\sqrt{1-\dfrac{0.6024^4}{(1-30.78\times 1{,}088{,}000^{-0.5})^2}}} - 0.2232 = 0.6067 \qquad (4\text{-}13.8)$$

The fitted coefficient of 0.6067 is identical, in this case, to the tested coefficient to four significant digits.

For the test point at a pipe Reynolds number of 1,664,300,

$$C = 0.6056 + 0.2232 \frac{\sqrt{1-0.6024^4}}{\sqrt{1-\dfrac{0.6024^4}{(1-30.78\times 1{,}664{,}300^{-0.5})^2}}} - 0.2232 = 0.6065 \qquad (4\text{-}13.9)$$

This time the fitted discharge coefficient is 0.03% different from the measured discharge coefficient of 0.6063.

The data points and fitted curves are shown in Fig. 4-13.3.

To extrapolate to higher Reynolds numbers above the highest calibrated point, the fitted curve is applied by substituting the Reynolds number to which the extrapolation is being made for the Reynolds number term in Eq. (4-13.7).

Notice that in extrapolating to a Reynolds number of 50 million based on the curve-fit, the extrapolated discharge coefficient of 0.6058 is only 0.1% lower than the fitted coefficient at the highest Reynolds number for which the metering run was calibrated (0.6064 at a Reynolds number of 1,791,000). The very low dependence of the discharge coefficient on Reynolds number at higher flows is one of the reasons for the orifice-metering run being an excellent and recommended choice whenever flow must be measured beyond the range of the calibration data.

4-14 SOURCES OF FLUID AND MATERIAL DATA

ASME MFC-3M, *Measurement of Fluid Flow in Pipes Using Orifice, Nozzle, and Venturi.* New York: American Society of Mechanical Engineers; 1989.

Bean, H. S., ed. *Fluid Meters: Their Theory and Application,* 6th edition. New York: The American Society of Mechanical Engineers; 1971.

ISO 5167-1(E), *Measurement of Fluid Flow by Means of Pressure Differential Devices Part 1: Orifice Plates, Nozzles, and Venturi Tubes Inserted in Circular Cross-Section Conduits Running Full.* Geneva: International Organization for Standardization; 1991.

ISO 5167-1(E), *Measurement of Fluid Flow by Means of Pressure Differential Devices Part 1: Orifice Plates, Nozzles, and Venturi Tubes Inserted in Circular Cross-Section Conduits Running Full.* Geneva: International Organization for Standardization; 1998.

Keyser, D. R. *How Accurate Are Flow Calibrations Anyway?* Proceedings of the 1996 International Joint Power Generation Conference, PWR-v.30, ASME publication H01077, pp. 131–137.

Keyser, D. R. *A New, Improved Equation for the Coefficient of Discharge of an Orifice Flow Meter.* ASME Fluids Engineering Division Annual Summer Meeting, Proceedings Paper FEDSM98-5286, June 1998.

Keyser, D. R. The Systematic Uncertainty of Laboratory Flow Calibrations. *Journal of Fluids Engineering* **120:**19–22; 1998.

Reader-Harris, M. J.; Sattary, J. A. The Orifice Plate Discharge Coefficient Equation. *Flow Measurement Instruments* **1:**67-76; 1990.

Reader-Harris, M. J.; Sattary, J. A.; Spearman, E. P. The Orifice Plate Discharge Coefficient Equation — Further Work. *Flow Measurement Instruments* **6**(2):101–114; 1995.

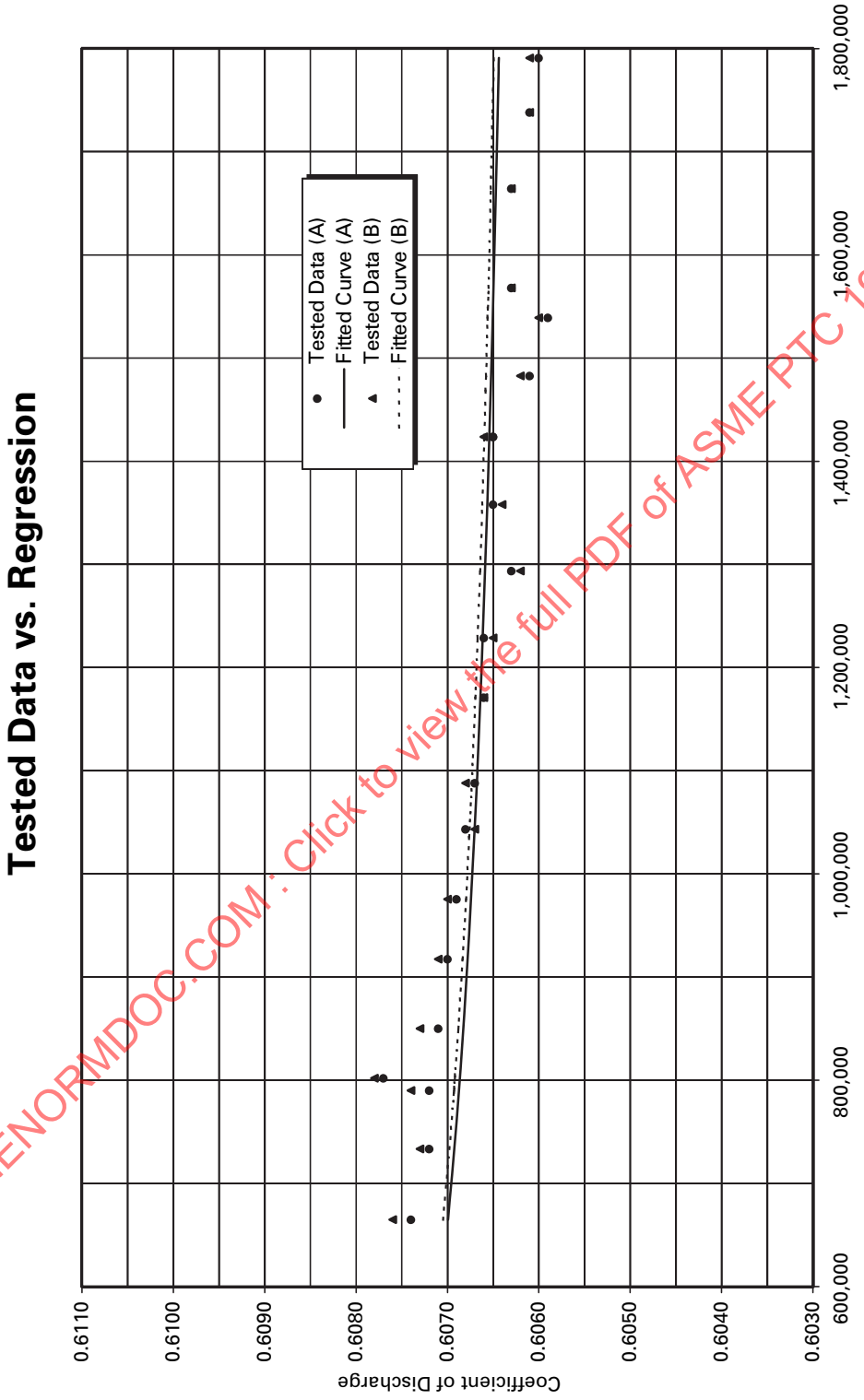

Fig. 4-13.3 Orifice-Metering Run Calibration Points and Fitted Curves (Test Data Versus Fitted Curves)

Section 5
Nozzles and Venturis

This Section must be used in concert with Section 3, which describes the theory of operation necessary for proper flow measurement, and Section 7, which provides guidance and recommendations for the installation of these primary elements into a flow section that then comprises the fluid meter.

Only four types of primary elements are described specifically in this Section.

(a) ASME low β ratio nozzles ($\beta \leq 0.5$)

(b) ASME high β ratio nozzles ($0.45 \leq \beta \leq 0.8$)

(c) ASME throat tap nozzles (only $\beta = 0.46$ or 0.5 have been used)

(d) ASME (classical Herschel) venturi

These are the ones for which the most experience and data exist in the current literature. They are also the ones most often used in Performance Test Codes work. Other nozzles and flow tubes may be used by agreement, and if equivalent care is taken in their fabrication and installation and if they are calibrated in a laboratory with the same care and precision as recommended herein, there is no reason for these fluid-metering sections not serving with equivalent accuracy, repeatability, and reliability.

The highest accuracy and confidence will result if the nozzle is installed in a flow section as shown in Fig. 5-0. The flow section consists of the primary element, the diffusing section if used, the flow conditioner, and the upstream and downstream pipe lengths. The upstream pipe section shall be at least 20 diameters of straight pipe and include an appropriate conditioner recommended in Section 7, which shall be installed approximately 16 pipe diameters upstream of the nozzle. The downstream section shall be at least 10 diameters of straight pipe. This flow meter assembly should be assembled, calibrated, left intact for the duration of the test, and recalibrated (or at least inspected for damage or deposits) after a test. Once calibrated, the flow-metering section should not be disassembled from the prescribed length upstream of the flow conditioner to the recommended length downstream of the nozzle exit. If it is necessary to disassemble the section to inspect it before or during the test, provisions for the accurate realignment and reassembly, such as pins, must be built into the section.

5-1 RECOMMENDED PROPORTIONS OF ASME NOZZLES

Figure 5-1 shows the proportions of each of the three types of ASME nozzles with respect to the throat and pipe inside diameter.

(a) Entrance Section. All ASME flow nozzles are long-radius nozzles that have the shape of a quarter ellipse in the entrance section. The values of the major axis and

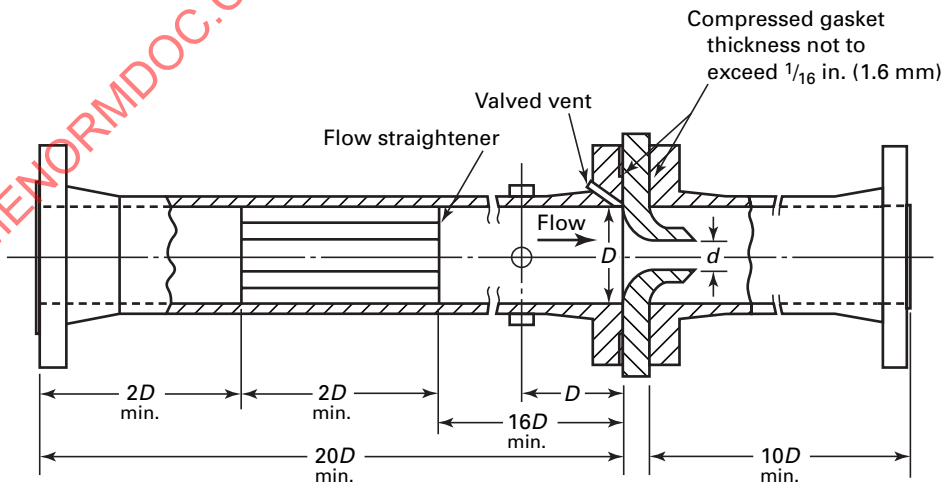

GENERAL NOTE: No obstruction, such as thermocouple wells, backing rings, etc.

Fig. 5-0 Primary Flow Section

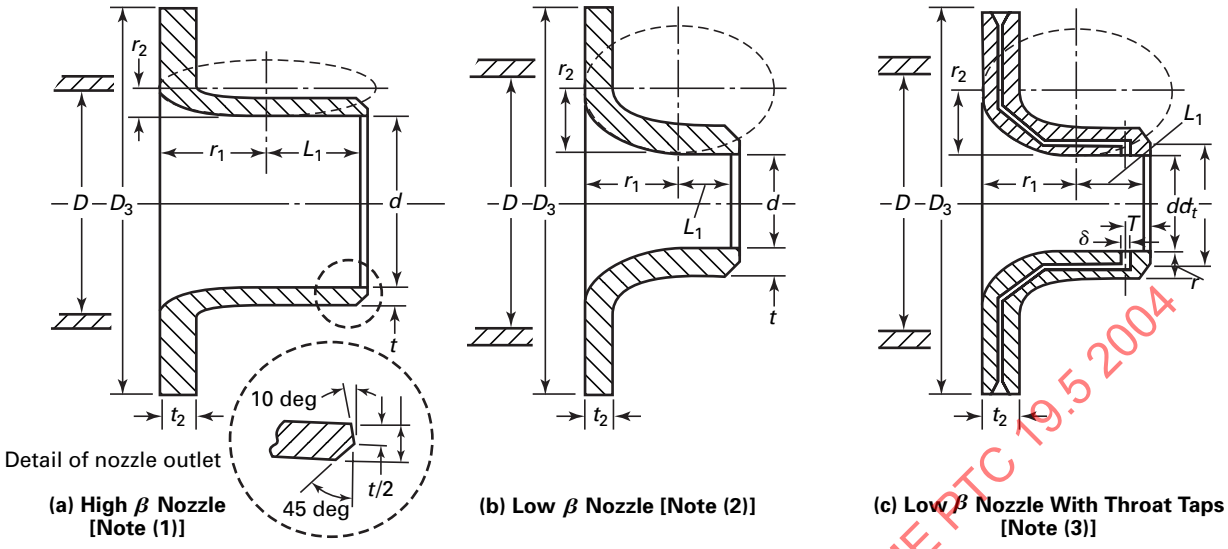

(a) High β Nozzle [Note (1)]

(b) Low β Nozzle [Note (2)]

(c) Low β Nozzle With Throat Taps [Note (3)]

NOTES:

(1) For sketch (a):

$$0.50 \le \beta \le 0.80$$

$$r_1 = D/2$$

$$r_2 = (D - d)/2$$

$$L_1 \le 0.6d \text{ or } \le D/3$$

$$2t \le D[\, - d + 0.13 \text{ in. } (3 \text{ mm})]$$

$$0.13 \text{ in. } (3 \text{ mm}) \le t_2 \le 0.15D$$

(2) For sketch (b):

$$0.20 \le \beta < 0.50$$

$$r_1 = d$$

$$0.63d \le r_2 \le 0.67d$$

$$0.6d \le L_1 \le 0.75d$$

$$0.13 \text{ in. } (3 \text{ mm}) \le t \le 0.5 \text{ in. } (12 \text{ mm})$$

$$0.13 \text{ in. } (3 \text{ mm}) \le t_2 \le 0.15D$$

(3) For sketch (c):

$$0.25 \le \beta < 0.50$$

$$r_1 = d$$

$$0.63d \le r_2 \le 0.67d$$

$$L_1 = 0.75d$$

$$d_t = 1.25d$$

$$t = 0.25d$$

$$t_2 = 1.5 \text{ in. } (38 \text{ mm})$$

$$0.13 \text{ in. } (3 \text{ mm}) \le \delta \le 0.25 \text{ in. } (6 \text{ mm})$$

$$T = 0.25d$$

Fig. 5-1 ASME Flow Nozzles

the minor axis of the ellipse are shown in Fig. 5-1 for each type of flow nozzle. The major center of the ellipse shall be parallel to the centerline of the nozzle within 0.1%. The ellipse shall terminate at a point no greater than D regardless of the value of the minor axis. The profile of the ellipse may be checked by means of a template.

(b) Throat Section. The throat section shall have a diameter d and a length as shown in Fig. 5-1. The measured value of d shall be the average of four equally spaced radial measurements of the throat diameter taken in each of three equally spaced planes along the length of the throat section, covering at least three-quarters of the throat length for a total of 12 diametral measurements. No diameter shall differ by more than 0.05% from the average diameter d. Under no circumstances shall the throat diameter increase toward the nozzle exit. A decrease in diameter d toward the exit end is acceptable if it is within the 0.05% variation allowed from the average diameter.

(c) Exit End Section. The exit end section is shown in Fig. 5-1.

(d) General Requirements for the ASME Flow Nozzles. The distance from the pipe inside diameter to the outside diameter of the nozzle throat shall be greater than or equal to 0.125 in. (3 mm).

It is recommended that a shoulder for centering the nozzle assembly in the pipe be provided. If this shoulder is provided, it should be no larger in outside diameter than $D - 0.060D$ and should be no longer than t_2. In no case shall the centering shoulder cover any part of the downstream tap.

The thickness t shall be sufficient to prevent distortion of the nozzle throat from the stresses of machining, installation, or conditions of use.

The surface of the inner face of the nozzle shall be polished or machined smooth and shall have a maximum roughness of 32 μin. (0.8 μm). The exit end must not have rounding or burrs.

The downstream (outside) face of the nozzle shall be cylindrical and machined smooth or otherwise constructed so as to eliminate any pockets or pits that might retain debris or matter that may be in the fluid.

ASME long-radius nozzles may be made from any material that does not wear easily and remains dimensionally stable with known thermal expansion properties.

5-2 PRESSURE TAP REQUIREMENTS

ASME long-radius nozzles shall use taps that conform to Section 7. The upstream tap shall be located in the pipe wall at a distance D ($+0.2D$, $-0.1D$) from the plane of the inlet face of the nozzle. Nozzles without throat tap shall use wall taps located at $0.5D$ ($\pm$ $0.01D$) from the plane of the inlet face of the nozzle. Under some installation geometries, this specification places the tap downstream of the nozzle exit plane and that is not permitted. Under no circumstances may any part of the downstream tap be located downstream of the nozzle exit.

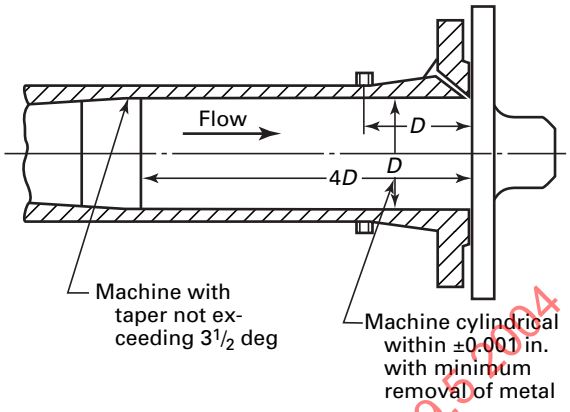

Fig. 5-3-1 Boring in Flow Section Upstream of Nozzle

5-2.1 Throat Tap Nozzles

It is recommended that this nozzle be manufactured with four throat taps located 90 deg apart. The pressure taps shall be between ⅛ in. (3 mm) and ¼ in. (6 mm) in diameter and at least 2 diameters deep. They shall be machined perpendicular to the bore surface, have sharp corners, and be free from nicks, burrs, scratches, or wire edges. The surface finish should be 4 μin. or better and be free from ripples, scratches, and burrs. The holes should be drilled and reamed before the final boring and polishing of the throat section. A plug may be pressed into the hole and removed after this final finishing of the throat. Any slight burr may be removed by rolling a tapered piece of maple around the edge.

5-3 INSTALLATION REQUIREMENTS

In addition to the recommendations given in Section 7, the pipe internal surface roughness should not exceed 0.001 in. (25 μm) over an area of $4D$ preceding and $2D$ following the plane of the inlet face of the nozzle. If boring and/or honing are required, such machining should extend for a distance of at least $4D$ upstream and $2D$ downstream of the plane of the inlet face of the nozzle. The machined portion shall be tapered into the unmachined portion of the pipe at an included angle of less than 3½ deg. The depth of the machining should be the minimum required to obtain the surface finish. The machined inside diameter D of the pipe should be uniform throughout the machined length ±0.25%. All machining should be accomplished after all necessary welding of flanges, pressure taps, or other attachments has been accomplished (see Fig. 5-3-1).

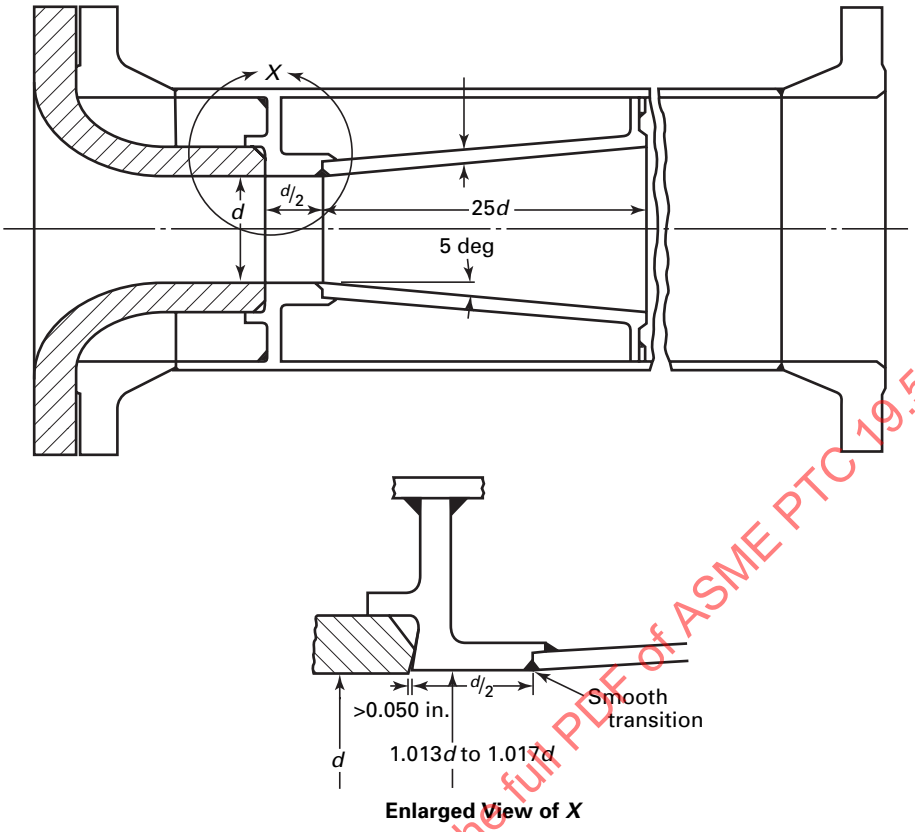

Fig. 5-3-2 Nozzle With Diffusing Cone

(a) Flanged Installation. ASME nozzles shown in Fig. 5-0 are designed to be installed between raised face pipe flanges. Nozzles may also be used with other styles of flanges if such use does not interfere with the flow.

(b) Installation Without Flanges. ASME nozzles may also be installed directly in pipe by welding or pinning the nozzle to the pipe inside diameter. If such a method is used, care should be taken to ensure against any protrusions into the flow upstream or downstream of the nozzle.

(c) Centering. The nozzle shall be manufactured so that the clearance between the nozzle shoulder and the pipe inside diameter shall be uniformly greater than 0.03 in. (0.8 mm) of the pipe into which it is installed.

(d) Straight Piping Lengths. The upstream and downstream straight piping lengths are the same for ASME nozzles as for orifice plates, specified in Section 4.

(e) Flow Conditioners. One of the appropriate flow conditioners discussed in Section 7 should be used for best repeatability between laboratory and field test installations.

(f) Diffusers. A diffuser section may be added to the exit of the nozzle to reduce the amount of permanent pressure loss. It must be installed in accordance with Fig. 5-3-2. This transforms the throat tap nozzle into a nozzle-venturi, and this primary element must be calibrated and used with the diffuser always attached.

5-4 COEFFICIENT OF DISCHARGE

The coefficient of discharge, which is defined and explained in Section 3, has the same form for all nozzles and venturis because the physics of the flow in all such devices is similar. There is a smooth and gradual reduction in flow area from the pipe size to the throat size, and then a variety of transitions returning the flow to the pipe size. The coefficient of discharge is influenced by three major physical effects of decreasing importance: Bernoulli's equation, boundary layer thickness at the downstream pressure tap, and any tap effects or errors. The first is discussed in detail in Section 3. The effect of the boundary layer is derived and discussed thoroughly elsewhere [1–3]. The physical concept is simply that the displacement boundary layer forms a ring around the cylindrical throat section that subtracts flow area from the dry area measured and corrected for conditions of use before it is calibrated and used. The ratio of the constricted area actually available for the flow to the dry measured area (corrected for the temperature and pressure of use or calibration) is in fact the coefficient of discharge.

The error caused by the pressure tap is caused by the same physics that result in drag on an aerodynamic body with such a hole in its surface. Just as the coefficient of drag of a hole is constant over the range of Reynolds numbers within the experimental uncertainties of their measurements, likewise the effect of the tap is constant over the range of flow measurement Reynolds numbers, according to a very large body of data examined by the ASME PTC 19.5 committee.

(a) Equation for the Coefficient of Discharge. The equation for the coefficient of discharge becomes the sum of three major terms: a constant, a tap effect, and a complicated function of the boundary layer displacement thickness. The constant is unity, because in the practical matching of real flows to the ideal flow assumptions made in applying Bernoulli's equation in Section 3, these ideals are approached asymptotically as the Reynolds number approaches infinity. The tap effect is a constant added to unity, and its average value is 0.0054 based on copious data [3]. The complicated function of the boundary layer depends primarily on several Reynolds numbers and the ratio of the laminar/turbulent shape factors. Those Reynolds numbers are

(1) based on the tap diameter

(2) based on the distance from the entrance of the nozzle to the plane of the downstream pressure measurement

(3) at which transition from laminar to turbulent boundary layers is determined to begin

For any given geometry of a primary element (e.g., an ASME throat tap nozzle), all of these become proportional to the throat Reynolds number, and these proportionality constants are included in the equations below.

The transition Reynolds number may vary with different installations because it depends on the intensity of the upstream turbulence, which depends in part on the pipe roughness and upstream fittings. A good estimate of this value in the flow meter installations prescribed herein is about 500,000. Transition to fully turbulent boundary layers does not occur at a single value; instead, it extends over quite a range, often up to a throat Reynolds number of 20,000,000. The major part of its effect occurs between 1 and 3.5 million. The following equation is applicable for throat Reynolds numbers above 1,000,000 and may be used, if necessary, down to 700,000 depending on transition.

$$C = 1 + \text{tap effect} - \frac{T}{Re_d^{\,1/5}} \times \left\{1 - \frac{Re_t}{Re_d}\left[1 - \frac{(H_T/H_L)^{5/4}\,(L/T)^{5/4}}{Re_t^{\,3/8}}\right]\right\}^{4/5} \qquad (5\text{-}4.1)$$

For the dimensions and proportions of ASME nozzles, this becomes

$$C = C_o - \frac{0.185}{Re_d^{\,1/5}}\left[1 - \frac{361{,}239}{Re_d}\right]^{4/5} \qquad (5\text{-}4.2)$$

where, in Eq. (5-4.1),

H_L = laminar shape parameter (2.59)
H_T = turbulent shape parameter (1.28)
L = laminar slope (numerical value from [2] = 6.88)
Re_t = transition Reynolds number
T = turbulent slope (0.185)

For ASME nozzles without throat taps, there is zero correction to be added in their use. The throat tap, being in the area of the highest velocity, is very sensitive to very small defects in its shape and to any damage immediately upstream; whereas, in the case of the wall tap nozzle arrangement, the downstream pressure tap is in a relatively quiet back eddy in the flow, which is in communication with the exit flow of the nozzle.

(b) Nozzle Calibration. The main purpose of the flow calibration is to determine by measurements the leading constant term in Eq. (5-4.2). The flow calibration laboratory selected for this work should be reputable and responsible, its instrumentation should be traceable to national standards, and it should be agreeable to all parties.

At least 20 calibration points should be run over the widest range of Reynolds numbers possible, which applies to the performance test. The spacing of the points is recommended to be in equal intervals of $Re_d^{-1/5}$. The calibration curve should always maintain the same shape as shown in Eq. (5-4.2), since the variation of the coefficient of discharge with Reynolds number is well established both theoretically and empirically. This is the form of equation to use whenever an extrapolation is necessary beyond the calibration data to higher operating Reynolds numbers during the test.

(c) Procedure for Fitting and Evaluating the Curve for the Coefficient of Discharge

(1) Determining the Average Value of the Leading Constant C_o. For each calibration datum, substitute into Eq. (5-4.2) the throat Reynolds number and the measured coefficient of discharge and solve for C_o.

$$C_o = C_{\text{meas}} + \frac{0.185}{Re_d^{\,1/5}}\left[1 - \frac{361{,}239}{Re_d}\right]^{4/5} \qquad (5\text{-}4.3)$$

Calculate the arithmetic mean of each of these C_o; then that is the leading constant term for the calibration curve for that nozzle. Substitute that value into Eq. (5-4.2) and the result is the fitted calibration curve for that nozzle. This curve may be used for extrapolation if necessary without additional uncertainty.

Calculate the standard deviation of the mean for the C_o data; that will be required for the random uncertainty portion of the calibration curve when ASME PTC 19.1 is applied.

(2) Determining Whether the Calibration Curve Parallels the Theoretical Curve. For each of the calibration data, calculate the differences between C_{meas} and the fitted curve calculated in (1) above and plot each of these

differences versus their Reynolds number. (It would be more correct to plot them versus $Re_d^{-1/5}$, but the necessary condition here is a line of zero slope, a horizontal plot. Such an ideal result is unlikely to occur statistically.) All that can be done is to determine whether or not there are statistically justifiable grounds for stating that a calibration curve is not parallel to the theoretical curve [Eq. (5-4.2)]. Next, determine the best-fit straight line through the differences, in the least squares sense, and examine the slope of this curve. It most likely will not be exactly zero; however, it can be determined whether or not it is statistically different from zero. If it is probably not different from zero statistically, one must assume the slope to be zero; therefore, the nozzle calibration is indeed parallel to the theoretical curve.

To determine such parallelism, calculate the confidence limits for the slope of the aforementioned linear regression. These confidence limits give a ± range about the calculated slope. If this range includes zero, the nozzle calibration curve must be accepted as parallel to the theoretical curve. These calculations are explained in detail in ISO-7066-Part 1 [4].

Denoting the calculated, best-fit slope by b,

$$\text{The variance of } b = \frac{\left(\begin{array}{c}\text{variance of the}\\ \text{data from}\\ \text{the best fit line}\end{array}\right)(n - 2dof)}{(n-1)\left(\begin{array}{c}\text{variance of the}\\ \text{Reynolds number}\\ \text{of the calibration}\end{array}\right)} \tag{5-4.4}$$

where

dof = degrees of freedom
n = the number of calibration points

The square root of the variance is the standard deviation of the slope, which, when multiplied by the appropriate Student's t for 95% confidence, provides the desired range for the slope.

(d) Coefficient of Discharge for the Regime of Wholly Laminar Boundary Layers. This equation is valid from very low Reynolds numbers up to about 500,000 for ASME nozzles and venturis.

$$C = C_o - 6.88\ Re_d^{-1/2} \tag{5-4.5}$$

(e) Coefficient of Discharge for the Regime of Partly Laminar and Partly Turbulent Boundary Layers. This is a very narrow regime that could be ignored except that it provides the physics of the beginning of the transition hump often discussed in the literature in connection with throat tap nozzle calibrations. It had been assumed that, once the data were over the hump, the flow was in the fully developed turbulent boundary layer regime.

$$C = C_o - \frac{6.88(Re_t^{-1/2})}{Re_d} \tag{5-4.6}$$

in which Re_t is the throat Reynolds number at which transition begins, usually between 500,000 and 800,000, which is also approximately the range of validity for this equation.

(f) Uncertainty of the Coefficient of Discharge

(1) Calibrated Flow Sections. The uncertainty of a calibrated flow section shall be determined using the methods in ASME PTC 19.1, Test Uncertainty, applied to both the laboratory facilities and the calibration data. Normative values of the bias uncertainties found between calibration laboratories that have participated in transfer standard comparisons are

(a) ±⅓% for water calibrations (when everything is ideal, perhaps ±¼%)

(b) ±½% for hydrocarbon liquids and viscous fluids

(c) somewhere between these two values for well-known gases

(2) Uncalibrated Flow Sections. When the nozzle is made and installed in accordance with this Supplement and when β and the Reynolds number are assumed to be known without error, the uncertainty in the coefficient of discharge is as follows:

(a) ASME high β with wall taps, ±1%; ±1.5% for $\beta > 0.7$

(b) ASME low β with wall taps, ±1%

(c) ASME throat tap nozzle, always calibrated

(g) Unrecoverable Pressure Losses. For ASME nozzles, the fraction of the signal differential pressure that is permanently lost may be estimated by

$$\frac{\text{pressure loss}}{\text{differential pressure}} = 1 + 0.014\beta - 2.06\beta^2 + 1.18\beta^3 \tag{5-4.7}$$

5-5 THE ASME VENTURI TUBE

The venturi tube combines into a single unit a short, constricted portion between two tapered sections and is usually inserted between two flanges in a pipe. Its purpose is to accelerate the fluid and temporarily lower its static pressure. Suitable pressure connections are provided for observing the difference in pressures between the inlet and the constricted portion or throat.

The proportions of venturi tubes used for metering liquids or gases are usually substantially the same as those originally adopted in 1887 by its inventor, Charles Herschel. A typical form of construction is shown in Fig. 5-5. Starting at the upstream flange, the first portion is a short, cylindrical inlet that is a continuation of the upstream pipe line. This part is either machined inside or cast smooth so that its diameter can be accurately

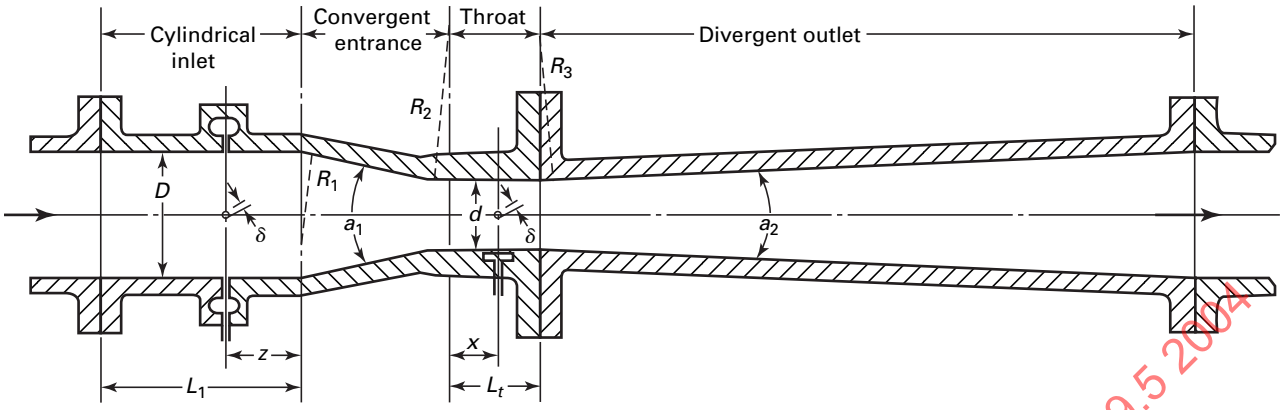

$$L_1 \geq D$$

$$z = D/4$$

$$L_t = D \pm 0.05d$$

$$x = d/2$$

$$R_1 = 1.375D \pm 20\%$$

$$R_2 = 3.625d \pm 0.125d$$

$$5d \leq R_3 \leq 15d$$

$$a_1 = 21 \text{ deg} \pm 1 \text{ deg}$$

$$7 \text{ deg} \leq a_2 \leq 15 \text{ deg}$$

Pressure tap size: $^{5}/_{32}$ in. (4 mm) $\leq \delta \leq$ $^{25}/_{64}$ in. (10 mm) and
Upstream tap: $\delta \leq 0.1D$ or
Downstream tap: $\delta = 0.13d$

Fig. 5-5 Profile of the ASME Venturi

determined. The static pressure of the fluid at the inlet may be obtained through a single side-wall hole, preferably there may be several holes evenly spaced around the inlet section, or it may be measured individually.

Following the preliminary straight part is the entrance cone that has an included angle of 21 deg. The straight and converging parts are joined by a curved surface. The entrance cone leads to the short cylindrical throat that is accurately machined. The pressure taps in the throat measure static pressure in the throat. The transition from the entrance cone into the straight throat is rounded off by an easy tangential curve to avoid the resistance caused by a sharp corner and also to preclude the possibility that the fluid might break away from the wall at high speeds and not fill the throat completely. The diameter of the throat is usually between one-third and three-fourths of the entrance or pipe line diameter, and in its vicinity there is usually located a joint, a handhole, or even a manhole in the large sizes, which permits inspection of the condition of the throat and side holes and facilities measurement of the throat diameter.

The end of the throat leads, by another easy curve, into the exit or diffuser cone, which has an included or total angle between 7 deg and 15 deg. This terminates in the outlet flange, or other type of end, for connecting the venturi to the pipeline.

Small venturi tubes are commonly made of brass, bronze, and stainless steel and smoothly finished all over the inside to reduce the resistance. Larger venturi tubes are usually of cast iron, the throat and sometimes the straight entrance portion being lined with brass, bronze, or stainless steel and machined to a smooth finish. Very large venturi tubes, up to 20 ft in diameter,

have been made almost entirely of smooth-surface concrete with only the throat being of finished metal.

5-6 DESIGN AND DESIGN VARIATIONS

Small variations from the proportions shown in Fig. 5-5 may or may not affect the flow measurements appreciably. For example, small changes of the angle of convergence of the entrance cone from the usual value of about 21 deg may be expected to have some slight influence on the discharge coefficient, but very little information is available on this point. An essential feature is that the transition from the cone to the throat be made by an easy tangential curve.

The angle of the diverging cone does not influence the discharge coefficient, which is not appreciably affected by removing the exit cone altogether. The original 5 deg to 7 deg total angle was adopted because it gives the lowest resistance at ordinary speeds of flow and ratios of throat diameter to pipe diameter commonly used at that time. If the amount of the overall drop is not important, the diverging cone can be omitted (i.e., equivalent to an exit cone angle of 180 deg) and the loss characteristics of such a venturi tube will resemble those of a flow nozzle. However, when the cone angle exceeds about 15 deg, the differentials produced are quite unsteady.

(a) Entrance Section. The entrance section shall have an inside diameter D and shall be at least one pipe inside diameter long. The inside diameter of the entrance section shall not vary from the matching pipe inside diameter by more than $0.01D$ and it shall be concentric with the matching upstream pipe when examined visually. The inside diameter of the entrance section shall be measured in the plane of the pressure taps at a minimum of four equally spaced (approximately 45 deg) measurements passing through the centerline of the section. These measurements must be made so that at least one measurement is taken at, or near, each pressure tap. No inside diameter measurement shall vary from the average of these measurements by more than ± 0.5%.

(b) Convergent Section. The convergent section shall be conical with an included angle of 21 ± 1 deg. The profile of the convergent section may be checked with a straight template and shall not deviate from the template by more than $\pm 0.005D$.

(c) Throat. The throat shall have an inside diameter D that shall be cylindrical to within ±0.1% of the average inside diameter. The throat shall be parallel with the centerline of the venturi tube assembly. The throat begins at the radius R_2 and ends at the radius R_3, and it has a length of $1.0d \pm 0.05d$. The radii at each end of the throat shall be as provided in Fig. 5-5, and, compared with the template, they shall not deviate from the template by more than $0.02d$.

The inside diameter d shall be measured in the plane of the pressure taps at four equally spaced radial measurements passing through the centerline of the throat. The location of these measurements may be made beginning at any point on the internal circumference as long as at least one measurement is taken at or near each pressure tap. No inside diameter measurement shall vary from the average of these measurements by more than ± 0.1%.

(d) Divergent Section. The divergent section shall be conical and shall have an included angle between 7 deg and 15 deg. It is recommended that an angle of 7 deg be chosen for minimum unrecoverable pressure loss. The smallest diameter of the divergent section shall be not less than the inside diameter d. There must be no protrusion, step, or shoulder impeding the flow from the throat. The larger end of the divergent section shall have an inside diameter D and shall terminate at the matching pipe inside diameter, unless truncated as allowed by agreement. When furnishing venturi tubes without flanged ends, the venturi may be supplied with an exit cylinder section attached to the divergent section to accommodate installation to the matching downstream pipe.

A venturi tube may be shortened by up to 35% of the divergent section length by truncation. A venturi tube is truncated when the inside diameter of the venturi outlet end is less than the diameter D. Such truncation may increase the unrecoverable pressure loss.

(e) Roughness. The entrance section, convergent section, and divergent section shall have a maximum roughness of 20 in. (0.5 m), except that, for the larger sizes, the roughness relative to the diameter should be the same or that recommended for a throat tap nozzle.

(f) Materials. Venturi tubes must be manufactured from a material that does not wear excessively and remains dimensionally stable in continued use. It is recommended that the convergent section and the throat be manufactured from one piece of material. If this is not possible, it is recommended that either one of the following applies:

(1) The throat section is machined after it is joined to the convergent section.

(2) The throat section is of sufficient length to allow for the machining of the radius R_2 and a portion of the convergent angle, requiring the joining of the convergent section to the throat at a diameter greater than d.

(3) In joining the divergent section to the throat, care shall be taken to ensure that the divergent section is centered with the throat. There shall be no steps between the inside diameters of the two parts.

5-7 VENTURI PRESSURE TAPS

(a) Number of Taps. A minimum of two upstream and two throat taps shall be provided. It is recommended

that four upstream and four throat taps be provided and that they be individually measured.

(b) Tap Location. Upstream taps shall be located on the entrance section at a distance of $0.50D$ ($+0.0D$, $-0.25D$) from the beginning of the convergent section. Throat taps shall be located at $(0.5 \pm 0.02)d$. Both upstream and throat taps shall be located at equal spacings (i.e., 180 deg or 90 deg apart).

(c) Tap Hole Edge. The edge of each pressure tap hole shall be square, sharp, and free from burrs or nicks at the inner surface.

(d) Tap Length. The pressure tap hole shall be circular and cylindrical for a length at least 2.5 times the diameter of the hole measured from the inside diameter of the venturi.

(e) Tap Size. The recommended size of the tap hole is between 0.15 in. (4 mm) and 0.4 in. (10 mm) inclusive, but not greater than $0.1D$ for upstream taps and $0.13d$ for throat taps. It is also recommended that pressure taps be as small as possible while still considering the possibility of tap hole plugging by contamination.

(f) Taps With Annular Chambers. The cross-sectional area of the annular chamber, if used, should be greater than half the sum of the pressure tap hole areas. It is recommended that the annular chamber be doubled in cross-sectional area if the venturi is to be installed with insufficient upstream piping from a disturbance that may cause swirls or vortices in the measured fluid.

5-8 DISCHARGE COEFFICIENT OF THE ASME VENTURI

The discussion of coefficients of discharge in para. 5-4, in particular those parts relevant to throat tap nozzles, applies equally well to the venturis. This is because it is a primary element with a set of throat taps, and the same physics apply to this design. If the ratio of the boundary layer thickness to the diameter is in the same range as that found for throat tap nozzles, the operating range of the Reynolds number based on tap diameter is of similar magnitude, and the remaining flow conditions are similar, the coefficient of discharge should be identical to the equations in para. 5-4 relevant to the appropriate range of throat Reynolds numbers. These equations are the best estimate for the coefficient of discharge for an uncalibrated venturi. Since it is a primary element with throat taps, the leading coefficient C_o should be 1.0054; recent data on a few venturi calibrations support this statement.

In cases such as very large venturis, for which the similarity proportions with the throat tap nozzle are found not to hold, reference [1] provides the theory and practical application to estimate the coefficient of discharge.

(a) Uncertainty of the Coefficient of Discharge. Again assuming the upstream and throat diameters and the Reynolds numbers are known without error, the bias uncertainty of an uncalibrated venturi is about ±0.7%. For a calibrated venturi, para. 5-4(f) applies.

(b) Overall Pressure Loss for an ASME Venturi. The static pressure along a venturi tube decreases rapidly from its maximum at the entrance to its minimum at the throat, after which it increases, rapidly at first and then more slowly, until its second maximum value is reached near the junction of the exit cone and the pipe. This second maximum is lower than that at the entrance by approximately 10% to 20% of the pressure difference between the inlet maximum and the throat minimum. In other words, between 80% and 90% of the venturi differential is recovered in the diverging cone. As previously indicated, the function of the diverging cone is to decelerate the fluid steam uniformly and with minimum turbulence so that the outlet maximum pressure will approach the inlet pressure as nearly as possible. This restoration is imperfect. The percentage of pressure loss (i.e., the 10% to 20% mentioned above) decreases as the speed of flow increases or as the size of the venturi tube is increased.

5-9 INSTALLATION REQUIREMENTS FOR THE ASME VENTURI

The venturi has been criticized for being a long meter; however, when its length is combined with the upstream lengths given in Table 7-2.4-2 so that no additional uncertainty accrues, its length is less than that recommended for a flow nozzle. For the example of a 0.5β venturi, this total length is 7.85 pipe diameters compared to the 30 diameters of a nozzle flow section. This is because the convergent cone is effective as a flow conditioner for the throat section, although the venturi, like all meters, is sensitive to swirl. If swirl is expected or known to exist, an appropriate conditioner reputed to reduce swirl should be selected and installed as discussed in Section 7.

(a) Upstream Line Diameter. The average upstream pipe diameter, measured in at least four places, shall be within ±0.25% of the average diameter for at least $2D$, measured upstream from the entrance section.

(b) Roughness of Upstream Pipe. The upstream pipe shall not have a relative roughness k/D greater than 10^{-3} for at least $2D$ from the upstream end of the entrance section of the venturi tube.

(c) Alignment of the ASME Venturi. The offset between the centerlines of the upstream pipe and the venturi shall be less than $0.005D$ and shall be aligned with the upstream piping to within 1 deg.

(d) Recommended Lengths of Straight Piping for ASME Venturis. Paragraph 7-2.4 and Table 7-2.4-2 give details regarding the piping installation requirements for these meters.

5-10 SOURCES OF FLUID AND MATERIAL DATA

[1] Murdock ; Keyser, D. R. A Method for Extrapolating Calibration Data for Flow Nozzles. ASME/Joint Power Generation Conference, 85-JPGC-PTC-2, October 1985.

[2] Murdock ; Keyser, D. R. Theoretical Basis for Extrapolation of Calibration Data of PTC 6 Throat Tap Nozzles. *Journal of Engineering for Gas Turbines and Power* **113**: 228–232; 1991.

[3] Murdock ; Keyser, D. R. A Method for the Extrapolation of Calibration Data of PTC 6 Throat Tap Nozzles. *Journal of Engineering for Gas Turbines and Power* **113**: 233–241; 1991.

[4] ISO 7066, Part 1, *Assessment of Uncertainty in the Calibration and Use of Flow Measurement Devices — Linear Calibration Relationships*. Geneva: International Organization for Standardization; 1989.

Section 6
Pulsating Flow Measurement

6-1 INTRODUCTION

There are basically two kinds of unsteady flow: transient flow and oscillating flow. In Performance Test Codes work there is practically no interest in transient flow, since almost all tests are conducted at a steady state operating point for the system under test. Slowly varying flow can be measured using steady state theory and equations, so long as it can be shown that the flow is quasisteady; the rate of variation is negligible relative to the steady flow terms in the equation. Rapid transient flow is not discussed in this Section.

Nearly periodic pulsating flow is a fact of life in many performance testing situations in the field, and this is the primary focus of this Section. These situations fall into two broad categories: those in which pulsating flow is an unpleasant surprise and those in which it is expected to occur during the test. When it is an expected condition of the test, the flow measurement system can be designed to defeat or attenuate the effects of the pulsating flow on the performance measurement. It may be made responsive enough to the flow rate so that the metering indication is correct at each instant, and the additional inaccuracy is within the goals for the test.

On the other hand, the piping system may be designed to attenuate such pulsations with the installation of low-pass filters, gas-filled accumulators in liquid systems, or volume-choke flow pulsation dampers in gas flow systems. Numerous passive filter designs are effective for various pump types operating at various speeds. Design of such passive filters with regard to their volume, restrictor size, and location in the piping for the expected frequency range is a well-covered subject. Also, there are many flow measurement techniques that are quite insensitive to pulsating flow, which may be an alternative in certain testing situations. These include electromagnetic flow meters, tracer techniques, some positive displacement mechanical meters, and sonic flow nozzles.

When pulsating flow is an unpleasant surprise, the test engineer often has no choice but to assess by how much his test uncertainty, both bias and random, has increased as a consequence of nonsteady flow. Sometimes minor modifications to the flow-metering system can ameliorate the problem, such as using a faster-responding transducer or changing the length of the pressure-sensing lines to a differential pressure transducer. However, installing restrictors in these pressure-sensing lines to reduce pulsations cannot be permitted.

There are only two favorite types of flow meters for which there are sufficient reported studies to provide any useful guidance: turbine meters and, more commonly described, all types of orifices, nozzles, and venturis.

6-2 ORIFICES, NOZZLES, AND VENTURIS

Actually, almost all of the published investigations have been concerned with orifices. However, since the physical equations are fundamentally identical for all types of head class meters, it is assumed that the conclusions and results concerning orifices apply as well to the others. Summaries of and excerpts from technical papers and articles have been selected because of their relevance and applicability to performance testing. A more complete listing of source publications is at the end of this Section.

The very first mistake to avoid is the square root error, which is the difference between the flow calculated using the square root of the mean Δp instead of correctly averaging the individual square roots of each Δp observed during the test period. The error arises as follows: in Section 3 Bernoulli's equation is derived, which relates the differential pressure signal to the square of the velocity, the square of the flow. Averaging the differential pressures equates to averaging the square of each observed instant flow, which result is not the same as the average flow unless the observed variations are negligible.

6-2.1 History

Efforts to measure unsteady flow fall broadly into three categories. The first included attempts to isolate, attenuate, or remove the pulsations in the observed pressures or flows. Since this approach is often unsuccessful, many attempts have been made to define a pulsation number or pulsation threshold over which it would be unwise to measure. An even more optimistic third group hopes to devise or discover a correlation between such a pulsation number and actual oscillating flow, or at least its true temporal mean. Approximately half of these investigations concern flow at low Reynolds number often with interest in biomedical application, which is of lesser interest to performance testing.

Among the pulsation numbers published, two have been experimentally investigated in some detail: the

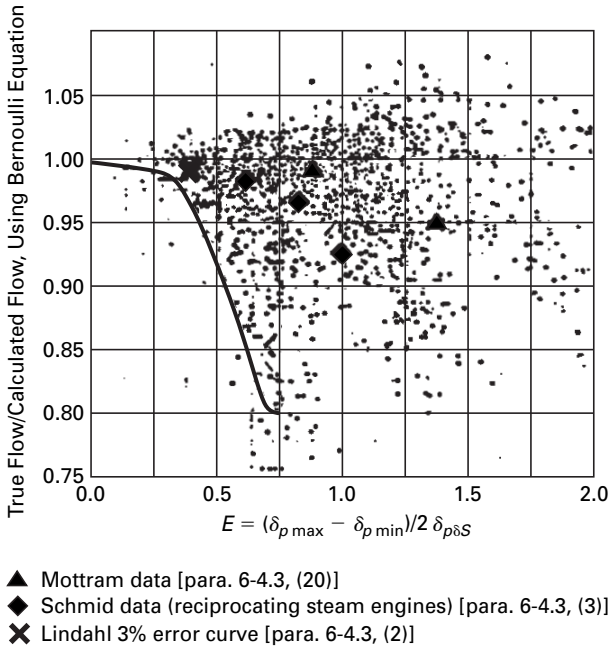

Fig. 6-2.1 Measured Errors Versus Oscillating Differential Pressure Amplitude Relative to the Steady State Mean

Hodgson number and the Strouhal number. The Hodgson number is an attempt to relate the fluid volume and pipe length between the meter and the source of pulsations (such as the pump, tank, or valve) to the error induced by these pulsations. Some authors have decided that the Hodgson number might be useful as a pulsation threshold but that it does not correlate well with the observed errors. Others have analyzed the Hodgson number further and have found it to be proportional to the product of the Strouhal number along with other geometric and parametric ratios.

The possibilities of applying the Strouhal number to pulsating flow have generated great interest, which has resulted in several serious attempts at correlation. The Strouhal number is, after all, the only well-defined, experimentally verified, dimensionless fluid dynamic number incorporating an oscillation frequency. Unfortunately, none of the experimental investigations have been successful in discovering a correlation between the Strouhal number and their unsteady flow results. With the benefit of perfect hindsight, this is perhaps not so surprising. A physically meaningful dimensionless number must represent or summarize a phenomenon or be derived from relevant equations of physics; the equations to which the Strouhal number applies is not the drag of immersed bodies. The conclusion must be that future efforts at correlating unsteady flow errors and observations with Strouhal number will be fruitless also because a correlation is irrelevant.

Table 6-2.1
Error Threshold Versus Relative Amplitude of ΔP

E, ratio	Error, %
0.167	0.25
0.187	0.34
0.215	0.5
0.268	1.0
0.327	2.0
0.422	5.0

The problem of measuring unsteady flow is serious; this is generally appreciated. However, that the errors can be surprisingly large is less well known. There is not an abundance of useful data in the literature, but much of what exists has been summarized in Fig. 6-2.1. This previously published figure [1] has superimposed data that were published in other reports. It is strikingly apparent that the preponderance of error is such that the true flow is less than calculated from the Bernoulli equation using the mean square root of the observed pressure differentials. Furthermore, if an attempt were made to fit a curve through that cloud of data less than unity, at least three branches would be required. Interestingly enough, the superimposed data seem to lie along each of the three branches. Why there are three branches remains unknown at this time; if one thing is certain, it is that error and the amplitude of the differential pressure oscillations are not a sufficient number of parameters to describe this phenomenon. One would like to know also the frequency, phase angle, and fluid properties at which these observations were made. The solid curve on the left of Fig. 6-2.1 represents an attempt at defining an empirical pulsation threshold. It is merely one tail of a normal distribution curve fitted to include 90% of the data for E between zero and 0.75. The equation of this curve is

$$\text{Error} = 0.2 \exp \frac{\left[-(1.5 - 2E)^2\right]}{0.3103} \qquad (6\text{-}2.1)$$

The error calculated from the curve versus some observed amplitudes of differential pressure is presented in Table 6-2.1. No recommendations are being made concerning the use of this curve; its purpose is only to show the progression of observable magnitudes for various error thresholds in the measurement of unsteady flow.

6-2.2 Theoretical Background

The Bernoulli equation usually is derived from either the Navier-Stokes equation or from the principle of conservation of energy. The equation preceding it in the derivation is the Euler equation, which explicitly includes temporal variation.

$$\frac{\partial V}{\partial t} + \frac{V \partial V}{\partial s} + \frac{1}{\partial} \frac{\partial \rho}{\partial s} = 0 \qquad (6\text{-}2.2)$$

With the assumption of steady state, the first term becomes zero and this differential equation can be integrated along any streamline from the upstream tap to the downstream tap to yield the Bernoulli equation. Without the assumption of steady state, but using the assumptions of incompressible and one-dimensional flow,

$$Q(t) = V(s,t)\, A(s) \qquad (6\text{-}2.3)$$

Equation (6-2.3) can be integrated along a streamline between the upstream and downstream tap as follows:

$$\frac{\partial Q}{\partial t} \int_{S_1}^{S_2} \frac{\partial S}{A(s)} - \left(\frac{1}{A_2^2} - \frac{1}{A_1^2}\right) \frac{Q^2}{2} = \frac{1}{\rho}\left[\rho_1(t) - \rho_2(t)\right] \qquad (6\text{-}2.4)$$

This is the proper theoretical point of departure for one-dimensional, inviscid, unsteady flow analysis. Sources using other approximations to calculate pulsating flow errors have been found to deduce incorrect conclusions. Equation (6-2.4) must be solved numerically.

There is a quantitative difference between two cases. In the first case, differential pressure oscillations are driving the flow. In the second case, the flow is unsteady, consequently the differential pressure oscillates. In the first case, the error is positive and increases in proportion to the $\frac{3}{2}$ power of the relative amplitude of the differential pressure. In the second case, it is negative because the mean differential pressure increases in proportion to the square of the relative amplitude of flow oscillation q.

For example, a pipe with a closed valve at the end can have standing pressure waves in it, generated by a machine somewhere else on the line. Because of the different pressure reflections from the upstream and downstream sides of the meter and because of the separation of the pressure taps, a mean and an RMS differential pressure can be observed across the meter even though the flow is known to be zero. On the other hand, if a control valve in the line is oscillating slightly, it will cause the flow to oscillate and an oscillating differential pressure will result, including harmonics. The flow oscillation might be quite small, but if one of the pressure frequencies were to excite a resonance in some other component of the metering system (e.g., the connecting tubing), then obviously any estimate of the mean flow or even the size of the flow oscillation would be seriously in error.

The deficiency of standard head class meter installations in unsteady flow is that the differential pressure observation is not sufficient. Sensing only the differential pressure, the difference between pressure pulsations and unsteady flow cannot be distinguished. Additional information is needed. Schmid's data are for reciprocating steam engines. Lindahl's experiments used an oscillating butterfly valve downstream, as did Bajura's. In these cases, it is apparent that the flow was oscillating and the errors shown in Fig. 6-2.1 are negative, in agreement with this theory. Mottram's test rig used a piston compressor in series with a steady mean flow sonic element. Depending on frequency and displacement, his data should reflect mixed effects of both flow and pressure oscillations. Outside the laboratory, for industrial or performance test in field installations, it is less clear what an oscillating differential pressure implies; but, when it is observed, an independent measurement of the flow or velocity variation ought to be made (using, for example, hot wire anemometers, lasers, or probes that might be inserted through existing taps). Then at least a quantitative estimate of the effects of unsteadiness can be made.

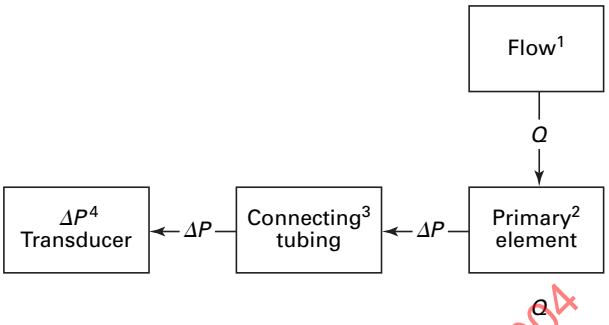

Fig. 6-2.2 Fluid–Metering System Block Diagram

On the other hand, an absence of oscillations in differential pressure measurements does not guarantee that the flow is steady. Pressure oscillations easily can be attenuated by relatively long connecting tubing and by the frequency response of the transducer. All components of the system must be considered.

Simplified System Description

The head class flow meter system is assembled from the four major components shown in Fig. 6-2.2. These are the flow to be measured, the primary element (orifice, nozzle, or venturi), connecting tubing, and the differential pressure transducer.

A great deal of research has been done and remains to be done on flow-velocity profiles, unsteady flow, computer simulations of flow, and so on. Here a rather simple model of sinusoidal unsteady flow was used as an analytical test function.

6-2.3 Frequency Response of the Primary Element

The corner frequency or bandwidth of an orifice meter has been calculated [2, Eq. (14)]

$$\Omega_c = 2CQ\left[1 - \frac{3}{16}(\partial Q/Q)^2\right]^{1/2} \qquad (6\text{-}2.5)$$

in which C is a geometric constant of the meter installation that varies with its size.

$$C = \frac{D(1 - \beta^4)}{2A_2^2(4/\pi + 0.8913/\beta^2)} \quad (6\text{-}2.6)$$

The bias uncertainty of C is about ±14%, and it is probably a good approximation to use for any differential pressure primary element. Pulsating flow measurements in which the frequency is greater than half the corner frequency ought to be avoided. Below $\Omega_c/2$, the Bernoulli equation may be used, and the consequent errors may be estimated from the linear time constant model of the primary element.

NOTE: This statement applies only to the primary element and not the entire flow-measuring system shown in Fig. 6-2.2.

For most industrial flows of interest in performance testing, findings indicate that the bandwidth of the primary element is considerably greater than the reported flow oscillation frequencies. When this is so, it means that the Bernoulli equation satisfactorily infers the volumetric flow for frequencies approximately an octave below the corner frequency of the primary element. Equation (6-2.5) states that the corner frequency increases with the mean flow Q.

6-2.4 Frequency Response of the Instrument Tubing

Research has been done on the effects of connecting tubing [3]. The U.S. Navy supported an intensive experimental investigation of the frequency response of connecting pressure tubing and especially the effects of various source and termination devices on the dynamic response [3].

The results indicate that it is this component of the system that ought to be highly suspect when differential pressure oscillations are observed. The reported pulsation frequencies were usually in the range of 1 Hz to 20 Hz, which coincides with the range of resonant frequencies for typical connecting tubing lengths, for instance, from the meter run to the top of the manometer. The effects of tubing on the pressure signal vary from attenuation to amplification, and the effects of the transducer, as a load termination, are equally important. The net effect can be anything from obscuring an actual unsteady flow to amplifying an inconsequential pulsation to where it appears serious. The effects of connecting tubing are in fact complex.

The following recommendations relevant to fluid metering are presented:

(a) To achieve maximum bandwidth, the length of tubing connecting the differential pressure sensor to the pressure taps should be as short as possible. The first resonant frequency occurs at

$$f = \frac{\alpha}{4L} \quad (6\text{-}2.7)$$

where

α = the speed of sound in the fluid

(b) The tubing diameter should be selected to achieve unity damping factor. This will tend to curtail resonant pressure peak amplitudes and maintain tubing as a linear element of the system. Both the attenuation and amplification of the unsteady portion of the signal will be minimized. The tubing size nearest to the following calculated diameter should be selected.

$$d = 4\sqrt{\frac{L}{\alpha}}\ (\text{m, ft}) \quad (6\text{-}2.8)$$

In most cases, this diameter is very much smaller than the half-inch tubing and pipe sizes recommended by *Fluid Meters* or the Performance Test Codes. Consequently, the probable bias is toward amplifying the perceived unsteady flow in installations conforming to various codes.

6-2.5 Frequency Response of the Pressure Transducer

Considering only the frequency response, the transducer should behave as much as possible as a solid end to the tubing. Its flow impedance should be greater than the connecting tubing, and its fluid compliance (capacitance) should be less. A small (2 mm diameter) gas bubble trapped in a liquid-filled transducer is a significantly large capacitance in terms of its effect on frequency response. Care must be exercised to remove these bubbles. The traditional U-tube manometer obviously does not stand up well to the above criteria for unsteady flow conditions. For the myriad designs of commercial transducers, the user is at the mercy of the manufacturer's data unless he chooses to conduct frequency response tests. Fortunately, their bandwidth is often high enough that the transducer can be considered linear for all frequencies of interest.

6-2.6 Pulsation Thresholds

The most comprehensive survey and experimentation on pulsating flow measurement was reported by Head [4] in 1956. This report covers turbine meters, positive displacement meters, variable-area meters, and head class meters, but the great majority of the data concern orifices, nozzles, and venturis. The statement is made that whenever the peak-to-peak amplitude Γ of the flow variation is less than 10% of the mean flow, the primary element will be operating in a quasisteady mode and negligible flow measurement error will result. It is restated here, as above, that an independent means, such as a hot-wire anemometer, is required for determining this amplitude.

A bias error ratio is defined

$$u_{\text{bias}} = Q_i/Q_{\text{mean}} = (1 + \alpha\Gamma^2)^n \quad (6\text{-}2.9)$$

where

n = an exponent determined by meter type and kind of flow
α = a wave-shape coefficient
Γ = $2\delta Q/Q$ = peak-to-peak amplitude of flow pulsation

Values of n depend on meter type and kind of flow. For variable-differential and variable-area flow meters in incompressible flow, $n = 0.5$ when flow is turbulent and $n = 0$ when flow is purely viscous; in the transition region or the compressible flow region, where q is proportional to Δp^m, the exponent n is closely approximated by $n = 1 - m$. In critical flow (sonic velocity in the throat of the nozzle), where mass rate is proportional to upstream pressure in a region of negligible approach velocity, $n = 0$. For turbine, propeller, or positive-displacement meters, $n = 1$.

Values of the wave-shape coefficient α are as follows:

(a) For sinusoidal variation of flow about the average, $\alpha = 1/3$.

(b) For a sawtooth wave, $\alpha = 1/12$.

(c) For any rectangular wave where the maximum flow persists for a fraction x of the period T and minimum flow persists for the remaining fraction $(1 - x)$ of the period, $\alpha = x(1 - x)$.

The highest known value of α is that for a symmetrical rectangular wave where $x = 0.5$ and $\alpha = 0.25$.

Previously published data [4] are summarized and presented in Fig. 6-2.6, and the conclusions therefrom are recommended for guidance and advice. It is further recommended that all of the techniques discussed in this Section be applied to the specific pulsation problem presently manifest and that the worst case estimate of the additional flow measurement uncertainty be used in reporting the performance test results.

6-2.7 Conclusions and Recommendations

(a) It has been shown that, from the viewpoint of accurate measurement of average flow, pulsation is potentially significant only when the intensity Γ is greater than 0.1. This value of Γ is recommended as a practical pulsation threshold for official publication, acceptable for the most exacting accuracy requirements.

(b) Pulsation-error magnitude has been shown to depend primarily on pulsation intensity and wave shape in a manner readily calculable from Eq. (6-2.9) when b is assumed unity, and, secondarily, on frequency-response characteristics of the flow meter.

(c) Flow measurement errors are best eliminated by the use of pulsation-attenuation equipment selected to reduce Γ to the threshold value. When this is impossible because of large attenuator size needed for low frequencies, errors may be minimized by selecting a high-response instrument for which b is negligible.

(d) Flow meters are least affected when viscous or inertial damping is minimized and when the principle of operation is such that a large part of the flow oscillation can be absorbed by small response. Variable-area and turbine-type meters are of such a character, but this advantage disappears above frequencies near the low end of the audio range.

(e) Accurate corrections can only be made when pulsation effects are forced to the maximum as by viscous damping and high inertia to force the coefficient b to unity. Additional instrumentation for accurate determination of intensity and wave shape will be required. The Q is equal to the indicated rate divided by the pulsation factor, as given by Eq. (6-2.6). A tolerance, or twice the standard deviation (4) of ±20% of the value of the error, must be assumed until more precise experimental data become available.

(f) Proper measurement of instantaneous or average values of secondary qualities has been assumed throughout this Performance Test Code. Secondary sources of pulsation error, particularly troublesome in variable-differential meters, are associated with nonsymmetrical damping and capacity in differential manometer lines. To a much smaller extent, similar errors in measurement of absolute pressure may affect the accuracy of gas measurement with any type of flow meter. No flow-pulsation threshold can ensure elimination of such errors, but the art of proper measurement of these secondary quantities is quite well developed.

6-3 TURBINE METERS IN PULSATING FLOW

Turbine flow meters have been accepted for high accuracy flow measurement of both liquids and gases in steady flow. In many applications such as in nuclear reactor systems, fossil-fuel power plants, oil refineries, and natural gas facilities (e.g., gas production fields and compressor stations), the flow may not be steady but pulsating. It is important and sometimes essential to know whether the turbine meter will perform accurately or will have significant error when operating under pulsating conditions determined by the installations. For flow measurement of liquids that have relatively high density, the response of a turbine meter to pulsating flow is generally good, resulting in small meter error due to pulsating flow. On the other hand, for flow measurement of gases that have relatively low density, the response of a turbine meter is generally not so good and significant meter error may result when operating in pulsating flow of large amplitude.

The maximum flow velocity through the meter must be at a low Mach number so that the compressibility effect of the gas on the meter performance can be neglected. It is assumed that the inlet velocity V_1 is axial and has a uniform velocity distribution.

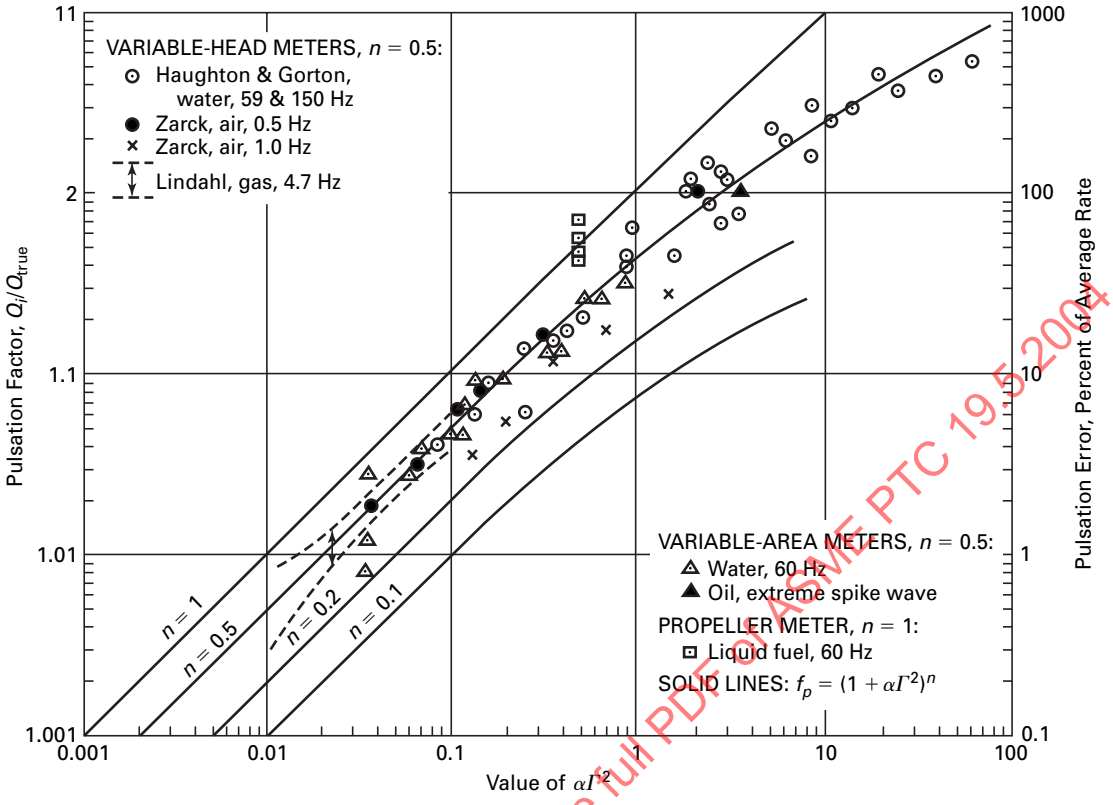

Fig. 6-2.6 Experimental and Theoretical Pulsation Error

6-3.1 Dimensional Analysis

There are three important dimensionless parameters affecting turbine meter performance in pulsating flow [5].

D_1 = dragless rotor time constant/period of flow pulsation

D_2 = fluid drag torque/fluid driving torque (on rotor)

D_3 = bearing friction drag torque/fluid driving torque

The methods for calculating these numbers are given in [5, 6].

Of course, changes in the parameters D_1, D_2, and D_3 do affect the magnitude of meter pulsation error. These changes are brought about from variations in meter design and meter size and variations in the pulsating flow. Knowledge of the effects of these variations on meter error can provide a basis for modifying the nature of the pulsating flow, modifying the meter design, selecting the proper meter size, or changing the location of the meter to minimize the meter error or to perhaps make the meter error predictable (i.e., if the pulsating flow is better defined in one location versus another).

For large values of D_1 where the rotor response is not good, Fig. 6-3.1 indicates that the meter pulsation error increases with increasing values of D_3. D_3 does not affect the value of the overrun for large values of D_1, but an increase in D_3 decreases the steady state rotor speed, thus changing the meter calibration.

Even though these figures are for a sine wave flow fluctuation and for specific values of the parameters D_2 and D_3, the effects are characteristic of other wave shapes and other values of D_2 and D_3.

6-3.2 Rotor Response Parameter D_1 and Pulsation Period T

With reference to Fig. 6-3.1, it is seen that three significant regions exist on the error graphs based on the value of the rotor response parameter D_1. Region 1 is where $D_1 = t_m/T \geq 1$ (i.e., the flow pulsation period T is equal to or less than the dragless meter time constant t_m). The error curves are practically horizontal. Here, the meter has little ability to follow the flow fluctuation because of the rotor inertia and just dithers at a definite overspeed. This overspeed, and thus the meter pulsation error, can be quickly calculated by the asymptotic solution. Region 2 is where $1 > D_1 > 0.05$. The error curves drop off for decreasing values of D_1 and reflect the increasing ability of the rotor to follow the flow fluctuation, resulting in a decrease in meter pulsation error. Region 3 is where $D_1 \leq 0.05$ (i.e., the flow pulsation period T is 20 times that of the dragless meter time constant t_m or longer). The error curves have already

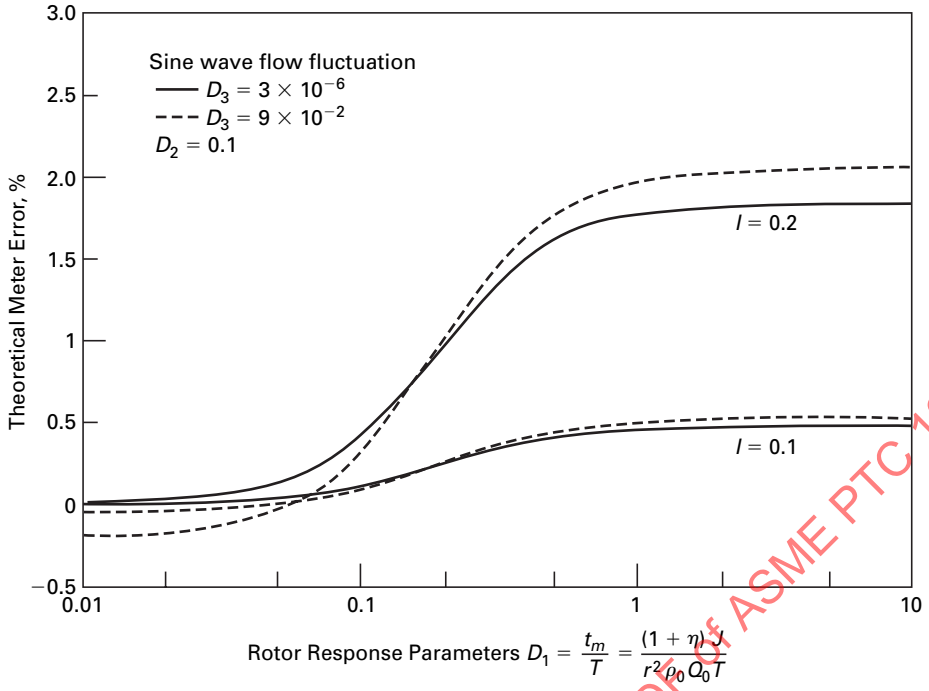

Fig. 6-3.1 Semi-Log Plot of Theoretical Meter Pulsation Error Versus Rotor Response Parameter for Sine Wave Flow Fluctuation, $D_2 = 0.1$, and Pulsation Index, $I = 0.1$ and 0.2

dropped to near the horizontal level. Here, the rotor is able to follow the fluctuation, resulting in only small meter pulsation error due to rotor inertia (the negative meter pulsation error shown is a result of nonfluid drag effect D_3).

It should be noted that the frequency or period T of the pulsating flow by itself does not determine the degree of rotor response or the value of D_1. The rotor response is determined by the ratio of the dragless meter time constant t_m to the pulsation period T. Also, the meter property term $(1 + \eta)J/r^2$, which can be considered as the effective mass of the rotor system, by itself does not determine the meter time constant $t_m = (1 + \eta)J/r^2\ \rho Q_0$. The meter time constant is determined by the ratio of the effective mass of the rotor system to the mass rate ρQ_0 passing through the meter at the operating condition.[1]

6-3.3 Fluid Drag Parameter D_2

Although the effects of a change in D_2 are not shown, calculations will show the increasing D_2 always reduces the meter error caused by either D_1 or D_3. If D_1 and D_3 are zero, there is no meter pulsation error and the change in D_2 will only affect meter calibration.

[1] The meter time constant, which includes drag effect, can be determined from a closed-form solution to a differential equation for a step change in flow and is where the flow rate Q_0 required for t_m and D_3 is the value after the step change and J is the rotor inertia.

6-3.4 Nonfluid Drag Parameter D_3

For dragless meter rotor system (i.e., $D_2 = 0$ and $D_3 = 0$), the meter pulsation error is due to rotor inertia effect D_1 only. Since the rotor responds better at high flow than at low flow $[t_m \alpha (1/Q)]$, the rotor overruns more during the low-velocity portion of the flow cycle than it underruns during the high-velocity portion of the flow cycle, thus resulting in a net overrun or positive meter error in measuring pulsating flow. As the rotor response parameter D_1 decreases toward zero, the rotor inertia effect becomes smaller and the positive meter pulsation error decreases to zero. However, for a real rotor system where $D_3 \neq 0$, the meter pulsation error is caused by both the rotor inertia effect D_1 and the nonfluid drag effect D_3. Figure 6-3.1 indicates that D_3 causes the meter to underrun in pulsating flow for small values of D_1 ($D_1 < 0.15$) where the rotor response is good. The physical reason for this is that the meter has more slip due to the D_3 effect during the low-velocity portion of the flow cycle than it does during the high-velocity portion of the flow cycle, resulting in underrun of negative meter error due to nonfluid drag torque.

Therefore, the meter pulsation error will become negative as D_1 approaches zero, especially for high values of D_3, because the meter underrun due to the D_3 effect may exceed the overrun due to the D_1 effect (which approaches zero as D_1 approaches zero).

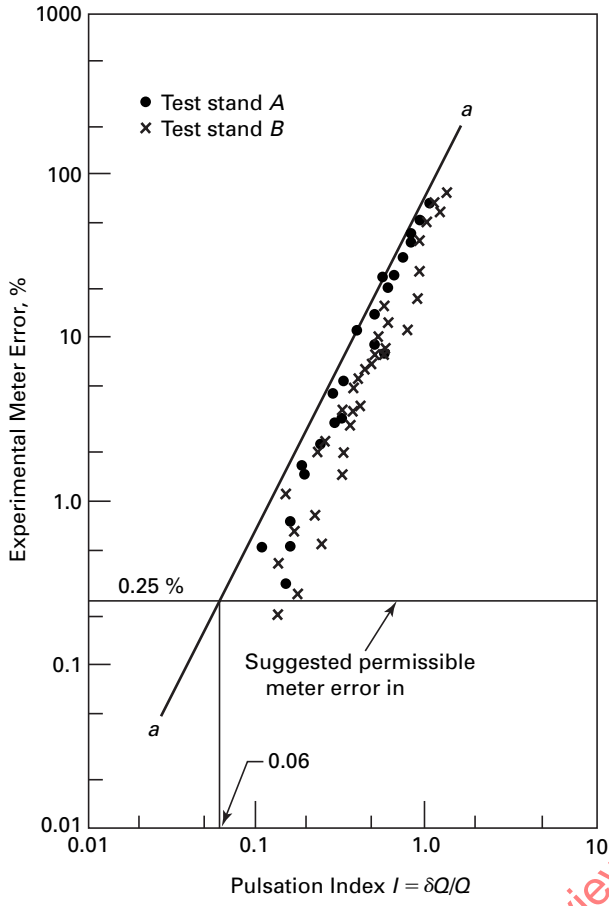

Fig. 6-3.5 Experimental Meter Pulsation Error Versus Pulsation Index

For large values of D_1 where the rotor response is not good, Fig. 6-3.1 indicates that the meter pulsation error increases with increasing values of D_3. D_3 does not affect the values of the overrun for large values of D_1, but an increase in D_3 decreases the steady state rotor speed, thus changing the meter calibration.

6-3.5 Experimental Pulsation Data

The experimental meter pulsation error data [5] are shown in Fig. 6-3.5. There is quite a range in the data for a given amplitude of pulsation. It is recommended that the upper bound (line a-a) be used to estimate conservatively the additional bias uncertainty resulting from the unsteady flow. It may be calculated using Eq. 6-2.8.

$$u_b(\%) = 69(\delta Q/Q)^2 \qquad (6\text{-}3.1)$$

In Fig. 6-2.6, the pulsation index $I = \delta Q/Q$ and it is the relative amplitude of flow variation or half the peak-to-peak oscillation. In the reported experiments, it is safe to say that no wave shape was like another, so that variations in meter error because of wave shape variation is a likely cause for the spread in the data at a given pulsation condition. Also, the effect of varying values of D_1 (especially for $D_1 \leq 1$), D_2, and D_3 causes additional spread in the data.

As has been mentioned previously, the wave shapes encountered in the laboratory experiments vary substantially — from near sinusoidal to rounded-off square waves to all types of triangular-like waves and to harmonic alterations of these wave shapes — and are probably not unlike the variety of wave shapes encountered in the field.

A theoretical analysis of gas turbines flow meter in the measurement of pulsating flow, including both fluid drag and nonfluid drag on the rotor system and dealing with pulsating flow of arbitrary wave shape, appears to be validated by a wide range of test results except for large pulsations where the situation is more complex and needs further investigation. Careful design and execution of properly instrumented tests are essential in determining meter pulsation error that is free from extraneous errors caused by poorly conditioned flow or improper operation of the test stands.

The meter pulsation error of a gas turbine flow meter may be estimated with reasonable accuracy for a known pulsating flow situation using steady state values of fluid drag and nonfluid drag.

Test results indicate a gas turbine flow meter retains its excellent steady state repeatability in pulsating flow, which is a necessary condition for possible measurement of pulsating flow.

6-4 SOURCES OF FLUID MATERIAL AND DATA

6-4.1 Literature Referenced in Section 6

[1] Keyser, D. R. Unsteady Orifice Flow Measurement: Its Theory and Observations. In *Flow, Its Measurement and Control in Science and Industry* (Durgin, W., ed.), vol. 2. Research Triangle Park, NC: Instrument Society of America; 1981.

[2] Keyser, D. R. Oscillating Flow Measurement Using Differential Pressure Fluid Meters. ASME 83-JPGC-PTC-5.

[3] Woods, R. L., et al. Comparison of Theoretical and Experimental Fluid Line Responses with Source and Load Impedances. ASME publication H00278, Fluid Transmission Line Dynamics, 1983.

[4] Head, V. P. A Practical Pulsation Threshold for Flowmeters. ASME Trans. October 1956.

[5] Lee, W. F. Z., et al. Gas Turbine Flowmeter Measurement of Pulsating Flow. *Journal of Engineering Power* **97:**231-241; 1975.

[6] Lee, W. F. Z.; Evans, H. J. Density Effect and Reynolds Number Effect on Gas Turbine Flowmeter. *Journal of Basic Engineering* **87**(4):1043–1057; 1965.

6-4.2 Other Literature Relevant to Section 6

Bean, H. S., ed. *Fluid Meters: Their Theory and Application*, 5th edition. New York: The American Society of Mechanical Engineers; 1959.

Dowdell, R. B.; Liddle, A. H. Measurement of Pulsating Flow With Propeller and Turbine Type Meters. Trans. ASME **75**: 961–968.

Evans, H. J. Private communication, Rockwell International, November 1972.

Grey, J. Transient Response of the Turbine Flowmeter. *Jet Propulsion*: 98–100; 1956.

Haalman, A. Pulsation Error in Turbine Flowmeter. *Control Engineering* **12**: 89–91; 1965.

Head, V. P. A Practical Pulsation Threshold for Flowmeters. Trans. ASME **78**:1471–1479; 1956.

Higson, D. J. The Transient Performance of a Turbine Flowmeter in Water. *Journal of Scientific Instruments* **41**: 317-320; 1964.

ISO Draft Proposal, Characterization of Steady Flow. ISO/TC 30/SC 2/WG 7 (Secr.-1) 1, 1973.

Jepson, P. Currentmeter Errors Under Pulsating Flow Conditions. *Journal of Mechanical Engineering Science* **9**(1): 45–54; 1967.

Jepson, P. Transient Response of a Helical Flowmeter. *Journal of Mechanical Engineering Science* **6**(4): 337–342; 1964.

Kastner, L. J.; Williams, T. J.; Sowden, R. A. Critical-Flow Nozzle Meter and Its Application to the Measurement of Mass Flow Rate in Steady and Pulsating Streams of Gas. *Journal of Mechanical Engineering Science* **6**(1): 88–98; 1964.

Lee, W. F. Z.; Evans, H. J. A Field Method of Determining Gas Turbine Meter Performance. Trans. ASME **92**(4): 724–731; 1970.

Lee, W. F. Z.; Evans, H. J. Density Effect and Reynolds Number Effects on Gas Turbine Flowmeter. Trans. ASME *Journal of Basic Engineering* **87**(4):1043–1057; 1965.

Ower, E. On the Response of a Vane Anemometer to an Air Stream of Pulsating Speed. *Philosophical Magazine* **23:**992–1004; 1937.

van Mill, C. H. The Dynamic Behaviour of a Turbine-Flowmeter. **6:**169–173; 1964.

6-4.3 Bibliography

Ainslee, A. R. The Effects of Transmission Lines and Orifices on Dynamic Pressure Measurement. Master's thesis, Princeton University, 1966.

Bajura, R. A.; Pellegrin, M. T. Studies of Pulsating Incompressible Flow Through Orifice Meters, NBS Special Publication 484. Proceedings of Symposium on Flow, Open Channels and Closed Conduits, October 1977.

Bean, H. S., ed. *Fluid Meters: Their Theory and Application*, 5th edition. New York: The American Society of Mechanical Engineers; 1959.

Bean, H. S., ed. *Fluid Meters: Their Theory and Application*, 6th edition. New York: The American Society of Mechanical Engineers; 1971.

Chilton, E. G.; Handley, L. R. Pulsations in Gas-Compressor Systems. Trans. ASME **74:**931–943; 1952.

Clamen, M.; Minton, P. J. An Experimental Investigation of Flow in an Oscillating Pipe. *Fluid Mechanics* **81:**421–431; 1977.

Deckker, B. E. L.; Male, D. H. Fluid Dynamic Aspects of Unsteady Flow in Branched Ducts. *Proceedings of the Institution of Mechanical Engineers* 182(Pt 3H):167–174; 1967.

Earles, S. W.; Jeffery, B. J.; Williams, T. J.; Zarek, J. M. Pulsating Flow Measurement Using an Orifice-Manometer System. *The Engineer*: 821–825; 1967.

Engel, F. Fluid Dynamic Problems Awaiting Solution. *Measurement and Control*: T6–T14; 1971.

Goldscmeid, F. Experimental Study of Pulsating Viscous Flow in Rigid Pipes. *Non-Steady Flows: 185–195; 1970.*

Habib, M. A.; Whitelaw, J. H. Velocity Characteristics of a Confined Coaxial Jet. ASME paper 79-WA/FE-9, 1979.

Hall, N. Orifice and Flow Coefficients in Pulsating Flow. Trans. ASME **74**: 925–929; 1952.

Hanchett, M. T. The Design of a Certification Instrument for Flow Meters Subjected to Pulsating Flow. Interim Report, July 1960.

Head, V. P. A Practical Pulsation Threshold for Flowmeters. Trans. ASME **78**: 1471–1479; 1956.

Hoppmann, W. H.; Liu, J. C. C. Flowmeter for Pulsating Flow. *Non-Steady Flows*: 209–213; 1970.

Investigations of Pump Pressure Pulsation Measurement Techniques and Related Problems, Dearborn, DE, Naval Engineering Experiment Station, Anna, MD, AD874-218L.

ISO Draft Proposal: Characterization of Steady Flow, ISO/TC30/SC2/WG7, July 1975.

Kirmse, R. E. Investigations of Pulsating Turbulent Pipe Flow. ASME paper 79-WA/FE-12, 1979.

Koloseus, H. J.; Ahmad, D. Response of Biased Manometers Subjected to Sinusoidal Pressure Variations. *Non-Steady Flows*: 215–227; 1970.

Lindahl, E. J. Pulsation and Its Effect on Flowmeters. Trans. ASME **68**: 883–894; 1946.

Mattingly, G. E.; Chang, C. C. Unstable Waves on an Axisymetric Jet Column. *Journal of Fluid Mechanics* **65:**541–560; 1964.

McCloy, D. Effects of Fluid Inertia and Compressibility on the Performance of Valves and Flow Meters Operating Under Unsteady Conditions. *Journal of Mechanical Engineering Science* **8:**52–61.

Miller, R. J. A Report of a Study Relating to Errors in the Metering of Pulsating Fluid Flow and an Electronic Analog to Analyze These Errors. University of Wyoming, 1957.

Moore, J.; Moore, J. G. A Calculation Procedure for Three-Dimensional, Viscous, Compressible Duct Flow. Part I: Inviscid Flow Considerations; Part II: Stagnation Pressure Losses in a Rectangular Elbow. ASME papers 79-WA/FE-4 and 79-WA/FE-5, 1979.

Moretti, G. Complicated One-Dimensional Flows. AD-731-494, September 1971.

Mosely, D. S. Orifice Metering of Pulsating Flow. American Gas Association Project NQ-15, Southwest Research Institute, Experimental Program Utilizing a Special Purpose Water Test Facility, May 1958.

Mottram, R. C. The Measurement of Pulsating Flow Using Orifice Plate Meters. *Non-Steady Flows*: 197–208; 1970.

Numerical Solution of Viscous Flow Equations Using Integral Representations, Proceedings of the Fifth International Conference on Numerical Methods. In *Fluid Dynamics Lecture Series in Physics* (Wu, J. C.; Wahbah, H. H., eds.), vol. 59.1976:448–453.

Oppenheim, A. K.; Chilton, E. G. Pulsating Flow Measurement: A Literature Survey. Trans. ASME **77**: 231–248; 1955.

Paidoussis, M. P.; Issid, N. T. Experiments on Parametric Resonance of Pipes Containing Pulsatile Flow. *Journal of Applied Mechanics*: 198–202; 1976.

Pellegrin, M. T.; Bajura, R. A. Pulsating Flow of an Incompressible Fluid Through a Sharp-Edged Orifice Meter, Report ENG-74-10399-A. West Virginia University, Morgantown, WV, NSF Grant ENG-74-10399, June 1976.

Pick, G. S. Experimental Determination and Correlation of Pressure-Time Response in Measuring Systems. AD-675-498, July 1969.

Pollard, F.; Cannizzaro, S. Investigation of Pulsating Flow Hydraulic Concepts. AD-473-815, November 1965.

Rainville, E. D. *Intermediate Differential Equations*. New York: John Wiley & Sons; 1961.

Render, W. A. The Effect of Air in Damping Water Borne Pressure Pulses. AD-481-353.

Sarpkaya, T. Mechanism of Turbulence Generation in Pulsating Viscous Flow. AD-438-511, March 1964.

Sauer, H. J.; Smith, ; Field, L. V. Metering Pulsating Flow in Orifice Installations. *Instrument Technology*: 41–44; 1969.

Schirk, R. J. Orifice Meter Errors Produced by Pulsating Flow. Master's thesis, University of Wyoming, June 1963.

Seymour, B. R.; Varley, E. Pulsatile Flow in Flexible Tubes. AD-695-710, August 1969.

Shames, I. H. *Mechanics of Fluids*. New York: McGraw-Hill; 1962.

Slaughterbeck, D. C. Flow Meter Characteristics With Pulsating Compressible Flow. Master's thesis, University of Wyoming, June 1965.

Sparks, C. L., et al. The Use of Short Run Tracer Detection Techniques for Pulsative Flow Measurement. Final Technical Report, December 1961.

Ury, J. F.; Goldscmidt, A. I. Measurement of Pulsating Flow of Liquids Through Orifices. *Trans ASME*: 25–32; 1964.

Walks, R. E. The Effect of Acoustic Excitation on the Measurement of Fluid Flow. University of Wyoming, May 1964.

Weber, P. Measurement of the Natural Frequency of Pulsating Flow Equipment. University of Wyoming, May 1965.

Williams, T. J. Pulsation Damping in Pressure Gauge Connections. *The Engineer*: 378–379; 1959.

Wood, D. J.; Kao, T. Y. Evaluation of Quasi-Steady Approximation for Viscous Effects in Unsteady Liquid Pipe Flow. AD-714-539, January 1968.

Wu, J. C. Numerical Boundary Conditions for Viscous Flow Problems. *AIAA Journal* **14**(8):1042–1049; 1978.

Wu, J. C., et al. Numerical Solution of Unsteady Flow Problems Using Integro-Differential Approach. ASME Symposium Volume on Non-Steady Fluid Dynamics: 245–251; 1978.

Yellin, E. L.; Peskin, C. S. Large Amplitude Pulsatile Water Flow Across an Orifice. *Journal of Dynamic Systems, Measurement, and Control* **97**: 92–95; 1975.

Young, B. Differential Error in Measurement of Pulsating Compressible Fluid Flow. Master's thesis, University of Wyoming, January 1965.

Section 7
Flow Conditioning and Meter Installation Requirements

7-1 INTRODUCTION

The primary element shall be installed in the pipeline at a position such that the flow conditions immediately upstream sufficiently approach those of a fully developed profile and are free from swirl.

The theory of practically any flow meter begins with the assumption that the velocity in the conduit is everywhere the same — all the flow velocity vectors are parallel to the axis of the pipe or duct and all have the same value. This is called the assumption of a uniform, one-dimensional velocity profile. This exists in theory only and never in the field. The best flow condition to be found in the field is that of a fully developed, turbulent velocity profile. These words describe an axially symmetric, bullet-shaped velocity profile that is mostly uniform across the central area of the conduit and rounded toward the wall where it eventually goes into the turbulent boundary layer, to the laminar sublayer, and then to zero velocity at the conduit surface. Superimposed on this profile is a kind of random isotropic turbulence of some undetermined intensity. The difference between this profile and the uniform one assumed in the theory gives rise to the published (average) calibration coefficients for various classes of flow meters. Flow calibration laboratories make every effort to attain this type of velocity profile by using sufficient lengths of straight pipe upstream and downstream of the metering section, such piping having representative commercial smoothness on the inside. Such a velocity profile is rarely to be found in the field or plant where a performance test is to be conducted.

Whenever flow goes around a bend, the higher velocities are found on the outside (of the bend) downstream and some angular momentum is imparted to the flow. The velocity profile has become skewed. When two such bends are found close to each other and out of plane, a helical streamline pattern called swirl may be generated. Swirl is particularly harmful to the accuracy of turbine meters and propeller meters and it degrades the accuracy of differential pressure meters. It takes quite some time (and, therefore, quite some straight pipe) for the fluid viscosity to affect the decay of such angular momentum and to redistribute the velocity profile. There are many upstream piping arrangements discussed in this Section, and if insufficient straight pipe length remains in the metering section, the use of flow conditioners is recommended. There are those that are effective in removing swirl, those that are effective in redistributing the axial velocity profile, and some that are effective for both. The tradeoff comes in how much permanent pressure loss can be tolerated.

7-1.1 Recommended Practice

The most accurate flow measurement can be attained by calibrating the entire metering section in a flow calibration laboratory suitable to the needs of the test. Metering section is herein defined as all the straight conduit upstream and downstream of the primary element (e.g., the flow meter and nozzle), including the flow conditioner installed as it is during test and the instrumentation fittings, plumbing, and the transducers. Following calibration, the entire metering section assembly should remain intact from end to end (to the maximum extent possible at least) and installed at the test site in the as-calibrated condition. The use of a flow conditioner is recommended because it nullifies the effects of the remaining differences between the laboratory and test installation. With such care taken in the pretest calibration of the metering section, it does not matter which primary element is selected; all will result in equivalent accuracy.

When the temperature of the fluid is above or below ambient so that the difference in temperature may affect the fluid properties, thermal insulation of the entire meter section may be advisable. Refer to ASME PTC 19.3, Temperature Measurement.

During the test, the primary element should be clean and undamaged. The inlet edge of an orifice must be square and sharp; the inlet and throat sections of a nozzle or venturi should be clean, smooth, and free of scale or encrustations. Such conditions should be established by inspection, both before and after use. Therefore, especially for orifices, means must be provided to remove the orifice plate for inspection and to reinstall it in exactly the same position as when it was calibrated, such as locating pins; see Sections 3, 4, and 5 for details.

7-1.2 Calibrations

Normally, calibration of a particular differential pressure producer is desired or required whenever the flow measurement uncertainty must be less than 1% (for nozzles and venturis) and < 0.6% to 0.7% for orifice-metering sections. For new, clean devices installed in accordance with Sections 4 and 5, calibration should be made with the adjacent sections of pipe in which such a primary element is to be used. The length of the actual piping

Table 7-1.2-1 Recommended Straight Lengths for Orifice Plates and Nozzles

	On Upstream (Inlet) Side of the Primary Device							On Downstream (Outlet) Side
β	Single 90 deg Bend or Tee (Flow From One Branch Only)	Two or More 90 deg Bends in the Same Plane	Two or More 90 deg Bends in Different Planes	Reducer ($2D$ to D Over a Length of $1.5D$ to $3D$)	Expander ($0.5D$ to D Over a Length of D to $2D$)	Globe Valve Fully Open	Gate Valve Fully Open	All Fittings Included in This Table
≤ 0.20	10 (6)	14 (7)	34 (17)	5	16 (8)	18 (9)	12 (6)	4 (2)
0.25	10 (6)	14 (7)	34 (17)	5	16 (8)	18 (9)	12 (6)	4 (2)
0.30	10 (6)	16 (8)	34 (17)	5	16 (8)	18 (9)	12 (6)	5 (2.5)
0.35	12 (6)	16 (8)	36 (18)	5	16 (8)	18 (9)	12 (6)	5 (2.5)
0.40	14 (7)	18 (9)	36 (18)	5	16 (8)	20 (10)	12 (6)	6 (3)
0.45	14 (7)	18 (9)	38 (19)	5	17 (9)	20 (10)	12 (6)	6 (3)
0.50	14 (9)	20 (10)	40 (20)	6 (5)	18 (9)	22 (11)	12 (6)	6 (3)
0.55	16 (8)	22 (11)	44 (22)	8 (5)	20 (10)	24 (12)	14 (7)	6 (3)
0.60	18 (9)	26 (13)	48 (24)	9 (5)	22 (11)	26 (13)	14 (7)	7 (3.5)
0.65	22 (11)	32 (16)	54 (27)	11 (6)	25 (13)	28 (14)	16 (8)	7 (3.5)
0.70	28 (14)	36 (18)	62 (31)	14 (7)	30 (15)	32 (16)	20 (10)	7 (3.5)
0.75	36 (18)	42 (21)	70 (35)	22 (11)	38 (19)	36 (18)	24 (12)	8 (4)

	Fittings	Minimum Upstream (Inlet) Straight Length Required
For all β values	Abrupt symmetrical reduction having a diameter ratio ≥ 0.5	30 (15)
	Thermometer pocket or well of diameter ≤ $0.03D$	5 (3)
	Thermometer pocket or well of diameter between $0.03D$ and $0.13D$	20 (10)

GENERAL NOTES:

(a) All straight lengths are expressed as multiples of diameter D. The pipe roughness shall not exceed that of a smooth, commercially available pipe approximately $k/D < 10^{-3}$.

(b) Required straight lengths to meet the discharge coefficient uncertainties delineated herein are represented by the values without parentheses. Straight lengths can be reduced down to the values in parentheses, but then an additional uncertainty of 0.5 percentage points must be added to the uncertainties as delineated herein for each meter if made any shorter than the full required lengths shown without parentheses.

to be used in the calibration should be at least as shown in Tables 7-1.2-1 and 7-1.2-2. For best results, any fitting that immediately precedes the inlet of the metering section should be used in the calibration. Whenever possible, the calibration range should encompass the entire range of Reynolds numbers corresponding to the rates of flow to be encountered. When the calibration facilities are inadequate to attain the highest Reynolds numbers to be encountered in the test, the indications of the calibration may be extrapolated using procedures in the relevant Sections (i.e., 4 and 5).

NOTE: The extrapolation should not be extended to a condition that would correspond to a pressure ratio p_2/p_1 below about 0.8 since a change in flow regime may occur in this pressure-ratio region. This note does not apply to sonic-flow nozzles; refer to Section 8 for compressible flow measurement.

7-2 FLOW CONDITIONERS AND METER INSTALLATION

Metering section assemblies are prescribed with criteria for including or omitting flow conditioners. Most of these recommendations are based on tests using orifices as the primary element (see para. 7-2.4g). In the absence of better data or information, these specifications are recommended as good practice for practically any type of meter or primary element.

7-2.1 Flow Conditioners

The recommended designs of flow conditioners are shown in Fig. 7-2.1. For removing both swirl and smoothing the velocity profile, flow conditioner types (a) and (b) are preferred. Tube bundle designs [flow conditioner type (a)] have been used successfully with the number of tubes between 19 and 41; only marginal improvement in effectiveness has been reported for designs using more than 19 tubes. The design criteria for the perforated plates [flow conditioner type (b)] is that the total flow area of the sum of the holes is less than half of the inside area of the pipe. The tradeoff for this effectiveness is a higher loss coefficient, as shown in Table 7-2.1, in which the loss coefficient is the unrecoverable portion of the upstream dynamic pressure of the flow.

Table 7-1.2-2 Recommended Straight Lengths for Classical Venturi Tubes

Diameter Ratio	Single 90 deg Short Radius Bend [Note (1)]	Two or More 90 deg Bends in the Same Plane [Note (1)]	Two or More 90 deg Bends in Different Planes [Notes (1) and (2)]	Reducer 3*D* to *D* Over a Length of 3.5*D*	Expander 0.75*D* to *D* Over a Length of *D*	Gate Valve Fully Open
0.30	0.5 [Note (3)]	1.5 (0.5)	(0.5)	0.5 [Note (3)]	1.5 (0.5)	1.5 (0.5)
0.35	0.5 [Note (3)]	1.5 (0.5)	(0.5)	1.5 (0.5)	1.5 (0.5)	2.5 (0.5)
0.40	0.5 [Note (3)]	1.5 (0.5)	(0.5)	2.5 (0.5)	1.5 (0.5)	2.5 (1.5)
0.45	1.0 (0.5)	1.5 (0.5)	(0.5)	4.5 (0.5)	2.5 (1.0)	3.5 (1.5)
0.50	1.5 (0.5)	2.5 (1.5)	(8.5)	5.5 (0.5)	2.5 (1.5)	3.5 (1.5)
0.55	2.5 (0.5)	2.5 (1.5)	(12.5)	6.5 (0.5)	3.5 (1.5)	4.5 (2.5)
0.60	3.0 (1.0)	3.5 (2.5)	(17.5)	8.5 (0.5)	3.5 (1.5)	4.5 (2.5)
0.65	4.0 (1.5)	4.5 (2.5)	(23.5)	9.5 (1.5)	4.5 (2.5)	4.5 (2.5)
0.70	4.0 (2.0)	4.5 (2.5)	(27.5)	10.5 (2.5)	5.5 (3.5)	5.5 (3.5)
0.75	4.5 (3.0)	4.5 (3.5)	(29.5)	11.5 (3.5)	6.5 (4.5)	5.5 (3.5)

GENERAL NOTES:

(a) All straight lengths are expressed as multiples of diameter *D*. The pipe roughness shall not exceed that of a smooth, commercially available pipe approximately $k/d < 10^{-3}$.

(b) Downstream fittings or other disturbances situated at least four throat diameters downstream of the throat pressure tapping do not affect the accuracy of the measurement.

(c) Required straight lengths to meet the discharge coefficient uncertainties delineated herein are represented by the values without parentheses. Straight lengths can be reduced down to the values in parentheses, but then an additional uncertainty of 0.5 percentage points must be added to the uncertainties as delineated herein for each meter if made any shorter than the full required lengths shown without parentheses.

NOTES:

(1) The radius of curvature of the bend shall be equal to or greater than the pipe diameter.

(2) Since the effect of these fittings may still be present after 40*D*, no unbracketed values can be given in the Table.

(3) Since no fitting can be placed closer than *D*/2 to the upstream pressure tapping in the Venturi tube, the "zero additonal uncertainty" value is the only one applicable in this distance.

If removing swirl is the main concern (e.g., with turbine or propeller meters), then the use of flow conditioner type (a) with nineteen tubes, flow conditioner type (c) with the minimum number of plates, and flow conditioner type (d) the etoile are recommended. Data presented [1] for flow conditioner type (d) indicate it is the most effective at removing swirl; the etoile also may be shortened to 1*D* in length with negligible loss in effectiveness.

(a) Tube Bundle Straightener. This type of straightener consists of several parallel tubes fixed together and held rigidly in the pipe. It is important in this case that the various tubes are parallel with each other and with the pipe axis. If this requirement is not met, the straightener itself might introduce disturbances into the flow. There shall be at least 19 tubes. Their length shall be at least 20*d*. The tubes shall be joined in a bundle and installed tangent to the pipe wall.

(b) Sprenkle Straightener. This straightener consists of three perforated plates in series with a length equal to one pipe diameter between successive plates. The perforations should be chamfered on the upstream side, and the total area of the holes in each plate should be greater than 40% of the cross-sectional area of the pipe. The ratio of plate thickness to holes shall be at least unity, and the diameter of the holes shall be less than $\frac{1}{20}$ of the pipe diameter. The three plates should be held together by bars or studs located around the periphery of the pipe bore. These should be as small in diameter as possible, consistent with providing the required strength.

7-2.2 Metering Section Assemblies for Various Piping Configurations

The metering section is composed of two sections whose lengths are determined from Tables 7-1.2-1 or 7-1.2-2. The primary element is placed between these sections. Pressure differential measuring taps are located in accordance with the specifications for each primary element. Temperature-measuring connections may be required under certain conditions and are specified in para. 7-4.

7-2.3 Fabrication of Piping

The normal methods of fabricating piping and components are not satisfactory for accurate flow measurement. The requirements set forth must be followed, and no deviations may be permitted for satisfactory results. In the design stages, check the installation drawing for clarity and precision of fabrication instructions. After initial fabrication, inspect and document that all requirements are met and record when the necessary corrections

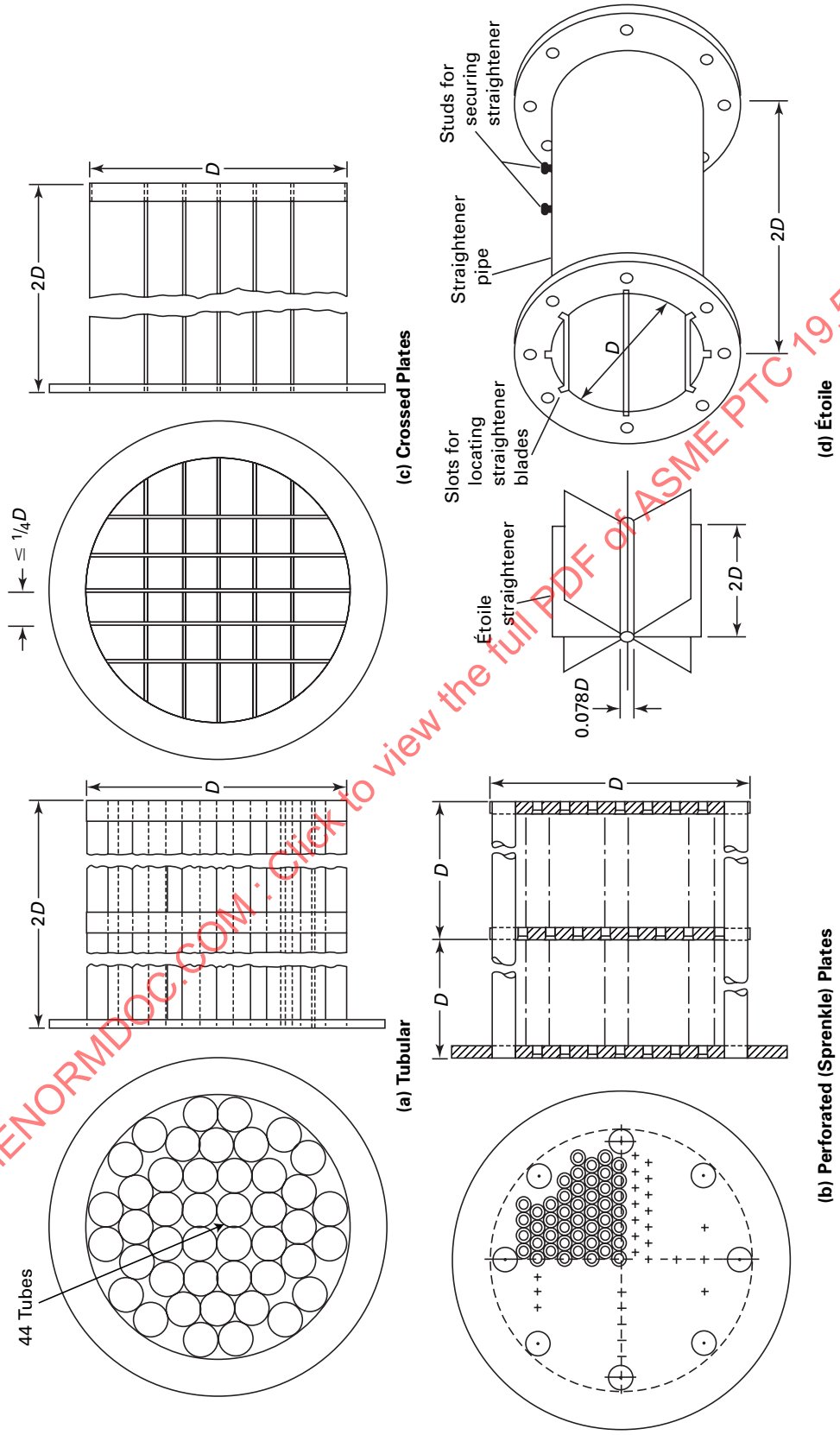

Fig. 7-2.1 Recommended Designs of Flow Conditioner

Table 7-2.1
Loss Coefficients for Flow Conditioners

Flow Conditioner Type		k
(a) Tube bundle	41 tubes	8.0
	19 tubes	5.0
(b) Perforated plates	Beveled holes	11.6
	Straight holes	13.0
(c) Crossed plates	. . .	2.2
(d) Étoile	. . .	1.1

GENERAL NOTES:
(a) $\Delta P_{loss} = k(\frac{1}{2}\rho V_1^2)$. k is the multiple of the upstream dynamic pressure.
(b) Refer to Table 3-1. If the units of lines (1) or (3) are used, then k is dimensionless. For other units, conversions must be made in accordance with Section 2.

have been made. Measurements shall be made as required.

(a) Inside pipe walls shall not be polished but should be as smooth as is commercially practical. When pipe walls are machined or ground, the finish should simulate that of new smooth pipe. Seamless pipe or cold-drawn seamless tubing may be used.

(b) Grooves, scoring, pits, raised ridges resulting from seams, distortion caused by welding, offsets, backing rings, and similar irregularities, regardless of size, that change the inside diameter at such points by more than $k/D < 10^{-3}$ shall not be permitted. When required, the roughness may be corrected by filling in, grinding, or filing off to obtain smoothness within.

(c) Under no circumstances will changes of diameter (e.g., shoulders, offsets, and ridges) greater than $0.003D$ be permitted within $4D$ of the primary element. All upstream valves shall fully open. It is recommended that control be affected by valves located downstream of the primary element. Isolating valves located upstream preferably shall be of the gate type and shall be fully open.

(d) When measuring steam in a horizontal pipe, suitable drains or blowoffs should be provided on the underside of the pipe on the inlet and outlet sides of the primary element. If the pressures are measured through annular chambers, there should be drains in these chambers also. In other than horizontal installations, the pipe adjacent to the primary element should be drained at the point of minimum elevation. The valves or cocks used on these drains should be ones that will close tightly.

(e) When measuring an incompressible fluid, vents should be located on the upper side of the horizontal pipe to eliminate any entrapped gas. In other than horizontal installations, the piping system should be vented at the highest point.

7-2.4 Metering Section Piping Adjacent to the Primary Element

(a) The primary element or flow section shall be fitted between two sections of straight cylindrical pipe of constant cross-sectional area, in which there is no obstruction or branch connection (whether or not there is flow into or out of such connections during measurement) other than those specified in Tables 7-1.2-1 and 7-1.2-2. The pipe is considered straight when it appears so by visual inspection. The required minimum straight lengths of pipe, which conform to the description above, vary according to the nature of the fittings, the type of primary element, and the diameter ratio. They are indicated in Tables 7-1.2-1 and 7-1.2-2, which show the upstream and downstream straight lengths required for installation between various fittings and the primary element.

(b) Recommended Lengths of Straight Piping. Tables 7-1.2-1 (for orifices and nozzles) and 7-1.2-2 (for venturis) recommend the piping installation for these meters. For lengths between the two listed, a systematic uncertainty of $\pm\frac{1}{2}\%$ must be added to the coefficient of discharge component. For lengths shorter than those given in parentheses, the amount of uncertainty that should be added is undetermined but most likely greater than $\frac{1}{2}\%$. In such instances, it is good practice to calibrate the meter in the piping arrangement of the performance test to achieve high accuracy. In other words, the actual piping of the test, or a replica thereof, should be installed in the flow laboratory for a distance upstream of the flow section, as specified for the worst case for the β ratio to be used, to obtain the calibration for the test.

(c) The internal pipe diameter D shall be measured on four or more diameters in the plane of the inlet pressure tap. Check measurements shall be made on three or more diameters in two additional cross-sections at least two pipe diameters from the inlet face of the orifice plate or flow nozzle, or past the weld, whichever is the greater distance. The values of all such upstream diameters shall agree within 0.4% when the diameter ratio β of the orifice or flow nozzle is 0.2 and within 0.5% when the diameter ratio is 0.75. For intermediate values of β, a linear relation can be used. The average of all diameters near the plane of the inlet pressure tap shall be used in computing the diameter ratio of the primary element.

(d) Measurements of the diameter of the outlet section shall be made in the plane of the outlet pressure tap to ensure that the diameter of the outlet section agrees with that of the inlet section, within twice the tolerance given above for the diameters of the inlet section.

(e) The internal surface of the pipe immediately preceding and following an orifice or flow nozzle shall be straight and free from mill scale, pits or holes, reamer scores or rifling, bumps, and other irregularities. The surface roughness shall not be greater than 350 μin. The

pipe shall be near enough to a cylindrical shape that no diameter departs from the average diameter D by more than 0.25%. If boring or honing is necessary to secure this degree of surface smoothness and pipe roundness, such final finishing shall extend for at least 4D preceding and 2D following the inlet face of the orifice or nozzle. The bored or honed portion shall be faired into the pipe at an included angle of less than 30 deg. The depth of material removed shall be the minimum required to obtain the desired condition, and all finishing operations shall be done after welding of flanges and pressure connections. Flanges, when used, shall be constructed and attached to the pipe so that there is no recess greater than $\frac{1}{4}$ in. (6 mm) between the primary element and the end of the pipe, measured parallel to the axis of the pipe.

(f) Tables 7-1.2-1 and 7-1.2-2 summarize the recommendations for the length of metering section to be fabricated as a function of the piping surrounding the flow measurement location [4]. It is not practical to show every possible installation; each must be considered on its own merits. For installations not covered explicitly or where the piping configuration and fittings are not known at the time of design, the worst case shall be used (the maximum lengths of straight pipe). When more than one type of piping configuration is found upstream of the metering section, each one may have some effect, because it is not always the first fitting configuration upstream that governs. If there is less than the recommended straight pipe between any two configurations shown on the relevant schedules in Tables 7-1.2-1 and 7-1.2-2, then the metering section shall be fabricated in accordance with the maximum lengths specified on the applicable schedules. Better yet, a calibration should be performed in accordance with para. 7-2.4b. The straight lengths given in Tables 7-1.2-1 and 7-1.2-2 are minimum values, and straight lengths longer than those indicated are always recommended.

(g) If the upstream piping configuration is worse or more complicated than any of those listed in Tables 7-1.2-1 and 7-1.2-2, then the use of a flow conditioner is recommended. Use 20D of straight pipe upstream of the flow conditioner, followed by 22D downstream straight pipe to the inlet of the primary element. If sufficient straight pipe upstream is not available, the flow conditioner may not be placed closer than 16D upstream of the primary element with another 2 to 4D upstream of the conditioner, and then calibration of the metering section is required; otherwise the flow measurement uncertainty may exceed 1.5%. If there is sufficient upstream straight pipe but the use of a conditioner is desired as well, then at least 20D of straight pipe must be left between the conditioner and the inlet of an orifice.

(h) Minimum straight lengths are required between various fittings located upstream or downstream of the primary element and the primary element itself.

(i) The minimum straight lengths required for classical venturi tubes are less than those defined for orifice plates, nozzles, and venturis because they are derived from different experimental results and different correlation approaches and the convergent portion of the venturi tube is designed to obtain a more uniform velocity profile at the throat of the device. Tests have shown that, with identical diameter ratios, the minimum straight lengths upstream of the venturi tube may be less than those required for orifice plates and nozzles.

Table 7-3 Recommended Maximum Diameters of Pressure Tap Holes

Pipe Inside Diameter	Tap Diameter (Maximum)
2 to 3	$\frac{3}{8}$
4 to 8	$\frac{1}{2}$
> 10	$\frac{3}{4}$

GENERAL NOTE: All dimensions are given in inches.

(j) The values given in these tables were obtained experimentally with very long straight lengths of pipe upstream of each kind of fitting, and it could be assumed that the flow upstream of the disturbance was close enough to a fully developed and swirl-free flow.

(1) When the primary element is installed in a pipe leading from an upstream open space or large vessel, either directly or through any fitting, the total length of pipe between the open space and the primary element shall never be less than 30D. In the absence of experimental data, it has seemed wise to adopt the conditions required for orifice plates and nozzles for the ASME venturi tubes. For any fitting installed, the straight lengths given in Tables 7-1.2-1 and 7-1.2-2 shall apply between this fitting and the primary element.

(2) If several fittings (other than 90 deg bends) are placed in series upstream from the primary element, the following rule shall be applied: between the closest fitting to the primary element and the primary element itself, there shall be a straight length as specified for the fitting and for the actual value of β. Also, between this fitting and the preceding one, there shall be a straight length equal to one half of the value given for the second upstream fitting as specified for a diameter ratio = 0.7, no matter what the actual value of β may be. This requirement does not apply when that fitting is an abrupt symmetrical reduction covered above.

(3) If one of the minimum straight lengths so adopted is between an unbracketed and a bracketed one, a ±0.5% additional uncertainty shall be applied to the flow coefficient uncertainty.

7-3 PRESSURE TRANSDUCER PIPING

The locations of pressure tap holes used with orifices and flow nozzles are referred to the inlet face of the orifice plate or flow-nozzle flange as the datum plane, except for flange taps used with orifices. The locations

of pairs of pressure taps are specified in the chapter dealing with each differential pressure producer. Any piping arrangement that meets the shutoff, drainage, and other installation requirements of the transducers and the primary element selected for the test shall suffice.

Pressure tap holes shall be of specified diameter at the inner surface of the pipe and at right angles to it. The depth of the cylindrical portion of the hole shall be at least two tap diameters. These holes shall not be drilled until after their position has been accurately located. The edges of the pressure tap holes on the inner surface shall be free from burrs and slightly rounded. Very often the pressure tap locations are such that part or all of the drilling must be done in the flange. The outer end of the pressure tap shall be strengthened as necessary and drilled and tapped for the appropriate instrument connection.

The pressure taps shall be located in accordance with the specific sections for the primary elements.

For taps after a single change of direction (bend or tee), it is recommended that the tappings (if pairs of single tappings) be installed in such a way that their axes are perpendicular to the plane of the bend or tee.

The recommended maximum diameter of pressure tap holes through the pipe wall or flange is given in Table 7-3. With clean fluids, smaller diameters may be desirable.

There must be no burrs, wire edges, or other irregularities on the inside of the pipe at the nipple connections or along the edge of the hole through the pipe wall. The diameter of the hole should not decrease within a distance of 2σ from the inner surface of the pipe but may be increased within a lesser distance.

Where the pressure hole breaks through the inner surface of the pipe, there must be no roughness, burrs, or wire edge. The edge (corner) of the hole may be left truly square or it may be dulled (rounded) very slightly.

Connections to the pressure holes should be made in accordance with ASME PTC 19.2. When using nipples, couplings, or adapters, it is important that no part of any such fitting projects beyond the inner surface of the pipe. Methods of making pressure connection to pipes are shown in Fig. 7-3.

7-4 INSTALLATION OF TEMPERATURE SENSORS

For a thorough description and recommendations for accurate temperature measurement, the reader is referred to ASME PTC 19.3, Temperature Measurement. This paragraph specifies the installation of thermometers in the metering section.

When thermometers must be installed in wells, they should be located at least as far upstream of the primary element as the lengths specified in Tables 7-1.2-1 or 7-1.2-2, preferably upstream of the flow conditioner if one was used. Downstream they may not be placed closer than $5D$ to the exit of the primary element.

When peened thermocouples are installed, they cause no interference with the flow. Thermocouples can be peened into the walls of piping and pressure vessels only when the wall thickness is greater than twice their hole depth.

7-5 SOURCES OF FLUID AND MATERIAL DATA

[1] Kinghorn, F. C.; McHugh, A.; Dyet, W. D. The Use of Etoile Flow Straighteners with Orifice Plates in Swirling Flow, ASME paper 79-WA/FM-7, 1979.

[2] Lewis, E. L., ed. *Instrument Standards,* 13th edition. Philadelphia: Naval Ship Engineering Center; 1966.

[3] ISO 5167-1, *Measurement of Fluid Flow by Means of Pressure Differential Devices Part 1: Orifice Plates, Nozzles, and Venturi Tubes Inserted in Circular Cross-Section Conduits Running Full.* Geneva: International Organization for Standardization; 1991.

[4] Bean, H. S., ed. *Fluid Meters: Their Theory and Application,* 6th edition. New York: The American Society of Mechanical Engineers; 1971.

[5] Miller, R. W. *Flow Measurement Engineering Handbook,* 2nd edition. New York: McGraw-Hill; 1983.

Morrow, Thomas B., "Metering Research Facility Program, Orifice Meter Installation Effects: A′ = 29*d* Sliding Flow Conditioner Tests", Southwest Research Institute Project No. 04-7274, Technical Memorandum GRI Report No. GRI-97 / 0083; June 1997

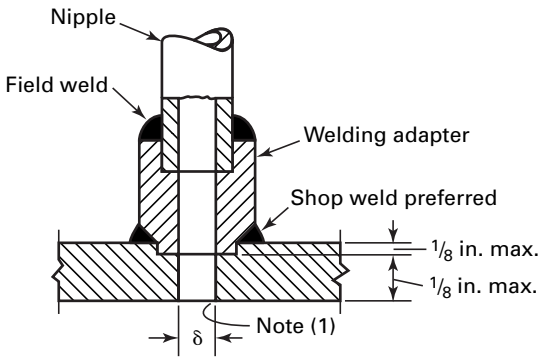

(a) For Temperatures up to 800°F

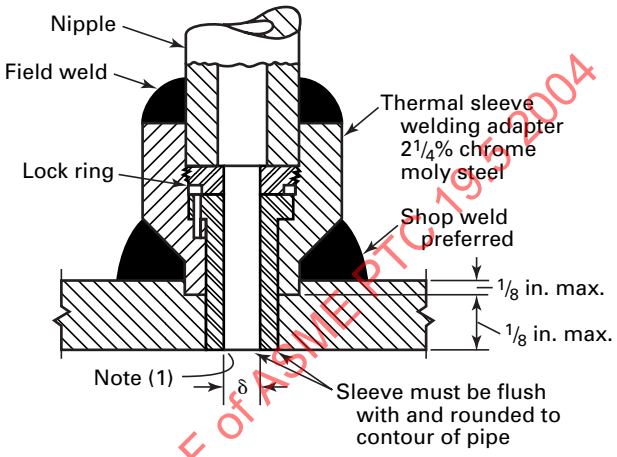

(b) For Temperatures Above 800°F and a Secondary Element With Appreciable Displacement

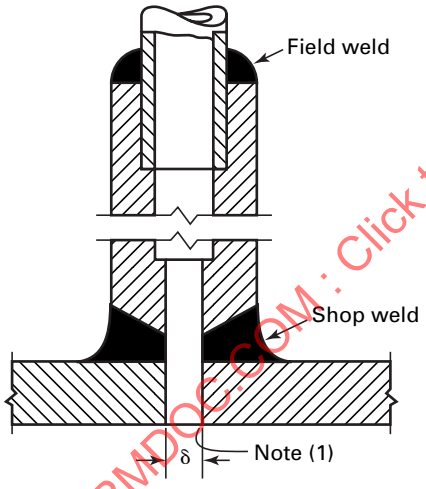

(c) Optional Design Where Full Penetration Weld Is Required

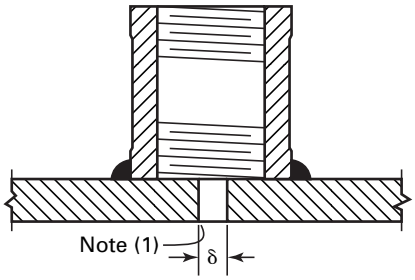

(d) For Temperatures Up To 400°F

NOTE:
(1) Edge of hole must be clean and square or rounded slightly, free from burrs, wire edges, or other irregularities.

Fig. 7-3 Methods of Making Pressure Connections to Pipes

Section 8
Sonic Flow Nozzles and Venturis — Critical Flow, Choked Flow Condition

8-1 INTRODUCTION

The critical flow meter may be classed with variable-head meters in that it requires a constriction in the conduit, inlet pressure and temperature measurements, and knowledge of thermodynamic properties for the calculation of the mass flow of gases and vapors. The feature that distinguishes sonic flow nozzles and venturis from subsonic head meters is that the fluid stream is accelerated to sonic velocity at the throat.

Critical flow exists when the mass flow is the maximum possible for the existing upstream conditions. Sonic flow nozzles and venturis operate at critical flow and have an average throat velocity that closely approximates the local sonic velocity, which is the choked flow condition [1]. Sonic velocity is assumed in the plane of the throat in the one-dimensional flow model used to determine theoretical flow.

Figure 8-1-1 shows a venturi designed for critical flow measurements [2] and includes a comparison of the Mach number distribution through the venturi during subsonic and sonic flow operation. The average throat Mach number cannot exceed a nominal value of 1.0 in any critical flow device. References in the literature to supercritical nozzles indicate that the velocities downstream of the throat are supersonic.

(a) Advantages and Disadvantages of Sonic Flow Meters. All critical flow meters have certain characteristics in common. Because the mass flow is determined solely by the state of the fluid stream at the inlet to the nozzle, there is no need for a differential pressure measurement to calculate the flow as in subsonic variable-head devices. Thus, two measurements instead of three are required, eliminating the need for a throat pressure tap. The nearly linear relationship between the mass flow and the inlet stagnation pressure, at constant temperature, is an advantage over the square-root relationship between the flow and the differential pressure measurement in a subsonic variable-head meter. The linear relationship permits approximately three times the range of flow measurements, compared to the square-root relationship, for equal instrument ranges for the pressure and differential pressure measurements.

The greater range of the critical flow meter does not come without a penalty. At fixed downstream conditions, the total pressure loss across the critical flow meter is approximately proportional to the flow. These losses are caused by fluid friction losses from turbulence (vortices) and losses across shock waves in addition to boundary layer losses. Therefore, the pumping power required increases in proportion to the flow range covered. This is not a characteristic of subsonic flow devices as these have comparatively small total pressure losses.

A related disadvantage of the critical flow meter is the acoustical disturbance created in the downstream fluid. At the high end of the flow range, with low downstream pressure, the exit velocities can be in the high supersonic range. The resulting shock waves cause acoustical noise and turbulence, which may affect apparatus performance and downstream measurements in some applications. Special attention must be paid to this potential problem in calibration activities.

The fact that the flow is both measured and controlled by the inlet conditions to a critical flow meter may be an advantage or a disadvantage depending on the particular application. In calibration applications this feature can be an advantage. However, in most industrial applications it is a disadvantage. Subsonic devices will measure the fluid flow in a conduit without greatly affecting the flow, because the total pressure loss over their flow range from frictional effects is low. This is not true for sonic flow nozzles and venturis.

Critical flow meters are relatively unaffected by disturbances in the inlet fluid stream, other than swirl, compared to their subsonic counterparts. Flow measurement errors caused by pulsation and nonstandardized inlet velocity profiles are at least an order of magnitude smaller for critical flow meters than for subsonic variable-head flow meters. This is due to two factors. Firstly, the acceleration of the stream to sonic velocity mitigates (washes out) the inlet disturbances before they reach the throat. Secondly, the inlet pressure measurement is affected far less by these disturbances, by a factor of 15 [2], compared with the differential pressure measurement required by subsonic devices.

The relatively large pressure drop from the inlet to the throat of the critical flow meter, as required to reach sonic velocity, results in a correspondingly large variation in the fluid properties. Compared with subsonic devices, this requires more accurate fluid properties and more sophisticated calculation methods in some operating regimes to realize the critical flow meter's potential for high accuracy. Alternatively, it would be

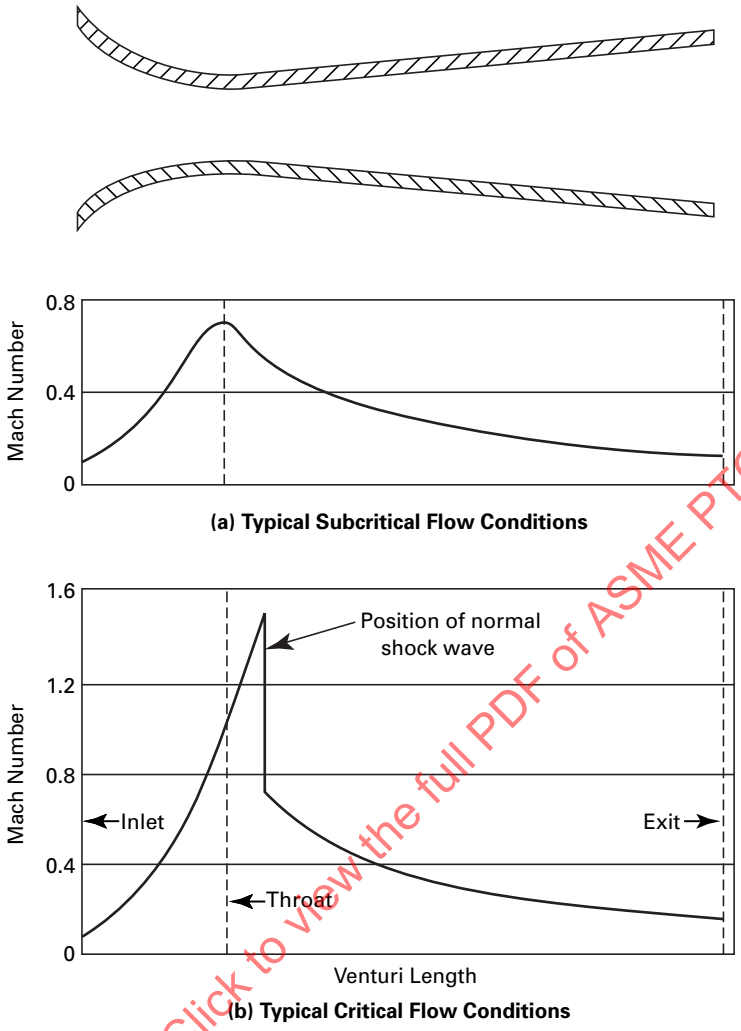

Fig. 8-1-1 Ideal Mach Number Distribution Along Venturi Length at Typical Subcritical and Critical Flow Conditions

necessary to accept a larger error tolerance, as was done for the expansion factors of variable-head flow meters at the highest throat velocities [3]. Fortunately, these limitations were largely overcome by fluid property research and the development of rigorous electronic computations. Highly accurate data have long been available for steam and more recently for several gases.

The Mach number is fixed at every location from the inlet to the throat, where it is nominally equal to Mach 1, in a critical flow meter. Therefore, the discharge coefficient is only a function of the throat Reynolds number. Because the Mach number varies with the flow in a subsonic variable-head flow meter, the discharge coefficient is a function of both the Mach number and the Reynolds number. Consequently, the predicted discharge coefficients of critical flow meters can have substantially lower uncertainties than their subsonic counterparts [4].

Varner [5] used 49 critical flow venturi nozzles in parallel for aircraft gas turbine development. The nozzles had throat diameters of 9.7 in. (24.64 cm) and the flow of air was 25 lbm/sec (11.34 kg/s) through each nozzle when the inlet was at standard atmospheric pressure and temperature.

The stability and accuracy of sonic flow devices make them particularly well suited for use as transfer standards. Stevens [6] used 162 venturi nozzles in parallel with throat diameters of 0.313 in. (7.93 mm) and estimated the uncertainty to be ±0.05% (bias + 2σ).

(b) Special Applications of Sonic Flow Nozzles and Venturis. The critical flow meter is most commonly used to measure and control the mass flow of a gas or vapor. Special meters with the same name should be mentioned to avoid confusion.

The sonic flow choke has a long history of use as a flow-limiting device. The accuracy with which the mass

flow through a choke must be known may vary with the particular application.

The flow through a rupture disk and pressure relief valve are related applications. A mass flow determination under critical flow conditions may be important, but the accuracy requirement is not as great as for critical flow meters.

There is a need to distinguish between critical flow meters used for measuring the flow of gases and vapors and critical flow devices used to measure the discharge of flashing liquids. (These were once called cavitating venturis.) The use of the same names may create some confusion since they operate on different principles. When near-saturated or supercooled liquids enter a nozzle or venturi, they change phase from liquid to vapor (flash), which causes a choked flow condition. These devices share some operational similarities with critical gas flow devices in that the mass flow is nearly linear with the inlet pressure. Liquid critical flow meters are used in the nuclear power field [7].

There is another specialized application that makes use of the unique characteristics of the critical flow meter. The volumetric flow upstream of a critical flow meter is nearly constant, while the mass flow is varied, if certain conditions are met over the operating range. These conditions are as follows:

(1) The stream is nearly an ideal gas (i.e., the variation in the compressibility factor is insignificant).

(2) The discharge coefficient of the meter does not vary significantly over the flow range.

(3) The critical flow function is constant. This is true for an ideal gas.

(4) The Mach number upstream of the meter is low such that the differences between the static and stagnation properties (pressures and temperatures) of the stream are insignificant.

Based on these assumptions, the volumetric flow upstream of the meter is nearly constant. Real gases and flow meters will deviate in varying degrees from these conditions.

(c) Historical Development of Concepts. G. A. Goodenough, Professor of Thermodynamics at the University of Illinois, presented the principles of compressible flow for an ideal gas in a textbook [8]. The equation for the flow of a gas from a plenum at state 1, through a short tube, to a pressure P_2 downstream of the tube was given as follows:

$$q_m = F\sqrt{2g\frac{\gamma}{\gamma-1}\frac{P_1}{1}\left[\left(\frac{P_2}{P_1}\right)^{2/\gamma}-\left(\frac{P_2}{P_1}\right)^{(\gamma+1)/\gamma}\right]} \qquad (8\text{-}1.1)$$

Figure 8-1-2 shows a plot of the mass flow versus the downstream pressure. The downstream pressure is reduced from an initial value equal to the inlet pressure (100), indicated as point A, down to zero at point C. The first derivative of the mass flow function, Eq. (8-1.1), versus the downstream pressure is equal to zero at the

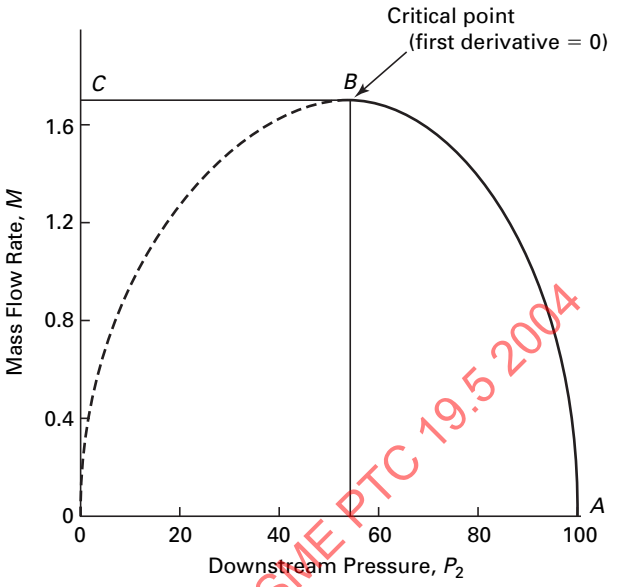

Fig. 8-1-2 Definition of Critical Flow As the Maximum of the Flow Equation, Eq. (8-1.1)

critical flow point, indicated as point B, which is the maximum of the curve.

The downstream pressure at which the flow reached a maximum value is called the critical pressure, and the critical pressure ratio is derived as follows:

$$\frac{P_2}{P_1} = \left(\frac{2}{\gamma+1}\right)^{\gamma/(\gamma-1)} \qquad (8\text{-}1.2)$$

This maximum flow condition, due to sonic velocity being reached at the throat, has been referred to as critical flow in thermodynamics, gas dynamics, and in the early literature.

In the 1930s, gas dynamists recognized the advantage of using Mach number as a parameter and the isentropic stagnation properties in compressible flow analyses [9]. The isentropic flow functions for ideal gases with constant ratio of specific heats are given in Eqs. (8-1.3) through (8-1.6).

$$\frac{P}{P_0} = \left(1+\frac{\gamma-1}{2}M^2\right)^{-\gamma/(\gamma-1)} \qquad (8\text{-}1.3)$$

$$\frac{\rho}{\rho_0} = \left(1+\frac{\gamma-1}{2}M^2\right)^{-1/(\gamma-1)} \qquad (8\text{-}1.4)$$

$$\frac{T}{T_0} = \left(1+\frac{\gamma-1}{2}M^2\right)^{-1} \qquad (8\text{-}1.5)$$

$$\frac{A}{A^*} = \frac{1}{M}\left[\left(\frac{2}{\gamma+1}\right)\left(1+\frac{\gamma-1}{2}M^2\right)\right]^{(\gamma+1)/2(\gamma-1)} \qquad (8\text{-}1.6)$$

The relationships in Eqs. (8-1.3) through (8-1.6) at critical flow are shown in Eqs. (8-1.7) through (8-1.9).

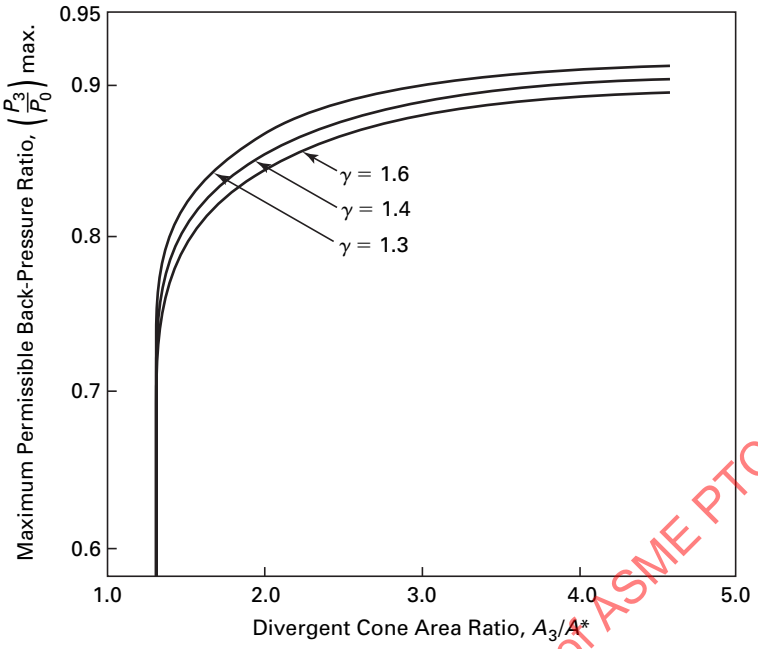

GENERAL NOTE: Reynolds numbers greater than 2×10^5.

Fig. 8-2-1 Requirements for Maintaining Critical Flow in Venturi Nozzles

$$\frac{T^*}{T_0} = \frac{2}{\gamma + 1} \tag{8-1.7}$$

$$\frac{P^*}{P_0} = \left(\frac{2}{\gamma + 1}\right)^{\gamma/(\gamma-1)} \tag{8-1.8}$$

$$\frac{\rho^*}{\rho_0} = \left(\frac{2}{\gamma + 1}\right)^{1/(\gamma-1)} \tag{8-1.9}$$

The relationships in Eqs. (8-1.3) through (8-1.9) became widely used in fluid metering, gas turbines, rockets, aeronautics, and other technical fields.

8-2 GENERAL CONSIDERATIONS

The common characteristic of all critical flow meters (i.e., that the speed of sound is reached at the throat) has lead to the following names:

(a) sonic flow nozzle, venturi, or venturi nozzle

(b) critical flow nozzle, venturi, or venturi nozzle

(c) critical flow orifice (rounded but abrupt inlet contour without a diffuser section)

(d) supersonic nozzle (converging-diverging contour with supersonic velocities)

(e) laval nozzle (converging-diverging contour, named after the pioneer de Laval)

When critical flow is established, the flow is referred to as choked. This is because the flow cannot be regulated by adjustments in valves located downstream of the constriction, as can be done with subsonic flow meters. Thus, when critical flow is established, the mass flow is controlled by the inlet conditions to the critical flow device and is independent, or nearly independent (depending on the wall contour), of the downstream pressure.

It is necessary to have a downstream pressure at or below the value required to maintain sonic velocity at the throat of a critical flow meter. Monitoring of the downstream pressure is therefore necessary to ensure that this requirement is met. The choking pressure ratio is defined as the minimum ratio of the inlet stagnation pressure to the downstream static pressure required for sonic flow. The operating conditions must meet or exceed the choking pressure ratio of the meter for operation under critical flow theory. Conversely, the unchoking back-pressure ratio is defined as the ratio of the downstream static pressure to the inlet stagnation pressure at which the velocity at the throat becomes subsonic. The operating conditions must provide back-pressure ratios lower than the unchoking back-pressure ratio. Figure 8-2-1 gives maximum back-pressure ratios for critical flow venturi nozzles [1].

The design of the diffuser, the fluid density, and other fluid properties all affect the unchoking characteristics of a venturi nozzle. A good diffuser design increases the efficiency with which the kinetic energy of the sonic jet is converted to flow work, resulting in a higher exit static pressure.

The back-pressure ratio requirements given in Fig. 8-2-1 are based on standardized designs for critical flow venturi nozzles.

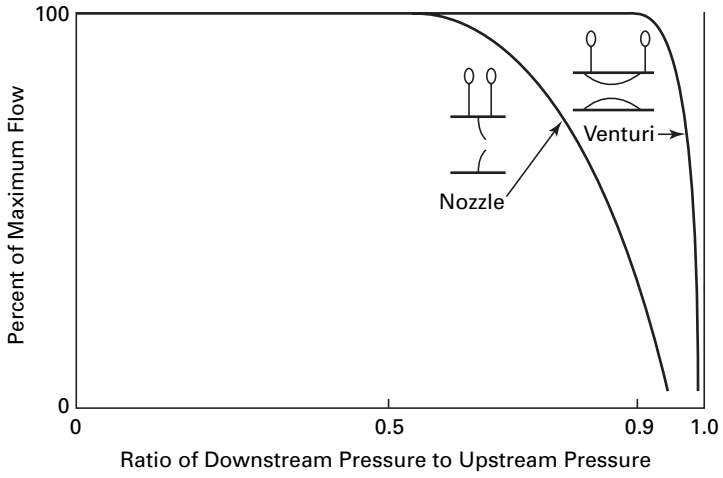

Fig. 8-2-2 Mass Flow Versus Back-Pressure Ratio for a Flow Nozzle Without a Diffuser and a Venturi Nozzle With a Diffuser

A very abrupt approach section, such as the square-edged orifice used in subsonic flow measurements, causes a choked flow condition that is affected by the pressure downstream of the device. Thus, at fixed inlet conditions, the mass flow can increase up to 11% as the downstream pressure is reduced from the value required to first establish sonic velocity, down to zero pressure [10]. This is because of the changing shape of the contracting jet downstream of the orifice (vena contracta). Whereas this is a sonic flow device, it does not meet the essential requirement of a critical flow meter (i.e., that the mass flow is determined solely by the inlet conditions).

It is sometimes necessary to operate in both subsonic and sonic flow regimes. A compromise must then be made in selecting a flow meter design. A critical flow venturi nozzle must have a throat pressure tap added for operation in the subsonic regime. Because there is no performance data for subsonic operation, it must then be calibrated. It may be preferable to select a subsonic meter for which a calibration is available, such as the ASME low-β throat tap flow nozzle, which will also perform reasonably well in the sonic flow regime [11].

Providing a diffuser section downstream of the throat, as shown in Fig. 8-1-1, increases the unchoking back-pressure ratio, as indicated in Fig. 8-2-2.

8-3 THEORY

(a) Definitions

critical flow mass flux: mass flow per unit area perpendicular to the flow.

mass flow defect: the difference between the actual mass flow and the theoretical mass flow based on the assumptions made in calculating the theoretical value. This is the sum of the velocity defect, due to the average velocity at the throat being less than the speed of sound, and the density defect, due to the average density being different from the value calculated from the assumption of one-dimensional isentropic flow.

sonic surface: the location in a fluid stream where the velocity has reached the local speed of sound. This is an imaginary surface with a parabolic or spherical shape near the throat of an axially symmetric sonic flow nozzle or venturi.

(b) General. The theoretical basis for critical flow calculations follows the theory for subsonic variable-head flow meters. The assumptions, upon which critical flow theory is based, are as follows:

(1) The chemical composition of the flowing fluid does not change. (This excludes chemical reactions and elevated temperatures where dissociation of molecules becomes significant.)

(2) The flowing fluid is in a state of thermodynamic equilibrium, such that the equations of state that relate the thermodynamic properties are valid. (This excludes nonequilibrium or metastable states whose properties are time functions.)

(3) The fluid stream is in steady state (i.e., the thermodynamic properties remain constant with time at each point or location in the stream). (This excludes inlet temperature gradients and variations with time due to inadequate upstream mixing.)

(4) The fluid steam is in steady flow. The mass flow is constant through each cross-sectional surface normal to the axis of the fluid stream. (This excludes transient and pulsating flows.)

(5) The flow process from the inlet to the meter throat is reversible (frictionless). The actual flow deviates from this assumption in that the boundary layer is

not frictionless. The coefficient of discharge provides a correction for this deviation.

(6) The fluid flow is one-dimensional, such that the velocity and thermodynamic properties vary only along the axis of the meter from the inlet to the throat. Conversely, the velocity of the stream and all of the thermodynamic properties are invariant in planes normal to the axis of the meter. (Deviations of the actual flow from this assumption due to the existence of two-dimensional flow are corrected by the coefficient of discharge.)

(7) The flowing fluid is a homogeneous compressible fluid, such that each thermodynamic state is totally defined by two independent properties. Examples of fluids that meet these conditions adequately for engineering calculations are as follows:

(a) Pure substances in the gaseous phase (e.g., helium, argon, oxygen, nitrogen, carbon dioxide, steam, and other chemically homogeneous gases).

(b) Gaseous mixtures that may be treated as pure substances, (e.g., air, intimate mixtures of air, and other gases with water vapor).

(c) Intimate mixtures of two or more phases that are finely and uniformly dispersed such that they behave as if they were homogeneous (e.g., a high-quality mixture of saturated water vapor and fine droplets of saturated liquid or similar mixtures of multiple phases that are in thermodynamic equilibrium).

(8) The flow is adiabatic (i.e., without heat transfer). (This can be especially significant in small meters where the surface area of the meter walls is large relative to the cross-sectional flow area of the fluid stream. It is important that the wall temperature of the meter be close to the temperature of the flowing fluid to reduce heat transfer to an insignificant level.)

The frictionless requirement of para. 8-3(b)(5) along with the adiabatic requirement of para. 8-3(b)(8) make the process isentropic.

In accordance with para. 8-3(b)(2), equilibrium is assumed for the thermodynamic states of the fluid in all derivations of theoretical flow. Some nonequilibrium exists immediately following all changes of state since small but finite time is required to reach equilibrium. The theory of equilibrium thermodynamics assumes an idealized quasiequilibrium process to eliminate any time dependence of the thermodynamic states. Sonic flow devices are more apt to encounter significantly nonequilibrium states than subsonic fluid meters because of their higher throat velocities. This is particularly true for very small nozzle sizes.

Venturi designs that have continuous wall curvature from the inlet through the throat provide no time for an equilibrium state to be reached, because the fluid expands continuously through the throat. Designs that have a cylindrical section prior to the sonic flow point provide time for equilibrium to be established. It is unlikely that a significant increase in uncertainty results from nonequilibrium states in most critical flow applications. However, this possibility should be considered when using fluids with complex molecules that might have relatively long relaxation times, such as carbon dioxide.

Acceptable homogeneous fluids include air and other gases containing water vapor, as stated in para. 8-3(b)(7)(b). The volumetric flow correction for water vapor is a linear function of the molar fraction of vapor. A correction of 0.3% in the volumetric flow of air and water vapor with a relative humidity of 75% has been calculated by Aschenbrenner [12].

As previously noted, parenthetically in the list of assumptions, the actual fluid flow process usually deviates from the theoretical assumptions in only two respects. Firstly, the velocity and fluid properties vary in the radial direction in addition to the axial direction of the meter, making the actual flow pattern two-dimensional instead of one-dimensional, as required by para. 8-3(b)(6). (All critical flow meters considered herein have an axially symmetric geometry such that two dimensions define the actual flow condition.) Secondly, there is significant viscous friction in the boundary layer, making the real flow process irreversible, instead of frictionless (isentropic) flow as required by para. 8-3(b)(5).

Figure 8-3-1 shows how these two deviations from the assumptions reduce the actual mass flow below the theoretical value. The radial distribution of mass density, due to centrifugal force effects, increases the actual flow above the theoretical value. This is more than compensated for by the radial distribution of Mach number, which is below the theoretical sonic velocity (i.e., below Mach 1). The sum of these two effects provides the mass flow defect in the inviscid potential flow regime. The viscous friction in the boundary layer provides the second mass flow defect. The mass flow defects are the amounts that each of these effects reduces the actual flow below the flow that would result from the theoretical model defined by the assumptions.

The coefficient of discharge is relied upon to compensate for these two deviations of the actual flow from the theoretical model. The sum of the mass flow defects is equal to one minus the discharge coefficient ($1 - C_d$). Throat Reynolds number is used to correlate the coefficient of discharge. (Theoretical solutions indicate that the discharge coefficient is a weak function of the specific heat ratio, in addition to the throat Reynolds number, but this effect is usually ignored and accepted as scatter in experimental results.) The precision with which this correlation can be realized depends on how closely the assumptions are met. Every deviation of the actual flow from the theoretical model, other than the two for which the Reynolds number can correct, will cause loss of accuracy in the flow measurement. This is especially true with greater differences between calibration and application conditions.

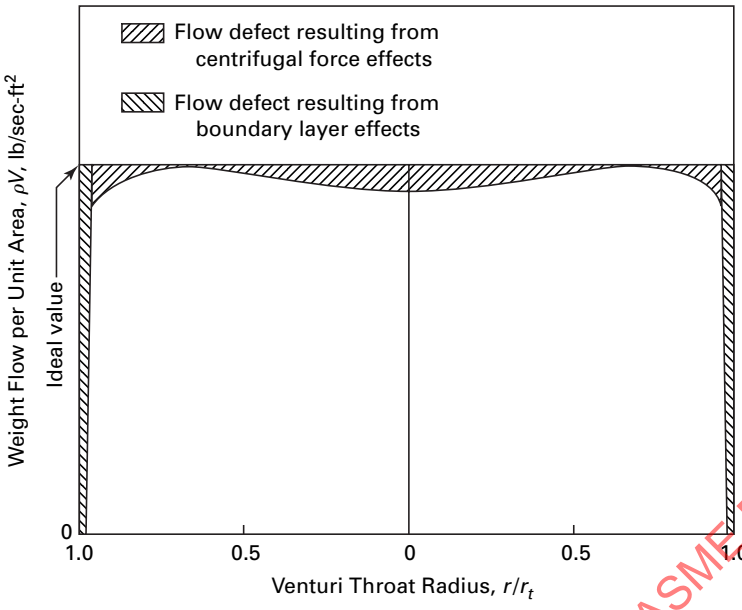

Fig. 8-3-1 Schematic Representation of Flow Defects at Venturi Throat (Smith and Matz 1962)

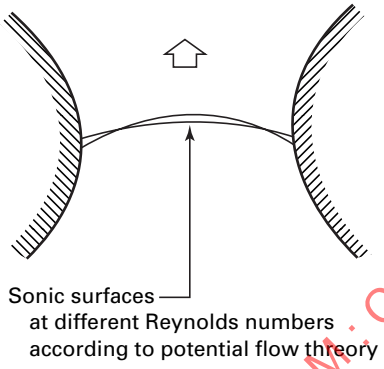

Fig. 8-3-2 Schematic Diagram of Sonic Surfaces at the Throat of an Axially Symmetric Critical Flow Venturi Nozzle (Arena and Thompson 1975)

A schematic diagram of flow profiles at the venturi throat is shown in Fig. 8-3-2, indicating the sonic surface to be a paraboloid of different proportions at different Reynolds numbers.

8-4 BASIC THEORETICAL RELATIONSHIPS

Basic equations and relationships derive from the eight assumptions given in para. 8-3(b) as follows:

(a) Continuity Equation. Conservation of mass for one-dimensional flow, which is applicable to each area of the fluid stream perpendicular to the axis of the meter, is given by

$$q_m = \rho A V \tag{8-4.1}$$

(b) Steady Flow Energy Equation. Conservation of energy, the first law of thermodynamics, applied from the inlet stagnation state to the sonic state at the throat, is given by

$$V^{*2}/2 = h_0 - h^* \tag{8-4.2}$$

(c) Equations of State. Equations of state establish relationships among thermodynamic properties: pressure, temperature, density, compressibility factor, enthalpy, specific heats, ratio of specific heats, and entropy. The relationships depend on the fluid model (i.e., ideal gas, real gas, or vapor).

(d) Isentropic Relationships

$$s_0 = s^* \tag{8-4.3}$$

(e) Local Speed of Sound. Equations for the local speed of sound depend on the fluid model and state properties. The equation for an ideal gas is simple, while the equation for a real gas is complex.

8-5 THEORETICAL MASS FLOW CALCULATIONS

(a) General. Several equations and methods are available for determining the theoretical critical flow. Not all of the methods are applicable to all compositions of gases and vapors in all operating regimes due to limitations in the availability and accuracy of thermodynamic property data and other factors. The choice of a method is governed by the property data available, the flow measurement accuracy required, and the degree of complexity that is acceptable in the computation for the

particular application. Each of these considerations is briefly reviewed here and treated in some detail for each of the equations and methods as they are presented.

(b) Uncertainty in Critical Flow Function Calculations. Accuracy considerations are complicated by two fundamentals. Firstly, all measurements contain errors. Secondly, the absolute accuracy of a measurement is never known. Procedures are well established for calculating the propagation of errors to determine the uncertainty in the result. It is recommended that one of the standardized practices be used (e.g., ASME PTC 19.1). But the basis for applying these procedures is the estimated error in each error source. The mathematical rigor of the error propagation calculations can give the false impression that the uncertainty in the result has been precisely determined. A practical indication of uncertainty is obtained by comparing the results from different methods. The amount of discrepancy often does more to indicate the level of accuracy and confidence that can be placed in the results than formalized uncertainty analyses based on error estimates. For this reason, comparisons of results from different flow measurement methods should be made whenever possible.

Convenience and accuracy may both be important in obtaining a flow measurement. A sophisticated data reduction procedure that provides better accuracy might be essential in some cases, but for practical reasons not desirable in others. One of the several error components in an uncertainty analysis is the error in the critical flow function. A trade-off may be made between a more rigorously accurate calculation and a more convenient simplified calculation that could contain a larger bias. Arnberg and Seidl [13] give errors and corrections that take real gas properties into account for critical flow functions for air calculated in several ways using ideal gas theory.

(c) Methods for Determining Critical Flow Functions. A list of references for critical flow functions is given in the standard [1].

The methods for determining the theoretical mass flow are grouped into three classifications.

(1) Closed Form Solutions. The simplest theoretical critical flow equation is for an ideal gas with the specific heats idealized as constants. This equation has sufficient accuracy in many real gas applications over restricted operating regimes, primarily with regard to pressure limitations.

Approximate methods are given for some improvement in accuracy over broader operating regimes for real gases compared to the ideal gas mode. These methods use the compressibility factor Z correction to the equation of state. Also, ratios of specific heats are obtained in various ways to approximate the isentropic exponent during expansion from the inlet to the throat of the nozzle or venturi.

(2) Iterative Methods Using Gas or Vapor Property Tables. Tables of thermodynamic properties can be used to calculate the flow for various assumed states at the throat of the nozzle. The critical flow state is then determined where the flow reaches a maximum. Tables of thermodynamic properties have been compiled for many substances for their vapor regimes. Gas tables assume the ideal gas equation of state to be valid but permit the variation of specific heats with temperature to be taken into account.

(3) Iterative Methods Using Complex State Equations. The best accuracy over broad operating regimes using real gases and vapors can be obtained by using complex computerized procedures and the most accurate equations of state [14]. Results from these calculations are given in Appendix A for air. Sullivan [15] used more accurate equations of state later published by Jacobsen [16], the results from which are used as the basis for calculating the error in the other methods. Appendix B gives the deviations of the Johnson results from those of Sullivan.

(d) Method for Determining the Deviation From Ideal Gas State. The extent of deviation of the compressibility factor Z from unity is an indication of how nonideally a gas is behaving in a particular state. This must be known to select a method for determining the critical flow function to achieve the desired accuracy. Pressure-temperature-density data are correlated by the compressibility factor as follows:

$$Z = P/(\rho RT) \tag{8-5.1}$$

It is important that the same ideal gas constant R be used with the compressibility factors as was used in compiling the compressibility factor tables and charts. Most compressibility factor data are based on the universal gas constant [see para. 8-5(e)(1)]. Inconsistent use of gas constants with compressibility factors will result in additional error.

The compressibility factor Z is a function of the state of the gas. The real gas equation of state includes the compressibility factor and is correct, subject only to the error in the compressibility factor. Compressibility factors are determined from experimental data, aided by statistical mechanics, and tabulated for each gas composition [17].

In the absence of data for a particular gas, an estimate of the compressibility factor can be obtained from generalized charts. These charts correlate the compressibility factor by reduced pressures (P/P_c) and reduced temperatures (T/T_c). The reduced properties normalize the data using the critical point properties (P_c, T_c) based on the principle of corresponding states.

Use the following steps to obtain an estimate of the compressibility factor for a given state (P, T) of a specified gas:

(1) Obtain the critical point pressure P_c and temperature T_c from critical property tables available in thermodynamics textbooks.

(2) Calculate the reduced properties for the given state using P/P_c and T/T_c.

(3) The compressibility factor can be found in a chart, such as that shown in Fig. 8-5-1 for air, using the reduced properties for parameters.

The universal gas constant is used as a basis for correlating the compressibility factors Z for real gases [17].

(e) Closed Form Solutions for Critical Flow Functions

(1) Ideal Gas Relationships. The assumption is made that the fluid is an ideal gas for which the equation of state by definition is

$$P = \rho(R_u/M)T \tag{8-5.2}$$

where

M = molecular mass
R_u = universal gas constant; U.S. Customary units: 1545 ft-lbf/lbm-mole°R; SI units: 8.314 kJ/kg·moleK

In addition to being an ideal gas, the further assumption is made that the specific heat values are constant, such that the ratios of specific heats are constant. The isentropic functions given in Eqs. (8-1.6) through (8-1.9) are then applicable.

$$P^*/P_0 = (T^*/T_0)^{\gamma/(\gamma-1)} = (\rho^*/\rho_0)^{\gamma} \tag{8-5.3}$$

The speed of sound at the throat for an ideal gas is as follows:

$$c = (\gamma^* R^* T^*)^{0.5} \tag{8-5.4}$$

With the assumption that the ratio of specific heats is constant ($\gamma^* = \gamma_0 = \gamma$), the ideal gas critical flow function is

$$C^*_i = \sqrt{\gamma\left(\frac{2}{\gamma+1}\right)^{(\gamma+1)/(\gamma-1)}} \tag{8-5.5}$$

The corresponding theoretical flow for an ideal gas with constant specific heats is then

$$q_{mi} = \frac{A^* C^*_i P_0}{\sqrt{(R_u/M)T_0}} \tag{8-5.6}$$

Some methods for calculating the ideal gas critical flow function C^*_i are given below.

(a) Method 1: Ideal Gas, Ratio of Specific Heats Assumed Constant. Note from Eq. (8-5.5) that, for an ideal gas with a constant ratio of specific heats, the critical flow function, C^*_i depends only on the composition of the gas (i.e., it is a constant for each gas composition). Whereas no gas is ideal, all gases approach the ideal state at low pressure and most gases behave in a more idealized manner with increasing temperature. In many applications, the simplicity of the flow calculation using Eq. (8-5.5) is a desirable feature and may provide a practical approach, assuming the error that is incurred is tolerable.

Values of the critical flow function from Eq. (8-5.5) and the critical property ratios from Eqs. (8-1.7) through (8-1.9) are given in Table 8-5-1 for monatomic gases (3 deg of freedom), diatomic gases (5 deg of freedom), and triatomic gases (6 deg of freedom).

The critical flow functions C^*_i given in Table 8-5-1 are quite accurate for monatomic gases because their specific heats are nearly constant.

The constant critical flow function for a diatomic gas from Eqs. (8-1.7) through (8-1.9) can be corrected to the real gas value for air by means of correction factors given in Appendix C [13].

The following ideal gas relationships show that the ratio of specific heats is related to the specific heat at constant pressure and the gas constant:

$$R = c_p - c_v \tag{8-5.7}$$

Ratio of specific heats: (8-5.8)

$$\gamma = c_p/c_v$$

Gamma function: (8-5.9)

$$\frac{\lambda - 1}{\lambda} = \frac{R}{c_p} = \frac{\overline{R}}{\overline{c}_p}$$

Consequently, the critical flow function C^*_i will vary for any particular ideal gas as the specific heat at constant pressure varies. This imposes restrictions on the operating states and/or flow measurement accuracy obtainable from Methods 1, 2, and 3 wherein the variation of specific heats is not taken into account.

(b) Method 2: Ideal Gas, Ratio of Specific Heats at Inlet Stagnation State. The easiest way to partially compensate for changes in specific heats is to use the ratio of specific heats corresponding to the inlet stagnation state, instead of a fixed value for each gas, as in Method 1. The error in Method 2 is shown in Fig. 8-5-2.

Example 1
Gas: air
Inlet stagnation pressure $P_0 = 100$ atm
Inlet stagnation temperature $T_0 = 550$°R
Real gas [15] $C^* = 0.7083$
Real gas [16] $\lambda_0 = 1.5944$
From Eq. (8-5.5), based on $\lambda_0 = 1.5944$, Method 2: $C^*_i = 0.7156$; Error $e = +1.03\%$
From Fig. 8-5-2: Error $e = +1.00\%$ (agreement to the readability of the graph)

Based on Method 1, from Table 8-5-1:
Ratio of specific heats $\gamma = 1.4$
$C^*_i = 0.68473$
Error $e = -3.33\%$

Compared with Method 1, Method 2 reduced the absolute error from 3.33% to 1.03%.

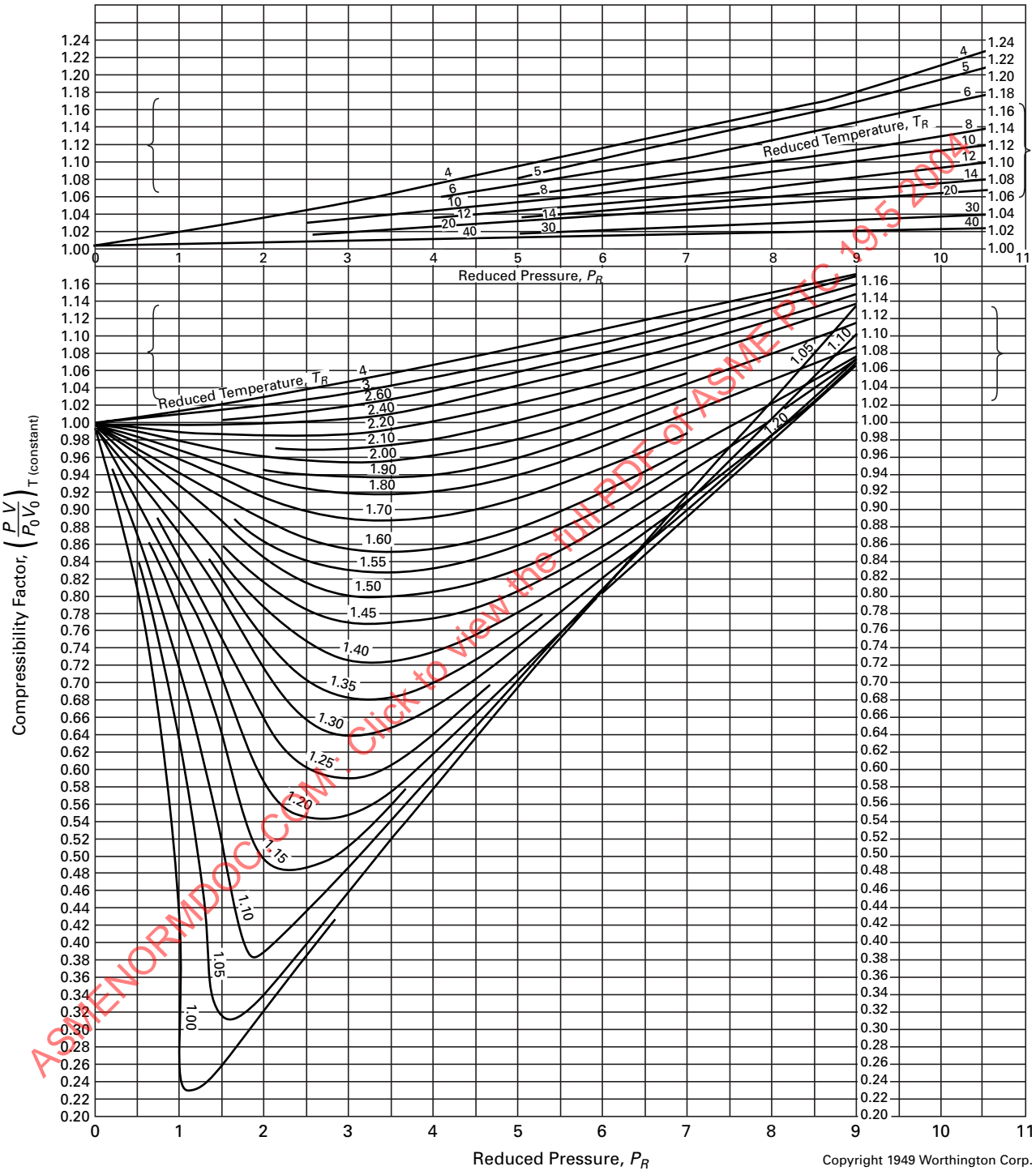

Fig. 8-5-1 Generalized Compressibility Chart

GENERAL NOTE: Compressibility factor for gases:

$$P_R = \text{reduced pressure} = \frac{P}{P_c}$$

$$T_R = \text{reduced temperature} = \frac{T}{T_c}$$

$$\left(\frac{P\,V}{P_0\,V_0}\right)_{T\,(\text{constant})} = 1 \text{ for ideal gases;}$$

P, P_c, T, and T_c are in absolute units.

NOTE:

(1) In this range, at reduced temperature approximately equal to 4, the compressibility factor reaches a maximum, and then decreases with an increase in reduced temperature values, to avoid confusion in reading, the reduced temperature lines greater than 4 are offset on an identical scale.

Fig. 8-5-1 Generalized Compressibility Chart (Cont'd)

Table 8-5-1 Critical Flow Function C^*_i and Critical Property Ratios [Ideal Gases and Isentropic Relationships, Eqs. (8-1.7) through (8-1.9)] Versus Type of Ideal Gas

Type of Gas	Ratio of Specific Heats	Critical Flow Function, C^*_i	Critical Temperature Ratio	Critical Pressure Ratio	Critical Density Ratio
Monatomic	$5/3 = 1.666\,7$	0.726 18	0.750 00	0.487 14	0.649 53
Diatomic	$7/5 = 1.4$	0.684 73	0.833 33	0.528 28	0.633 93
Triatomic	$8/6 = 1.333$	0.673 22	0.857 14	0.539 77	0.629 44

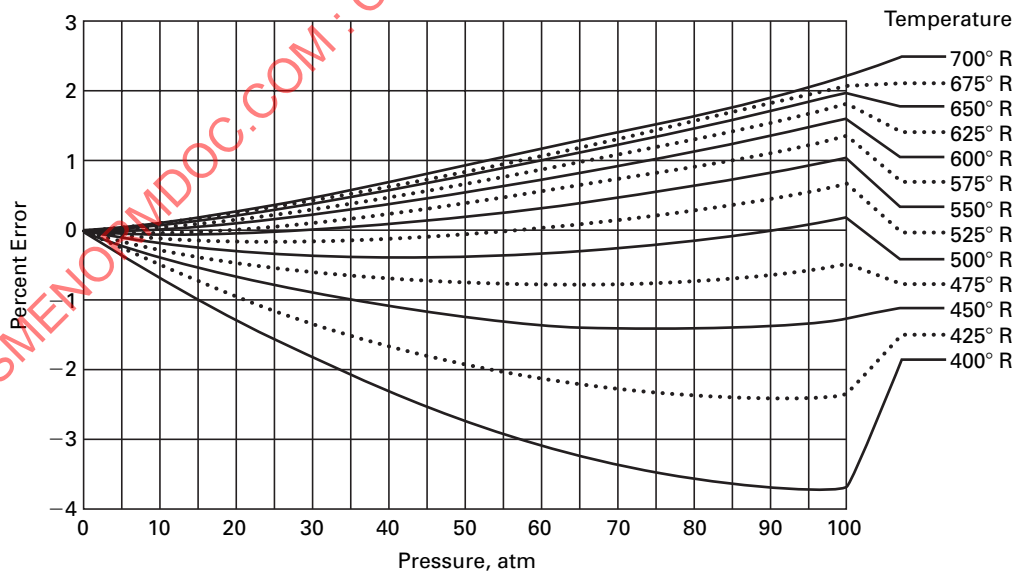

GENERAL NOTE: Error in ideal gas critical flow function for air, based on inlet ratio of specific heats γ_0.

Fig. 8-5-2 Error in Critical Flow Function C^*_i for Air Using Method 2 Based on Ideal Gas Theory With Ratio of Specific Heats Corresponding to the Inlet Stagnation State [13]

Table 8-5-2 Percentage Error in Method 3 Based on Critical Flow Functions [19] and Air Property Data [17]

Temperature, °R	Inlet Stagnation Pressure, atm				
	5	10	20	40	80
475	+0.17	+0.33	+0.65	+1.18	+1.67
500	+0.13	+0.25	+0.50	+0.91	+1.23
550	+0.06	+0.15	+0.30	+0.52	+0.60
600	+0.03	+0.08	+0.15	+0.26	+0.18
700	−0.03	−0.04	−0.03	−0.09	−0.31

(2) Real Gas Relationships. Sullivan [18] gives an historical review of theoretical isentropic flow models for real gases.

The real gas equation of state is as follows:

$$P = \rho ZRT \tag{8-5.10}$$

The most elementary correction of the ideal gas critical flow equation for real gas effects is to add the compressibility factor correction to the ideal gas constant [i.e., substituting ZR for the gas constant R in Eq. (8-5.6)], as follows:

$$C^*_{Ri} = \frac{C^*_i}{Z^{0.5}} \tag{8-5.11}$$

The theoretical equation for the mass flow of a real gas can be calculated from the following:

$$q_{mR} = \frac{P_0 A^* C^*_i}{(ZRT_0)^{0.5}} \tag{8-5.12}$$

(a) Method 3: Real Gas Approximation Using the Ideal Gas Critical Flow Function Corrected by the Compressibility Factor. This method uses Eqs. (8-5.5) and (8-5.11) to obtain an approximation for the real gas critical flow function. The compressibility factor and ratio of specific heats used in the solution correspond to the inlet stagnation state.

The error in the real gas critical flow function for air using Method 3 based on Sullivan [15] is shown in Fig. 8-5-3 [13]. Table 8-5-2 gives errors in Method 3 based on critical flow functions from Johnson [19].

At an inlet temperature of 475°R and a pressure of 80 atm, the error from Fig. 8-5-3 is 1.18% compared with 1.67% from Table 8-5-2. Since Johnson and Sullivan used nearly identical calculation methods, the difference of 0.49% in the results is attributed to discrepancies between the property data of Hilsenrath et al. [17] and Jacobsen [16].

(f) Iterative Methods Using Gas or Vapor Property Tables

(1) Ideal Gases, Using Gas Tables

(a) Method 4: Ideal Gas, Gas Tables. Most textbooks on thermodynamics and gas dynamics published since 1948 have included gas tables abridged from Keenan and Kaye [20]. These tables permit solutions for isentropic processes to be calculated for ideal gases with the variation of specific heats with temperature taken into account. These tables make it possible to calculate critical flow more accurately than by Methods 1 and 2, the latter of which will be shown in the following example:

Example 2
Gas: air
Gas property data obtained from Keenan and Kaye [20].
An inlet state will be chosen at a sufficiently low pressure to meet the ideal gas requirement quite well, and at a high temperature where a large variation in the ratio of specific heats is expected.
Inlet state: pressure $P_0 = 10$ atm (146.96 psia)
Temperature $T_0 = 700$°R
$h_0 = 167.56$ Btu/lbm
$Pr_0 = 3.446$

The first approximation of the sonic state at the throat will be made using the isentropic, constant γ values from Table 8-5-1.

$T^* = T_0(T^*/T_0) = (700)(0.83333) = 583.3$°R
$h^* = 139.46$
$Pr^* = 1.8161$
$P^* = P_0\,(Pr^*/Pr_0) = 146.96\ (1.8161/3.446) = 77.4504$ psia
$\rho^* = P^*/RT^* = (144)(77.4504)/(53.34)(583.3) = 0.35850$ lbm/ft^3
$V^* = [2g_c 778(h_0 - h^*)]^{0.5} = [(2)(32.174)(778.26)(167.56 - 139.46)]^{0.5} = 1186$ ft/sec
$q_m/A = \rho V^* = (0.35850)(1186) = 425.2$ lbm/sec ft^2

The above calculation is repeated for a range of temperatures in the region of the first approximation of T^* from which the critical flow state is determined as the point at which maximum flow occurs.

The throat state is established at 584.0°R corresponding to the maximum mass flow of 425.164 lbm/sec ft^2. This result is in error by −0.12% compared with Sullivan [15].

(2) Real Gases, Using Thermodynamic Property Tables

(a) Method 5: Real Gases and Vapors, Thermodynamic Property Tables. This method is applicable to real gases and vapors for which thermodynamic property tables are available. These tables contain properties such as entropy, enthalpy, and mass density (or more commonly the reciprocal, the specific volume) as functions of two variables, usually the pressure and temperature. The accuracy of the result using this method is very sensitive to the accuracy and resolution of the property tables.

This method is similar to Method 4 where gas tables were used. The gas tables gave properties as a function of temperature and were applicable only at low pressures, where deviations from ideal gas properties would be small. The thermodynamic property tables account for

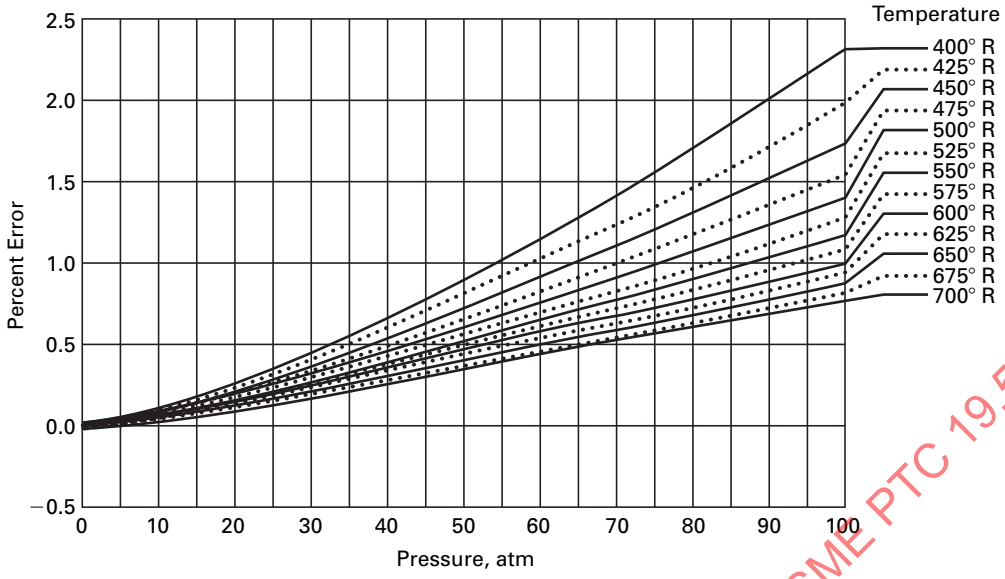

GENERAL NOTE: Error in real gas critical flow function for air, based on ideal gas critical flow function, inlet ratio of specific heats γ_0, and inlet compressibility factor Z_0.

Fig. 8-5-3 Error in Method 3 for Air Based on Critical Flow Functions [15] When Using Air Property Data [13] [16]

real gas effects by taking both temperature and pressure into account. With two independent variables instead of one, interpolation of the tables becomes more complex. When the thermodynamic properties have been computerized, the iterative calculations are much easier to perform. Solutions are shown using a table lookup of properties. The same method would apply using computerized properties.

Example 3
This example uses thermodynamic property tables and linear interpolation between quantities in the tables. This method is not the most accurate, but it is useful because of the wide availability of thermodynamic property tables for many substances.
Gas: steam
Gas property data obtained from Keenan and Keys [21]

For this example, a plenum state is selected where the steam is a very nonideal gas (a vapor). This is indicated by a large change in enthalpy at constant temperature, indicating the properties change significantly with pressure as well as temperature.

Inlet stagnation state: pressure P_0 = 1,000 psia
Temperature T_0 = 700°F (1,160°R)
Enthalpy h_0 = 1,125.3 Btu/lbm
Entropy s_0 = 1.5141 Btu/lbm

An iterative solution establishes the throat state. An even temperature from the table is chosen for the first guess.

T^* = 600°F (1,060°R)
s^* = s_0 = 1.5141

The following values are found from the tables at this state:

h^* = 1,282.9
v^* = 0.827 ft^3/lbm

The throat velocity and mass flow per unit area are as follows:

V^* = $[(2)(32.174)(778.26)(1{,}325.3 - 1{,}282.9)]^{0.5}$ = 1,457.2 ft/sec
G^* = V/v = 1,457.2/0.8205 = 1,762 lbm/sec ft^2

Iteration is continued to find the maximum flow, which is the critical flow point.

The throat temperature and entropy fixed the sonic flow state. Thus, interpolation from the tables gives the state at the throat to be

s^* = 1.5141 Btu/lbm R
T^* = 550°F
P^* = 546.7 psia

An ideal gas estimate for the throat temperature for a triatomic gas, although it would not be expected to be very accurate, is made using the critical temperature ratio from Table 8-5-1 as follows:

$$T^*_i = T_0(T^*/T_0) = (1{,}160)(0.85714) = 994.3°\text{R}\ (534°\text{F})$$

In spite of the very nonideal gas states over this flow process, the ideal gas estimate of the throat temperature would have provided a useful guide for the first estimate, thus reducing the number of iterations required.

The real gas theoretical (isentropic) mass flow at a throat temperature of 550°F, corresponding to the critical flow point, was found to be q_{mR}/A = 1,831 lbm/sec ft^2.

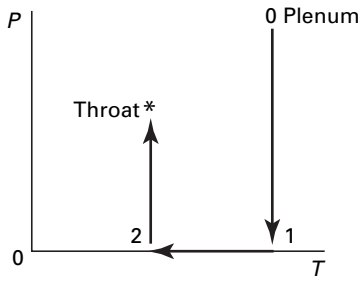

Fig. 8-5-4 Calculation Processes for the Isentropic Path From Inlet to Sonic Throat for a Real Gas Using the Method of Johnson [14]

The discrepancy between the result from Example 3 and the result from Johnson [14] is 0.36%. Note that the steam tables were first published in 1936 from a different database than Johnson's value, which was primarily based on Hilsenrath [17]. Presumably, the later property data are the most accurate.

(3) Real Gases, Using Complex Property Equations

(a) Method 6: Real Gases, Virial Equation of State. Johnson [14] published rigorous solutions and extensive tables of critical flow functions based on real gas properties. Sullivan [15] added refinements to Johnson's method. These are complex solutions that must have the equations of state programmed for practical evaluation by the iterative procedures they entail.

The difference between Methods 5 and 6 stems from the type of property data they use. Method 5 uses the enthalpy and entropy values correlated by researchers in compiling the thermodynamic property tables. Method 6 uses the more fundamental correlation of specific heat at constant pressure and compressibility factor, or alternatively, the equations of state that are the basis for determining the compressibility factors. A brief summary of the method used by Johnson [14] is given.

Two requirements must be met in this method to solve the critical flow process from the plenum to the throat of the sonic nozzle. Firstly, the plenum and throat entropies must be equal. Secondly, the throat velocity must be equal to the speed of sound. The processes followed during the calculations to proceed from the plenum to the throat are as shown in Fig. 8-5-4.

Equations for the change of entropy during these processes are as follows:

For the isothermal processes,

$$(s_1 - s_2) = -ZR\ln(P_1/P_0) \qquad (8\text{-}5.13a)$$

$$(s^* - s_2) = -ZR\ln(P^*/P_2) \qquad (8\text{-}5.13b)$$

For the constant pressure process,

$$(s_2 - s_1) = -c_p\ln(T_2/T_1) \qquad (8\text{-}5.13c)$$

For the entropy to be equal at the plenum and throat, the following must be true:

$$(s_1 - s_0) + (s_2 - s_1) + (s^* - s_2) = (s^* - s_0) = 0 \qquad (8\text{-}5.13d)$$

The equations for the entropy changes must be expressed in differential forms to account for the variation of the compressibility factor and specific heat at constant pressure. The variation of specific heat with temperature is taken into account when integrating along the zero pressure path. (The gas is ideal at zero pressure where the most accurate data for the specific heat at constant pressure are available.) The compressibility factor must be known and its variation taken into account along the two isothermal processes.

The calculation determines the throat state by iteration to satisfy the first requirement, Eq. (8-5.13d), that the throat and plenum entropies are equal.

To meet the second requirement, the throat velocity and the local speed of sound at the throat must be calculated and iteration continued until the state is found where they are equal. The velocity at the throat is calculated from the energy equation, using the enthalpy decrease from the plenum to the throat. This is determined by integration along the three processes shown in Fig. 8-5-4. The speed of sound is a function of the state at the throat, for which Eq. (8-5.14) was used.

$$\alpha^2 = \left(\frac{\delta p}{\delta \rho}\right)_s \qquad (8\text{-}5.14)$$

$$= RT\left[Z+\rho\left(\frac{\delta Z}{\delta \rho}\right)_T + \frac{\left[Z + T\left(\frac{\delta Z}{\delta T}\right)_\rho\right]^2}{\frac{C_{p0}}{R} - 1 - T\left(\frac{\delta}{\delta T}\left\{\int_0^\rho \left[Z - 1 + T\left(\frac{\delta Z}{\delta T}\right)_\rho\right]\frac{d\rho}{\rho}\right\}\right)_\rho}\right]$$

The theoretical sonic state at the throat has been determined when both the isentropic and sonic velocity requirements have been met.

A graph of critical flow functions for air is given in Appendix A [19].

The uncertainty in the critical flow functions for air [19], based on results from Sullivan (1989), is given in Appendix B. It is seen that the largest discrepancy is 0.4% at the inlet stagnation state corresponding to the highest pressure (100 atm) and lowest temperature (400°R). Below 25 atm, the two methods agree to within 0.02% at temperatures from 400°R to 700°R.

An approximate graphical method for obtaining critical flow functions for air is given in Appendix C. The correction factors provided by the graphs convert the ideal gas critical flow function for air (0.6847315) to real gas values [15]. The graphs extend to a pressure of 300 atm and cover temperatures from 400°R to 700°R.

(b) Method 7: Real Gases, Table Lookup or Curve Fitting to the Results of Method 6. When accurate solutions

have been obtained for a particular gas over the operating range of interest, it may be preferable to use these results rather than recalculating using Methods 1 through 6. Depending on the application, either table interpolation or curve fitting could be used. Both of these provide close to the maximum available accuracy without the complexity of repeating the calculations. Equations that fit the surface of critical flow function versus pressure and temperature may be obtained with good accuracy over limited ranges.

8-6 DESIGNS OF SONIC NOZZLES AND VENTURI NOZZLES

(a) General. The main feature of a sonic nozzle or venturi design is the variation in the cross-sectional flow area in the axial direction from the inlet pipe or plenum to the discharge pipe or plenum (i.e., the meter contour). The contour, and possibly the surface roughness, determine the essential features (i.e., the coefficient of discharge and choking pressure ratio over the operating range). Related features include inlet flow conditioning, the locations and details of the inlet temperature probe(s), the inlet pressure tap(s), and the location of an exit pressure tap for the measurement of the back pressure on the meter.

The flow-metering characteristics are mainly determined by the inlet contour. The diverging portion to a location slightly beyond the throat may slightly affect the performance of some meters in some operating regimes due to effects on the throat boundary layer and on the shape of the sonic surface. These possible effects have not been documented. The exit section, primarily the angle and length of the diffuser, determines the efficiency of the diffusion process. The efficiency along with the meter size and operating parameters determine the choking pressure ratio.

Meter designs are most commonly described in terms of the shape of the walls confining the fluid stream in a longitudinal-section vies. Thus, a circular-arc inlet refers to the wall shape of the inlet portion of the meter hardware. Similarly, the inlet of an ASME flow nozzle is described as a quadrant of an ellipse. An alternative description gives the full three-dimensional shape. Thus, a circular-arc inlet revolved about the axis of the meter forms a torus. Thus, a toroidal throat venturi nozzle is an alternative description for a nozzle with a circular-arc inlet. The ASME/ANSI standard [1] uses the term toroidal throat venturi nozzle.

The discharge coefficient versus Reynolds number relationship and the choking pressure ratio characteristics must be determined for each meter design. Extensive testing is required to obtain a high accuracy over a large Reynolds number range. High confidence in the absolute accuracy of the discharge coefficient can only be obtained by comparing the results of tests that use different primary measurement methods. This would be facilitated by limiting the number of designs studied, which in turn would be encouraged by standards with small tolerances. The tolerances of the present standards [1, 22] are large enough to cause substantial differences in discharge coefficients and, thus, necessitate a larger uncertainty in the mean calibration curve than might otherwise be required.

(b) Design Criteria

(1) Repeatability. It is futile in most applications to attempt to obtain an accuracy of flow measurement higher than the repeatability of the meter. Random errors can be reduced by repetition and averaging, but errors that are not truly random cannot be reduced in this manner. Repeatability in boundary layer transition regimes is poor due to the complexity of the mechanisms that trigger the transition. Therefore, it is desirable to develop meter configurations that have minimal changes in their discharge coefficients during transition.

(2) Inlet Contour. The inlet contour, to the location where sonic velocity is reached, should preferably produce a thin boundary layer. This would minimize the change in the discharge coefficient during transition, thereby minimizing loss of accuracy due to nonrepeatability in this regime. A thin boundary layer also contributes to a high coefficient of discharge, due to a low boundary layer mass flow defect (see Fig. 8-3-1). This is desirable because it indicates that the actual flow is close to the theoretical model, such that little empirical correction is required of the discharge coefficient. This in turn adds to the confidence with which the discharge coefficient versus Reynolds number correlation can be relied upon to maintain accuracy. This is especially important when there are large differences between calibration and application flow conditions (i.e., the range of states and gases over which the correlation can be applied with tolerable loss of accuracy).

The circular-arc inlet, with no cylindrical throat section, produces a thin boundary layer. The radius of curvature of the approach section is important in determining the mass flow defect (Fig. 8-3-1) and, thus, the value of the discharge coefficient. The variation of the discharge coefficient as a function of the inlet radius was calculated by Stratford for laminar and turbulent boundary layers versus Reynolds number [23]. The circular-arc nozzle with an inlet radius equal to twice the throat diameter is close to optimum for producing a high discharge coefficient. This is because an inlet radius of twice the throat diameter nearly optimizes the combination of boundary layer thickness and two-dimensional (centrifugal force) flow effects.

(c) Standardized Flow Nozzle and Venturi Designs

(1) Toroidal Throat Venturi Nozzle. A design known in the United States as the modified Smith/Matz venturi nozzle has been adopted by national and international

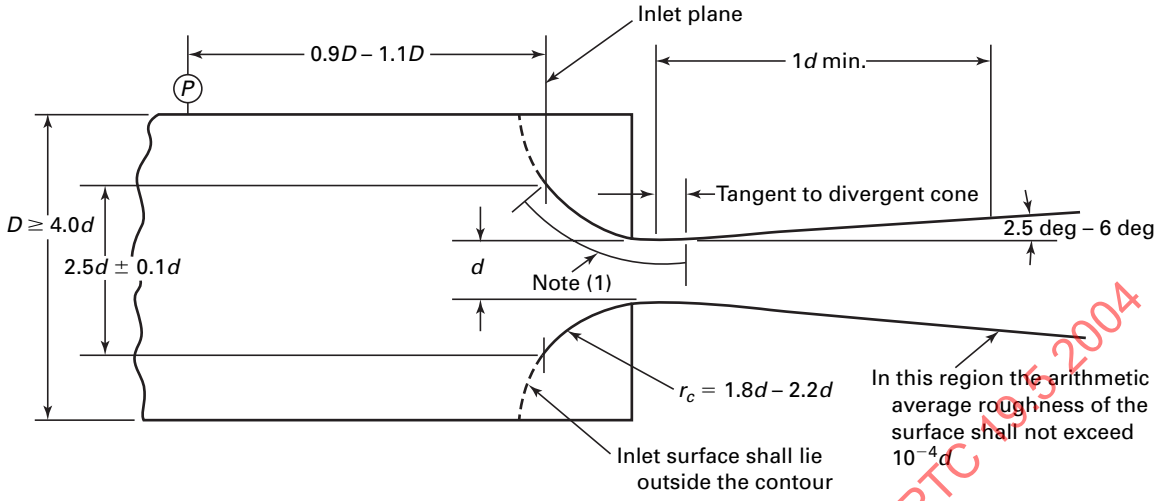

NOTE:
(1) In this region the surface shall not exceed $15 \times 10^{-6}d$ arithmetic average roughness and the contour shall no deviate from toroidal form by more than $0.001d$.

Fig. 8-6-1 Standardized Toroidal Throat Sonic Flow Venturi Nozzle

standards organizations [1, 22]. The modification was to the inlet radius, which was originally $1.816d$ [2] and was changed to $2.0d$ with a tolerance of $0.2d$ in the standards. This design is shown in Fig. 8-6-1.

One advantage of the toroidal throat critical flow venturi is that the continuous inlet curvature, passing through the throat, lends itself to analysis for the determination of theoretical discharge coefficients.

The design avoids the boundary layer buildup that occurs in a cylindrical section, with its near-zero pressure gradient, and the related problems of transonic shock, flow separation, and boundary layer pressure gradient reversal.

(2) Cylindrical Throat Venturi Nozzle. A sonic venturi with a cylindrical throat section may have manufacturing and metrological advantages over the toroidal throat venturi, especially in small sizes. It is essential that the cylindrical throat not have a taper that could cause the throat to occur at a location other than the exit, or, even less desirable, a sonic flow location that oscillates between the inlet and the exit. This venturi design has been accepted as a sonic flow standard [1, 22] and is shown in Fig. 8-6-2.

The cylindrical throat design offers some advantages, primarily in ease of manufacture, but is inferior to the toroidal throat design from fluid mechanics points of view. Firstly, the inlet radius is more abrupt in that it is equal to the throat diameter instead of twice the throat diameter. This produces larger centrifugal forces, resulting in a larger radial density gradient, compared with the toroidal throat design. Secondly, the flow discontinuity at the juncture of the inlet curvature and the beginning of the cylindrical throat poses the risk of flow separation, especially following the small inlet radius of curvature. Thirdly, the cylindrical section causes the boundary layer to become thicker than the toroidal throat design. These effects combine to reduce the discharge coefficient, which is an undesirable feature for any flow meter.

(3) ASME Low-β Flow Nozzles. Figure 8-6-3 shows two standardized ASME nozzles that were designed for subsonic application and offer possibilities for combined subsonic and sonic operation. The high-β ratio design [Fig. 8-6-3, sketch (a)] is not recommended for use as a sonic flow nozzle because of the high inlet Mach number. (A maximum β ratio of 0.25 is specified in the standards.) But, it can be used with appropriate correction for the inlet pressure and temperature measurements, with some sacrifice in accuracy. Figure 8-6-3, sketch (b) shows an ASME low-β ratio flow nozzle with throat pressure taps, which is recommended for combined subsonic and sonic flow operation.

See Section 5 for details and dimensions of the ASME flow nozzles.

8-7 COEFFICIENTS OF DISCHARGE

(a) Method of Correlation of Discharge Coefficients. The coefficient of discharge corrects for the deviation of the actual mass flow from the theoretical value. The throat Reynolds number correlates the discharge coefficients for critical flow meters. For axially symmetric flow meter designs, all flow sections are circular in cross-section, such that the throat Reynolds number is given by the following:

$$R_d = 4q_m/\pi d\mu \qquad (8\text{-}7.1)$$

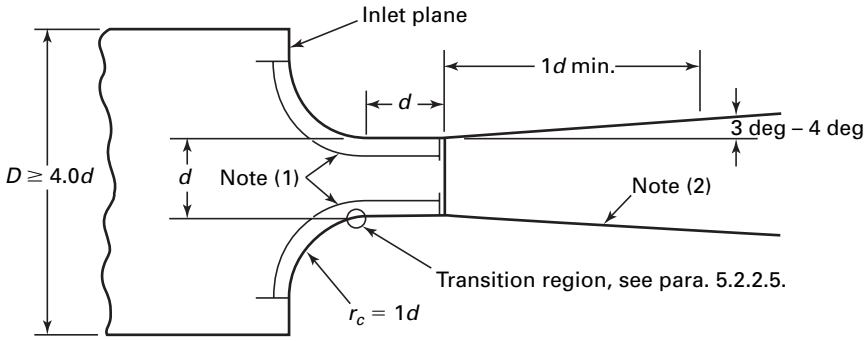

NOTES:
(1) In this region the arithmetic average surface roughness shall not exceed $15 \times 10^{-6}d$, and the contour shall not deviate from toroidal and cylindrical form by more than $0.001d$.
(2) In the conical divergent section, arithmetic average of the relative roughness shall not exceed $10^{-4}d$.

Fig. 8-6-2 Standardized Cylindrical Throat Sonic Flow Venturi

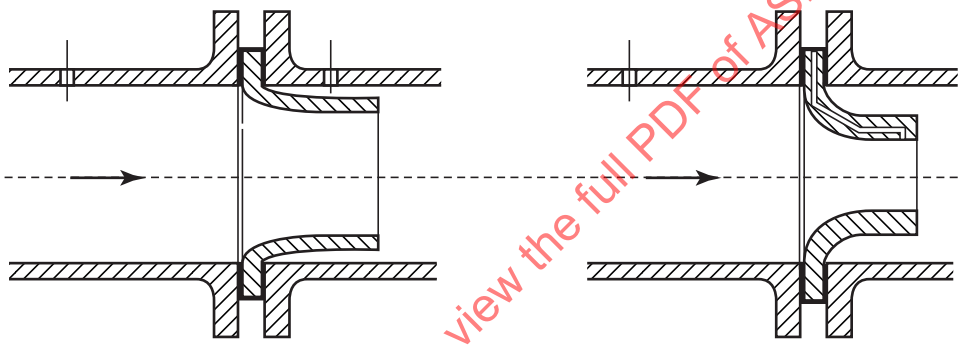

(a) High Beta, β (b) Low Beta, β

Fig. 8-6-3 ASME Long-Radius Flow Nozzles

The absolute viscosity μ is determined at the inlet stagnation temperature.

Theoretical solutions for the discharge coefficients of toroidal throat venturi nozzles indicate the discharge coefficient is a weak function of the ratio of specific heats in addition to the Reynolds number. This fact will cause some scatter when the data includes gases with different ratios of specific heat [24].

(b) Calibration Methods and Uncertainty Estimates for Discharge Coefficients

(1) General. Discharge coefficients are determined experimentally and analytically. Experimentally determined discharge coefficients are subdivided into primary and secondary measurements. Secondary measurements are performed with the test meter in series with one or more critical flow meters in parallel, which have been previously calibrated by primary methods. Many primary methods have been developed. Error estimates using standardized procedures are performed on the primary methods; however, confidence in the absolute accuracy of the primary methods can only be obtained by consistency in the results from the different methods.

(2) Experimentally Determined Discharge Coefficients. The accurate measurement of mass flow of gas is more difficult than for a liquid. But, liquid calibrations cannot be applied to critical flow measurements with accuracy. So, it has been necessary to develop several primary methods for measuring the mass flow of gases. Probe traverses, volume displacement (bell prover), change of state in a calibrated volume, and bulk mass flow measurements (gravimetric methods) have been employed.

(3) Analytically Determined Discharge Coefficients. Analytically determined discharge coefficients use boundary layer theory and potential flow theory to calculate the deviations of the actual flow from the ideal one-dimensional inviscid flow model. Stratford [23], Hall [25], and Ishibashi and Takamoto [26] provided analytical discharge coefficients for sonic flow nozzles. Smith and Matz [2] used theory and internal flow measurements to obtain discharge coefficients for critical flow venturi nozzles.

Table 8-7-1 Summary of Points Plotted in Fig. 8-7-1 and Coefficients for Eq. (8-7.2)

Reference	a	b	R_d, min.	R_d, max.	Nozzles	Diameter, mm	Avg. Pts.
Takamoto and Ishibashi (1998)	0.9985	3.412	2.40E+04	8.50E+04	23	3.4~19	23
Ishibashi et al (1998)	...	...	2.10E+04	1.70E+05	5	6.7–13.41	10
Takamoto et al (1994) (1999)	...	...	4.30E+04	1.40E+06	2	6.7 & 19	12
Wendt and von Lavante (2000)	0.9982	3.448	5.00E+04	1.30E+05	3	5~10	12
Karnik et al (1996)	...	...	1.00E+07	2.40E+07	2	10, 23.3	2
Stevens (1986)	0.9975	3.901	2.00E+05	1.20E+06	14	7.9	21
Smith & Matz (1962), Beale (1999)	...	...	4.00E+05	5.00E+06	1	143	7
Olsen (1972)	...	...	8.68E+05	3.37E+06	1	25	6
Arnberg et al (1974)	0.9974	3.306	4.00E+04	2.50E+06	16	3.8~35	18
Anonymous (1986)	...	...	1.60E+06	3.20E+07	10	25~59	10
Brain and McDonald (1977)	...	...	3.70E+05	7.20E+05	1	5~17	3
Brain and Reid (1978)	...	...	1.50E+06	1.17E+07	5	5~17	10
Brain and Reid (1981)	...	...	1.07E+06	1.07E+07	12	4.5~34.9	9
Stratford (1962), laminar	0.9984	3.032	1.00E+05	2.00E+06		$C_d = a - bR_d^{-1/2}$	11
Stratford (1962), turbulent	0.9984	0.0693	5.00E+05	1.00E+07		$C_d = a - bR_d^{-1/5}$	15

(c) Discharge Coefficients for Toroidal Throat Venturi Nozzles. For gases with a fixed ratio of specific heats, the analytical solutions indicate that the discharge coefficients can be correlated in the laminar boundary layer range by the following equation:

$$C_d = a - bR_d^{-0.5} \tag{8-7.2}$$

The same form of equation applies in the turbulent boundary layer range with the Reynolds number exponent changed from −0.5 to −0.2. Table 8-7-1 summarizes the results from approximately 690 measurements on 95 venturi nozzles compiled from 13 sources [4, 11]. Ten of these were secondary measurements and 680 were primary measurements of various types. Some of these measurements were averaged to reduce random error resulting in 143 points to be plotted. Added to these measured average points were 26 analytical points [23]: 11 for laminar boundary layer and 15 for turbulent. The total 169 points are shown in Fig. 8-7-1.

The mean curve in Fig. 8-7-1 is called a universal curve because it represents all toroidal throat venturi nozzles manufactured to the ASME [1] and ISO [22] standards. The scatter in the data is due to the manufacturing tolerances allowed in the standards, measurement errors, and, most importantly, boundary layer transition. An uncertainty range of ±0.3% (2σ) is shown. The universal curve is represented by the following equation:

$$C_d = 0.9959 - 2.72R_d^{-0.5} \tag{8-7.3}$$

Lower uncertainties can be obtained by manufacturing venturi nozzles to closer tolerances than permitted by the standards. When the flow range is limited (2.00E + 05 < R_d < 1.2E + 06) and falls within the laminar boundary layer regime, a particular design of venturi nozzle can be calibrated to an uncertainty as low as ±0.07% (bias + 2) [6]. This uncertainty can be statistically reduced to ±0.05% by placing several venturi nozzles in parallel.

High-precision venturi nozzles manufactured by superaccurate lathes have performance characteristics that are highly repeatable. The first three references listed in Table 8-7-1 used high-performance venturi nozzles. Equation (8-7.4) fits the data from this source, which covers a flow range: (2.1E + 04 < R_d < 1.4E + 06). At the lower Reynolds numbers, the estimated uncertainty is ±0.2%, which decreases to ±0.1% (bias + 2σ) at the higher Reynolds numbers.

$$C_d = 0.9985 - 3.396\ R_d^{-0.5} \tag{8-7.4}$$

Figure 8-7-2 compares several mean line discharge coefficient curves for toroidal throat venturi nozzles. The boundary layer transition for two sets of high-precision venturi nozzles is also shown. Whereas the transition curves occur at different Reynolds numbers, in both cases they proceed from the mean curve for high-precision venturi nozzles at laminar flow, Eq. (8-7.4), to the universal curve, Eq. (8-7.3).

(d) Discharge Coefficients for Cylindrical Throat Venturi Nozzles. The discharge coefficients for the cylindrical throat venturi nozzle are given in Table 8-7-2 [1, 22].

(e) Discharge Coefficients for ASME Low-β Throat Tap Flow Nozzles. Figure 8-7-3 gives a composite graph of discharge coefficients for the ASME low-β throat tap flow nozzles [11].

Mean curves are shown for several operating conditions: critical flow of air and steam, subsonic air flow

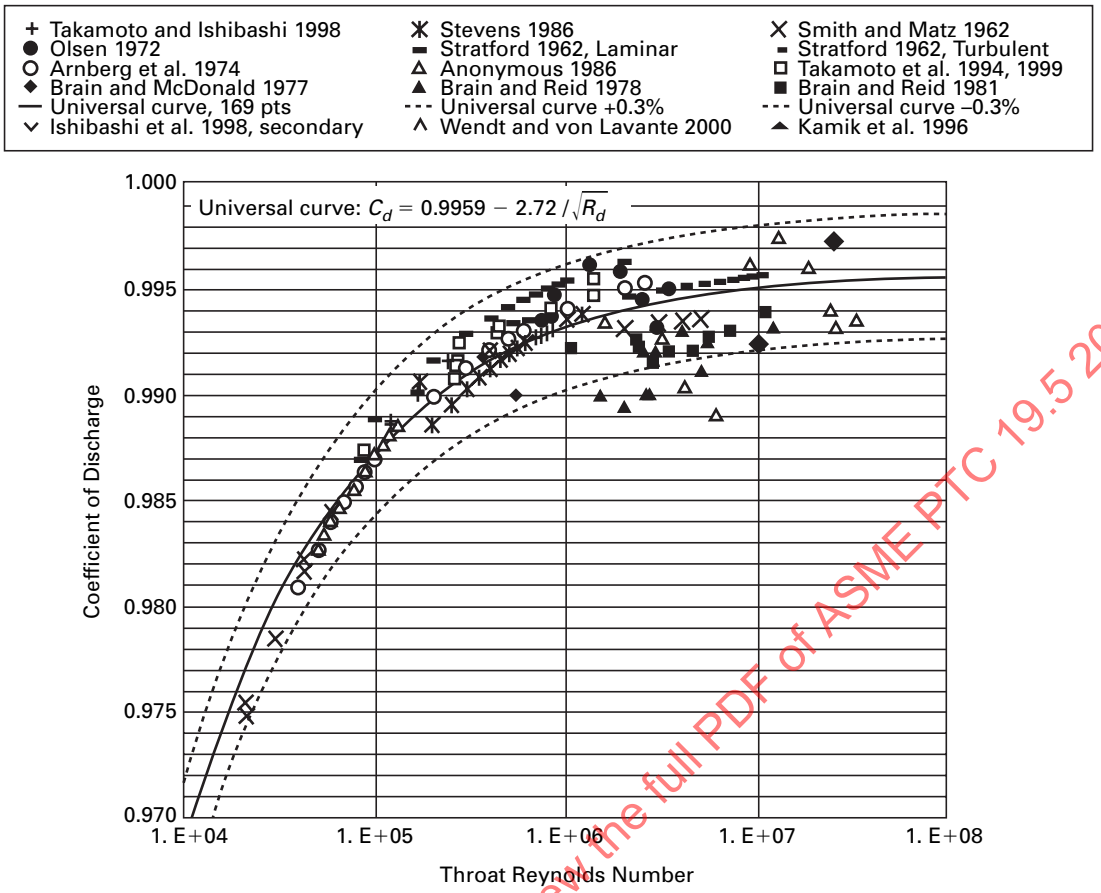

Fig. 8-7-1 Composite Results for Toroidal-Throat Venturi Nozzles

for Mach numbers from 0.2 up to 1.0, and water flow. Compared to the sonic flow nozzle, which has only one operating parameter, the subsonic flow nozzle has two parameters, the throat Reynolds number and the throat Mach number. Error in the theory and/or real gas properties may have caused the discharge coefficient to exceed 1.0 at the highest Reynolds numbers. Excluding this data, all of the results fall within a 1% band.

Where operation in both the subsonic and sonic regimes is required, the ASME low-β throat tap flow nozzle is recommended due to the availability of calibration data for both regimes. It is noted that the downstream pressure must be maintained at a lower value to have critical flow with the ASME flow nozzle due to the absence of a diffuser (see Fig. 8-2-2).

8-8 INSTALLATION

(a) General. The critical flow meter is relatively insensitive to disturbances in the inlet flow stream compared to some flow meters [27, 28]. This is largely because critical flow meters avoid phase lag and square root errors that are present in subsonic meters that rely on a differential pressure measurement. Tests on critical flow meters found little error from severe pulsations when using an average inlet pressure obtained by a throttled gage line [29]. This is a major advantage because pulsations are difficult to remove from the fluid stream.

Inlet flow conditioning to establish a standardized velocity profile, which is essential for subsonic flow meters, is not as important for sonic nozzles and venturis. The inlet profile will have a slight effect on the conversion of the inlet static pressure measurement to average inlet stagnation pressure.

Swirl may cause errors in critical flow meters, although no data were found to quantify this effect. Therefore, swirl should be removed from the fluid stream by means of an inlet flow straightener.

(b) Standardized Inlet Flow Conditioner. Inlet flow-conditioning methods have been standardized as shown in Fig. 8-8-1. Details of the inlet flow conditioner are specified in ASME [1] and ISO [22].

(c) Inlet Configurations for Sonic Venturi Nozzles. The ISO [22] and ASME [1] standards permit a range of inlet configurations as shown in Fig. 8-6-1. The most commonly used inlet configuration is the bulk-head

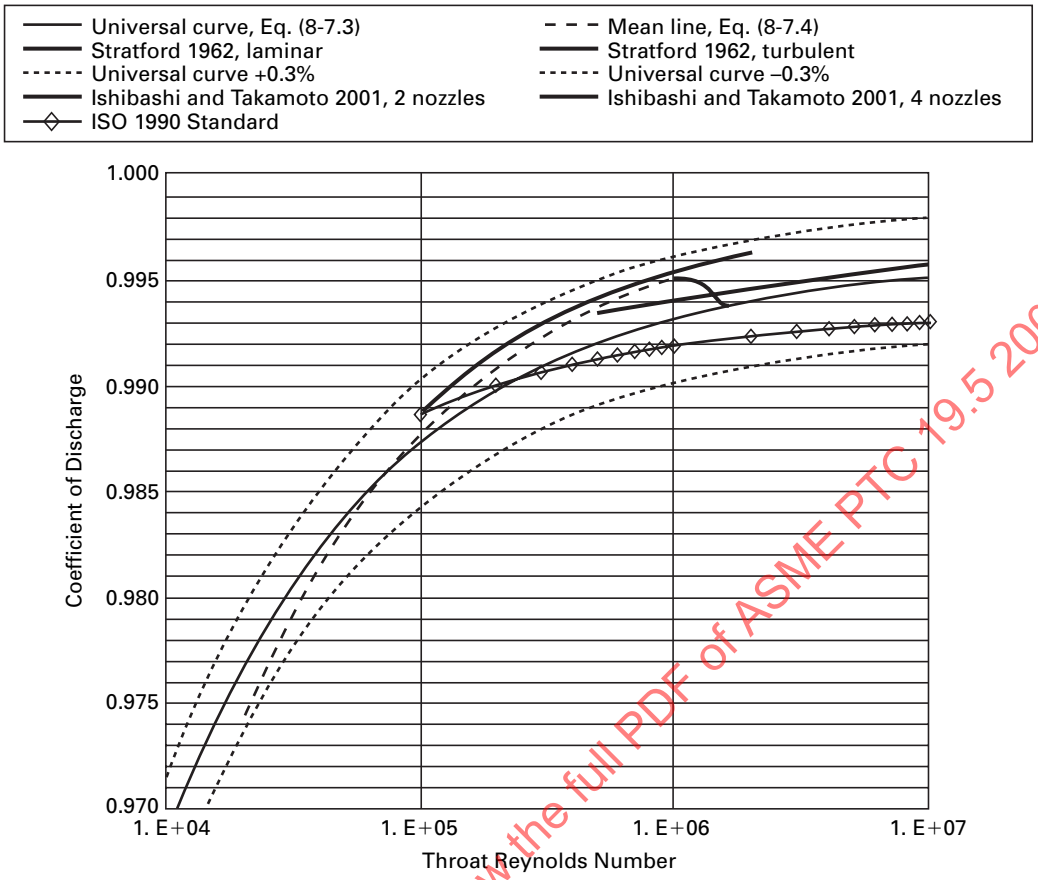

Fig. 8-7-2 Mean Line Discharge Coefficient Curves for Toroidal-Throat Venturi Nozzles

Table 8-7-2 Discharge Coefficients for Cylindrical-Throat Venturi Nozzles

Reynolds Number Re_d	Discharge Coefficient
3.5×10^5	0.988 7
5×10^5	0.988 7
2×10^6	0.988 7
3×10^6	0.989 0
5×10^6	0.990 1
7×10^6	0.990 7
1×10^7	0.991 4
2×10^7	0.992 5

installation shown in Figs. 8-6-2 and 8-6-3. Figure 8-8-2 shows the continuous curvature inlet used by Stevens [6] compared with the sharp-lip, free-standing inlet used by Smith and Matz [2].

The sensitivity of three designs of critical flow venturi nozzles to initial boundary layer thickness, as affected by the inlet configuration, was studied analytically [30]. Included in the study were the effects of inlet flow nonuniformity, separation, and the location of the boundary layer transition point. The differences among the sensitivities of the three designs of venturi nozzles for these effects were found to be small. A slight advantage was seen for the toroidal throat venturi nozzle of the Smith and Matz design with the free-standing inlet.

The loose specification on the inlet configuration in the ISO and ASME standards is based on the assumption that the permitted variations in the inlets do not significantly affect the performance. However, as more precise venturi nozzles are manufactured and calibrated by increasingly accurate methods, the differences in their discharge coefficients cast doubt on this assumption. Previously, these differences were attributed entirely to calibration errors. It is probable that tighter specifications will be needed in the standards before lower uncertainties in the universal curve can be obtained. Presently, the lowest uncertainties are obtained by calibrating each configuration of venturi nozzle.

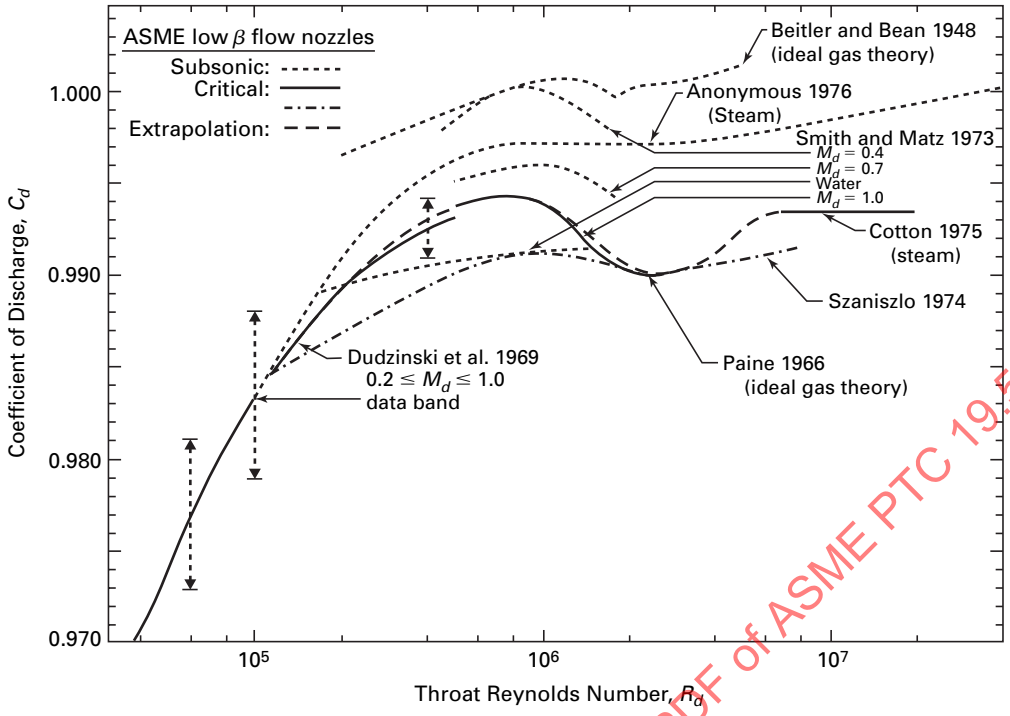

GENERAL NOTE: Reprinted with permission from Research on Flow Nozzles, Engineering Experiment Station Bulletin 131, Ohio State University, Columbus, Ohio.

Fig. 8-7-3 Composite Graph of Discharge Coefficients for the ASME Low-β Throat-Tap Flow Nozzles [11]

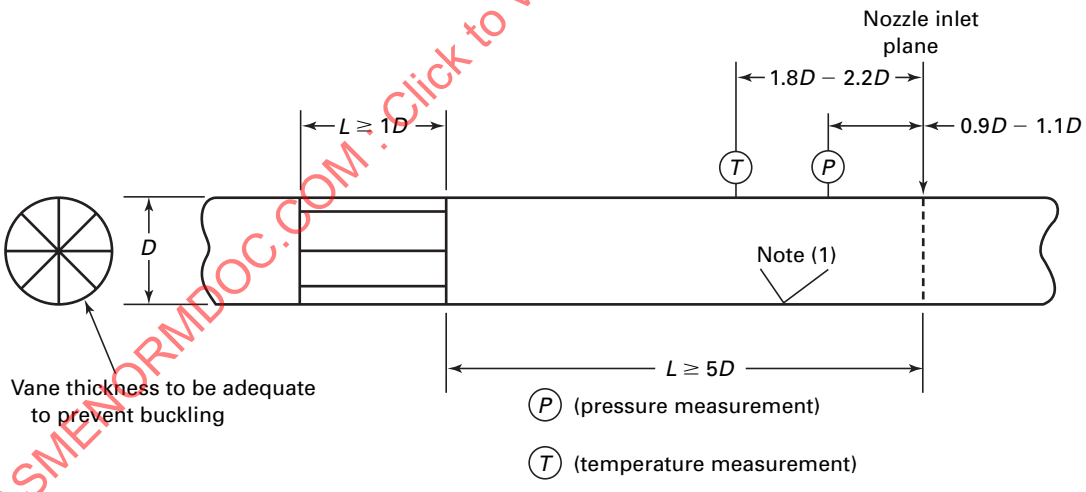

NOTE:
(1) Surface roughness shall not exceed $10^{-4}D$.

Fig. 8-8-1 Standardized Inlet Flow Conditioner and Locations for Pressure and Temperature Measurements

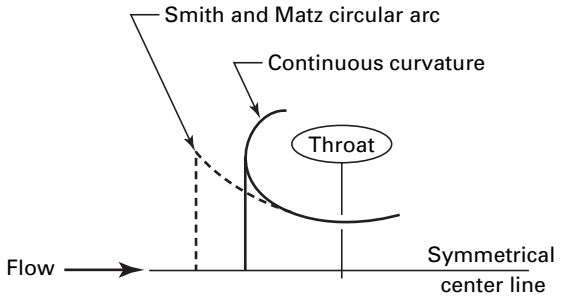

Fig. 8-8-2 Comparison of the "Continuous Curvature" Inlet [6] With the "Sharp-Lip, Free-Standing" Inlet [2]

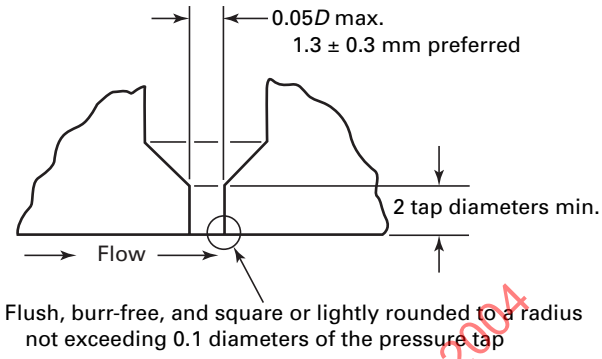

Fig. 8-9 Standardized Pressure Tap Geometry

8-9 PRESSURE AND TEMPERATURE MEASUREMENTS

(a) Pressure Measurements

(1) Beta Ratio. Beta is the ratio of the throat diameter of the nozzle to the inlet pipe diameter. This has special importance for mass flow measurements using sonic flow nozzles or venturi nozzles. This is because the inlet pressure measurement has followed the established practice for subsonic nozzles by using inlet pipe wall pressure tap(s) to measure the static pressure. An alternative could have been to use impact probes, which would have involved more complexity and caused disturbances in the inlet stream.

The conversion from static to stagnation pressure is accomplished by isentropic relationships based on one-dimensional flow of an ideal gas. This contains error from the fact that the flow is not one-dimensional. The velocity profile in the inlet section at the location of the wall tap(s) results in a corresponding stagnation pressure profile. The discrepancy caused by this deviation from one-dimensional flow is acceptably small if the correction from static to stagnation pressure is sufficiently small. This is the case when the β ratio is less than 0.25, which is required in the ISO [22] standard.

The velocity profile of a properly conditioned inlet stream will vary in a predictable manner with the Reynolds number. Consequently, the error in converting from static to stagnation pressure under ideal conditions is correlated by the discharge coefficient versus Reynolds number relationship.

When the standardized limit on the β ratio of 0.25 is not practical due to limitations on the size of the inlet pipe, a compromise is necessary between higher β ratios and some loss of accuracy in converting from measured inlet static pressure and the average inlet stagnation pressure. At a β ratio of 0.25, the correction from static to stagnation pressure is less than 0.1% and the error in this correction due to two-dimensional effects is estimated to be on the order of 0.01%, depending on the Reynolds number. For other β ratios, the correction can be calculated from the isentropic relationships in Eqs. (8-1-1) through (8-1-4) and a similar judgment made as to the possible error in the correction.

(2) Pressure Taps. Pressure tap geometry has been standardized, as shown in Fig. 8-9, and the details are specified in the ISO [22] and ASME [1] standards.

(3) Pressure Tap Corrections. Pressure tap corrections are not considered necessary for sonic flow meter installations with β ratios less than 0.25, in accordance with the ISO [22] standard.

(4) Downstream Pressure Measurement. The pressure downstream of the meter must be measured to ensure sonic operation. The standardized location is within 0.5 conduit diameters of the exit plane of the venturi nozzle. The ASME [1] standard permits other locations with corresponding precautions on the use of the choking pressure ratio requirements given in Fig. 8-2-1.

(b) Temperature Measurement. ASME PTC 19.3 shall be followed. The temperature sensed in a flowing stream by a bare temperature probe T_p, which does not stagnate the fluid stream, measures a value between the static and stagnation temperature. The correction to stagnation temperature is a function of two quantities.

(1) The first quantity is the recovery factor, as follows:

$$R_f = (T_p - T)/(T_0 - T) \tag{8-9.1}$$

The solution for T_0 from Eq. (8-9.1) is as follows:

$$T_0 = T_p/[(T/T_0)(1 - R_f) + R_f] \tag{8-9.2}$$

The value of the recovery factor varies with the shape of the probe, the Reynolds number, and the Mach number of the stream. An approximate value for the recovery factor is 0.85, which is sufficiently accurate when the inlet Mach number is low (e.g., when the β ratio is less than 0.25). Additional details are given in ISO [22].

(2) The second factor is the ratio of the static to stagnation temperature (T/T_0) that appears in Eq. (8-9.2). This can be calculated from the isentropic relationship in Eqs. (8-1.3) through (8-1.6). Alternatively, it can

be found from isentropic flow tables that appear in most textbooks on thermodynamics, gas dynamics, or aerodynamics, and in gas property tables [9, 20].

Example 4
Flowing fluid: air
Probe temperature $T_p = 520°R$
Recovery factor $R_f = 0.85$
Inlet Mach number $M = 0.04$
β ratio $= 0.2628$
$T/T_0 = 0.99968$
From Eq. (8-9.2), $T_0 = 520/0.999952 = 520.02°R$

Note that the β ratio in this example slightly exceeded the recommended maximum of 0.25, and the correction to stagnation temperature was still only 0.004%, which would correspond to 0.002% in flow measurement. A few percentage points error in the recovery factor would not have had a significant effect.

At β ratios significantly higher than the recommended value of 0.25, the correction becomes larger. In Example 4, if the β ratio were changed to 0.4144, the stagnation temperature would be 520.16°R, for a correction of 0.03%. Considering the square root relationship between the mass flow and absolute temperature, this amounts to a correction of 0.015% in the mass flow. The static to stagnation pressure correction for this same case is 1.007 or 0.7%, and the mass flow would also be corrected 0.7%.

The ASME long-radius, high-β ratio flow nozzle [Fig. 8-6-3, sketch (a)] allows β ratios as high as 0.8. At a β ratio of 0.8, the temperature correction would be 0.53°R or 0.5%, for a correction of 0.25% in the mass flow measurement. The pressure correction would be 1.122, for a correction of 12.2% in both the pressure and mass flow. Because this correction is based on one-dimensional isentropic flow theory for an ideal gas, the error in this correction could be on the order of 1%. This is one reason, in addition to uncertainty in the discharge coefficient, that this design is not recommended for critical flow measurements.

The above examples show that the correction from static to stagnation pressure has about 48 times as much effect on the mass flow measurement as the correction from the bare probe temperature measurement to stagnation temperature.

8-10 SOURCES OF FLUID AND MATERIAL DATA

[1] ASME MFC-7M, Measurement of Gas Flow by Means of Critical Flow Venturi Nozzles. New York: American Society of Mechanical Engineers; 1987.

[2] Smith, R. E., Jr.; Matz, R. J. A Theoretical Method of Determining Discharge Coefficients for Venturis Operating at Critical Flow Conditions. *Journal of Basic Engineering* **84**(4): 434–446; 1962.

[3] Bean, H. S., ed. *Fluid Meters: Their Theory and Application,* 6th edition. New York: The American Society of Mechanical Engineers; 1971.

[4] Arnberg, B. T.; Ishibashi, M. Discharge Coefficient Equations for Critical-Flow Toroidal-Throat Venturi Nozzles. Proceedings of ASME FEDSM2001 Paper No. 18030. New Orleans, May 29–June 1, 2001.

[5] Varner, C. E. A Multiple Critical Flow Venturi Airflowmetering System for Gas Turbine Engines. *Journal of Basic Engineering* **92**: 792–796; 1970.

[6] Stevens, R. L. Development and Calibration of the Boeing 18 kg/s (40 lbm/sec) Airflow Calibration Transfer Standard. International Symposium on Fluid Flow Measurement, Washington, DC, 1986.

[7] Reshetnikov, A.V., et al. An Experimental Unit for Investigating the Discharge of a Flashing Liquid Through Short Channels at Variable Back Pressures. *Fluid Mechanics* - Soviet Research **16**(5):61–65; 1987.

[8] Goodenough, G. A. *Principles of Thermodynamics,* 3rd edition. New York, NY: Henry Holt and Company; 1911, 1920, 1931.

[9] Shapiro, A. H. *The Dynamics and Thermodynamics of Compressible Flow,* volumes 1 and 2. New York, NY: The Ronald Press; 1954.

[10] Perry, Jr., J. A. Critical Flow Through Sharp–Edged Orifices, Trans. ASME, **71**: 737: 1949

[11] Arnberg, B. T.; Ishibashi, M. Review of Flow Nozzle and Venturi Designs and Discharge Coefficients. Proceedings, 47th International Instrumentation Symposium. Denver, May 6–10, 2001.

[12] Aschenbrenner, A. The Influence of Humidity on the Flowrate of Air through Critical Flow Nozzles. Flow Measurement Conference, Budapest, Hungary, 1983.

[13] Arnberg, B. T.; Seidl, W. F. A Comparison of Errors in Four Methods for Determining Critical Flow Functions for Sonic Flow Nozzles and Venturis. Proceedings of ASME FEDSM'00-Paper No. 11343. Boston, 2000.

[14] Johnson, R. C. Calculations of Real-Gas Effects in Flow Through Critical-Flow Nozzles. *Journal of Basic Engineering* **86**(3):519–526; 1964.

[15] Sullivan, D. A. Private communications, Fern Engineering Co. to Walter Seidl, Colorado Engineering Experiment Station Inc., 1989.

[16] Jacobsen, R. T., et al. A Thermodynamic Property Formulation for Air. Proceedings of the 11th Symposium on Thermophysical Properties, 1991.

[17] Hilsenrath, J., et al. Tables of Thermal Properties of Gases. National Bureau of Standards Circular 564, 1955.

[18] Sullivan, D.A. Historical Review of Real-Fluid Isentropic Flow Models ASME Journal of Fluids Engineering 103. Series 1: **25**:8-267; 1981.

[19] Johnson, R. C. Real Gas Effects in Critical-Flow-Through Nozzles and Tabulated Thermodynamic Properties. NASA Technical Note D-25655, Lewis Research Center, January 1965.

[20] Keenan, J. H.; Kaye, J.; Gas Tables; New York, NY, John Wiley & Sons, 1945.

[21] Keenan, J. H.; Keyes, F. G. *Thermodynamic Properties of Steam*. 1959.

[22] IS0 9300, *Measurement of Gas Flow by Means of Critical Flow Venturi Nozzles.* Geneva: International Organization for Standardization; 1990.

[23] Stratford, B. S. The Calculation of the Discharge Coefficient of Profiled Choked Nozzles and the Optimum Profile for Absolute Air Flow Measurement. *Journal of the Royal Aeronautical Society* **68:**237–245; 1962, 1964.

[24] Arnberg, B. T. Discharge Coefficient Correlation for Circular-Arc Venturi Flow Meters at Critical (Sonic) Flow. *Journal of Fluids Engineering* **96:** 111-123; 1974.

[25] Hall, I. M. Transonic Flow in Two-Dimensional and Axially Symmetric Nozzles. *Quarterly Journal of Mechanics and Applied Mathematics* **15**(4):487, 508; 1962.

[26] Ishibashi, M.; Takamoto, M. *Discharge Coefficient of Super Accurate Critical Nozzle at Pressurized Condition*, Proceedings of 4th International Symposium on Fluid Flow Measurement. Denver, CO.: June 1999.

[27] Sparks, C. R. *A Study of Pulsating Effects on Orifice Metering of Compressible Flow*, ASME Measurement Symposium: September 1966.

[28] Brennan, J. A.; McFadden, S. A.; Sindt, C. F.; Kothari, K. M. *The Influence of Swirling Flow on Orifice and Turbine Flow-meter Performance*, Flow Measurement and Instrumentation, **1**, No. 1, p. 5: October 1989.

[29] Kastner, L. J.; Williams, T. J.; Sowden, R. A. *Critical Flow Nozzle Meter and Its Application To the Measurement of Mass Flow-Rate in Steady and Pulsating Streams of Gas, Mech. Eng. Science*, **6**, No. 1: 1964.

[30] Brown, E. F., et al. A Comparison of Three Critical Flow Venturi Designs. Trans. ASME **107:**316–321; 1985.

NBS Sonic Nozzle Calibrations, NBS-Boulder, NGPLA, and API committee. Private communication, J. Murdock and D. Keyser to T. Arnberg, 1986.

ASME PTC 6, *Performance Test Code on Steam Turbines.* New York: American Society of Mechanical Engineers; 2005.

ASME Supplement to Power Test Codes, Instruments and Apparatus, Chapter 4. New York: American Society of Mechanical Engineers; 1959.

Beale, D. K. Experimental Measurement of Venturi Discharge Coefficient Including Sensitivity to Geometric and Flow Quality Variables. Arnold Air Force Base, TN: Sverdrup Technology, Inc.; 1999.

Bean, H. S., ed. *Fluid Meters: Their Theory and Application,* 5th edition. New York: The American Society of Mechanical Engineers; 1959.

Bean, H. S. Communications. Proceedings, Institution of Mechanical Engineers **173**:36; 1959.

Beitler, S. R.; Bean, H. S. Research on Flow Nozzles. Columbus, OH: Ohio State University; 1948.

Brain, T. J. S.; Macdonald, L. M. Evaluation of the Performance of Small-Scale Critical Flow Venturi Using the NEL Gravimetric Gas Flow Standard Test Facility. In *Flow Measurement in the Mid 1970s.* Edinburgh: HMSO; 1977:103–125.

Brain, T. J. S.; Reid, J. Primary Calibration of Critical Flow Venturis in High-Pressure Gas. In *Flow Measurement of Fluids* (Dijstelbergen, H. H.; Spencer, E. A., eds.). Amsterdam: North Holland Publishing Co.; 1978:54–64.

Brain, T. J. S.; Reid, J. An Investigation of the Discharge Coefficient Characteristics and Manufacturing Specification of Toroidal Inlet Critical Flow Venturi Nozzles Proposed as ISO Standard Flowmeters. International Conference on Advances in Flow Measurement Techniques, East Kilbride, UK, 1981.

Cotton, K. C. Coefficient of Discharge for Three Steam Flow Nozzles, Critical Flow. Private communication to B. T. Arnberg, General Electric Co., Schenectady, NY, 1975.

Dudzinski, T. J., et al. Venturi Meter With Separable Diffuser. *Journal of Basic Engineering* **91**116–120; 1969.

Ishibashi, M.; Takamoto, M. Discharge Coefficient of Critical Nozzles Machined by Super-Accurate Lathes. Proceedings, 1998 Workshop and Symposium of National Conference of Standards Laboratories, Albuquerque, July 19–23, 1998.

Ishibashi, M.; Takamoto, M. Discharge Coefficient of Super-Accurate Critical Nozzles Accompanied With the Boundary Layer Transition Measured by Reference Super-Accurate Critical Nozzles connected in Series. Proceedings of ASME FEDSM'01, New Orleans, 2001.

Ishibashi, M.; Takamoto, M. Theoretical Discharge Coefficient of a Critical Circular-Arc Nozzle With Laminar Boundary Layer and Its Verification by Measurements Using Super-Accurate Nozzles. *Flow Measurement and Instrumentation* **11:**305–313; 2000.

Ishibashi, M., et al. Calibration of Critical Nozzles by Critical Nozzles. Proceedings of the 9th International Flow Measurement Conference, Lund, Sweden, June 15–17, 1998.

Olsen, L. O. Personal communication, National Bureau of Standards, letter ref. 213.06 to T. Arnberg, Jan. 12, 1972.

Olsen, L. O.; Baumgarten, G. Gas Flow Measurement by Collection Time and Density in a Constant Volume. In *Flow: Its Measurement and Control in Science and Industry.* Research Triangle Park, NC: Instrument Society of America; 1971:1287–1295.

Paine, C. J. Determination of ASME Convergent Nozzle Discharge Coefficients by Probe Measurements. East Hartford, CT: United Aircraft Research Laboratories; 1966.

Seidl, W. F. Primary Calibration of the Boeing 18 kg/s (40 lbm/sec) Airflow Calibration Transfer Standard. International Symposium on Fluid Flow Measurement, Washington, DC, 1986.

Smith, R. E., Jr.; Matz, R. J. Performance Characteristics of an 8-in.-Diameter ASME Nozzle Operating at Compressible and Incompressible Conditions. *Journal of Fluids Engineering* **95:**542–550; 1973.

Szaniszlo, A. J. Experimental and Analytical Sonic Nozzle Discharge Coefficients for Reynolds Numbers up to 8 × 106. ASME Fluid Meter Division, Paper 74-WA/FM-8, 1974.

Takamoto, M.; Ishibashi, M.; Watanabe, N.; Aschenbrenner, A.; Caldwell, S. Inter-comparison Tests of Gas Flow Rate Standards. Bulletin of NRLM 43(3)308/314, Japan, 1994.

Thompson, P. A.; Arena, C. C. Prediction of the Critical Massflow and Related Problems in the Flow of Real Gases. *Journal of Fluids Engineering* paper presented at Joint Fluids Engineering and Lubrication Conference, Minneapolis, May 5–7, 1975.

Section 9
Flow Measurement by Velocity Traverse

9-0 NOMENCLATURE

A = flow area, L^2
C = coefficient
K = structural blockage coefficient
Pr = Prandtl number
Q = volumetric flow, l^3/s
R = pipe inside radius, l
Re = Reynolds number
S = frontal area, support structure impeding flow
V, v, u = velocity, l/s
c = thermal heat capacity
d = diameter, L
f = frequency, 1/s
h = convective heat transfer coefficient
k = thermal conductivity and beam-crossing half angle, rad
p = pressure, f/l^2
r = radial dimension, l
w = weighting factor
Σ = summation of terms
δ = differential, difference
ρ = density, m/l^3
σ = standard deviation
τ = time constant, s

9-1 INTRODUCTION

Only circular or rectangular conduits flowing full of gas or liquid are covered by this Section. Pitot tubes, pitot-static tubes and pitometers, current and propeller meters, hot-wire anemometers, and laser Doppler velocimeters measure velocities at given locations in the flow, which then must be summed or integrated over the whole cross-section to obtain the total volumetric flow or mean velocity. These devices, therefore, have similar requirements for their installation and flow computations.

9-1.1 Flow Computation

Independent of which velocity traverse method is used, the total volumetric flow is obtained by numerical integration (a summation) of the form:

$$Q = A \Sigma_i (w_i v_i) \qquad (9\text{-}1.1)$$

where
A = total area of the conduit
i = index of the sensor location
v_i = observed mean velocity at the i^{th} traverse station
w_i = associated weighting factor

It is highly recommended that 20 to 30 data be taken at each sensor station in the traverse to obtain a good mean value of v_i and reduce the statistical random error. Plotting the observed velocity profiles is highly recommended to check the degree of asymmetry in the flow profile and whether it is reasonable to expect such a profile in the subject installation. A sample graphical integration is recommended to cross-check the numerical integration procedure for each test installation.

9-2 TRAVERSE MEASUREMENT STATIONS

In order of preference, the three approved techniques are the Gauss, Tchebycheff, and log-linear radial spacings. The reason for the preferred order is that the Gauss and Tchebycheff methods work for any arbitrary function describing the velocity profile and they are significantly more accurate than the log-linear method when using the same number of sensors. The converse also holds: equivalent accuracy can be attained using fewer sensors in the traverse. The log-linear method is designed to work only for velocity profiles that can be described by a linear combination of a logarithmic term and a linear term of the distance from the wall, as shown in Eq. (9-2.1).

$$v(r) = a + b[\log(1 - r/R)] + c(1 - r/R) \qquad (9\text{-}2.1)$$

The reason for providing a choice in the traverse pattern is that the sensor locations are different for each, and physical and installation constraints found in the field may dictate the choice of traverse pattern. In general, it is good engineering practice to use five sensors per radius or 10 per diameter. In small pipes or when the velocity profile and/or installation dimensions as stated in para. 9-3 are nearly ideal, three stations per radius suffice. In cases where the installation conditions are much worse than specified in Section 7, more than five sensors per radius are required to maintain accuracy. The effect of adding or subtracting sensors from the traverse array (or rake) can be estimated by choosing a suitable analytic formula for the expected velocity profile and integrating it using the calculus. The analytic

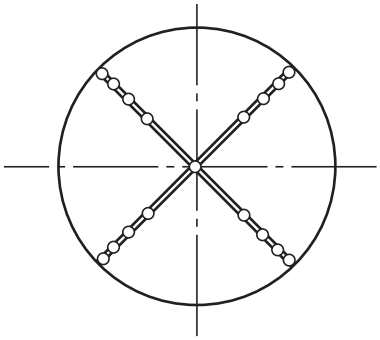

Stationary array mounted on crossbars in a circular conduit

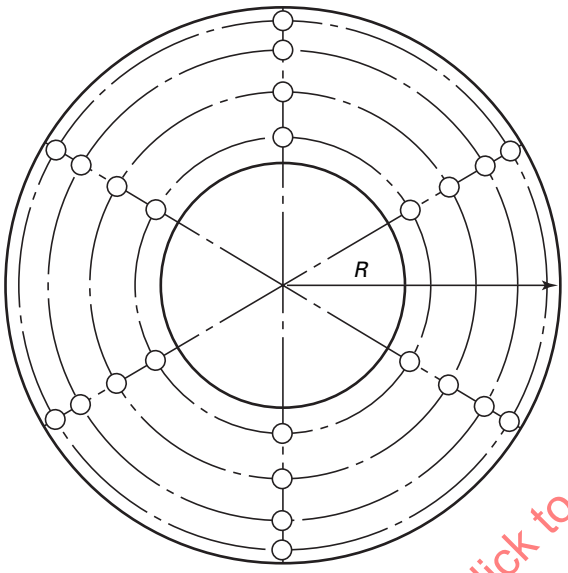

Fig. 9-2.1 Pipe Velocity Measurement Loci

result from the calculus can be compared to the result given by the numerical summation of velocities (also given by the same formula for the expected profile), using the recommended numerical integration procedures.

9-2.1 Pipes

Velocities in pipes shall be measured along at least two diameters. Typical diametral patterns are shown in Fig. 9-2.1. There are several acceptable methods of numerical integration that specify slightly different loci for the measuring stations along the diameters. Tables 9-2.1-1 through 9-2.1-3 specify these stations along the radii. The minimum number of stations per radius is three, five is the usual practice, and even more are recommended for large conduits or for adequate resolution of abnormal or skewed velocity profiles. A reference velocity shall be measured at the center of the area, but this observation is not always included in the flow computation methods described in this Section. The velocity at the center is always used in the measurement procedures to detect departures from the criteria of velocity profile skewness and unsteadiness, as in para. 9-3(b).

Table 9-2.1-1 Abscissas and Weight Factors for Gaussian Integration of Flow in Pipes

$$\int_0^1 x^k f(x)\,dx \approx \sum_{i=1}^{n} w_i f(x_i)$$

n	x_i	w_i
1	0.66666 66667	0.50000 00000
2	0.35505 10257	0.18195 86183
	0.84494 89743	0.31804 13817
3	0.21234 05382	0.06982 69799
	0.59053 31356	0.22924 11064
	0.91141 20405	0.20093 19137
4	0.13975 98643	0.03118 09710
	0.41640 95676	0.12984 75476
	0.72315 69864	0.20346 45680
	0.94289 58039	0.13550 69134
5	0.09853 50858	0.01574 79145
	0.30453 57266	0.07390 88701
	0.56202 51898	0.14638 69871
	0.80198 65821	0.16717 46381
	0.96019 01429	0.09678 15902
6	0.07305 43287	0.00873 83018
	0.23076 61380	0.04395 51656
	0.44132 84812	0.09866 11509
	0.66301 53097	0.14079 25538
	0.85192 14003	0.13554 24972
	0.97068 35728	0.07231 03307
7	0.05626 25605	0.00521 43622
	0.18024 06917	0.02740 83567
	0.35262 47171	0.06638 46965
	0.54715 36263	0.10712 50657
	0.73421 01772	0.12739 08973
	0.88532 09468	0.11050 92582
	0.97752 06136	0.05596 73634
8	0.04463 39553	0.00329 51914
	0.14436 62570	0.01784 29027
	0.28682 47571	0.04543 93195
	0.45481 33152	0.07919 95995
	0.62806 78354	0.10604 73594
	0.78569 15206	0.11250 57995
	0.90867 63921	0.09111 90236
	0.98222 00849	0.04455 08044

$k = 1$
w_i = weight factors
x_i = abscissas

GENERAL NOTE: Reprinted with permission from Mathematical Table Aids to Computation, Vol. 11, National Academy of Science.

Table 9-2.1-2
Abscissas and Weight Factors for Tchebycheff Integration of Flow in Pipes

n	*r*	*w*	*n*	*r*	*w*	*n*	*r*	*w*
2	(e)	(e)	6	0.2586		9	0.2103	
	0.4597			0.5373			0.4466	
	0.8881	1/2		0.6057			0.4854	
				0.7958	1/6		0.6450	
3	0.3827			0.8434			0.7071	1/9
	0.7071	1/3		0.9660			0.7642	
	0.9239						0.8743	
			7	0.2410			0.8947	
4	0.3203			0.4849			0.9776	
	0.6382			0.5814				
	0.7699	1/4		0.7071	1/7	10	(g)	(g)
	0.9473			0.8136			0.2046	
				0.8745			0.3954	
5	0.2891			0.9705			0.5000	
	0.5592						0.5862	
	0.7071	1/2	8	(f)	(f)		0.6768	1/10
	0.8290			0.2266			0.7361	
	0.9572			0.4513			0.8102	
				0.5444			0.8660	
				0.6698	1/8		0.9185	
				0.7425			0.9788	
				0.8388				
				0.8924				
				0.9740				

GENERAL NOTES:
(a) Averaging for linear interval $0 \le x \le 1$.
(b) Averaging for circular duct, in interval $0 \le r \le 1$.
(c) All measurements are weighted equally.
(d) Part of Table I-7-I, Station Locations and Weights Averaging, from Fluid Meters, 6th Ed.

Table 9-2.1-3
Abscissas and Weight Factors for the Log-Linear Traverse Method of Flow Measurement in Pipes

No. Sensors/Radius	R_i/R	W_i	Wall Dist., y/D
2	0.914	0.5	0.043
2	0.42	0.5	0.29
3	0.936	0.3333	0.032
3	0.73	0.3333	0.135
3	0.358	0.3333	0.321
4	0.958	0.25	0.021
4	0.766	0.25	0.117
4	0.632	0.25	0.184
4	0.31	0.25	0.345
5	0.962	0.2	0.019
5	0.848	0.2	0.076
5	0.694	0.2	0.153
5	0.566	0.2	0.217
5	0.278	0.2	0.361

GENERAL NOTE: Water Power, June 1957, p. 226.

9-2.2 Rectangular Ducts

Velocities in rectangular ducts shall be measured at the loci specified in Tables 9-2.2-1 and 9-2.2-2, depending on the method selected. In ducts, the spacing applies to half the wall-to-wall dimensions unless explicitly specified otherwise. At least five measurement loci are recommended for each line across the duct. More should be used if the flow is expected to be highly skewed or otherwise abnormal. Three sensors per line may be used if the duct is small or the flow profile is expected to be nearly symmetric and smooth with an unchanging sign of its curvature.

9-3 RECOMMENDED INSTALLATION REQUIREMENTS

(a) The measurement section should be in a straight run of conduit at least 20 diameters downstream and 5 diameters upstream from the nearest bend, change in area, or other flow obstruction.

(b) The mean velocity at the measurement section should be at least 75% of the maximum velocity observed. The velocity distribution should be that of a

Table 9-2.2-1 Loci for the Lines of Intersection Determining Measurement Stations for Flow Measurement in Rectangular Conduits Using Gaussian Integration

$$\int_{-1}^{+1} f(x)dx \approx \sum_{i=1}^{n} w_i f(x_i)$$

$\pm x_i$	w_i
$n = 2$	
0.57735 02691 89626	1.00000 00000 00000
$n = 3$	
0.00000 00000 00000	0.88888 88888 88889
0.77459 66692 41483	0.55555 55555 55556
$n = 4$	
0.33998 10435 84856	0.65214 51548 62546
0.86113 63115 94053	0.34785 48451 37454
$n = 5$	
0.00000 00000 00000	0.56888 88888 88889
0.53846 93101 05683	0.47862 86704 99366
0.90617 98459 38664	0.23692 68850 56189
$n = 6$	
0.23861 91860 83197	0.46791 39345 72691
0.66120 93864 66265	0.36076 15730 48139
0.93246 95142 03152	0.17132 44923 79170
$n = 7$	
0.00000 00000 00000	0.41795 91836 73469
0.40584 51513 77397	0.38183 00505 05119
0.74153 11855 99394	0.27970 53914 89277
0.94910 79123 42759	0.12948 49661 68870
$n = 8$	
0.18343 46424 95650	0.36268 37833 78362
0.52553 24099 16329	0.31370 66458 77887
0.79666 64774 13627	0.22238 10344 53374
0.96028 98564 97536	0.10122 85362 90376
$n = 9$	
0.00000 00000 00000	0.33023 93550 01260
0.32425 34234 03809	0.31234 70770 40003
0.61337 14327 00590	0.26061 06964 02935
0.83603 11073 26636	0.18064 81606 94857
0.96816 02395 07626	0.08127 43883 61574
$n = 10$	
0.14887 43389 81631	0.29552 42247 14753
0.43339 53941 29247	0.26926 67193 09996
0.67940 95682 99024	0.21908 63625 15982
0.86506 33666 88985	0.14945 13491 50581
0.97390 65285 17172	0.06667 13443 08688
$n = 12$	
0.12523 34085 11469	0.24914 70458 13403
0.36783 14989 98180	0.23349 25365 38355
0.58731 79542 86617	0.20316 74267 23066
0.76990 26741 94305	0.16007 83285 43346
0.90411 72563 70475	0.10693 93259 95318
0.98156 06342 46719	0.04717 53363 86512
$n = 16$	
0.09501 25098 37637 44018 5	0.18945 06104 55068 49628 5
0.28160 35507 79258 91323 0	0.18260 34150 44923 58886 7
0.45801 67776 57227 38634 2	0.16915 65193 95002 53818 9
0.61787 62444 02643 74844 7	0.14959 59888 16576 73208 1
0.75540 44083 55003 03389 5	0.12462 89712 55533 87205 2
0.86563 12023 87831 74388 0	0.09515 85116 82492 78481 0
0.94457 50230 73232 57607 8	0.06225 35239 38647 89286 3
0.98940 09349 91649 93259 6	0.02715 24594 11754 09485 2
$n = 20$	
0.07652 65211 33497 33375 5	0.15275 33871 30725 85069 8
0.22778 58511 41645 07808 0	0.14917 29864 72603 74678 8
0.37370 60887 15419 56067 3	0.14209 61093 18382 05132 9
0.51086 70019 50827 09800 4	0.13168 86384 49176 62689 8
0.63605 36807 26515 02545 3	0.11819 45319 61518 41731 2
0.74633 19064 60150 79261 4	0.10193 01198 17240 43503 7
0.83911 69718 22218 82339 5	0.08327 67415 76704 74872 5
0.91223 44282 51325 90586 8	0.06267 20483 34109 06357 0
0.96397 19272 77913 79126 8	0.04060 14298 00386 94133 1
0.99312 85991 85094 92478 6	0.01761 40071 39152 11831 2
$n = 24$	
0.06405 68928 62605 62608 5	0.12793 81953 46752 15697 4
0.19111 88674 73616 30915 9	0.12583 74563 46828 29612 1
0.31504 26796 96163 37438 7	0.12167 04729 27803 39120 4
0.43379 35076 26045 13848 7	0.11550 56680 53725 60135 3
0.54542 14713 88839 53565 8	0.10744 42701 15965 63478 3
0.64809 36519 36975 56925 2	0.09761 86521 04113 88827 0
0.74012 41915 78554 36424 4	0.08619 01615 31953 27591 7
0.82000 19859 73902 92195 4	0.07334 64814 11080 30573 4
0.88641 55270 04401 03421 3	0.05929 85849 15436 78074 6
0.93827 45520 02732 75852 4	0.04427 74388 17419 80616 9
0.97472 85559 71309 49819 8	0.02853 13886 28933 66318 1
0.99518 72199 97021 36018 0	0.01234 12297 99987 19954 7

w_i = weight factors
$\pm x_i$ = abscissas (zeros of Legendre polynomials)

GENERAL NOTE: Compiled from P. Davis and P. Rabinowitz, Abscissas and weights for Gaussian quadratures of high order, J. Research NBS 56, 35–37, 1956, RP2645; P. Davis and P. Rabinowitz, Additional abscissas and weights for Gaussian quadratures of high order. Values for $n = 64$, 80, and 96, J. Research NBS 60, 613–614, 1958, RP2875; and A. N. Lowan, N. Davids, and A. Levenson, Table of the zeroes of the Legendre polynomials of order 1–16 and the weight coefficients for Gauss' mechanical quadrature formula, Bulletin of the American Mathematical Society 48, 739–743, 1942 (with permission).

Table 9-2.2-2 Abscissas for Equal Weight Chebyshev Integration

$$\int_{-1}^{+1} f(x)dx \approx \frac{2}{n} \sum_{i=1}^{n} f(x_i)$$

n	$\pm x_i$	n	$\pm x_i$	n	$\pm x_i$
2	0.57735 02692	6	0.86624 68181	9	0.91158 93077
			0.42251 86538		0.60101 86554
3	0.70710 67812		0.26663 54015		0.52876 17831
	0.00000 00000				0.16790 00000
		7	0.88386 17008		0.00000 00000
4	0.79465 44723		0.52965 67753		
	0.18759 24741		0.32391 18105		
			0.00000 00000		
5	0.83249 74870				
	0.37454 14096				
	0.00000 00000				

$\pm x_i$ = abscissas

GENERAL NOTE: Table 25.5, p. 920, Handbook Math Functions; compiled with permission from H.E. Salzer, Tables for facilitating the use of Chebyshev's quadrature formula, J. Math. Phys. 26, 191–194, 1947.

fully developed, turbulent flow in a straight conduit.

(c) If flow conditioners are required to satisfy the preceding requirement (b), they should be placed at least 10 diameters upstream from the measurement section.

(d) If the conduit is of lapped construction, the plane of measurement shall be located in the section of smaller diameter.

9-4 CALIBRATION REQUIREMENTS FOR SENSORS

The only differential pressure Pitot probes that do not require calibration are those shown in Fig. 9-4. When fabricated according to these specifications, their calibration coefficient is 1.000, defined for example in Eq. (9-5.1).

9-4.1 Pitot-Static Sensors

There are many acceptable Pitot-static tubes that may be used as velocity sensors, including the Prandtl and several ASME designs shown in Fig. 9-4.1. These sensors measure the differential pressure corresponding to the dynamic pressure of the flow according to Bernoulli's equation (covered in Section 3). Their calibration coefficient C_d is a premultiplying factor that corrects this measurement to give the true value in exactly the same way as the orifice discharge coefficient. These Pitot-static sensors may be used in liquid or subsonic gas flows (Mach $\leq$ 0.3). They shall be calibrated in a mutually acceptable laboratory if it is necessary to obtain a more accurate coefficient. If the blockage correction is estimated to be more than one-quarter of the desired test uncertainty, they should be calibrated under conditions duplicating the mutual interference conditions of the test installation.

9-4.2 Cole Reversible Pitometer

The advantage of this sensor is that it produces a larger differential pressure for a given flow velocity. It must be calibrated. The calibration coefficient will include the velocity effects at the orifices and the friction head loss between them. Depending on the calibration installation, the coefficient may include the stem blockage effect; if so, this must be stated in the calibration report. If stem blockage was not included in the calibration, it may be estimated as follows: the gross cross-sectional area at the measuring section at the plane of the impact orifice shall be reduced by 1.25 times the projected area of the pitometer structure.

This sensor has been used extensively for water flow measurement in conduits wherein the mean velocity was between 2 ft/sec (0.6 m/s) and 20 ft/sec (6 m/s). The pitometer support structure must be reinforced as shown in Fig. 9-4.2 when installed in conduits larger than 4 ft (1.25 m). When readings are being taken, the pitometer orifices are rotated 180 deg apart and aligned with the axis of the conduit. Each orifice is connected to one leg of a differential manometer or pressure transducer as shown in Fig. 9-4.2.

9-4.3 Calibration of Current and Propeller Meters

Current or propeller meters shall be calibrated in a towing tank or free stream with the same mounting that will be used for the test. Where the meters are closely spaced, the calibration shall include the effects of the adjacent meters. The calibration shall include data on oblique flow up to 10 deg off the meter axis. The calibration curve may not be extrapolated. These meters shall be inspected before and after the test. Any blade deformation or defect found subsequent to the calibration may require recalibration of the meter if requested by either party to the test.

9-4.4 Hot-Wire and Hot-Film Anemometers

These instruments are used extensively in measuring the velocities in gas flow, especially when rapid velocity

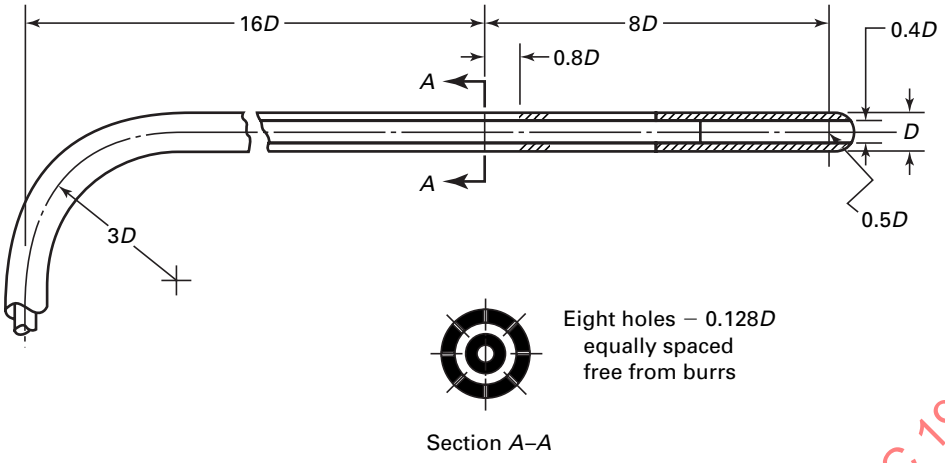

(a) NAFM and ASME

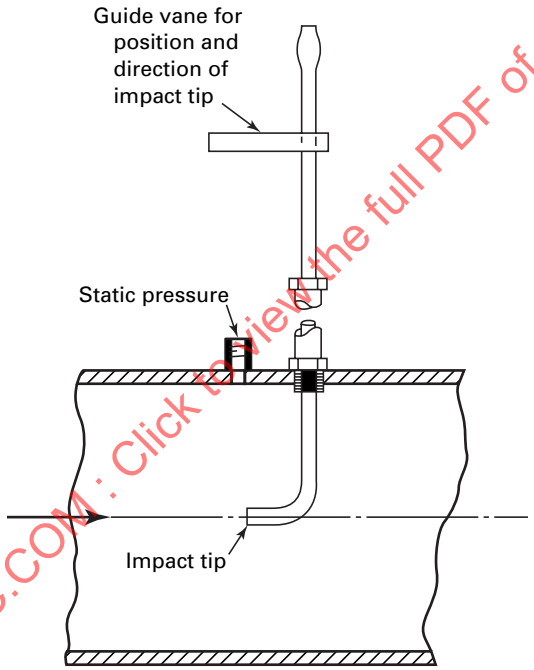

(b) A Type of Basic Pitot Tube or Impact Tube

GENERAL NOTES:
(a) Two designs of pitot-static tubes.
(b) Values of diameters between $^{3}/_{16}$ in and $^{5}/_{16}$ in. are suitable.

Fig. 9-4 Pitot Tubes Not Requiring Calibration (Calibration Coefficient = 1.000)

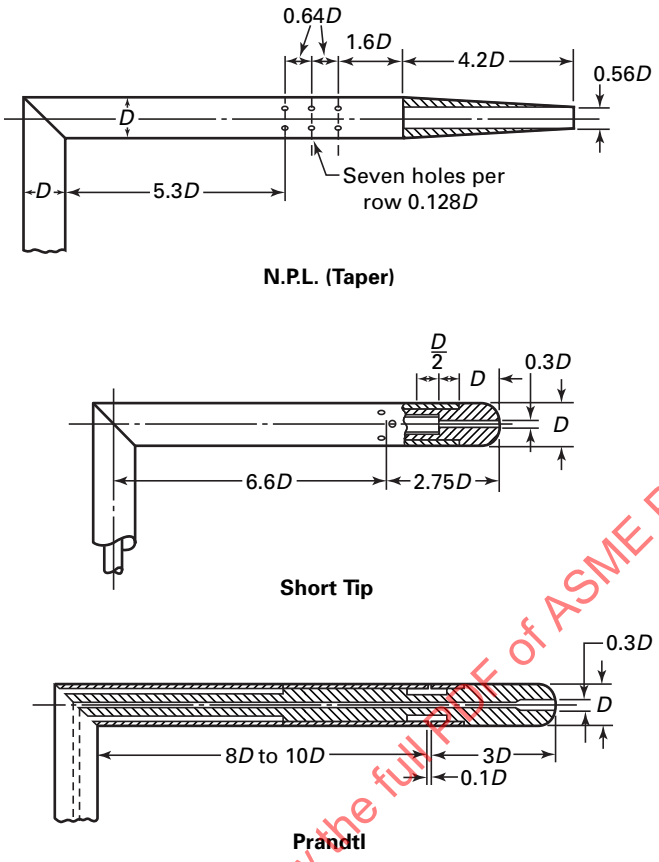

Fig. 9-4.1 Pitot Tubes Needing Calibration But Acceptable

pulsations and turbulent fluctuations must be detected. The traditional heated probe is a single-wire element stretched between two supports and held perpendicular to the velocity. The wire length should be at least 100 wire diameters. This sensor is equally sensitive to all velocity changes perpendicular to the wire. Using a single wire, the direction of the velocity is not known if the velocity is not parallel to the conduit walls. It may not sense the velocity component normal to the flow area. Its inherent frequency response will detect velocity fluctuations with periods that are six times or more the thermal time constant of the wire [Eq. (9-4.1)]. If higher frequency response is required, electronic compensation must be used. The sensing material should have a high temperature coefficient of resistivity, such as provided by tungsten, nickel, platinum, or special alloys. For metallic wires between 0.001 in. and 0.003 in. in diameter and for velocities between 5 ft/sec and Mach 1, the wire time constant is given by

$$\tau = [c_w d_w (p)_w]/4h \qquad (9\text{-}4.1)$$

where

$$h = k/d_w[Pr^{0.3}][0.35 + 0.47(Re_w)^{0.52}] \qquad (9\text{-}4.2)$$

There are two basic types of electric circuits used with such anemometers: constant current and constant temperature. The heated surface is one element of a Wheatstone or Kelvin bridge circuit. Frequency response greater than 300 Hz, which is usually sufficient for performance testing, has been obtained from variations of these basic circuits using relatively rugged wires. Often the theoretical computation of the anemometer calibration is adequate, based on the electrical circuit equations and the known convective heat transfer from the geometry of the probe to the fluid. For example, if the convective heat transfer coefficient h and the properties of the wire and the fluid are known, Eq. (9-4.2) can be used to compute the velocity. The uncertainty of this computed calibration shall be calculated using ASME PTC 19.1. Where better accuracy is required, the anemometer system must be calibrated under flowing conditions as nearly duplicating the performance test conditions as possible. The calibrating flow must be exceptionally free from turbulence to obtain a good mean velocity calibration.

9-4.5 Laser Doppler Velocimeters

Laser Doppler velocimetry (LDV) techniques may be used to measure flow velocities at the specified traverse

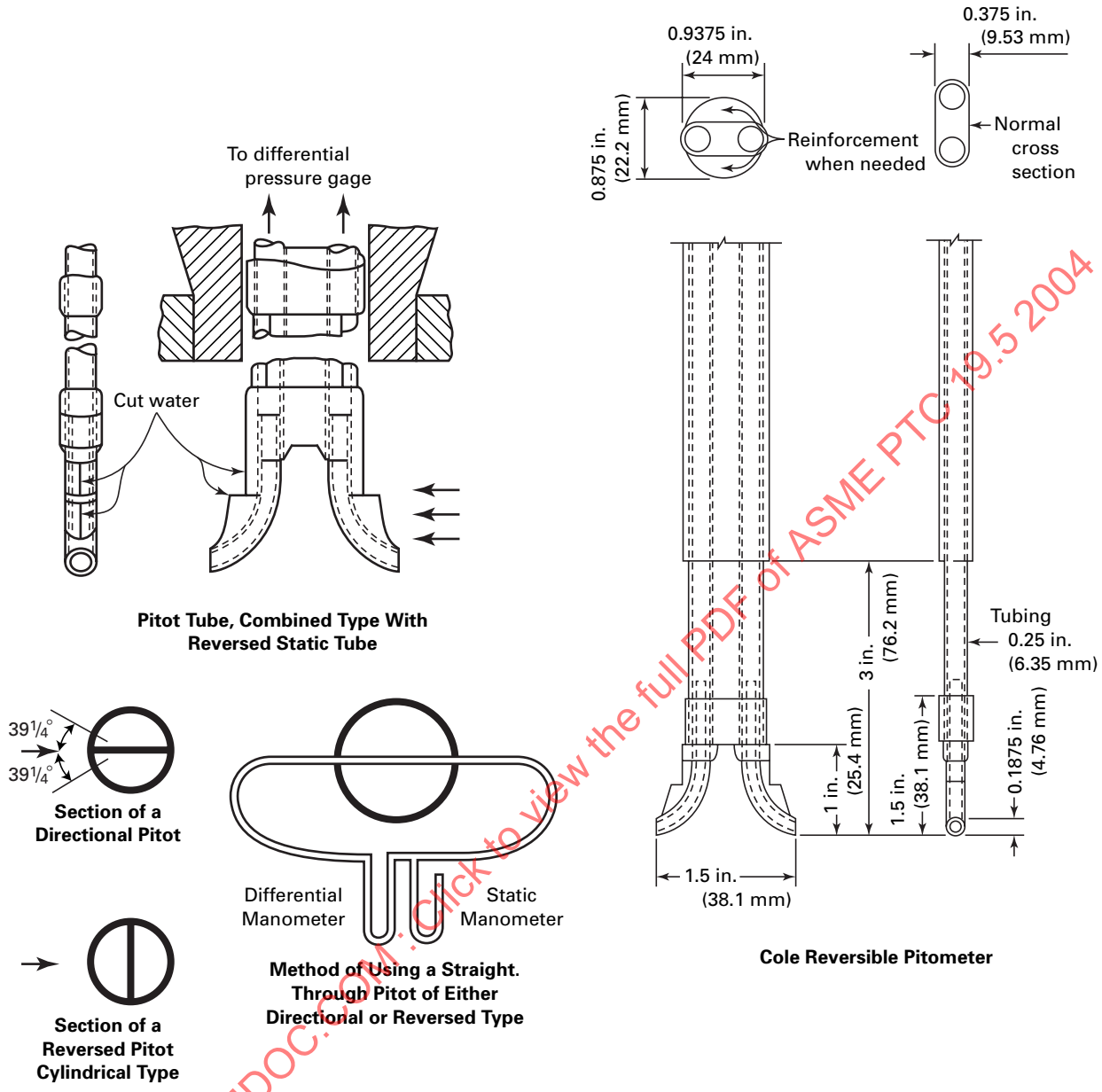

Fig. 9-4.2 Cole Reversible Pitometer Structural Reinforcements

locations. Because of the expense and complexities of this measurement system, the velocities are observed sequentially at each point in the traverse. Consequently, the conditions of para. 9-5.5 apply to this technique. There must be at least one window in the conduit for the light beam to enter and the velocity to be observed in the back scatter mode. The forward scatter mode yields a stronger signal, and for this technique another window must be added somewhere on the opposite side of the conduit. The fluid, of course, must be reasonably transparent. The fluid must have a sufficient density of particles that follow the flow and reflect light so that an adequate signal may be obtained. The flow is often seeded with particles to this end. Currently, there is not an accurate method intrinsic to the laser system for locating the focal point of the light beams; therefore, an independent mechanical device must be used to locate each measurement point of the traverse upon which the light beams are focused. Two such techniques have been used successfully: a grid of crossed wires and a removable probe that is positioned from outside the conduit. In this latter case, the crossed beam is focused on the point of the probe, the probe is removed and the velocity is measured, and then the procedure is repeated at the next traverse location.

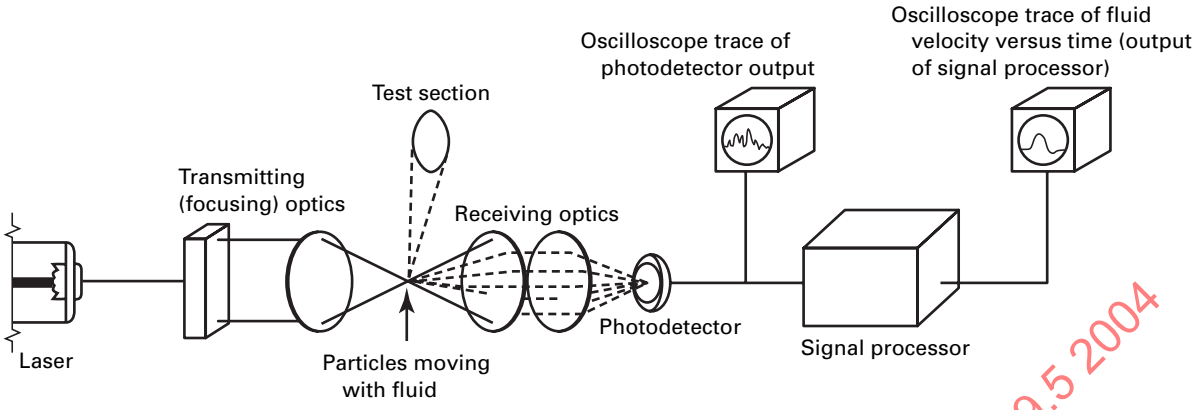

Fig. 9-4.5.1 Laser Doppler Velocimeter System

9-4.5.1 LDV System Description. A dual, crossed-beam LDV system is recommended for most applications. Figure 9-4.5.1 shows the arrangement of the basic components for a typical complete velocity measurement system. Helium-neon types can be used in applications where low power will suffice, and argon-ion types are often used where more power is required to penetrate the fluid. The laser provides a source of collimated and coherent light. The beam splitter separates the collimated beam into two parts of equal intensity. The focusing lens both focuses the two beams and causes them to cross at the measuring point. The crossed beams form a very small ellipsoid of light in which an interference pattern of light and dark lines is formed normal to the plane of crossing. When a particle passes through this fringe pattern, it reflects a frequency proportional to its velocity. The collecting optics focus this reflected light onto the photodetector, which transduces it to an electrical signal for the signal processor. The filtered frequency signal is subsequently converted statistically into a reading of mean velocity, rms velocity, velocity distribution, and so on.

For each application, the measurement system must be optimized, but for air and water flow these techniques are well established. The major system requirements are

(a) particles that are small enough to follow the flow accelerations but also large enough to reflect the light and provide an adequate signal.

(b) laser, optics, and the photodetector that are selected to provide an optimum signal-to-noise ratio.

(c) a signal processor that extracts the statistical information from the photodetector and converts it to a mean velocity.

(d) a data processor that can store and average the histogram built up from intermittent signals, since the flows of interest often have a low density of suspended particles.

9-4.5.2 LDV System Calibration. A rotating wheel whose dimensions and speed are also measured provides a convenient and accurate method of calibrating the entire LDV system from input to output. Such calibrations should be performed at several locations in the crossed-beam sensing volume to measure any variations within.

An accurate measurement of the beam-crossing half-angle k also provides a calibration if there are no distortions from the optics. The fringe spacing d_f depends only on k and the wavelength of the laser light, usually known within 0.01%.

$$d_f = \frac{\text{wavelength}}{2 \sin k} \tag{9-4.3}$$

$$u_x = d_f f \tag{9-4.4}$$

This LDV system senses only one component of the velocity vector. A second component can be measured by rotating the optics, but to sense all three components of the fluid velocity another LDV system must be installed at a different angle to the flow.

9-5 FLOW MEASUREMENT PROCEDURES

9-5.1 Flow Measurement by Pitot Rake

A Pitot rake is a battery of plane-ended total pressure tubes arranged along two or three pipe diameters as shown in Figs. 9-2.1, 9-5.1-1, and 9-5.1-2. This is the traditional primary method of all the recommended traverse methods of flow measurement for ASME performance tests. The radial spacing of the total pressure holes is specified in Tables 9-2.1-1 through 9-2.1-3, corresponding to the numerical integration method selected for the test. All total pressure openings are to be coplanar. Four static pressure taps are to be made in the conduit wall in the same plane as the total pressure taps, if possible;

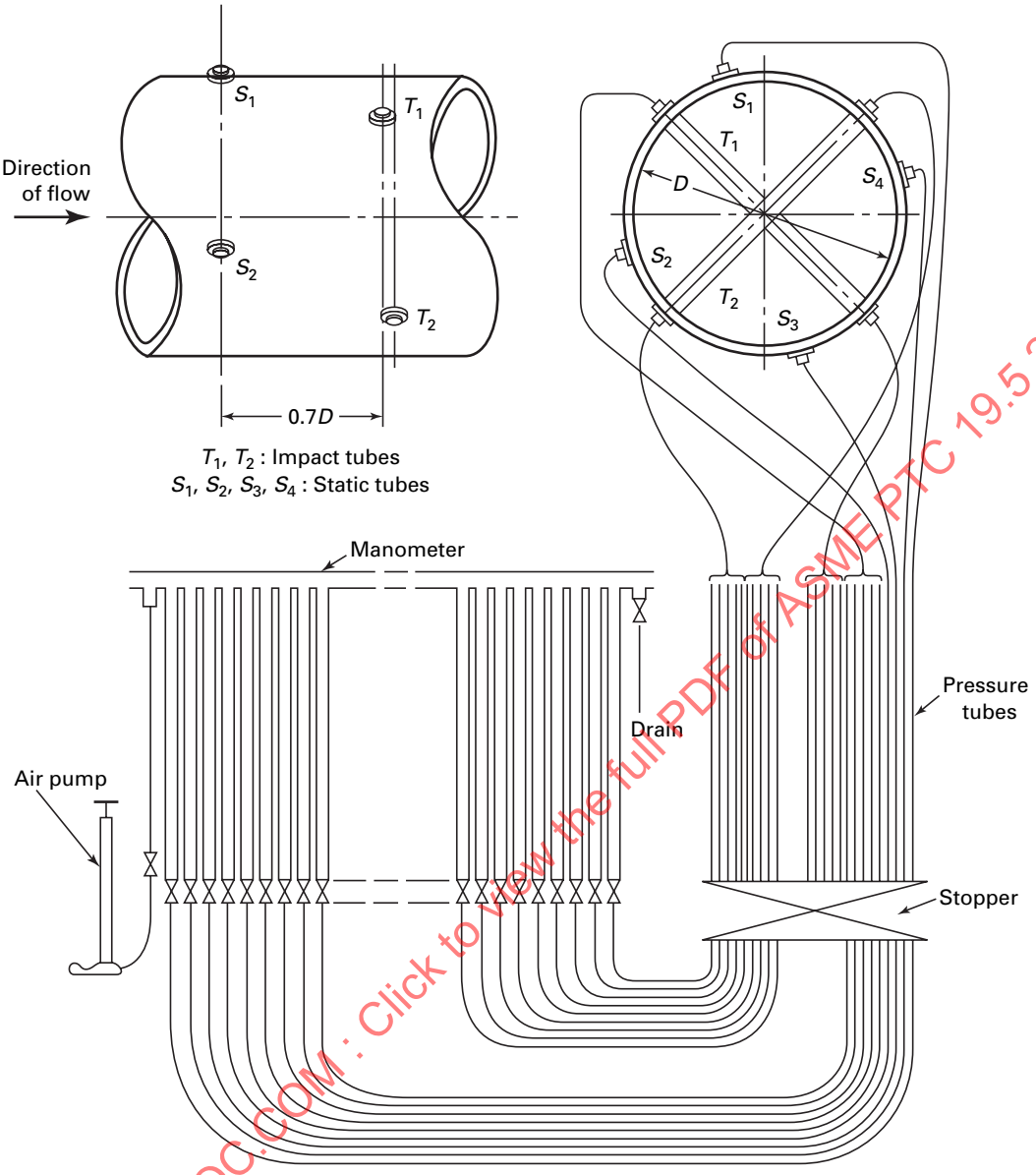

Fig. 9-5.1-1 Pitot Rake

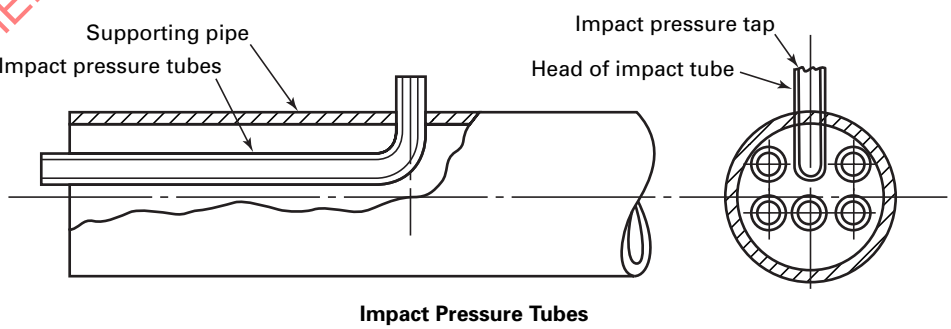

Fig. 9-5.1-2 Impact Pressure Tube Rake

if not, a correction for the pipe friction pressure loss shall be made to the data and the blockage correction altered, as described in para. 9-6.1. No static tap shall be located in either the top of a round pipe (because air bubbles may enter the manometer lines) or the bottom (because of the likelihood of particles clogging these sensing lines). A reference total pressure measurement shall be made at the center to satisfy paras. 9-3(b) and 9-5.5. Each static and total pressure tap is connected separately to one leg of a differential pressure manometer, or other agreed and calibrated transducer, through a set of ganged stopcocks, so that all may be isolated from the flow simultaneously for reading. Closure of the stopcocks shall not change the pressure measurement by more than 0.04 in. or 1 mm H_2O.

9-5.2 Pressure-Sensing Lines

Pressure-sensing lines shall be of noncorrosive material and not less than $\frac{1}{4}$ in. or 6 mm inside diameter. These lines must be free from leaks and shall be installed to avoid air entrapment in the connections. The lines and the manometers shall be protected from thermal sources such as direct sunlight, exhaust air from heat exchangers, or drafts.

9-5.3 Required Resolution and Density Determination

To maintain 1% accuracy, manometer deflections shall be at least 2 in. or 50 mm. If a manometer fluid other than water or mercury is used, its density shall be measured in situ.

9-5.4 Required Number of Readings

Manometers have been the primary differential pressure measurement standard and are recommended for use. ASME PTC 19.2 describes their application to these measurements and shall be used for reference.

Differential pressure transducers of at least equivalent accuracy may be used provided they are calibrated before and after the test in accordance with ASME PTC 19.2. Their uncertainties shall be evaluated according to ASME PTC 19.1. Manometer readings may be taken visually or by suitable photographic means. Ten to twenty observations shall be recorded at each station at each rate at uniform time intervals to cover at least two complete periods of any acceptable level of flow variations. Each manometer reading yields one observed velocity given by

$$v = C\,(2\delta p/\rho)^{1/2} \qquad (9\text{-}5.1)$$

where

C = 1.000 for a plane-ended total pressure tube
v_i = at the ith station, mean of the specified number of readings in Eq. (9-1.1).

9-5.5 Velocity Traverse — Moveable Sensor

Flow measurement by velocity traverse may be made by moving the sensor to the locations specified in para. 9-2. Using this method, the flow must remain steady throughout the period required to complete the traverse. The steadiness of the flow shall be monitored by a fixed sensor in the center of the conduit. An additional uncertainty accrues because of the observation period; this shall be estimated as a random uncertainty using the flow variation data from the fixed sensor during the period of the velocity traverse.

9-6 FLOW COMPUTATION

The arithmetic mean of the observed velocities — not differential pressures — at each measuring station shall be calculated. All corrections shall be included (e.g., calibration coefficient and blockage or stem and mutual interference corrections). The flow is computed by numerical integration (a finite summation) of these velocity data as an approximation to the integral of the velocity profile over the area.

9-6.1 Blockage Correction for Static Taps Upstream of Pitot Tubes

The pitot tube support structure must be stiff enough so that the effect of sensor vibration on all flow velocity measurements is negligible. The presence of this supporting structure causes a reduction in the observed static pressures without changing the total pressure. The observed flow measurement must be corrected [reduced according to Eq. (9-6.1) to account for this blockage]. The blockage factor K_s directly follows in which S is the frontal area of the support structure, x is the distance between the static pressure taps and the supporting structure, and A is the conduit flow area. (The factor 0.7 below has an uncertainty of ±0.05.)

$$\delta p_{\text{actual}} = (1 - 0.7K_s/S)\delta p_{\text{meas}} \qquad (9\text{-}6.1)$$

where

$$K_s = 1.0226 - 0.9948x/A - 0.8723(x/A)^2 + 1.223(x/A)^3$$

9-6.2 Blockage Correction for Current and Propeller Meters

There is a blockage correction that must be applied to the flow measurement, which is caused by the installation of the measurement system. The traverse array of meters reduces the flow area in the measurement section, which in turn causes the flow velocities there to increase. The flow measurement must be corrected using Eq. (9-6.2).

$$Q = [1 - 0.125\,(S/A) - 0.03\Sigma_i\,(S_m/A)]Q_m \qquad (9\text{-}6.2)$$

where the frontal area of each meter is $S_m = \pi\tau_m{}^2$.

9-6.3 Flow Computation in Pipes

$$Q_n = \int_0^R 2\pi r V(r)\,dr = A\left[\sum_{i=1}^{n} w_i V_i\right] \qquad (9\text{-}6.3)$$

The log-linear method uses equal weighting factors as shown in Table 9-2.1-3, but the Gauss and Tchebycheff methods specify a unique set of weighting factors w_i given in Tables 9-2.1-1 and 9-2.1-2. The summation over each radius of the pipe will give a separate estimate of the total flow. The arithmetic mean of each of these flows Q_n shall be the computed total flow. The differences between each of these estimates will give an indication of asymmetry in the velocity profile and/or the degree of approximation in the numerical integration technique.

Plotting the observed velocity profiles is highly recommended to check the degree of asymmetry in the flow profile and whether it is reasonable to expect such a profile in the subject installation. A sample graphical integration and summation are recommended to assess the validity of the numerical integration procedure and eliminate mistakes.

9-6.4 Example of Pipe Flow Computation

An example of pipe flow computation is given at the end of this Section.

9-6.5 Flow Computation in Rectangular Ducts

Numerical integration of the flow in conduits of rectangular cross-section is a two-dimensional problem using coordinates y and z along the height and width of the duct. The only methods recommended are the Gauss and Tchebycheff spacings and weighting factors given in Tables 9-2.2-1 and 9-2.2-2. No other published techniques approach the numerical accuracy of these two. The velocity is represented by a product function.

$$V(Y, Z) = F(Z)G(Y) \qquad (9\text{-}6.4)$$

and the differential area is $dA = dY dZ$.

As with circular conduits, the total flow is the integral of the velocity over the area.

$$Q = \int V(Y, Z)\,dA = \int_{-w/2}^{w/2}\int_{-h/2}^{h/2} F(Z)G(Y)\,dY\,dZ \qquad (9\text{-}6.5)$$

Since F and G are functions only of independent variables, the integration may be performed independently and the results multiplied. To align the actual physical dimensions of the duct with the values presented in Tables 9-2.2-1 and 9-2.2-2, the dimensions are normalized as ratios to the half-height and half-width of the conduit.

$$x = 2Z/w \text{ and } dx = 2dZ/w$$

$$y = 2Y/h \text{ and } dy = 2dY/h \qquad (9\text{-}6.6)$$

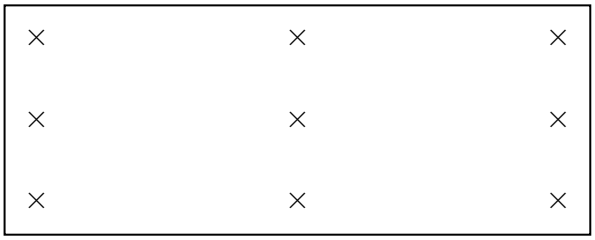

Fig. 9-6.5 Velocity Traverse Measurement Loci for a 3 × 3 Array

This simply has the effect of changing the lower limit of integration to -1 and the upper one to +1. Performing this transformation and calculating the numerical integration leads to

$$\int_{-w/2}^{w/2} F(Z)dZ = (w/2)\int_{-1}^{1} f(x)dx = (w/2)\sum_{n=1}^{n} w_i f(x_i) + R_n \qquad (9\text{-}6.7a)$$

and

$$\int_{-h/2}^{h/2} G(Y)dY = (h/2)\int_{-1}^{1} g(y)dy = (h/2)\sum_{j=1}^{m} u_j g(y_j) + R_m \qquad (9\text{-}6.7b)$$

where R_n and R_m denote the remainder or numerical error involved in truncating the series at n and m terms, the consequence of making n measurements across the width and m measurements over the height for a total of $n \times m$ velocity measurements in the traverse pattern.

The numerical approximation to the integral of the velocity profile, which gives the total flow, becomes

$$Q = (wh/4)\sum_{i=1}^{n} w_i f(x_i)\sum_{i=1}^{m} u_i g(y_i) \qquad (9\text{-}6.8)$$

This is the product of two finite series, term by term. Note also that $f(x_i)g(y_j) = V_{ij}$, the velocity observed at the i, j designated point in the traverse, as defined in Tables 9-2.2-1 and 9-2.2-2 and shown by example in Fig. 9-6.5. The given spacing provides lines across the rectangular cross-section in both the width and the height. The velocity sensors are placed at the intersection of these lines. For instance, $f(x_2)g(y_1) = V_{21}$, where $n = m = 3$ as follows:

$$\begin{aligned} Q = wh/4(&w_1u_1V_{11} + w_1u_2V_{12} + w_1u_3V_{13} \\ &+ w_2u_1V_{21} + w_2u_2V_{22} + w_2u_3V_{23} \\ &+ w_3u_1V_{31} + w_3u_2V_{32} + w_3u_3V_{33}) \end{aligned} \qquad (9\text{-}6.9)$$

This format appears similar to a matrix, but it is simply the sum of terms over the indices of velocity measurement loci. Note that the loci in Tables 9-2.2-1 and 9-2.2-2 are given as proportions of the half-width and half-height and that the weighting factors are symmetric about the origin, which is the center of the duct. For the

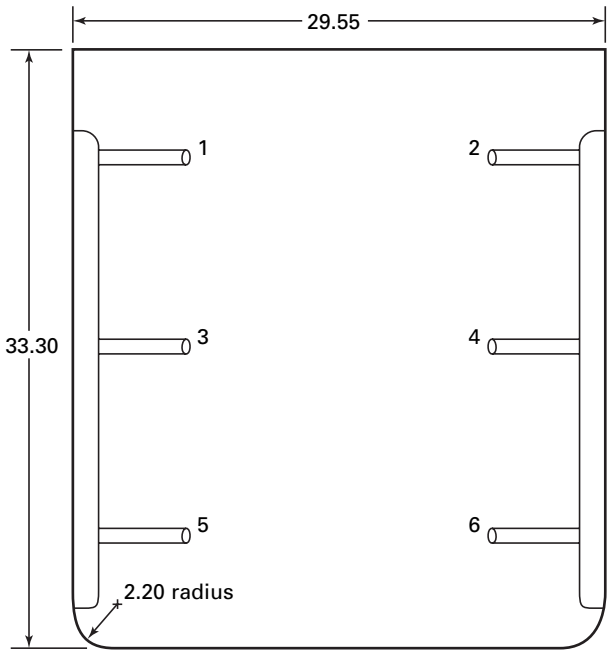

Fig. 9-7.1 Inlet Duct With Pitot-Static Rake Installed

odd values of n and m, the velocity must be measured in the center to compute the flow. For even values of n and m, this observation shall be obtained to evaluate skewness of the velocity profile and also to monitor the temporal steadiness of the flow during the period of reading the sensors and/or moving them between measurement stations.

9-7 EXAMPLE OF FLOW COMPUTATION IN A RECTANGULAR DUCT

This example treats the measurement of air flow to the engine of an aircraft in flight. This is one of a series of similar measurements relating to the engine performance/inlet-airframe integration tests. Because there was a limit on the number of telemetering channels, only six measurement loci were available. Operational constraints prevented drilling static pressure taps into the sidewalls of the inlet duct; therefore, ASME Pitot-static probes were selected for this test. These were fabricated from ¼-in. o.d. stainless steel tubing in accordance with Fig. 9-4. These probes were 6 in. in length before the bend and their side supports were aerodynamic shapes for stiffening without interfering with the flow to the engine any more than necessary.

9-7.1 Flow Area

The flow area of the inlet is shown in Fig. 9-7.1 with the dimensions in inches. It was measured at 39°F by taking six readings of the height and width at four stations each, for a total of 48 measurements. The bias uncertainty of these physical dimensions was estimated to be ±0.025 in., and repeated measurements were found to range ±0.03 in. The flow area was the height times the width minus the two rounded corners minus the six probe circles. (It is good practice to perform the uncertainty analysis simultaneously with the instrumentation and test design.) To determine the random effect on the flow area, it was necessary to use the range of dimensions to calculate an equivalent random uncertainty from Table 2.1 in ASME PTC 19.1. For four samples of six readings each, $d2 = 2.57$ and the equivalent degrees of freedom are 18.1. This provides $t_{95} = 2.1$,

$$s = \sigma = 0.03/2.57 = 0.0116 \text{ in.} \qquad (9\text{-}7.1)$$
$$t_{95}s = \pm 0.025 \text{ in.}$$

This happens to equal the bias estimate; therefore, both components of the flow area uncertainty are about ±0.16%.

9-7.2 Traverse Pattern Selection

Since only a few sensors could be employed, Gaussian integration spacing was selected because it provides the least error in the calculation of the total flow. The measurement locations were taken from Table 9-2.2-1 for n = 2 and n = 3. Across the width they are located at ±0.5773 times the half-width from the center. Across the height they are located at the centerline and at ±0.7746 times the half-height. This places the lines of intersection at ±8.529 in. from the centerline in width (6.245 in. from the sidewall), ±9.990 in. from the centerline in height (6.666 in. from the top and bottom), and at the centerline (16.65 in. from the top).

9-7.3 Blockage Correction

The Pitot-static array was fastened to the inlet walls by a welded bracket whose frontal projection was 1.00 in. × 26.50 in., one on each side as shown in Fig. 9-7.1. Each velocity probe was supported by an aerodynamically shaped spar whose frontal projection measured 0.50 in. thick × 5.25 in. long. The structure on each side resembled a rake, hence the name Pitot rake. The blockage correction factor is calculated using Eq. (9-6.1). Terms required for this equation are the following:

$$\text{Flow area, } A = 981.64 \text{ in.}^2$$

$$\text{Static holes to stem, } x = 4.0 \text{ in.}$$

$$x/\sqrt{A} = 0.1277$$

$$K_s = 0.8839$$

$$\text{Blockage correction factor} = [1 - 0.7(0.8839)(68.75/981.64)] = 0.9566 \pm 0.0032$$

Table 9-7.4
Transducer Calibration Linearized Calibration Data

No.	*a*	*b*	*δ*, %
1	−0.0235	9.93	0.08
2	0.0158	9.98	0.12
3	−0.0057	9.94	0.07
4	0.0254	10.03	0.18
5	0.0095	10.01	0.10
6	−0.0112	9.96	0.11

All differential pressures observed must be post-multiplied by this factor to arrive at the true, raw data on differential pressure.

9-7.4 Transducer Calibration

Six differential pressure transducers were used in the flight test. Each was calibrated in the laboratory before installation in the aircraft against a water manometer. Each had a calibration curve fit given in the following form:

$$\delta p = a + b\,(\text{voltage output}) \tag{9-7.2}$$

Eighteen observations were made for each curve, ascending and descending in pressure. The voltage was measured with a laboratory-quality, calibrated DVM, the largest error of which was reported 0.02% of reading. Each transducer had a random variation about this linear graph, as given in Table 9-7.4.

It was found during flight tests that these transducers would drift slowly throughout the day. Their constant a was not, in fact, constant. The slope b was 40 times more constant than a and was taken to be essentially constant in the data processing. In conducting the test, the a was adjusted during preflight as close as possible to zero (±0.003 V) with the engines off. At the conclusion of the flight test, the transducer output was again measured to determine the drift. This drift was by far the largest component uncertainty in the pressure measurement; it was classified as a ± bias uncertainty with the value of one-half the drift from startup to shutdown.

9-7.5 Flight Testing and Data Processing

The purpose of the flight test program was to measure the velocity profile in the intake at various air speeds, altitudes, and attitudes and to measure the total air flow to the engine as well. Only the starboard engine nacelle was instrumented, and damage to the engine from the Pitot rake coming loose was a major safety-of-flight concern. Flight data were logged once per second for a 1-min period using the on-board eight-channel recorder. The other two channels recorded the outside air temperature and the pressure altitude. These data were processed after the flight.

Table 9-7.6 Test Data Summary

		Bias (drift)		*σ*	
Station	*v*, ft/sec	mV	%	mV	%
1	374.9	4	0.7	6	1.05
2	337.4	6	1.05	10	1.75
3	377.9	3	0.52	12	2.09
4	332.6	1	0.17	8	1.40
5	385.1	10	1.75	15	2.62
6	365.8	8	1.40	12	2.09

air density (ICAO Tables) = 0.001267 slug/ft^3
OAT = −22.5°C
pressure = 13.86 in. Hg

Since it is the time-average velocity data that are of interest, the voltage outputs by the transducers were not averaged. Rather, each of the 6 × 60 data were used to calculate the air velocities, and then these were averaged to give the true mean velocity for that period as follows:

(a) The average of the pre- and postflight values of a were used in the calibration equations for each transducer giving the pressure for each datum in psi.

(b) Each pressure was corrected for the blockage as determined by para. 9-7.3 and Eq. (9-6.1).

(c) Each velocity was computed using Bernoulli's equation as follows:

$$v = [2\delta p(144)/\rho]^{0.5}\ (\text{psi ft}^3/\text{slug})^{0.5} \tag{9-7.3}$$

(d) The temporal mean velocity was calculated for each station as well as its variance.

(e) The air temperature and pressure did not vary during the 1-min period.

9-7.6 Typical Set of Test Data

In the following instance, the aircraft was in level flight at 20,000 ft msl at 214 kts. true air speed (measured from ground stations) and at 5 deg of steady sideslip to port (measured by onboard instrumentation). This flight condition was maintained for 2 min. Data acquisition was initiated by the pilot when he was satisfied that conditions were steady. The data are shown in Table 9-7.6.

This velocity profile shows a pronounced skewness on the outboard side of the inlet, plausibly resulting from the steady sideslip. A graphical plot of the profile was made to give an indication of the flow distribution and reasonableness. The flow was computed using the method shown in para. 9-6.5 with the weights for $n = 2$ and $n = 3$ in Table 9-2.2-1.

$$\begin{aligned} Q &= \underline{w}_1\underline{u}_1\underline{V}_1 + \underline{w}_2\underline{u}_2\underline{V}_2 + \underline{w}_3\underline{u}_3\underline{V}_3 \\ &\quad + \underline{w}_4\underline{u}_4\underline{V}_4 + \underline{w}_5\underline{u}_5\underline{V}_5 + \underline{w}_6\underline{u}_6\underline{V}_6 \\ &= (0.55555)(1)(374.9) + (0.55555)(1)(337.4) \\ &\quad + (0.88888)(1)(377.9) + (0.88888)(1)(332.6) \\ &\quad + (0.55555)(1)(385.1) + (0.55555)(1)(365.8) \\ &= 1444.4\ \text{ft}^3/\text{sec} \end{aligned} \tag{9-7.4}$$

Multiply this by $A/4$,

$$Q = 1444.4(6.817/4) = 2461.6 \text{ ft}^3/\text{sec}$$

The average velocity $Q/A = 361.1$ ft/sec; whereas the mean of the velocities is 362.3 ft/sec, which is 0.32% too high.

9-7.7 Error and/or Uncertainty Analysis

There are two major bias uncertainties in any numerical integration method using an array of sensors. The first is the fact that the entire array might be displaced from where it should be — that is, it is not centered in the duct. The second is the truncation inaccuracy caused by making a finite number of measurements to infer the entire flow field. This installation dictated a limited number of sensors, fewer than is usually recommended. Still, the numerical error turned out to be negligible — 0.008% low.

The clearest and easiest way to estimate these effects is to model the observed velocity profile with an analytic one, which can be integrated analytically and from which the velocity values can be calculated for use with the selected (Gaussian) numerical integration technique (for comparison). In this case, a suitable velocity profile is

$$V = 360 + 12.18x + 10.81y$$

$$-1.231 \text{ ft} \le x \le 1.231 \text{ ft and} \qquad (9\text{-}7.5)$$
$$-1.387 \text{ ft} \le y \le 1.387 \text{ ft}$$

$$Q = \int V\,dxdy = \int 360\,dx + \int 12.18\,xdx + \int 10.81\,ydx \qquad (9\text{-}7.6)$$

over x yields $360x + 12.18x^2/2 + 10.81yx - 1.231^{1.231}$.

Next, evaluating at the limits and then integrating with respect to y,

$$Q = \int 886.32dy + \int 26.61\,ydy$$
$$= [886.32y + 26.62y^2/2 - 1.387]^{1.387}$$
$$= 2458.65 + 0 \text{ ft}^3/\text{sec}$$

This becomes the true value for comparison and analysis. The model flow area is a rectangle of 6.829 ft^2.

The Gaussian integration calculations of the numerical value for this model flow are shown in Table 9-7.7-1, giving a value that is 0.008% low. This error is nothing more than −1 significant figure in the velocity profile [Eq. (9-7.5)]. This example problem is a (too) simple example illustrating the Gaussian quadrature, because it has been shown [1] that, for n points in the traverse, the Gaussian method returns the exact value for the integral for velocity profile functions that are of degree $2n - 1$ or less. In this particular example, there are two measurements in the x-direction, so that the x-component of the two-dimensional velocity profile could be as complicated as a cubic equation and yet be exactly calculated. Likewise, with three measurements in the y-direction, any velocity profile that can be represented adequately using a fifth degree polynomial will also be calculated exactly. The power of the Gaussian quadrature, and the Tchbeycheff as well, comes from the fact that these use twice as many parameters to fit the data than the other commonly known integration methods, such as Simpson's one-third rule and equal area methods.

Table 9-7.7-1
Numerical Error Analysis for Gaussian Model Flow

x_i	y_i	w_{xi}	w_{yi}	V_{ij}	Q_i
−0.710 7	1.074 7	1	0.555 555	362.961 1	201.645 0
0.710 7	1.074 7	1	0.555 555	380.273 8	211.263 2
−0.710 7	0	1	0.888 888	351.343 6	312.305 4
0.710 7	0	1	0.888 888	368.656 3	327.694 5
−0.710 7	−1.074 7	1	0.555 555	339.726 1	188.736 7
0.710 7	−1.074 7	1	0.555 555	357.038 8	198.354 8
				sum =	1 439.999

bias = −0.000 08
Q_{tot} = 2 458.439 ft^3/sec

The better approach is to take the measured velocity profile and electronically fit it best in a least-squares sense in one of two recommended forms:

$$V(x, y) = F(x)G(y)$$

or

$$V(x, y) = V_{mean} + F(x) + G(y)$$

if the variation from the mean is not too great. If an adequate fit for the purposes of the test is obtained using a polynomial of degree $2n - 1$ or less, where n is the number of measuring stations each in x and y directions, then the Gaussian method will add no uncertainty chargeable to numerical integration. If higher degree polynomials are required to fit the data, then these functions can be integrated analytically to compute the flow through the area and that result compared to the value given by the Gaussian method to estimate the uncertainty charged to the numerical integration.

If the Pitot rake were installed in the worst case, all x and y dimensions would be in error by 0.060 in. The effects of measuring the velocities in the wrong place and calculating with the same weighting factors are shown in Table 9-7.7-2. This causes a bias uncertainty of 0.032%. Since these misalignments could be in either direction, these are symmetric biases.

(a) Thermal Contraction Effects. The inlet duct was measured on the ground at 39°F; the flow measurement took place at −22°C. The flow area was obviously smaller under the flowing conditions. The range of linear thermal expansion coefficients was found to be 22 to 30 ×

Table 9-7.7-2
Effect of 0.060-in. Misalignment on Gauss Flow

x_i	y_i	w_{xi}	w_{yi}	V_{ij}	Q_i
−0.705 7	1.079 7	1	0.555 555	363.076 1	201.708 9
0.715 7	1.079 7	1	0.555 555	380.388 7	211.327 0
−0.705 7	0.005	1	0.888 888	351.458 6	312.407 6
0.715 7	0.005	1	0.888 888	368.771 2	327.796 6
−0.705 7	−1.069 7	1	0.555 555	339.841 1	188.800 6
0.715 7	−1.069 7	1	0.555 555	357.153 7	198.418 7
				sum = 1 440.459	

bias = −0.000 319 caused by 0.60 in. misalignment in x and y ±
Q_{tot} = 2 459.224 ft^3/sec

Table 9-7.7-3
Effect of Uncertainty in Pressure Measurements

Probe	Weight		Bias, %		Random, %
1	0.555 55	×	0.7	& ×	1.05
2	0.555 55	×	1.05	& ×	1.75
3	0.888 88	×	0.52	& ×	2.11
4	0.888 88	×	0.17	& ×	1.40
5	0.555 55	×	1.75	& ×	2.62
6	0.555 55	×	1.40	& ×	. . .
Weighted sum/4			3.335%/4		7.294%/4

Table 9-7.7-4 Summary of Uncertainty Analysis

Source	Bias effect on Q, %	Random effect on Q σ, %
Flow area A	0.16	0.16
δp measurements	0.417	0.912
Rake blockage	0.16	. . .
Density, tabular	0.08	. . .
Density, temperature	0.31	. . .
Numerical Integration	0.008	. . .
Root-sum-square	±0.56%	±1.85% (2σ)

10^{-6}/°C from the Handbook of Chemistry & Physics, Chemical Publishing Co. Note there is an uncertainty stemming from different reported values, which often occurs in material property data of all kinds. However, in this case, the overall change in area was negligible (4.3×10^{-6} ft^2).

(b) Air Density From Different Sources. There was found to be an uncertainty of 0.08% in the reported air data from two sources: The ICAO Standard Atmosphere, U.S. Government Printing Office, 1962 compared to the Compressed Air & Gas Data, Ingersoll-Rand, 1971, p. 34–121.

(c) Temperature Measurement Uncertainty. The aircraft temperature probe was certified accurate to within ±2°F; this implies an error in the measured density of ±0.31%.

(d) Sensitivity Coefficients. Since the velocity is calculated from Bernoulli's equation and the pressure, density, and blockage factor all appear under the square root, the sensitivity of these uncertainties is one-half. The uncertainty of the coefficient of the Pitot-static probe is negligible, and the sensitivity of the flow area is unity. See Table 9-7.7-3 for the effect of uncertainty in pressure measurements.

The calibration data bias and random effects are negligible compared to the test data. Applying the sensitivity factor of one-half, the aggregate effect of the pressure transducer errors in the rake on uncertainty of the total flow becomes ±0.417% bias and ±0.9118% random (one standard deviation). The combined effects of all uncertainties on the total flow measurement are summarized in Table 9-7.7-4, in which the random uncertainties have been normalized to that expected if more than 30 observations had been made.

The combined uncertainties then become, according to ASME PTC 19.1,

$$u_{95} = \pm 1.93\% \text{ (covers 95\% of the data)}$$

$$u_{add} = \pm 2.41\% \text{ (covers all but about 1\% of the data)}$$

It is permissible to ignore component uncertainties smaller than one-fifth of the largest one. To improve the test results, Table 9-7.7-4 shows the need for more stable pressure transducers and better temperature measurement. Then the total uncertainty could be brought down to about 1.25%. The random variations in the flow are believed to reflect the actual fluid dynamics, and, therefore, the random component of δ_p cannot be improved much.

9-8 SOURCES OF FLUID AND MATERIAL DATA

[1] Gerald, C. F.; Wheatley, P. O. *Applied Numerical Analysis,* 4th edition. Reading, MA: Addison Wesley Publishing Co.; 1968.

[2] Abramowitz, M.; Stegun, I. A. *Handbook of Mathematical Functions with Formulas, Graphs, and Mathematical Tables,* Chapter 25, NBS Applied Mathematics Series 55. Washington, DC: Superintendent of Documents, U.S. Government Printing Office; 1964.

[3] Keyser, D. R. Laser Flow Measurement. *Journal of Engineering Power* paper 77-WA/FM-2, 1978.

[4] Bean, H. S., ed. *Fluid Meters: Their Theory and Application,* 6th edition. New York: The American Society of Mechanical Engineers; 1971.

[5] *Handbook of Chemistry & Physics,* Chemical Publsihing Co.

Section 10
Ultrasonic Flow Meters

10-1 SCOPE

This Section applies to ultrasonic flow meters that base their operation on the measurement of transit times of acoustic signals. Furthermore, this Section is only concerned with the use of such meters to measure the volumetric flow of a liquid exhibiting homogenous acoustic properties, flowing in a completely filled and closed conduit.

Not covered by this Section are ultrasonic flow meters that derive volumetric flow measurement from the deviation, Doppler scattering, or statistical correlation of acoustic signals. Other travel time–based meter types (phase-shift, sing-around, including clamp-on transducer meters) may find application in some paragraphs below; however, they are not specifically included in this Section.

10-2 APPLICATIONS

Differential travel time acoustic flow meters are used in a wide variety of applications, with both factory-built spool pieces with integral transducer mounts in the 1-4-ft diameter range and, in larger pipes, field-installed transducers in the 3 ft and larger size range.

Multiple-path systems are used where high accuracy is required, such as for acceptance testing of pumps and turbines and in custody-transfer applications. An advantage of multiple-path meters is that they can be dry-calibrated in the field by making physical measurements in the meter section. This is particularly important when larger sizes are required, because field calibration of these large meters is expensive, time-consuming, and difficult.

Single-path systems are mainly used where accuracy is less important and low cost is required. Such applications include smaller pipes for water, waste water, and industrial flow rate measurement. Where process conditions are well-controlled, the single-path meter can have high accuracy and high repeatability after calibration.

10-2.1 Purpose

This Section provides

(a) a description of the operating principles employed by the ultrasonic flow meters covered in this Section

(b) a description of typical applications and accuracies achieved

(c) a description of error sources and performance verification procedures

(d) a common set of terminology, symbols, definitions, and specifications

10-2.2 Definitions

Terminology and symbols used in this Section, except for those defined below, are in accordance with ASME PTC 2.

(a) Terminology

acoustic path: the path that the acoustic signals follow as they propagate through the measurement section between the transducer pairs.

axial flow velocity: the component of liquid flow velocity at a point in the measurement section that is parallel to the measurement section's axis in the direction of the flow being measured.

cross-flow velocity: the component of liquid flow velocity at a point in the measurement section that is perpendicular to the measurement section's axis.

dry calibration: calibration of the flow meter without using transfer flow rate measurement standards. Calibration consists of an exact determination of pipeline diameter, path lengths, angles, and locations in the pipeline cross-section.

measurement section: the section of conduit in which the volumetric flow rate is sensed by the acoustic signals. The measurement section is bounded at both ends by planes perpendicular to the axis of the section and located at the extreme upstream and downstream transducer positions.

nonrefractive system: an ultrasonic flow meter in which the acoustic path crosses the solid/liquid interface at a right angle.

refractive system: an ultrasonic flow meter in which the acoustic path crosses the solid/liquid interface at other than a right angle.

secondary flow: a flow with streamlines that are not parallel to the conduit walls.

transducer: the combination of the transducer element and passive materials.

transducer element: an active component that produces either acoustic output in response to an electric stimulus and/or an electric output in response to an acoustic stimulus.

transit time: the time required for an acoustic signal to traverse an acoustic path.

velocity profile correction factor: a dimensionless factor based on the measured or estimated velocity profile used to adjust the meter output. This factor is necessary for some types of multiple-path numerical integration methods; it is also used for meter factor adjustment for single-path diametrical flow meters. Also, it is used to adjust the meter output to agree with wet calibration results.

(b) Symbols

A = the average cross-sectional area of the measurement section, L_2
C, C_p = velocity of sound in water, plastic, and so on
C_{down}, C_o, C_{up} = velocity of sound average (at rest), upstream, downstream
Q = the volumetric flow rate in the measurement section, L_3/T
S = velocity profile correction factor
V_{ax} = the average axial flow velocity along acoustic path i, L/t
W_i = a weighting factor for acoustic path i that depends on measurement section geometry and acoustic path location (dimensionless)
n = the number of acoustic paths
s = velocity profile correction factor S
t = transit time

10-3 FLOW METER DESCRIPTION

The transit time ultrasonic flow meter described in this Section is a complete system composed of the primary device, which is a measurement section with one or more pairs of transducers, and the secondary device, which is the electronic equipment necessary to operate the transducers, make the measurements, process the data, and display or record results.

10-3.1 Operating Principles

10-3.1.1 Introduction. At any given instant, the difference between the apparent speed of sound in a moving liquid and the speed of sound in that same liquid at rest is directly proportional to the liquid's instantaneous velocity. As a consequence, a measure of the average velocity of the liquid along a path can be obtained by transmitting an acoustic pulse along the path and subsequently measuring its transit time.

The volumetric flow of a liquid flowing in a completely filled and closed conduit is defined as the average velocity (averaged over a cross-section) multiplied by the area of the cross-section. Thus, by measuring the velocity profile to determine the average velocity of a liquid along one or more acoustic paths and combining the measurements with knowledge of the cross-sectional area, it is possible to obtain an estimate of the volumetric flow of the liquid through the conduit.

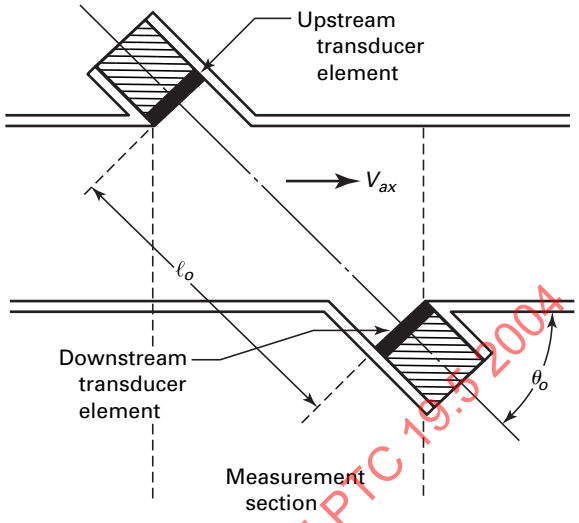

Fig. 10-3.1.2 Wetted Transducer Configuration

The theory behind these concepts is the subject of this paragraph.

10-3.1.2 Fluid Velocity Measurement. Several techniques can be used to obtain a measurement of the average effective speed of propagation of an acoustic pulse in a moving liquid to determine the average axial flow velocity V_{ax} along an acoustic path. This Section addresses the most popular method called transit time difference, although other methods are mathematically similar.

The basis of this technique is the direct measurement of the transit time of acoustic signals as they propagate between a transmitter and a receiver, both of which are in direct contact with the liquid. Different transmitter/receiver arrangements are described in para. 10-3.1.3. For an acoustic signal traveling upstream, the apparent sound speed at any point along the line of transmission, assuming only axial flow, is

$$C_{up} = C_o \sqrt{1 - \left(\frac{V_{ax}}{C_o}\right)^2 \sin^2 \theta} - V_{ax} \cos \theta \quad (10\text{-}3.1)$$

where C_o is the speed of sound in the liquid at rest, η is the angle between the acoustic path and V_{ax}, and V_{ax} is the axial flow velocity at the point in question (see Fig. 10-3.1.2). For a downstream pulse,

$$C_{down} = C_o \sqrt{1 - \left(\frac{V_{ax}}{C_o}\right)^2 \sin^2 \theta} + V_{ax} \cos \theta \quad (10\text{-}3.2)$$

In the ideal case of a uniform velocity profile, V_{ax} is constant throughout the liquid and the acoustic path is a straight line [i.e., η = constant = η_o (path angle for fluid at rest)]. Consequently, C_{up} and C_{down} are both constants along the acoustic path. In this case, the

upstream and downstream transit times (t_{up}, t_{down}) are given respectively by

$$t_{up} = \frac{l_o}{C_o \sqrt{1 - \left(\frac{V_{ax}}{C_o}\right)^2 \sin^2 \theta_o} - V_{ax} \cos \theta_o} \quad (10\text{-}3.3)$$

and

$$t_{down} = \frac{l_o}{C_o \sqrt{1 - \left(\frac{V_{ax}}{C_o}\right)^2 \sin^2 \theta_o} + V_{ax} \cos \theta_o} \quad (10\text{-}3.4)$$

where l_o is the straight-line distance between the centers of the faces of the acoustic transmitter and receiver. Taking the difference between the reciprocals of these transit times leads to

$$\frac{1}{t_{down}} - \frac{1}{t_{up}} = \frac{2V_{ax} \cos \theta_o}{l_o}$$

and, on rearranging, to

$$V_{ax} = \frac{l_o}{2\cos\theta_o}\left(\frac{1}{t_{down}} - \frac{1}{t_{up}}\right) = \frac{l_o}{2\cos\theta_o}\frac{\Delta t}{t_{up}\, t_{down}}$$

where
$\Delta t = t_{up} - t_{down}$

Since V_{ax} is constant, $V_{ax} = V_{ax}$ (the average flow velocity).

This analysis becomes more complicated in the absence of a uniform velocity profile. Nevertheless, to the degree that $(V_{ax}/C_o)^2_{max} << 1$, the result for the average of the axial liquid velocity along the acoustic path (V_{ax}) is identical, i.e.,

$$\overline{V}_{ax} = \frac{l_o}{2\cos\theta_o}\frac{\Delta t}{t_{up}\, t_{down}} \quad (10\text{-}3.5)$$

10-3.1.3 Transducer Considerations. In the preceding paragraph, it was assumed that the transducer element was in direct contact with the liquid and that the acoustic signal was propagated normal to the transducer/liquid interface. In most cases, it is desirable to protect the transducer element from the process liquid by using intervening materials (see Figs. 10-3.1.3-1 and 10-3.1.3-2). If such an arrangement is employed, Eq. (10-3.5) takes the following form:

$$\overline{V}_{ax} = \frac{l_o}{2\cos\theta_o}\left[\frac{1}{(t_{down} - t_o)} - \frac{1}{(t_{up} - t_o)}\right] = \frac{l_o}{2\cos\theta_o}\left[\frac{\Delta t}{(t_{down} - t_o) - (t_{up} - t_o)}\right] \quad (10\text{-}3.6)$$

where t_o, a function of temperature, is the transit time of the acoustic signals through the intervening materials.

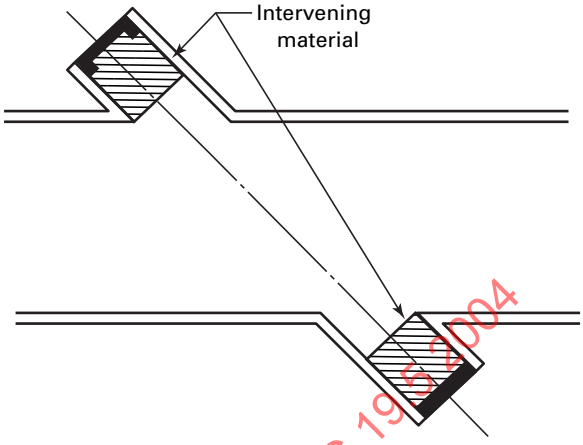

Fig. 10-3.1.3-1 Protected Configuration With Cavities

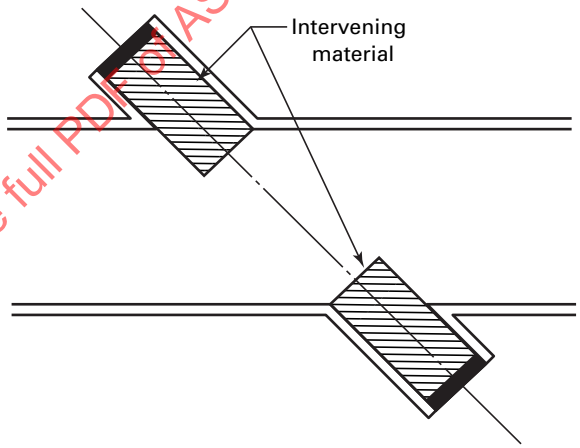

Fig. 10-3.1.3-2 Protected Configuration With Protrusions

Use of an intervening material also allows the possibility of acoustic signals entering and leaving the liquid along a path that is not normal to the solid/liquid interface. For example, the intervening material could be flush with the inside surface of the conduit as in Fig. 10-3.1.3-3. This further complicates the acoustic analysis since corrections for the refraction of the acoustic signals at the solid/liquid interface must be introduced also. This refraction takes place according to Snell's Law, i.e.,

$$\sin \varphi / C = \sin \varphi_p / C_p \quad (10\text{-}3.7)$$

where C is the sound speed in the liquid and C_p is the sound speed in the intervening material. As a consequence, η and t_o (f_o) in Eq. (10-3.6) now become functions of the sound speeds (C, C_p), and, in general, of the temperature, pressure, and composition of the process fluid and intervening materials.

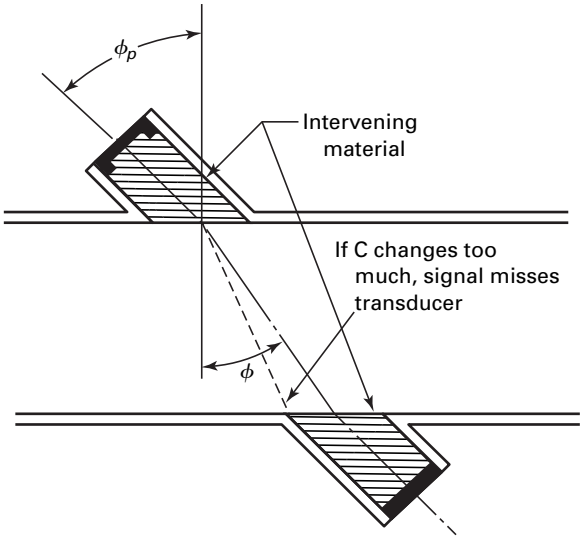

Fig. 10-3.1.3-3 Protected Configuration With Smooth Bore

10-3.2 Estimating Volumetric Flow

Once the average axial flow velocity along an acoustic path has been found, the volumetric flow can be calculated from the following equation:

$$Q = SA \sum_{i=1}^{n} W_i \overline{V}_{ax} \qquad (10\text{-}3.8)$$

Note that increasing n can reduce the sensitivity of S to flow profile variations.

10-4 IMPLEMENTATION

See Fig. 10-4 for acoustic flow measuring system block design.

10-4.1 Primary Device

The primary device consists of a separate spool piece with transducers installed or an existing section of conduit to which transducers are installed in the field.

10-4.1.1 Measurement Section. The section of conduit in which the volumetric flow is sensed by the acoustic signals is called the measurement section. This section is bounded at both ends by planes perpendicular to the axis of the section located at the extreme upstream and downstream transducer positions. The measurement section is usually circular; however, it may be square, rectangular, elliptical, or some other shape.

10-4.1.2 Transducers. The transducers transmit and receive acoustic energy. They may be factory-mounted or field-mounted by clamping, threading, or bonding. Transducers may be wetted by the liquid or not. Wetted transducers may be flush-mounted, recessed, or may protrude into the flow stream, as shown in Figs. 10-3.1.2 through 10-3.1.3-3. Some nonwetted transducers may be removed while the line is in service.

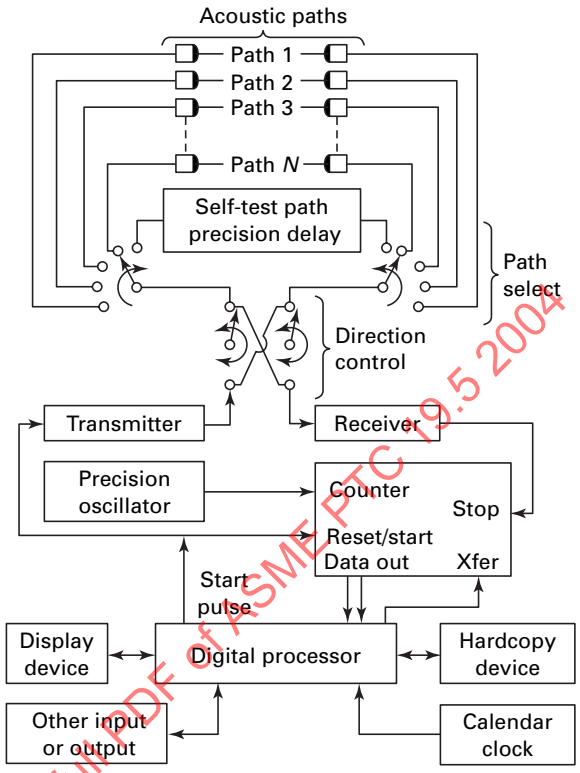

Fig. 10-4 Acoustic Flow Measuring System Block Design

10-4.1.3 Acoustic Paths. There may be one or more acoustic paths in the measurement section, each having a pair of transducers. Common arrangements are axial, diametric, and chordal, as shown in Fig. 10-4.1.3. See also para. 10-6.2.3 for a discussion of how the number of acoustic paths affects installed meter accuracy.

10-4.2 Secondary Device

The secondary device consists of the electronic equipment required to operate the transducers, make the measurements, process the measured data, and display or record the results. The secondary device should also contain means for automatic self-testing. These tests should include transmitter output power, receiver sensitivity, and timing accuracy as a minimum.

10-4.2.1 Operation of Transducers. The transducers on any given path may be excited simultaneously or alternately with one or more transmissions in each direction. In most cases, one transducer transmits a signal while the other receives. This is done in each direction on each path. The acoustic frequency and pulse repetition rate may vary depending on the application.

The transducers are connected to the electronics (secondary device) by shielded cables. The cable lengths

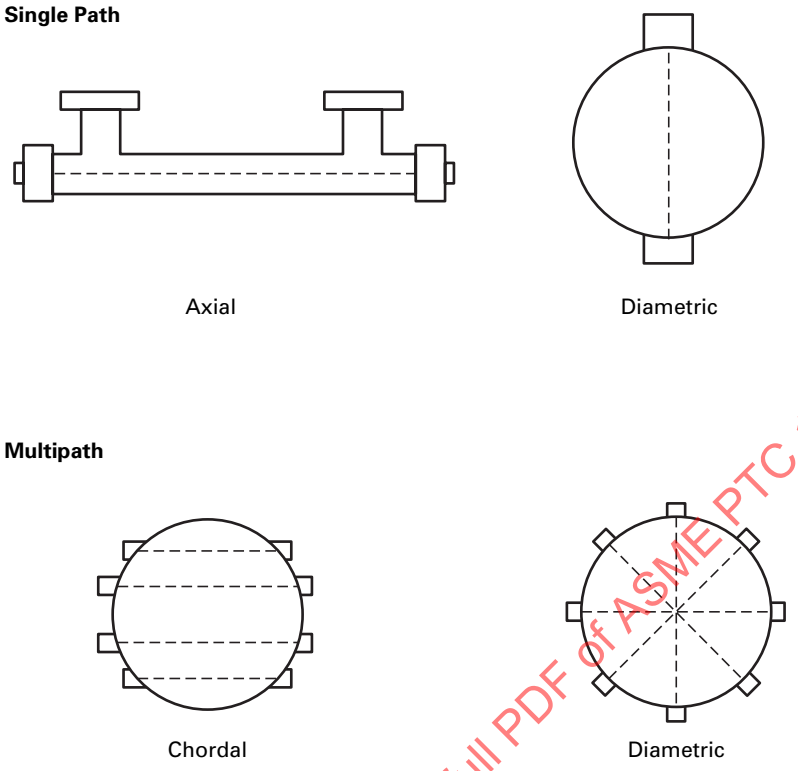

Fig. 10-4.1.3 Acoustic Path Configurations

between the secondary and primary devices are an important consideration, because longer cables introduce timing delays and signal losses. The timing delays can change the calibration factor if not accounted for; signal losses, when combined with path length (spreading loss) and acoustic attenuation in the liquid, can reduce the signal strength to the point where the meter will not operate properly. Cable specifications and maximum lengths are usually defined by the manufacturer.

10-4.2.2 Measurement Method. The transit time of an acoustic pulse is usually taken to be the interval between initial excitation of the transmitter and some characteristic point of the received signal. Exact details vary from one manufacturer to another.

10-4.2.3 Processing of Data. The secondary device, in addition to calculating the flow rate from measured transit times, should be capable of rejecting spurious signals, noise, and such. The measured flow may be the result of one or an average of many individual flow velocity calculations. Generally, it is necessary to average readings for more than several seconds and often for several minutes to reduce the output jitter of the flow meter resulting from the usually high level of turbulence in the pipeline, even when it is many diameters long. This variation in output due to turbulence follows a classic Gaussian distribution, with the uncertainty of the mean output easily calculated from the standard deviation and the total number of readings taken in the interval.

10-4.2.4 Displays and Outputs. Most meters have several outputs available, either as standard features or as optional additions to the equipment. Displays may show flow, integrated flow volume and/or direction, and may be analog or digital. Signal outputs usually include one or more of the following: current, voltage, digital, and a pulse rate proportional to flow. These outputs may or may not be electronically isolated. Flow meters may also include alarms and diagnostic aids.

10-5 OPERATIONAL LIMITS

Acoustic travel time flow rate measurement has potential operational limits. These should be investigated for each application.

10-5.1 Entrained Air

Air or other gases entrained in intake structures or created by upstream pumps, turbines, or obstructions such as partially closed valves can create sufficient attenuation in the acoustic signals to prevent operation.

10-5.2 Excessive Liquid Velocity

High liquid velocity combined with low pressure can cause local cavitation around the transducers, generating noise and entraining gas in the acoustic path.

10-5.3 Very Low Liquid Velocity

While acoustic transmission will not be affected by low velocities, the differential travel time may be so small that the system is incapable of measuring it with the required accuracy. The zero offset may also become unacceptably large. This is particularly true in smaller conduits and is highly dependent on the design of the transducers and travel time measurement electronics.

10-5.4 High Temperatures

Special designs may be required to accommodate high temperature service, and the operating pressure must be high enough to prevent liquid vapor from forming in the meter section.

10-5.5 Acoustic/Electronic Interference Between Meters

If meters are too close together they may interfere acoustically. However, this seldom happens in practice because the high frequencies used are attenuated rapidly. However, there can be electrical interference between meters with cables in close proximity such as when they run long distances in conduit or in a cable tray. These problems can usually be overcome with proper system and software design.

10-6 ERROR SOURCES AND THEIR REDUCTION

The purpose of this paragraph is to describe possible error sources for the types of ultrasonic flow meters covered by this Section. Although these errors may not be significant in some cases, they should all be addressed in detail when analyzing the uncertainties for a particular flow meter; ASME PTC 19.1 shall be used to estimate the overall uncertainty of the overall flow measurement process. ASME PTC 18 also contains standards for flow measurement in large pipes as well as error estimation methods.

10-6.1 Axial Velocity Estimate

Axial velocity errors are uncertainties in the determination of V_{ax} along an acoustic path. See Eqs. (10-3.5) and (10-3.6).

10-6.1.1 Acoustic Path Length and Angle. The determination of axial flow velocity V_{ax} is based on the acoustic path length l_o and angle θ. The error in V_{ax} is in direct proportion to the uncertainty in the acoustic path length and angle. Acoustic path length and angle errors are usually constant biases because of inaccuracies in the initial measurements or they may vary because of dimensional changes in the measurement section. In the case of refractive systems, changes in the index of refraction of the materials in the acoustic path, for example, by temperature variations can cause changes in the path length and angle (see Fig. 10-3.1.2).

Errors in the acoustic path length or angle for nonrefractive systems can be reduced by accurate geometric and acoustic measurements. For flow meters in which sound energy undergoes refraction, errors in acoustic path length or angle can be reduced by design and/or compensation based on knowledge of the speed of sound in the liquid and intervening materials between the transducer element and the flowing liquid.

In certain applications, changes in acoustic path length and angle that result from temperature- or pressure-induced pipe deformation may be compensated for in both the refractive or nonrefractive systems.

Systems where the transducers are field-mounted can achieve accuracies comparable to systems where the transducers are factory-mounted if the pipe centerline can be accurately determined, precise postinstallation measurements of path angles and lengths are made, and the electronics are adjusted to reflect these field-assembled dimensions.

Transducer protrusion into the pipeline can cause two types of errors. The protruding transducer may not measure a true average velocity all the way along the path because the flow between the transducer and pipe wall will be missed. Because this is usually the lowest velocity in the pipe, the effect of not including this in the line velocity average will be to overestimate this average. On the other hand, the flow streamlines in the vicinity of the transducer tend to increase the angle between the local velocity vector and the transducer, on both upstream and downstream transducers, causing the path velocity estimate to be low. There is also a wake downstream of the upstream transducer. Fortunately, these two effects are in the opposite direction and are not usually important in pipes larger than about 4 ft in diameter. For smaller size pipes, where relatively large transducers are used or where accuracy requirements are very high, it may be necessary to determine the effect of transducer protrusion experimentally or use a nonprotruding transducer design as shown in Fig. 10-3.1.2.

An important advantage in using crossed paths, particularly in field-installed systems, is where it is difficult to accurately determine the location of the centerline of the pipe to the required degree of accuracy. An example of this would be where the pipe is out-of-round or tapered. It is relatively simple to accurately determine the angle between the crossed paths, even when there is a relatively large uncertainty in the orientation of the acoustic paths relative to the true centerline of the pipe. Thus, errors in V_{ax} caused by the unknown path angles cancel because the angle between the paths is accurately known (see Fig. 10-4).

10-6.1.2 Transit Time. Uncertainties in the transit time measurements result from limits in the internal timing accuracy and resolution and lead to a corresponding uncertainty in V_{ax}. Errors in the measurement

of transit time may be reduced by the use of stable and accurate high-frequency oscillators and by averaging many individual transit time measurements. Transit time measurement errors are the easiest to analyze.

Transit time measurement errors from differences between upstream-to-downstream and downstream-to-upstream electronic signal paths may be reduced by using the same detection electronics and transmitter for both.

10-6.1.2.1 Signal Detection. Acoustic transit time measurements may be affected by inconsistencies in recognition of the received acoustic signal caused by variations in received signal level or waveform and noise.

(a) Variations in received signal level or waveform can occur as the acoustic properties of the liquid in the measurement section change because of excessive amounts of entrained air, suspended solids, temperature, or pressure or as transducer fouling occurs. These variations may result in uncertainty in determining the transit time, thus causing uncertainty in V_{ax}. The receiving circuits should be designed so as to prevent use of these distorted signals for the flow rate measurement.

(b) Noise can affect the accuracy of the transit time measurement. Noise sources may be either electrical or acoustic and either external or self-generated. Generally, externally generated electronic or acoustic noise is random with respect to the received signal. Self-generated acoustic noise, however, is usually synchronized with the received signal and is, therefore, much harder to compensate for in the secondary device.

Signal detection errors are reduced by operating with high signal-to-noise ratios. Methods can be provided that will reject excessively attenuated signals or those that are distorted by noise.

If the background noise is caused by external sources, the signal-to-noise ratio can be improved by increasing the transmitted signal level. However, in many cases the most troublesome noise is self-generated acoustic noise, particularly in refractive systems. This noise comes from energy being coupled directly into the pipe wall and then to the opposite transducer. This noise generally increases as the level of the transmitted signal increases. The signal-to-noise ratio, in these cases, may be improved by acoustically isolating the transducers from the measurement section by application of damping materials.

10-6.1.3 Sound Speed Dependency. The speed of sound in the liquid and in any intervening materials along the acoustic path varies with composition, temperature, and pressure. Depending on a particular ultrasonic flow meter's design, l_o, η, and t_o (f_o) [Eq. (10-3.6)] may be affected.

In nearly all cases, the errors caused by sound speed variations in the liquid are negligible for a properly implemented, nonrefractive, wetted transducer system.

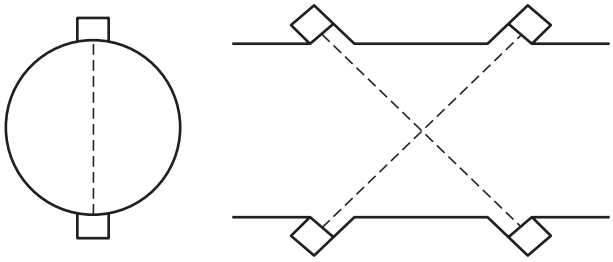

Fig. 10-6.1.4 A Typical Crossed-Path Ultrasonic Flow Meter Configuration

Changes in the speed of sound in the intervening material may, however, require compensation for nonwetted transducer systems.

In refractive systems, changes in the speed of sound in intervening materials and the liquid affect the acoustic path length and angle. It is possible to compensate for these effects. In rare cases, changes in the speed of sound in the liquid may refract the beam so much that it misses the opposite transducer. Accurate knowledge of the range of speed of sound in a particular liquid can prevent this possibility.

10-6.1.4 Secondary Flow. Secondary flow can produce an error in the determination of V_{ax} since it is normally assumed in the calculations that all flow is in the axial direction. Secondary flow is a result of flow perturbations occurring upstream or downstream of the measurement section from devices such as elbows, valves, and pumps. Secondary flow may result in an error in determining the transit time, which ultimately affects the calculation of V_{ax}.

The most effective way to reduce secondary flow errors is to avoid installations where severe secondary flow exists or to use additional, suitably placed acoustic paths. Reduction of secondary flow may require long, straight runs of pipe, depending on the nature of the secondary flow source and the accuracy required. (See para. 10-9 on installation effects for general guidelines.) Secondary flow errors can also be reduced by the use of an appropriate acoustic path orientation or by computing line velocities on multiple crossed chordal acoustic paths, as shown in Fig. 10-6.1.4, and averaging the resultant measured velocities.

10-6.2 Integration

Integration error is the error in the flow measurement that occurs in the computation of the flow from V_{ax}, A, S, and W_i.

10-6.2.1 Cross-Section Dimensional Errors. Error in the assumed cross-sectional area of the measurement section causes an error in the flow. This error may be from irregular shape, such as out-of-roundness, or it may be because of changes in the initial shape caused

by temperature, pressure, structural loading, or the formation of deposits or growths, such as algae, in the measurement section. Usually it is caused by combinations of the preceding conditions.

Cross-section dimensional errors can be reduced by manufacturing or choosing a measurement section that has constant dimensions along its length and can be measured accurately. Measurement section dimensional stability is important, because changes resulting from corrosion, material buildup, or loss of protective coatings will affect meter accuracy and may require recalibration. Furthermore, it is important that the pipeline not be distorted by mechanical stress, for example, if the pipeline was buried after dry calibration. Also, if temperatures or pressures are expected to be substantially different from reference conditions, it may be necessary to adjust the measured dimensions to compensate for dimensional changes that occur under operating conditions.

In circular pipes, dimensional errors can be reduced by minimizing the effects of out-of-roundness through averaging of radius (not diameter) measurements made at the upstream, middle, and downstream ends of the measurement section. To understand the importance of using radius measurement instead of diameter, consider a rounded, triangular-shaped pipe where all the diameters are equal. Clearly, the area derived by diameter measurement would be wrong.

The measurement section should be inspected periodically to determine if the dimensions have changed, and, if so, the meter factor should be adjusted appropriately. It is important to remember that the flow rate measured is linearly proportional to the cross-sectional area.

10-6.2.2 Acoustic Path Location. The acoustic path location is an important contributor to overall flow meter accuracy. The uncertainty in the position of the acoustic path can cause errors through improper assignment of a weighting factor W_i and by causing unnecessary sensitivity of V_{ax} to the velocity profile through nonoptimum placement of transducers.

Errors in acoustic path location can be reduced by suitable manufacturing techniques (in the case of a prefabricated measurement section) or by accurately determining the acoustic path for systems in which the transducers are assembled in the field. Path locations can be determined in a variety of ways; probably the most accurate one uses optical determination of both the acoustic path and angle within the measurement section.

10-6.2.3 Velocity Profile. An excellent and detailed discussion of turbulent flow profiles and the effects of upstream conditions on average velocity profiles has been published [1, Part C].

Ultrasonic flow meters are affected by variations in flow profile because uncertainty in the velocity profile causes an error in V_{ax} that may not be compensated for by the velocity profile correction factor S. This error may affect both the linearity and the value of the flow measurement. Velocity profile variations can be caused by changes in flow rate (both transient and steady state), wall roughness, temperature viscosity and viscosity change due to temperature, upstream or downstream hydraulic conditions, transducer projections, and transducer cavities. With sufficiently long, straight upstream piping and the absence of upstream and downstream hydraulic effects, the Reynolds number and friction factor of the measurement section and upstream piping would be sufficient to determine the velocity profile correction factor S. This is seldom the case for large diameter pipes.

There usually is a difference between the actual velocity profile and that assumed in the flow meter's computations. Since most flow meter computations assume a fully developed velocity profile, errors can be reduced by placing the measurement section as far as possible from bends, valves, tees, transitions, and so on (see Section 7). These errors can be reduced also by using a more accurate model of the actual velocity profile or, in general, by increasing the number of acoustic paths so that the meter can more accurately measure the flow even when the profile is unknown. Even when the meter section is located 50 or more diameters from an upstream obstruction, there will almost always be a swirl or spiral component to the flow. Therefore, to minimize errors produced by any swirl, the path placement should be symmetrical to the centerline.

10-6.3 Computation

There is a small error associated with the computations made by the electronic circuits because of the finite limits in processing accuracies. However, this error will normally be negligible. Computation errors due to electronic malfunction can be reduced by using built-in, self-checking features in the processor.

10-6.4 Calibration

Wet calibration is a primary means for reducing errors resulting from uncertainties in path length and angle, cross-section, and path location. Unfortunately, it is seldom possible or economically feasible to accurately calibrate large pipelines' flow meters in this manner. Velocity profile errors can be corrected with in situ calibration or by properly simulated laboratory calibrations.

There remains an uncertainty in the flow measurement that results from errors in the calibration procedure of ultrasonic flow meters. To reduce calibration uncertainty, calibration should be conducted according to national (ANSI) or international (ISO) standards.

10-6.5 Equipment Degradation

Performance errors may arise from fouling or physical degradation of the equipment. Equipment design should accommodate changes in component values and

process conditions. The equipment should indicate when degradation of flow meter performance occurs. The probability of error can be reduced considerably by including suitable self-test or diagnostic circuits in the equipment.

10-7 EXAMPLES OF LARGE (10–20 ft) PIPE FIELD CALIBRATIONS AND ACCURACIES ACHIEVED

Very few field calibrations of large acoustic flow meters have been published. Generally, field calibrations are extremely difficult and expensive and depend on other methods that, while code accepted, have uncertainty bands that are equal to or greater than the potential accuracy of the acoustic flow meter. The most recent and exhaustive tests were conducted by the Electrical Power Research Institute [2] and consisted of flow measurement intercomparisons at three different sites. These were a 22-ft diameter turbine penstock at Kootenay Canal in British Columbia, Canada, a 12-ft diameter penstock from a pump-generator at Grand Coulee Dam, Grand Coulee, Washington, USA, and a 10-ft diameter pump generator at TVA's Raccoon Mountain Pumping Generating Plant near Chattanooga, Tennessee, USA. The conditions were least favorable for high accuracy while pumping at the TVA site as the flow meter was installed directly at the spiral case outlet, did not have crossed paths, and was not oriented optimally with respect to the spiral case bend.

According to the Summary Report on page S-3-4, "It is concluded that the results from the acoustic methods as implemented by Westinghouse and Ferranti O.R.E. are as valid as the results from any of the code-approved methods. The random uncertainties (precision) of the acoustic methods were superior to any of the code methods. The systematic uncertainty (bias) of the acoustic method is probably between ±1% and ±2% and, in favorable installations, it may even be better."

It should be noted that the first series of tests was carried out under the most favorable conditions, and the results were, in the authors' opinion, closer to ±0.5% based on Tables 3-8 to 3-10.

10-7.1 Examples of Laboratory Calibrations of 2-ft Diameter Pipes

Numerous single- and multiple-path acoustic flow meter calibrations have been carried out in many different laboratories. Published data are mostly limited to manufacturer's data sheets.

10-7.1.1 A 24-in., four-path, recessed transducer straight-pipe calibration at Alden Research Laboratory used a weigh tank as the transfer standard. The spool piece was dry calibrated prior to testing. The accuracy obtained was better than ±0.5% over a 4-44 CFS range [3].

10-7.1.2 A 24-in., eight-path (two four-path planes) wet calibrated to remove the effect of protruding transducers was tested with short-radius, 90-deg elbow at 0, 2, and 4 diameters upstream of the meter spool piece. The results of this test are too complex to describe in detail here; in summary, if crossed planes are used, then 2–4 diameters are sufficient to separate an eight-path flow meter from the extreme disturbance caused by the upstream elbow, regardless of orientation, with an error of less than 0.5% with respect to the wet-calibrated, straight-pipe accuracy, over a 4–44 CFS range. To estimate overall dry-calibrated accuracy, therefore, the additional dry calibration uncertainty of typically 0.5% must be added to this, for a total accuracy of ±1% under these relatively unfavorable conditions [4].

10-8 APPLICATION GUIDELINES (SEE ALSO ASME PTC 19.1, TEST UNCERTAINTY)

By evaluating the performance parameters listed below, a user should be better able to predict the performance of a given ultrasonic flow meter in a specific application. These parameters are limited to those that can be substantiated by test or well-established computational methods. (It should be emphasized that the following performance parameters are determined by the manufacturer under specific reference conditions that will, in general, differ from the user's actual conditions.) Subjective or nonperformance parameters, such as convenience of installation, reliability, and cost, are left to the user for evaluation. In each case below, the range and conditions applicable to each parameter should be specified.

10-8.1 Accuracy

Accuracy describes the uncertainty of a measured value compared to its true value and is commonly reported as a percentage of actual flow, span, or full scale. The preferred method is to specify the maximum deviation (percentage) between measured flow and actual flow.

10-8.2 Linearity

The data obtained by test of any instrument consists of points scattered around a smooth curve that represents the nominal characteristic of the instrument. Linearity is the maximum deviation, at any flow rate, of that smooth curve from a least-squares linear fit to the data and should be reported as a percentage of that flow rate.

10-8.3 Repeatability

Repeatability is the ability of a flow meter to return to a previously indicated flow rate after a deviation in either direction and return to the flow conditions that caused that indicated flow rate. It also includes readout variations under constant flow conditions. Repeatability

should be reported as the maximum expected deviation between these indicated flow rates and expressed as a percentage of the flow rate indication.

10-8.4 Stability

Stability, also called drift, is a measure of change in accuracy with time. It should be reported as the maximum deviation in accuracy, as a percentage of actual flow, which can be expected to occur over a specified period (subject to constant hydraulic conditions).

10-8.5 Resolution

Resolution is the minimum change in actual flow required to produce an observable change in the output of the equipment.

10-8.6 Rangeability

Rangeability is the maximum and minimum flow over which the performance is specified.

10-8.7 Response Time

Response time is the time it takes, following a step change in the flow rate, for the flow meter's output to indicate a change in flow rate equal to 63% of the step change.

10-8.8 Power Requirements

The power requirements of the flow meter, including voltage and frequency tolerances necessary for proper performance, and the flow meter's power consumption should be clearly specified.

10-9 INSTALLATION CONSIDERATIONS

Many of the error sources listed in Section 3 can be reduced or eliminated by proper installation. Sources of error and installation problems the user should address during the design phase of a project are listed below.

10-9.1 Acoustic Path Length and Angle

Changes in acoustic path length and angle can be caused by significant temperature or pressure changes and external loading of the meter section. The installation location should be chosen to minimize these effects.

10-9.2 Signal Detection

Suspended solids, fouling, entrained air, or cavitation (caused by upstream equipment or even the meter itself) may degrade accuracy or prevent operation by attenuating the acoustic signal. It should be noted that, while excessive amounts of entrained air or sediment will not affect the accuracy of a well-designed acoustic flow meter, it will prevent operation. There are several tradeoffs to be considered when operation is required under these conditions. In particular, it may be possible to operate at a lower acoustic frequency, which is less susceptible to attenuation from entrained air and sediment. Also, it may be possible to locate the meter away from the source of entrained air, such as at a spillway or pump outlet. Alternatively, the meter could be mounted at a location with higher pressure; or, a smaller diameter section or larger path angle could be used to reduce path lengths and, hence, total acoustic attenuation.

Electrical interference and acoustic noise caused by mechanical vibration or cavitation can also interfere with the meter's operation.

10-9.3 Multiple Fluids

Metering fluids with widely differing acoustic properties may require multiple primary devices (spool pieces) due to excessive acoustic beam angular variations in refractive systems and/or excessive signal loss due to acoustic mismatch or attenuation. Under these conditions, the manufacturer should be consulted.

10-9.4 Secondary Flow and Distorted Velocity Profiles

Secondary flow directly affects a meter's performance and should be considered in the design of the installation and in the selection and orientation of a meter. Generally, the meter should be placed as far as possible from upstream elbows, transitions, valves, and such. When there is an unavoidable bend upstream of the meter, the acoustic paths, when viewed in cross-section, should be oriented perpendicular to the plane of the bend. Where accuracy is critical, crossed paths should be used. It should be remembered that there is almost always a swirl or spiral component to the flow, even after passing the fluid through a flow straightener. Therefore, it is important that a symmetrical path configuration be chosen to avoid errors from the source.

10-9.5 Integration

Flow profile changes and dimensional changes in the measurement section, including those caused by corrosion, erosion, or material buildup, directly affect meter performance and should be considered in the selection, location, and orientation of a meter.

The measurement section should be inspected periodically to determine if the cross-section area or profile correction factors should be adjusted to compensate for observed changes.

10-10 METER FACTOR DETERMINATION AND VERIFICATION

10-10.1 Calibration

Installation considerations and the required installed accuracy usually determine the methods of calibration.

There are three principal methods of meter factor determination:

(a) laboratory calibration
(b) field calibration
(c) analytical procedures (dry calibration)

The first two can be used to verify meter performance.

10-10.1.1 Laboratory Calibration. Laboratory calibrations should be conducted at facilities where the procedures are in accordance with national or international standards.

The calibration tests should generally be run using water that is free from entrained air or solid particles. Calibrations tests should be conducted using flows that are as free as possible from nonaxisymmetric flow and pulsation. Most often these conditions have been achieved by using sufficient lengths of straight pipe upstream and downstream of the measurement section and, if necessary, by installing upstream flow conditioners.

If the laboratory calibration is designed to model the field application, one of the advantages of multiple-path acoustic flow meters is that they can measure the actual velocity profile (to the extent possible with the number of paths installed). This can increase the confidence in the expected field accuracy by comparison of the velocity profiles achieved in the field with the laboratory data.

The extent to which the above conditions have been achieved can be determined by noting the sensitivity of the meter factor to rotation and translation of the primary device.

A statistically significant number of 30–100-sec runs (usually 10–20) should be made over a range of flows. Flow meter accuracy, within the uncertainty of the laboratory standards, should be determined by the combined random and systematic errors in the measurement of the volumetric flow following the methods of ASME PTC 19.1.

Special calibration tests may also be performed for those cases where piping in the final installation may produce an asymmetric flow or where other flow irregularities are suspected. These will require appropriate modeling of upstream and downstream piping.

10-10.1.2 Field Calibration. Field calibration, as opposed to laboratory calibration, has the advantage that true operating conditions are encountered. The major disadvantage may be a greater degree of uncertainty in the accuracy of the standards that are employed. In some cases, these secondary methods may be considerably less accurate than the ultrasonic flow meter being calibrated.

10-10.1.3 Analytical Procedures (Dry Calibration). Analytical procedures are often the only available techniques for meter factor S determination. This is particularly true for field installations in large line sizes. These procedures require physical measurements as well as instructions and data supplied by the manufacturer. These measurements and their contributions to the overall flow meter accuracy are discussed in para. 10-6. The uncertainty in the meter performance should reflect uncertainties associated with these procedures.

10-11 SOURCES OF FLUID AND MATERIAL DATA

[1] Schlichting, H. *Boundary Layer Theory: Part C,* 6th edition. New York: McGraw-Hill; 1968.

[2] Electrical Power Research Institute, Acoustic Flow Measurement Evaluation Project. Summary Report EPRI AP-5341, August, 1987.

[3] Alden Research Laboratory, Calibration of One 24-in. Acoustic Flowmeter, ARL No 149-82/c297, October 1982.

[4] Alden Research Laboratory, Calibration of One 24-in. Acoustic Flowmeter, ARL No 56-75-C297, July 1974, March 1975.

Section 11
Electromagnetic Flow Meters

11-1 INTRODUCTION

Electromagnetic flow meters have been used in many applications primarily because they do not obstruct the flow stream. They measure flow volumetrically, provided the fluid has an electrical conductivity above a threshold value. As a result of this restriction, their use has been limited almost exclusively to liquids.

11-1.1 Physical Principles

The operation of magnetic flow meters is analogous to the operation of an electric generator. Both follow the Faraday Law of Induction, which states that a voltage will be induced in a conductor moving through a magnetic field. In a generator, the conductor is the copper wire in the rotor; in a magnetic flow meter, the conductor is the fluid. In the generator, the induced voltage appears at the brushes; in the magnetic flow meter, the induced voltage appears at the electrodes.

The governing equation for the magnetic flow meter (see Fig. 11-1.1-1) has the following form:

$$e(t) = B(t)Lv \tag{11-1.1}$$

where

B = flux density, T (Telsa)
L = characteristic dimension, m
e = electrode voltage, V
(t) = function of time
v = average fluid velocity, m/s

The volumetric flow rate is related to the average velocity by

$$q = vA \tag{11-1.2}$$

where

A = flow area, m^2
q = flow rate, m^3/s

Combining Eqs. (11-1.1) and (11-1.2) results in

$$e(t) = \frac{B(t)Lq}{A} \tag{11-1.3}$$

Since the dimensions L and A in any one flow meter are constant, the electrode voltage is a linear function of both the flow rate and the flux density. [Various methods are used to eliminate the dependence of the electrode signal on the flux density. Equation (11-1.3) completely describes the flow measurement.]

The signal-generating mechanism within the magnetic flow meter consists of a continuum of individual generators throughout the measuring volume. The amplitude of each infinitesimally induced voltage is a function of the local fluid velocity, the local flux density, and their vector directions.

The ratio of the amplitudes of the induced local voltage to the output electrode voltage is a variable that is a function of the location of the generator and the geometry of the magnetic flow meter. This ratio is commonly known as the weighting function (see Fig. 11-1.1-2).

The total electrode voltage is the sum of all the voltages generated within the measuring volume because the laws of superposition apply. The electrode voltage is the integral of all the signals generated within the measuring volume, although the contributions of the two variables (velocity and flux density) will vary as a function of their distributions.

11-2 METER CONSTRUCTION

Electromatic flow meters consist of a primary device (the metering section) and a secondary device (the signal-processing system). The sizes of primary devices range from 0.008 in. to 96 in. (2 mm to 2,400 mm) in diameter. Metal or plastic housings enclose the primary and secondary devices for mechanical and environmental protection.

11-2.1 Primary Device

The primary device of a magnetic flow meter is mounted in the pipe. It consists of a nonmagnetic, nonconductive section of conduit, a pair of electrodes, and a flux generator. The metering section may be made of a nonconductive material, such as plastic, ceramic, or glass, or it may be of a nonmagnetic metallic conduit lined with an electrical insulating material inert to the fluid.

The electrodes are mounted diametrically. They may either contact the fluid or be mounted behind the liner, in which case the electrode voltage is measured capacitatively.

The magnet structure produces lines of flux that pass through the meter tube nearly perpendicular to both the tube axis and the electrode diameter. This magnetic flux field may be AC, pulsed DC, or DC, depending on the application.

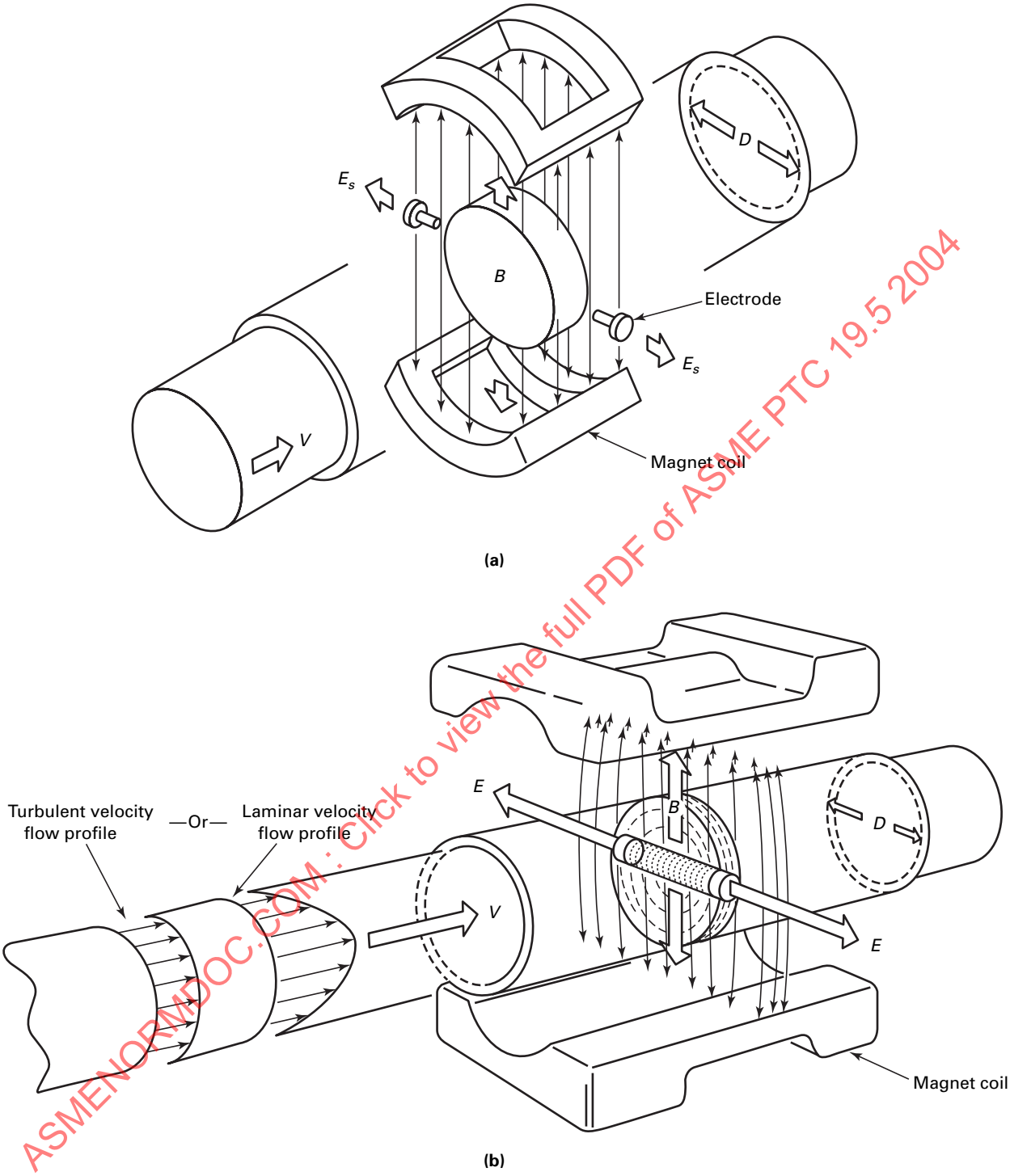

Fig. 11-1.1-1 Magnetic Flow Meter

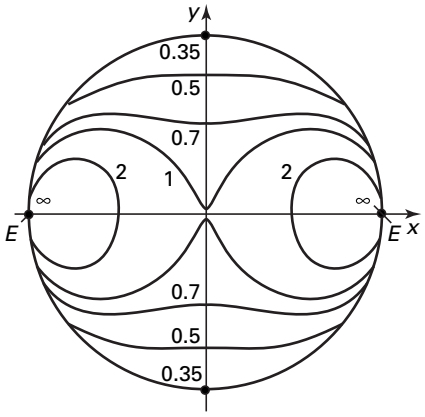

(a) Lines of Constant Weighting Function in the Plane of the Electrodes Based on the Value in the Center

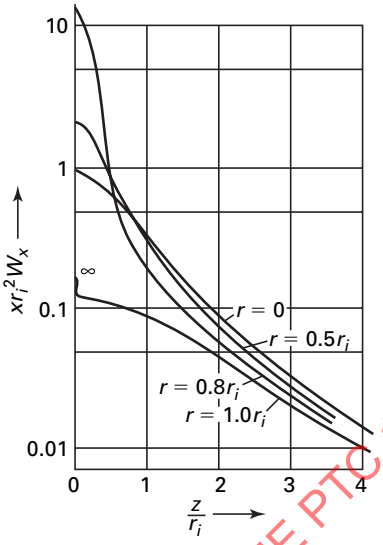

(b) Axial Relationship of the Weighting Function at Various Radii on the Electrode Axis

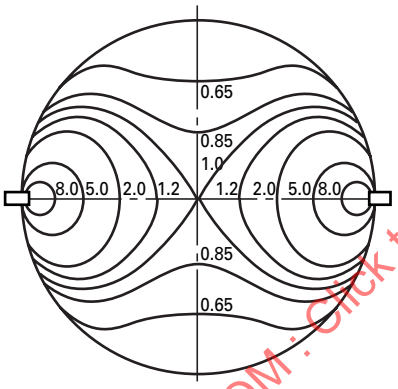

(1) Taken at Electrode Plane

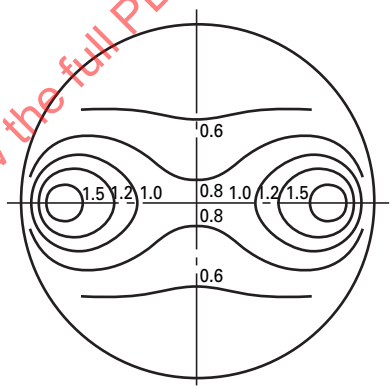

(2) Taken at 0.2 Diameters From the Electrode Plane

(c) Signal Generating Coefficients

Fig. 11-1.1-2 Weighting Function of the Magnetic Flow Meter

A reference signal proportional to the flux should be generated as necessary with varying flux amplitude. This reference signal may be obtained from the voltage induced in a coil located in the magnetic field from the amplitude of the magnet excitation current or from the magnet supply voltage.

11-2.1.1 Magnetic Drive System. The types of magnet drive systems commonly used for industrial magnetic flow meters are AC and pulsed DC (see Fig. 11-2.1.1). The AC systems produce a sinusoidal magnetic field. Although a range of frequencies (2 Hz to 250 Hz) can be used, 60 Hz is most common.

A variety of pulsed DC schemes are used. There are systems in which the magnet excitation current may be one polarity for part of the cycle and zero for the rest of the cycle; the current may be one polarity for part of the cycle and reversed polarity for the rest of the cycle; or the current may be a combination of both.

The flux amplitude follows various wave shapes such as rectangular, trapezoidal, or free-rising. In most systems, a constant DC flux is achieved during some portion of the cycle and it is during this period that the electrode voltage is sampled.

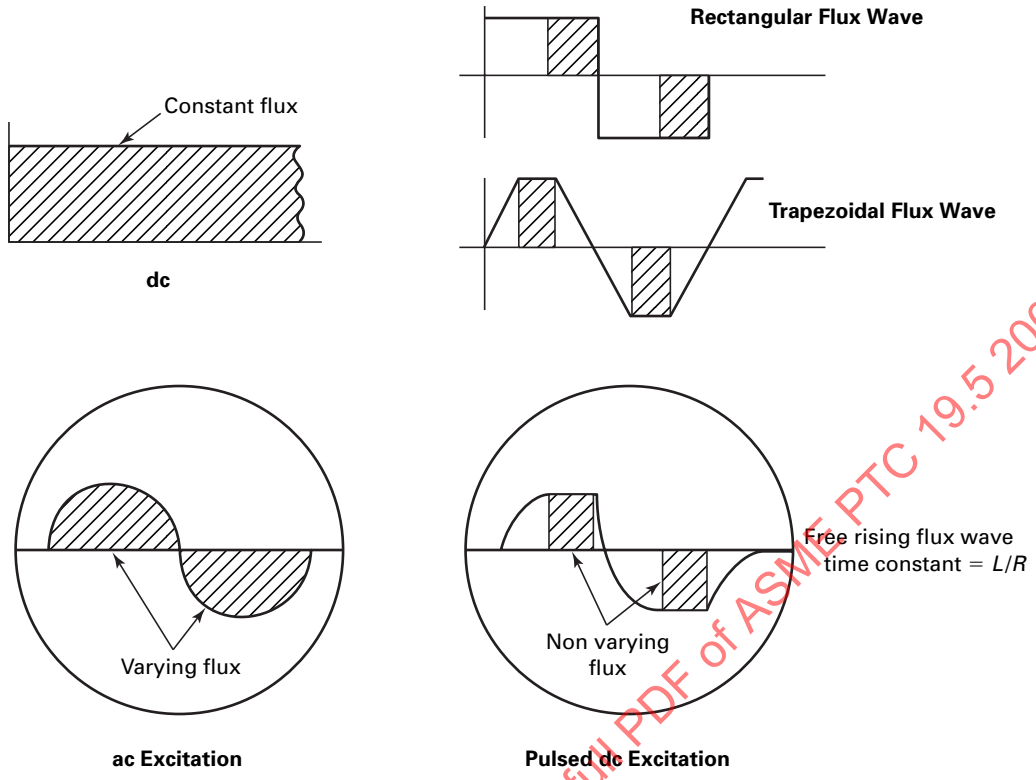

Fig. 11-2.1.1 AC and Pulsed DC Excitation Voltages

The electrode voltage is ignored when the flux is varying. The pulsed DC system operates at 2 Hz to 30 Hz. The pulsed DC systems were developed to eliminate the voltages induced by the time-varying flux unrelated to the flow.

For specialized applications, such as blood flow and liquid metals, constant DC magnet drive systems have been used.

11-2.2 Secondary Device

The secondary device includes the electronic circuitry required to convert the electrode voltage (typically between 0.01 mV and 10 mV) into a usable output signal. It may include a reference signal and the magnet control circuitry.

The secondary device may be remote from the primary device. The maximum flow setting of the secondary device can be adjusted over a range of 1 ft/sec to 30 ft/sec (0.3 m/s to 10 m/s) equivalent velocity, either manually or automatically. The turn-down ratio at any maximum setting is between ten and twenty to one. Some devices measure flow in either direction automatically.

The reference signal, which is proportional to the flux density, may be used to compensate for variations in flux density. This is accomplished by generating an output signal in the secondary device, which is a function of the ratio of the electrode voltage to the reference signal. This eliminates the flux B term in Eq. (11-1.3).

The reference signal may be derived from a coil located in the magnetic field whose output is a function of the flux density. This relation may be a direct one or an indirect one by way of a measurement of the current or voltage to the magnet coils to which the flux density is proportional.

The secondary device is designed to be compatible with an individual manufacturer's primary device and, therefore, cannot generally be used with another manufacturer's primary device. Within a particular primary mode group, secondary devices are usually interchangeable.

11-3 CALIBRATION

The calibration factors for magnetic flow meters are generally determined by a flow calibration (see Fig. 11-3), because it is time-consuming and costly to make the accurate measurements required to calculate the calibration factor. As noted in para. 11-1.1, the electrode voltage is the integral of all signals generated within the measured region. The calculation factor requires knowledge or measurements of the flux distribution, weighting function, dimensions, and flow velocity profile throughout the measuring section.

Magnetic flow meters are available (depending on manufacturer and design) with accuracy specifications, at reference conditions, between 0.5% and 2% of value.

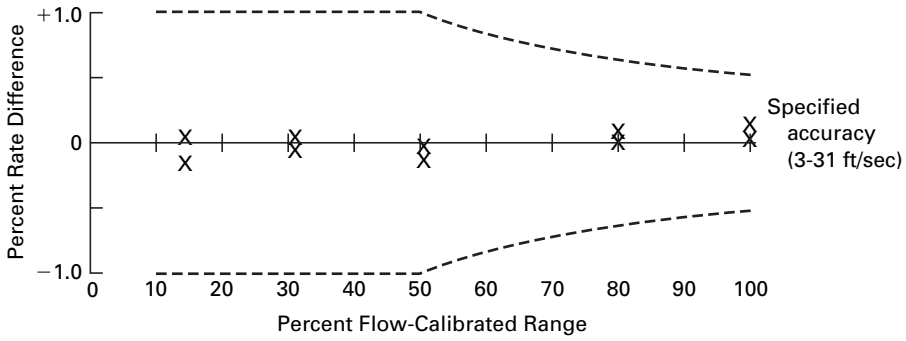

Calibration Test Report for Magnetic Flow Meter

Company Name:	XXXXX
Serial No.:	XXXXX
Model No.:	XXXXX
Date:	XXXXX
Maximum Flow:	500 GPM (U.S.)
Meter Factor:	4.197
Range Setting:	11.596 ft/sec for maximum flow

Test Data

Run No.	Actual GPM (U.S.)	Indicated GPM (U.S.)	Diff. % Rate
01	571.600	571.722	+0.021
02	571.600	572.288	+0.120
03	459.518	459.826	+0.067
04	459.803	459.842	+0.008
05	291.821	291.464	−0.122
06	291.649	291.577	−0.025
07	180.381	180.483	+0.056
08	180.282	180.215	−0.037
09	83.708	83.592	−0.139
10	83.648	83.696	+0.057

Fig. 11-3 Typical Flow Calibration Data

Accuracy is usually worse for flow velocities below 0.3 ft/sec (0.1 m/s).

The calibration factor of the magnetic flow meter relates to the secondary device output to flow. The calibration factor may be presented in several ways.

(a) Diameter is used when the output is expressed in terms of velocity units.

(b) Ratio of flow to velocity is used when the output is expressed in terms of velocity units.

(c) Ratio of flow-to-signal amplitude is used when the output is expressed in terms of electrode voltage units.

11-3.1 Field Calibration

In-place calibration of an installed meter system is preferred because all installation effects are included. This is impossible unless a certified standard method of measuring flow is used in series as a calibration transfer standard.

11-3.2 Model Testing

It is necessary that accuracy be determined by laboratory calibration of the magnetic meter system, including the piping and other requirements stated in para. 11-4.3.

11-3.3 Secondary Device Calibration

Verification of the secondary device performance is possible by using a secondary device calibrator. The calibrator provides precise signals instead of the primary device outputs and electrode and reference voltages, as required. These will check the signal conversions and control functions of the secondary device to an uncertainty better than one-fifth of the flow measurement

accuracy. The calibrator must be compatible with the secondary device.

11-4 APPLICATION CONSIDERATIONS

It is essential that the flow meter user clearly defines and describes the fluid and ambient conditions of the application so that a suitable meter can be selected.

11-4.1 Materials of Construction

Two major areas that must be considered when selecting the materials to be used in the design and construction of the flow meter are fluid properties and environmental conditions.

(a) Typical fluid properties are
- *(1)* corrosiveness
- *(2)* maximum line pressure
- *(3)* maximum fluid temperature
- *(4)* abrasiveness

(b) Typical environmental conditions are
- *(1)* temperature range
- *(2)* water pressure due to hosedown or submergence
- *(3)* hazardous atmospheres

Magnetic flow meters are available in many designs and are constructed from a variety of materials for applications over a wide range of conditions.

11-4.1.1 Corrosive Fluids. For very corrosive applications, the inner surface of the primary device may be made of a fluorocarbon, vitreous enamel, or ceramic. Electrodes are available in a wide variety of corrosion-resistant metals, including platinum.

11-4.1.2 Pressure. Standard designs up to ANSI class 300 are available, and special designs have been used at a much higher pressure.

11-4.1.3 Temperature. Designs are available for fluid temperatures as high as 392°F (200°C). The lower temperature limit is the freezing point of the fluid. Maximum ambient temperatures are usually limited to 150°F (65°C). Higher ambient temperatures can be accommodated by mounting the secondary device in a lower temperature region. The primary device is usually tolerant of ambient temperatures up to 250°F (120°C).

11-4.1.4 Slurries or Abrasive Fluids. For abrasive fluids, the primary device can be made of neoprene, polyurethane, or hard ceramic.

11-4.1.5 Adverse Ambients. Enclosures for both the primary and secondary devices are available in accordance with NEMA 4 (IEC Type IP66) requirements. Special designs are available for installations subjected to continuous submergence down to 30 ft (10 m). The standard designs are usually suitable for use in general purpose areas or in areas classified nonincentive Class I, Division 2, Groups B, C, and D. Special designs are available for use in areas classified Class I, Division 1, Group D.

11-4.2 Fluid Properties Affecting Meter Performance

11-4.2.1 Conductivity. The magnetic flow meter output is insensitive to the fluid conductivity provided that the conductivity is above a threshold value for that meter. The threshold value for generally available meters ranges from 5 μS/cm to 20 μS/cm (μmho/cm). Special systems are available that extend the lower limit to 0.1 μS/cm (μmho/cm). Low conductivity increases the source impedance within the fluid. The impedance is inversely proportional to fluid conductivity and proportional to electrode diameter. Together with any cable impedance, the fluid impedance can become appreciable relative to the secondary device input impedance and cause and error.

11-4.2.2 Density. The magnetic flow meter measures the volumetric flow [Eq. (11-1.3)]. Therefore, variations in density do not change the flow measurement.

11-4.2.3 Fluid Temperature and Pressure. The effects on accuracy of temperature and pressure are a result of area changes due to thermal expansion or pressure forces. The errors are usually negligible because the meters are designed to minimize dimensional changes.

11-4.2.4 Viscosity. The magnetic flow meter has been shown to be essentially independent of Reynolds number. Therefore, changes in viscosity will have a negligible effect on meter output.

11-4.2.5 Mixtures and Slurries. The weighting function discussed in para. 11-1.1 will change if the fluid has a nonhomogeneous conductivity. This will result in errors that are not only a function of the amount of nonhomogeneity but also a function of the nonhomogeneity's unpredictable distribution within the meter. Homogeneous mixtures of materials will not change the output of the secondary device so long as the conductivity of the mixture exceeds the threshold value. The mixture can consist of a nonconductive material in a conductive carrier (air in water, solid in liquid, liquid in liquid).

11-4.2.6 Fluid Coatings and Deposits. Coatings on the inside of the meter tube influence the meter performance in two ways. In the first case, the conductivity of the coating is above the threshold value and the output will be affected by the ratio of the conductivity of the coating to the conductivity of the fluid. This is, in effect, a special case of the inhomogeneous solid-in-liquid condition discussed in the preceding paragraph. If the conductivity of the coating is the same as the conductivity of the fluid, the change of output is negligible.

In the second case, the conductivity of the coating is below the threshold value and the source impedance is increased, thereby decreasing the signal. In the worst

case, the electrodes become totally insulated and the signal goes to zero. Capacitatively coupled electrodes are affected less by low conductivity coatings than are contacting electrodes.

11-4.3 Installation Effects

The manufacturer's instructions should be followed carefully when installing a magnetic flow meter. The following are the more important conditions that must be considered.

11-4.3.1 Electrical Grounding. It is usually required that the fluid on both sides of the meter be at ground potential. This is necessary to prevent large common mode voltages at the electrodes that could affect the output from the secondary device.

11-4.3.2 Full Pipe. The meter should be installed so that no air or gas bubble is trapped in the meter. Such a bubble would cause a change in the weighting function and result in an error. For vertical installations, upward flow will ensure a full pipe condition at all times. For horizontal installations, the electrode axis should be horizontal to prevent insulation of one of the electrodes by an occasional air or gas bubble traveling along the top of the pipe.

11-4.3.3 Shutoff Valves. Tight shutoff valves should be installed on both sides of the meter if the requirement for zero flow adjustment exists. They should not disturb the flow when wide open. Generally, pulsed DC systems do not require periodic zero checking but sinusoidal AC systems do.

11-4.3.4 Piping Requirements. The piping is a function of specific meter design. The minimum upstream length of straight pipe is 5 to 10 diameters and the minimum downstream length is 2 to 3 diameters to an elbow, tee, or reducer. The effect of an upstream control valve, whose opening will vary, is considerably greater. The use of a control valve upstream of the flow meter should be avoided, and the minimum downstream lengths to the control valve should be 2 to 3 diameters.

11-4.3.5 Electrical Connections. The electrode voltage is very small, from a few microvolts to a few millivolts. It is essential that special cables be used to prevent spurious signals from being included in the measurement. The interconnecting cables should be run in conduit, rigid or flexible, isolated from high-current wires.

11-4.3.6 Electromagnetic Interference (EMI). The meter signal may be affected by electromagnetic radiation unless suitably protected. The effect of portable radio transmitters and other EMI generators in the vicinity of the meter should be checked for interference.

Accessories are available to protect the meter in the event that interference exists.

11-4.3.7 Piping Strains. The installation should be designed to prevent piping strains from being transmitted to the meter. Such strains could deform or damage the meter.

11-5 SOURCES OF FLUID AND MATERIAL DATA

[1] Shercliffe, J. A. *The Theory of Electromagnetic Flow Measurement.* Cambridge, UK: Cambridge University Press; 1962.

[2] Schommartz, G. *Induktive Stroemungsmessung*. Berlin: VEB Verlagtechnik; 1974.

[3] Bean, H. S., ed. *Fluid Meters: Their Theory and Application,* 6th edition. New York: The American Society of Mechanical Engineers; 1971.

[4] Kuromori, K.; Mannherz, E. *Method for Calculating the Effects of Pipe Wall Contamination on the Calibration of Magnetic Flowmeters with Various Electrode Configurations. Flow 81, Its Measurement and Control in Science and Industry,* volume 2. Research Triangle Park, NC: Instrument Society of America; 1981.

[5] Measurements of Conductive Fluid Flow Rate in Closed Conduits: Method Using Electromagnetic Flowmeters. Technical Report ISO/TR 6817, 1980.

Section 12
Tracer Methods Constant Rate Injection Method Using Nonradioactive Tracers

12-0 NOMENCLATURE

C = mass concentration
D = diameter of conduit
DF = dilution factor
L = length of measuring section
Q = volumetric flow
Re = Reynolds number
x = maximum percentage variation in concentration across the conduit
λ = coefficient of resistance of the conduit (friction factor)

12-1 INTRODUCTION

This Section covers the measurement of water flow in closed conduits using nonradioactive tracer dilution methods. These methods apply to flow measurement in conduits into which a solution can be injected and effective mixing of the solution with the water flowing in the conduit can be achieved prior to a downstream sampling point. Dilution methods can be used to measure large flows and where other methods are impractical. This Section gives general guidelines for using tracer methods and discusses in detail the constant rate injection method.

The dilution technique is an accurate way to measure water flow in a closed conduit. The technique is based on the measurement of a tracer concentration in a liquid sample. Advantages of the dilution technique include the following:

(a) It is independent of geometric or hydraulic quantities.

(b) The measurement equipment is portable and can be used where other methods are difficult or inappropriate.

(c) High accuracy reference procedure: measure equipment performance in situ.

(d) It can be used to measure large flows (billions of gallons per day).

12-2 CONSTANT RATE INJECTION METHOD

The constant rate injection method is based on the injection of a tracer at a known constant rate into a flow stream. A sample is taken downstream enough of the injection point to allow for complete mixing. The flow is then determined by measuring the downstream concentration of the sample.

The dilution method is based on the conservation of mass and the control volume shown in Fig. 12-2. The governing equation is

$$Q_1C_1 + Q_2C_0 = (Q + Q_1)C_2 \qquad (12\text{-}2.1)$$

Since C_1 is typically much greater than C_2, sometimes by a factor of 10^7, Eq. (12-2.1) becomes

$$Q = Q_1C_1/(C_2 - C_0) \qquad (12\text{-}2.2)$$

To use this technique, the following conditions must be satisfied:

(a) Sufficient mixing length must exist between the injection and sampling points.

(b) The tracer must be injected at a known constant and measured rate.

(c) The tracer must have homogeneous concentrations at both injection and sampling points.

(d) The native background of the tracer in the measurement stream should be negligible or taken into account.

(e) No tracer should be lost between injection and sampling points.

(f) The observed property of the tracer used in measurement must vary in a known quantitative manner with tracer concentration, and the effect of any chemical reducing agent(s) in the flow stream must be taken into account.

(g) Uncertainties of 1% to 3% have been achieved in test depending on flow conditions.

12-3 TRACER SELECTION

There are numerous nonradioactive tracers that are used in water flow studies. These include sodium chloride, rhodamine B, rhodamine WT, and fluorescein. For a material to be used as a water tracer, it must

(a) mix easily with water.

(b) cause only negligible modifications to the main flow.

(c) be detectable at a concentration lower than the highest permissible concentration taking into account toxicity, corrosion, and so on.